Down-dip correlation and modelling of shallow-marine and estuarine deposits in the Sunnyside Member, Book Cliffs, Eastern Utah: Implications for the formation of non-depositional discontinuity surfaces

Master thesis in Petroleum Geology/Sedimentology

Tor Oftedal Sømme

University of Bergen,

Department of Earth Science,

November, 2005

Abstract

The Sunnyside Member is part of the Blackhawk Formation and consists of shallow-marine and estuarine deposits reflecting high-frequency changes in sea level. Detailed mapping of the unit reveals an intra parasequence architecture which is comparable to that of similar successions in the Blackhawk Formation. However, the Sunnyside Member comprises a unique set of coarsening upward sandstone packages, termed bedsets, which are bounded by non-depositional discontinuity surfaces and which were deposited during normal coastal progradation, expressing a sub-horizontal shoreline trajectory. In a palaeolandward direction, these bedset boundaries pinch-out into the lower shoreface. The surfaces are characterized by a landward shift of facies and an abrupt decrease in sediment supply.

Excellent 3D exposure in the study area allows careful down-dip correlation of the shallow-marine and estuarine units. The majority of successions are composed of interbedded mudstones and hummocky cross-stratified sandstones, representing a wave-dominated coastline; comprising uniform and basinward thickening wedges which can be traced for 5-10 km down-dip. However, one bedset demonstrates both wave and current-induced sedimentary structures in an overall basinward thinning wedge, indicating changes into a more mixed, fluvial and wave-influenced depositional environment, which has been interpreted to result from lateral migration of the river mouth.

Previous investigations of intra parasequence discontinuity surfaces in the Blackhawk Formation have suggested that they may form in response to high-frequency changes in sea level, wave base or sediment supply. The results from modelling obtained in this study indicates that non-depositional discontinuity surfaces similar to the ones observed in the Sunnyside Member form during a combined low in both sediment supply and wave base. A comparison between these data and field observations suggests a connection between reorientation of the shoreline resulting from river mouth migration, and a relatively abrupt decrease in sediment supply and wave base. The bedsets in the study area are therefore interpreted to result from reconfiguration of the coastal morphology, sediment starvation, and localized relative deepening due to loading and compaction. This interpretation implies first-order sand body connectivity both up depositional dip and along-strike between adjacent bedsets. Good understanding of the formation and pinch-out style of these units is of great importance in an exploration perspective as discontinuities will control fluid flow within a reservoir of parasequence scale.

Acknowledgements

Contents

Chapter One – Introduction, History and Stratigraphy

1.1 Introduction

This thesis presents a sedimentological interpretation and mapping of shallow-marine and estuarine deposits in the medial to distal part of the Sunnyside Member. It also presents a comparison between field observations and output data derived from a 2D simulation program, along with a model for the formation of non-depositional discontinuity surfaces examined in the study area.

The Sunnyside Member represents a series of stacked wave-dominated, shallow-marine parasequences, which were deposited on the western margin of the Late Cretaceous, Western Interior Seaway. Long-term collision between the North American plate and oceanic crust resulted in thrusting from the west and the formation of a major, north-south trending mountain chain, termed the Sevier Mountains, and an associated foreland basin. Throughout the Later Cretaceous and Early Tertiary, sediments were shed into the basin, depositing as an eastward thinning wedge. This deposition was mainly controlled by the relationship between thrusting, tectonics, subsidence and eustatic sea level. Superimposed cycles of relative sea level changes resulted in an intricate spatial distribution of both continental and shallow-marine sediments, which can be studied on various scales. The parasequences are regional extensive sandstone units reflecting high sedimentation relative to accommodation, and are bounded by surfaces representing an abrupt increase in accommodation and flooding in the marine environment (Van Wagoner et al., 1990). Internally, these units comprise discontinuity surfaces (clinoforms) which are interpreted to represent palaeosurfaces on the ancient shoreface-shelf (Hampson, 2000). The study of these internal packages along-strike and down-dip may reveal high-frequency changes of the ancient, wave-dominated depositional environment. This study will deal with some of these most high-frequency cycles encountered within shallow-marine deposits.

The first chapter in this thesis will focus upon the depositional and structural history of the Western Interior Seaway and its stratigraphy. An introduction to basic sequence stratigraphic history and terminology is also given, along with its appliance to the Sunnyside Member and the Blackhawk Formation. This chapter will also give a brief introduction to previous work in this subject area and discuss the methods which were used during fieldwork as part of this study, and in addition, address some of the uncertainties related to logging and

correlation. Chapter Two will give a detailed facies description and interpretation of the depositional environments encountered in the study area. Chapter Three will provide a brief introduction to shallow-marine, wave-dominated depositional environments, followed by a thorough description of the stratigraphical elements observed in the Sunnyside Member. It will also present a correlation panel, relating logged sections to each other, and further discuss the internal parasequence architecture and the palaeogeographical setting. Chapter Four will give a brief introduction to estuarine depositional environments, followed by a description and interpretation of the estuarine deposits encountered in the study area, as well as a detailed definition of the palaeogeographical setting. Chapter Five will give an introduction to the process-response modelling software used during simulations, and describe five different scenarios of shoreline progradation. Chapter Six will discuss the effects of changing sea level, wave climate and sediment supply on the shoreface-shelf profiles, and the potential mechanisms for the formation of non-depositional discontinuity surfaces. It will also compare the modelling result with field observations, and propose a model for bedset formation as seen in the Sunnyside Member. Chapter Seven will provide a summary and conclude the study.

1.2 Project aims

The main aim for this thesis was to document the sedimentological and stratigraphical elements of the shallow-marine and estuarine Sunnyside Member in the study area between Woodside Canyon and Gray Canyon (Figure 1.1). The architectural elements have previously been described proximally and distally of the study area by Howell et al. (in review). The outcrops which are exposed within the area allow a detailed description and interpretation of the pinch-out style of parasequences, bedsets and incised valley deposits. The aim was therefore to recognize the main characteristics associated with bedset boundaries, and to identify potential mechanisms responsible for their formation. Process-response modelling of discontinuity surfaces has previously been carried out by Storms and Hampson (2005), who presented a series of end-member scenarios and compared them to their observed results. The aim in this study is to reverse this methodology, and change the input variables to make the model respond in accordance with data gathered in the field.

Identification of the mechanisms responsible for bedset formation is very important to the understanding of coastal response to imposed changes in the depositional environment. Understanding of these features is also very important in hydrocarbon exploration, as wave-

dominated, shallow-marine deposits form important reservoirs worldwide. Due to bedsets here being separated by low-permeable zones of more distal facies, they will act as barriers to fluid flow, both vertically and horizontally. Good understanding of pinch out styles up and down-dip, and along-strike may therefore improve the knowledge of reservoirs and fluid behaviour. It may also be of great importance during well-correlation, allowing one to differentiate between bedset boundaries and parasequence boundaries within subsurface reservoirs (Hampson et al., in review).

1.3 Study area

The study area is located 250 km southeast of Salt Lake City, and approximately 30 km north of the town of Green River (Figure 1.1). The Sunnyside Member crops out in Woodside Canyon and Long Canyon, which is cut into the northwest-southeast trending Book Cliffs and defines the Beckwith Plateau. The Book Cliffs stretches from the town of Helper in the north, towards Grand Junction , Colorado, approximately 250 km southeast. Trail Canyon and Gray Canyon (a distance of approximately 15 km) and in the eastern 10 km of Long Canyon 1 (see Figure 1.8 for detailed map).
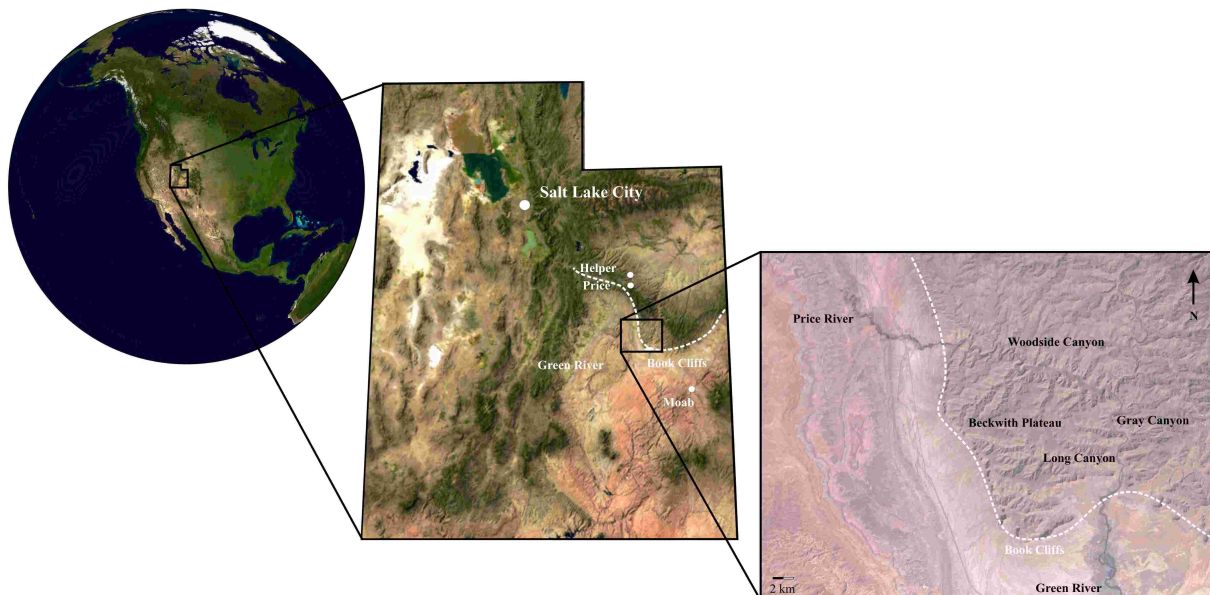
Figure 1.1. The study area is located in the south eastern part of Utah, USA. The main sections are in Woodside Canyon and Long Canyon. The outline of the Book Cliffs is marked by the white, broken line. Maps from NASA World Wind.

3

The Beckwith Plateau is elevated to 1500 m above sea-level, the regional climate is semi-desert, which therefore results in there being very little vegetation covering the outcrops (Howell and Flint, 2003). The region is generally not disturbed by tectonics, and was only mildly affected by the Late Paleocene San Rafael Swell (Hintze, 1988) to the west, resulting in an eastward dip of the bedding of 3-7° (Howell and Flint, 2003). However, the area underwent regional uplift and fluvial incision together with the Colorado Plateau during the Late Cenozoic (Hintze, 1988). This fluvial incision resulted in excellent 3D exposure of the cliffs and their internal stratigraphy.

1.4 Regional history and stratigraphy

In the Early Cretaceous, break-up of the supercontinent of Pangea was associated with westward drift of the North American continental plate, and the subsequent formation of a major thrust ridge along the western plate margin (Figure 1.2); this occurred in response to plate collision and subsidence of a dense oceanic crust (Burchfiel and Davis, 1975). This continuous thrusting from the west created the major, north-south trending, Cordilleran thrust belt and the associated Sevier mountain system; stretching from Canada and Alaska in the north, to the Gulf of Mexico in the south (Kauffman, 1984). As the mountain chain grew, flexural bulging of the lithosphere resulted in the development of a foreland basin (foredeep), which was bounded in the west by a forebulge; these are both oriented parallel to the main mountain chain (Decelles and Giles, 1996; Howell and Flint, 2003). Isostatic rebound of the lithosphere led to regional basement uplift 1000-1500 km east of the plate margin (Burchfiel and Davis, 1975). The foreland basin, termed the Western Interior Seaway, was progressively flooded from the north during the Aptian due to continuous subsidence and an overall high eustatic sea-level during the Late Cretaceous (Kauffman, 1984; Haq et al., 1988; Hintze, 1988). Throughout the entire period of basin development, the epicontinental seaway was controlled by tectonic activity, eustatic sea level variations and intensity, and timing of thrusting and subsidence along the western coastline (Kauffman, 1984).

Collision between the oceanic and the continental plates, microcontinents and island arcs continued throughout the basin's history, and several phases of thrusting have been recognized (Burchfiel and Davis, 1975; Kauffman, 1984; Hintze, 1988).
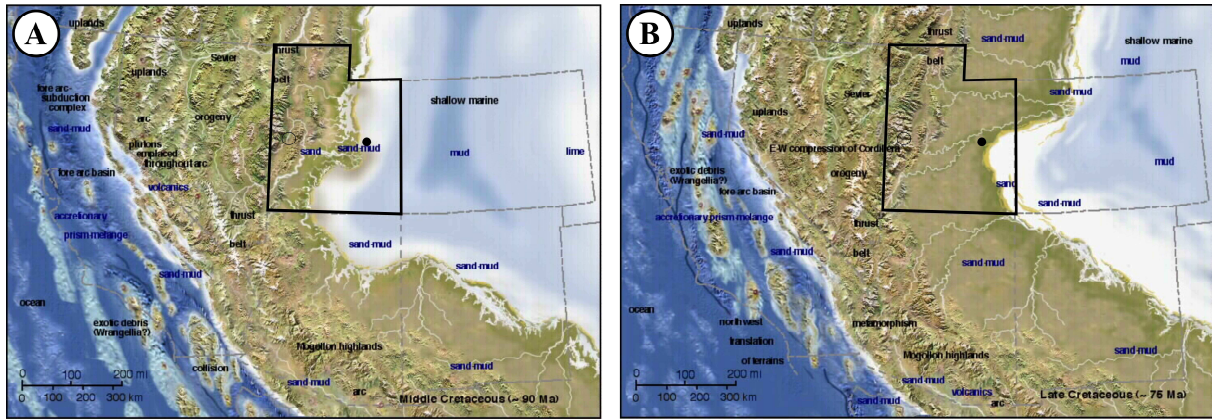
Figure 1.2. Palaeogeography of the central parts of present day USA during the (A) Middle Cretaceous and (B) Late Cretacous respectively. Utah is outlined in black. The approximate location of the study area is marked by a black dot. Maps are from http://jan.ucc.nau.edu/~rcb7/crepaleo.html.

These pulses directly affected the depositional pattern in the basin, and increased thrusting and uplift was accompanied by periods of rapid sedimentation and subsidence. This is evident from numerous volcanic ash layers which can be directly correlated with episodes of transgression and relative sea level rise (Kauffman, 1984).

Both subsidence and basin bathymetry was highly asymmetrical in the Western Interior Seaway, resulting in a highly asymmetrical depositional pattern (Kauffman, 1984). In the western part of the basin, proximal to the main Cordilleran thrustbelt where regional subsidence was high, thick sequences of coarse-grained, continental sandstones, conglomerates and marsh deposits along with marginal marine and shallow-marine clastics were laid down (Kauffman, 1984; Hintze, 1988). Farther east, in the deepest axial part of the basin, more fine-grained, calcareous and silty shales, and pelagic carbonates were deposited (Kauffman, 1984). In the eastern part of the basin, sedimentation was characterized by fine-grained, marine deposits composed of silty and calcareous shales, and shallow-water carbonates. In the Late Cretaceous, when the Sevier orogony was at its peak, the depositional pattern changed from being mainly aggradational in the early stages of the basin development, to being more progradational as the eustatic sea level ceased rising, and a considerable amount of sediments were shed into the basin from the west (Hintze, 1988). Superimposed on the overall aggradational and progradational stacking pattern, was several high-frequency cycles of transgression and regression, reflecting an intricate relationship between thrusting, tectonism, volcanism, subsidence, deposition and eustatic sea level (e.g. Burchfiel and Davis, 1975; Kauffman, 1984; Haq et al., 1988; Weimer, 1988)

In Late Cretaceous-Early Tertiary, the decreasing Western Interior Seaway was uplifted and split into several minor depositional basins as the thrustfront moved eastward and the angle of subduction decreased, resulting in more regional subsidence (Hintze, 1988; Krystinik and Dejarnett, 1995; Van Wagoner, 1995; Howell and Flint, 2003). The Uinta and the Paradox Basin are two of the minor basins and structural elements of the Western Interior Seaway during this period, and arelocated in the eastern part of present day Utah (Krystinik and Dejarnett, 1995; Van Wagoner, 1995). These basins captured a considerable amount of the sediments eroded from the western highlands, which today is observed as a mixture of interfingering continental and shallow-marine sediments along the western basin margin (Figure 1.3). The shallow-marine sediments of this north-south trending basin are known as the Mesa Verde Group (Spieker and Reeside, 1925; Howell and Flint, 2003). In the Book
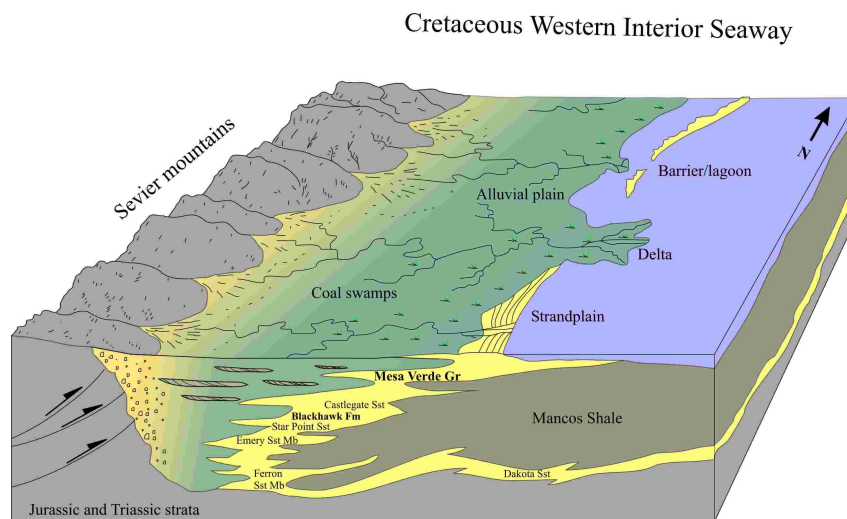
Figure 1.3. Depositional environments and selected stratigraphical units of the Western Interior Seaway. Gr = group, Fm = formation, Mb = member, Sst = sandstone. Modified from Hintze (1988) and Howell and Flint (2003).

Cliffs of eastern Utah, this group is further split up into the Star Point Formation, Blackhawk Formation and Price River Formation, reflecting an overall progradational unit largely composed of continental, marginal marine and shallow-marine deposits (Spieker and Reeside, 1925; Spieker, 1946; Young, 1955). Eastwards of these deposits, sandstone tongues interfinger with the grey and slightly bluish Mancos shale, which is 1500 m thick in central Utah (Spieker and Reeside, 1925; Spieker, 1946; Young, 1955). The Blackhawk Formation and Star Point Formation is interpreted to have been deposited during the latest part of Santonian to the middle part of Campanian (84-79.5 Ma) (Howell and Flint, 2003); however,

the timing depends on which set of dates is used (Obradovich, 1993; Van Wagoner, 1995; Howell and Flint, 2003).

According to Young (1955) , the Blackhawk Formation is up to 300 m thick, and consists of "six prominent littoral marine sandstone tongues and many lesser ones, all projecting eastward into the Mancos, where they loose their identity and grade into shale" (Figure 1.4). Each sandstone tongue is also overlain by lagoonal sandstone, shale and coal developed behind barrier bars, and overlain by white-capped sandstone. The six tongues are: the Spring Canyon Member, the Aberdeen Member, the Kenilworth Member, the Sunnyside Member, the Grassy Member and, the Desert Member, ordered from the stratigraphic base to the top. The six members of the Blackhawk Formation represent an overall upward shallowing succession, deposited during infilling and progradation of the shoreline into the basin. The interfingering between successive sandstone tongues and Mancos shale corresponds to alternating, high-frequency, changes in relative sea level in response to tectonism, subsidence, sedimentation and eustatic sea level (Young, 1955; Kauffman, 1984).
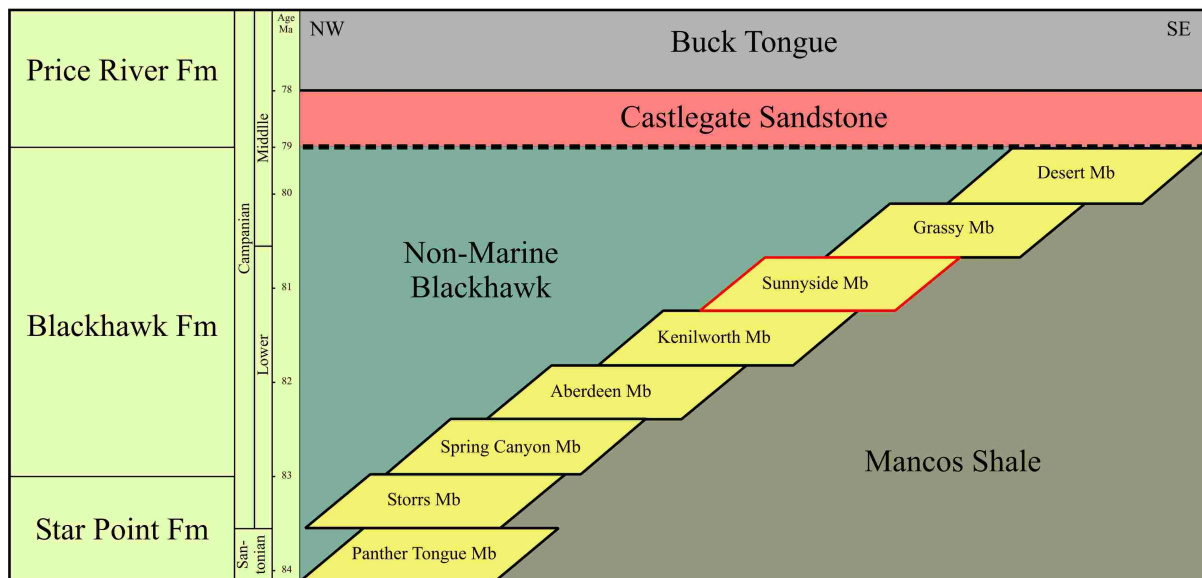
Figure 1.4. Lithostratigraphy of the Book Cliffs. The Sunnyside Member is outlined in red. Broken line below the Castlegate Sandstone represents a major erosional hiatus. Modified from Howell and Flint (2003).

The Sunnyside Member is composed of three main sandstone tongues which are separated by continental, marginal marine, shallow-marine and offshore deposits of varying thickness, and which pinch out basinwards (east) into the Mancos shale (Young, 1955; Howell and Flint, 2003). These three units represents three different stages of shoreline development, each reflecting 10-15 km of basinward progradation (Howell and Flint, 2003).

A typical succession displays an upward coarsening and upward shallowing unit, reflecting progradation of the shoreline. The tongues may also be truncated by an erosional surface, which represents a high-frequency fall in relative sea level, or by extensive coal beds (Davies et al., 2005). Both the internal architecture and the depositional environments of the Sunnyside Member will be discussed in detail throughout the forthcoming sections and chapters.

1.5 Sequence Stratigraphy

The concept of sequence stratigraphy was originally based upon seismic stratigraphy, and has been constantly developing from the late 70's, to the present day (e.g. Mitchum, 1977; Jervey, 1988; Posamentier et al., 1988; Posamentier and Vail, 1988; Van Wagoner et al., 1988; Van Wagoner et al., 1990; Mitchum and Van Wagoner, 1991; Hunt and Tucker, 1992; Kamola and Van Wagoner, 1995; Van Wagoner, 1995). It is defined as "the study of rock relationships within a chronostratigraphic framework wherein the succession of rocks is cyclic and composed of genetically related stratal units" (Mitchum, 1977). The concept has been widely used as a basis to understand and predict stratigraphic patterns in both modern and ancient deposition systems, both in response to sea level changes and deposition. Cycles of eustatic and relative sea level are usually superimposed upon each other to form a composite curve, these are divided into different time scales: first-order cycles (100-200 My), second-order cycles (10-100 My), third-order cycles (1-10 My), forth-order cycles (0.1-1 My) and fifth-order cycles (10-100 thousand years); this terminology is recognized by Mitchum (1977), Van Wagoner et al. (1990) and Mitchum and Van Wagoner (1991). Such composite sea level curves gives rise to a hierarchy of stratigraphical elements that reflects the various frequencies of sea level change. Composite sequences reflects third-order cycles, and are composed of several sequence sets, stacked in a progradational, aggradational or retrogradational pattern (Mitchum and Van Wagoner, 1991). These are again composed of higher-frequency sequences (Figure 1.5), reflecting fourth-order sea level cycles, and which are further composed of: systems tracts, parasequence sets, parasequences and bedsets, representing fifth-order cycles (Van Wagoner et al., 1990; Mitchum and Van Wagoner, 1991). In addition, some even recognize sixth-order cycles (thousand to tens of thousands of years) (e.g. Hampson and Storms, 2003).

The basic building block of sequence stratigraphy is the fourth or fifth-order, high-frequency sequence, which is composed of parasequence sets and parasequences (Van Wagoner et al., 1990). The sequence is defined as "a relatively conformable succession of genetically related strata bounded at its top and base by unconformities" (Mitchum, 1977; Van Wagoner et al., 1988; Van Wagoner et al., 1990). The bounding unconformity is described as "a surfaces separating younger from older strata along which there is evidence of subaerial erosional truncation and, in some areas, correlative submarine erosion, or subaerial exposure, with a significant hiatus indicated (Van Wagoner et al., 1988). Parasequence sets may be either progradational, aggradational or retrogradational (Figure 1.5), and are arranged into four systems tracts according to their stacking pattern. In the original sequence model there were three system tracts, these are the lowstand (LST), the transgressive systems tract (TST), and the highstand systems tract (HST). (Posamentier and Vail, 1988). More recent studies have also recognized the importance of deposition during falling sea level and defined an additional falling stage or forced regressive systems tract (Hunt and Tucker, 1992).

Two different types of high-frequency sequences are recognized (type I and type II). The most common (type I) is formed when the amount of sea level fall is greater than the rate of basin subsidence, whereas type II is formed when the rate of eustatic sea level fall is less or equal to the rate of basin subsidence (Posamentier and Vail, 1988). The type I sequence is bounded by below by a type I sequence boundary (SB), which is "characterized by subaerial exposure and concurrent subaerial erosion associated with stream rejuvenation, a basinward shift of facies, a downward shift in coastal onlap, and onlap over overlying strata" (Van Wagoner et al., 1988). A type II sequence is bounded by a type II sequence boundary and therefore is "marked by subaerial exposure and a downward shift in coastal onlap", but which lacks subaerial erosion due to stream rejuvenation and basinward shift in facies, in these cases the deposits above the SB are termed the shelf margin system tract (Van Wagoner et al., 1988). Both types of sequences described above are also bounded above by a type I or II SB.

Type I sequences are composed of three out of the four identified systems tracts (LST, the TST and the HST). The LST is formed during relative sea level fall and during subsequent slow rise of relative sea level (Posamentier and Vail, 1988). The lowstand fan is composed of fine-grained material, deposited as submarine fans during periods of incision and sediment by-pass in the proximal part of the basin. The lowstand wedge is deposited during stable or slowly rising sea level and is composed of finer-grained slope deposits or a relatively coarse-

9
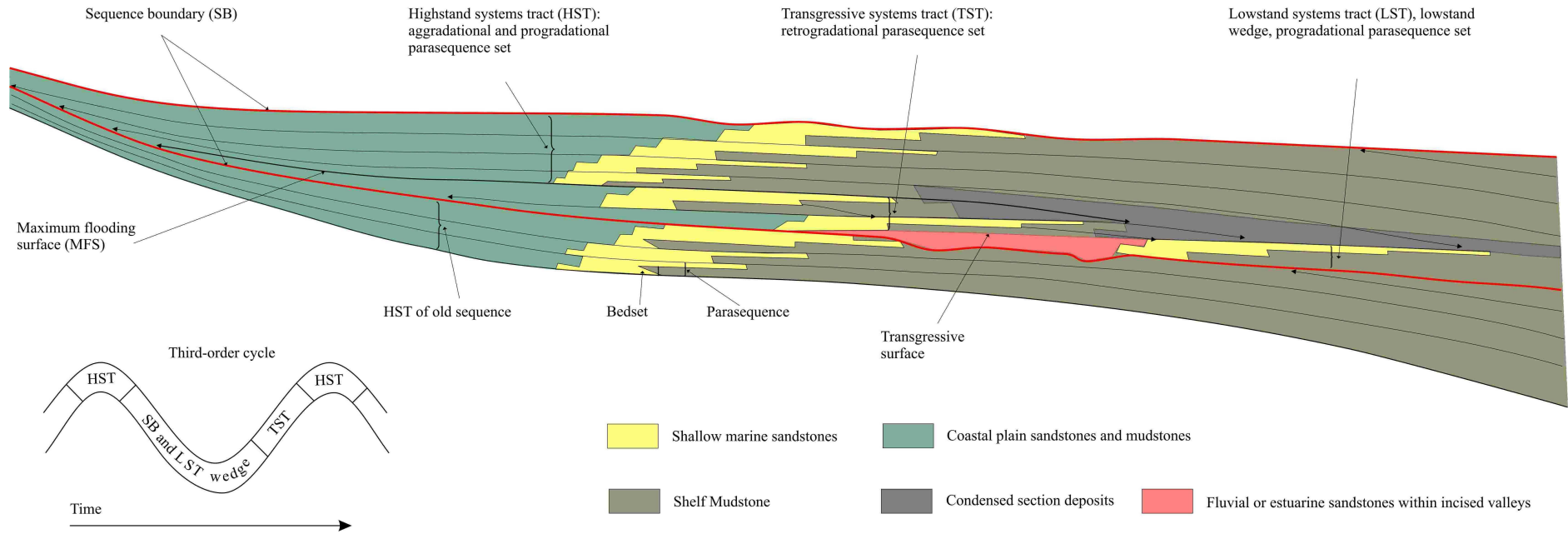
Figure 1.5. Internal architecture of an ideal ramp margin sequence which are bounded by a type I sequence boundary; from (Van Wagoner et al., 1990). In contrast to shelf-break margin sequences, ramp margin sequences lack a pronoundsed shelf-slope-basin floor topography, and there are no abrupt transition from shallow to deeper water. A result of this gently dipping topography is the general lack of muddy lowstand deposits, such as lowstand wedges or basin floor fans. Lowstand deposits in ramp margin sequences are therefore considered to consist of incised valley deposits and associated sandy deltaic deposits (Van Wagoner et al., 1988; Van Wagoner et al., 1990).

grained, basin restricted wedge, dependent on the shelf and slope geometries (Posamentier and Vail, 1988). The TST is deposited during sea level rise and is composed of a retrogradational parasequence set, which overlay the transgressive surface (flooding surface which may combine with the sequence boundary), which is itself overlain by the maximum flooding surface (MFS); this represents the maximum landward position of the shoreline (Van Wagoner et al., 1988). The subsequent HST is commonly composed of an aggradational and progradational parasequence set and is bounded above by the SB (Posamentier and Vail, 1988).

Parasequences are the main building blocks of high-frequency sequences and are defined as "a relatively conformable succession of genetically related beds or bedsets bounded by marine flooding surfaces and their correlative surfaces" (Van Wagoner et al., 1988). These flooding surfaces, or parasequence boundaries (PSB), "separate younger from older strata, across which there is evidence of an abrupt increase in water depth", and represent a landward dislocation of the shoreline (Van Wagoner et al., 1988). Most silisiclastic, shallow-marine parasequences are upward coarsening and upward shallowing, reflecting shoreline progradation (Van Wagoner et al., 1990). The main parasequence characteristics are: an overall upward thickening and coarsening of sandstone beds, an upward increase in sandstone/mudstone ratio, and an upward decrease in bioturbation (e.g. Van Wagoner et al., 1990; Boyd et al., 1992; Reading and Collinson, 1996). Farther landwards, parasequences can be identified in tidal, estuarine or fluvial environments; however, these are more difficult to identify (Van Wagoner et al., 1990). The PSB is characterised by a change in bed thickness, a landward shift of facies, a change in lithology from sandstone to mudstone or from coal to sandstone, and possibly by an erosional truncation (Van Wagoner et al., 1990). Parasequences are generally considered to be cycles of fourth or fifth-order, presumably one order higher than the high-frequency sequences they define (Mitchum and Van Wagoner, 1991).

The building blocks of parasequences are bedsets, which are defined as "a relatively conformable succession of genetically related beds bounded by surfaces (called bedset surfaces) of erosion, non-deposition or their correlative conformities" (Van Wagoner et al., 1990). The bedset surfaces, or bedset boundaries, are less extensive than the PSB, but demonstrates a similar upward increase in sandbed thickness and grain-size, and a decrease in bioturbation (Van Wagoner et al., 1990; Howell et al., in review). The main contrast, however, is that bedset boundaries are not flooding surfaces and are not associated with a landward

dislocation of the shoreline. Bedsets are generally considered as fifth or sixth-order cycles (Van Wagoner et al., 1990; Mitchum and Van Wagoner, 1991; Hampson and Storms, 2003).

The Blackhawk Formation represents a third-order, highstand sequence set (Mitchum and Van Wagoner, 1991; Howell and Flint, 2003), which reflect aggradation in the earliest and lowermost part of the formation, and more progradation towards the top during late highstand deposition (Figure 1.6). The sequence set is bounded by the Castlegate sequence boundary in the upper part. The six members identified by Young (1955) within the Blackhawk sequence set are composed of nine, high-frequency, fourth-order, sequences (Mitchum and Van Wagoner, 1991).
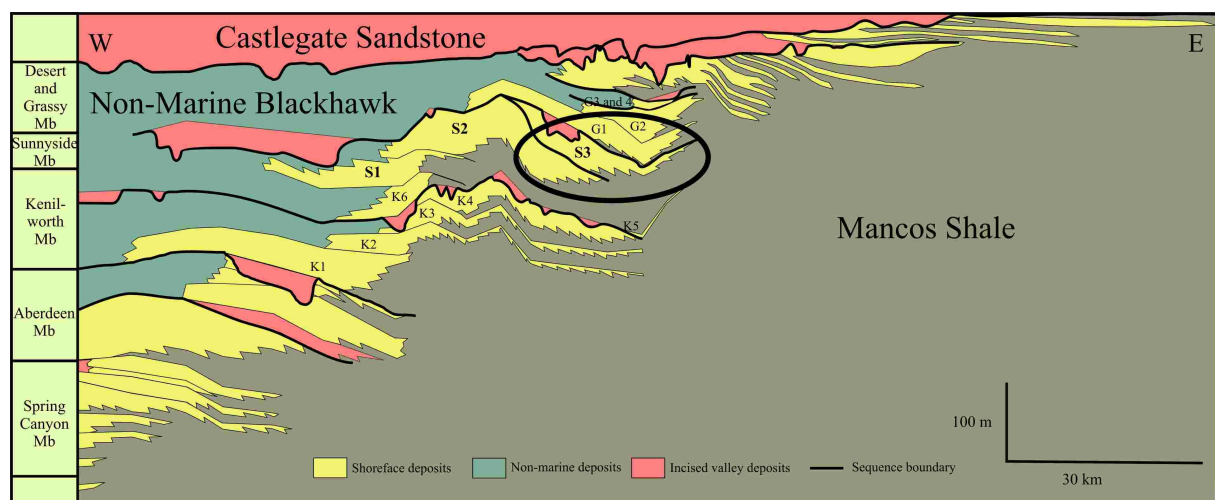
Figure 1.6. Cross-section showing selected sequence stratigraphical units in the Book Cliffs. The sequences exposed in the study area are encircled. Modified from Howell and Flint (2003).

The Sunnyside Member comprises parts of two of these nine, high-frequency sequences (Figure 1.6), and is represented by three parasequences, stacked in progradational parasequence sets (Van Wagoner et al., 1990; Howell and Flint, 2003). The lowermost Sunnyside Parasequence (S1), constitutes the lowermost unit in the HST, and is part of a high-frequency sequence where the TST and LST are located in the underlying Kenilworth Member (Figure 1.6) (Pattison, 1995; Taylor et al., 1995); the bounding surface between the two members is therefore a MFS. S1 is not present in the study area as it pinches out farther west (in the area close to B' Canyon) (Howell et al., in review). The second parasequence in the Sunnyside Member (S2), constitutes the uppermost unit of the same HST and is separated by the underlying S1 by a PSB, reflecting a relative sea level rise of approximately 10 m, and is bounded on top by the (lower Sunnyside) SB, reflecting a sea level fall of up to 20 m (Howell et al., in review). In the study area, the SB on top of S2 is a correlative SB as it is part

of the interfluve formed during incision (Figure 1.6). S2 is thicker (up to 45 m) than most of the parasequences in the Blackhawk Formation (Howell et al., in review). This is related to the limited basinward progradation of the two underlying parasequences, where the excess accommodation space created basinward of the shoreline prior to progradation of S2 was filled (Howell et al., in review). S2 is also capped by a thick coal bed (the "Sunnyside Coal", up to 5.5 m thick), which is split between South Lila Canyon and Woodside Canyon (a few kilometres west of the study area) into two minor beds, by a wedge of shallow-marine sandstone; this represents the maximum landward extent of the uppermost parasequence in the Sunnyside Member (S3) (Howell and Flint, 2003; Davies et al., 2005). The LST associated with the lowermost sequence is located somewhere east of the study area, but this has not been identified during this research as it is removed by later Cenozoic uplift and erosion. The TST is represented by the incised valley fill (exposed northeast of the study area,) and by a thin transgressive unit overlying the correlative SB in Woodside Canyon and Long Canyon 1 (see section 3.6). The following parasequence (S3) is the only parasequence in the subsequent HST, and it is bounded below by the MFS, and above by the next SB belonging to the lower most Grassy sequence (Figure 1.7), reflecting fall in relative sea level and subsequent fluvial incision (Howell et al., in review).
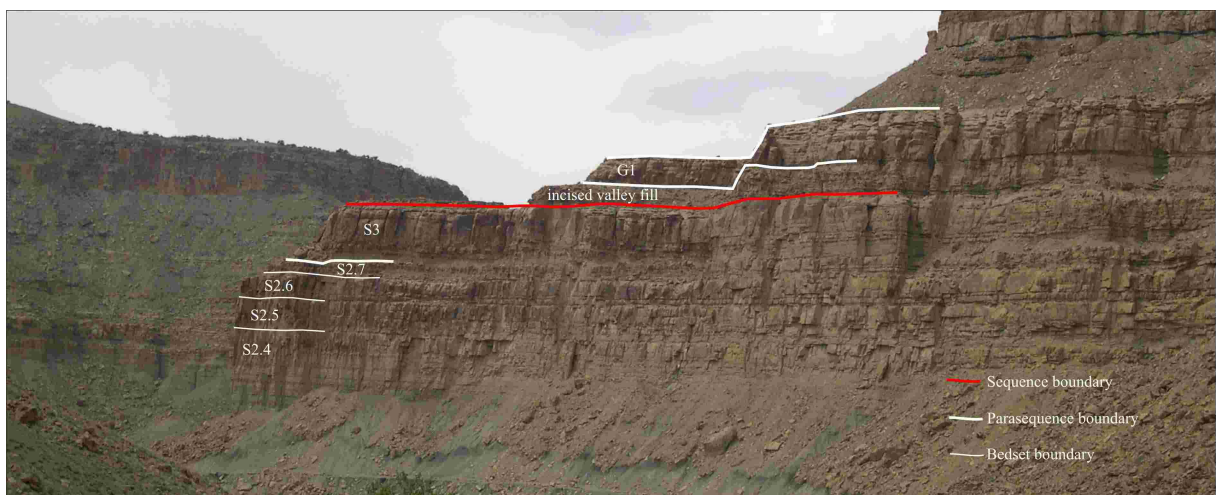
Figure 1.7. Stratigraphy in the proximal part of Woodside Canyon. Most of these units have been traced to their basinward extension, 10-15 km east of this locality. See text for more detailed description of the units. The heterolithic unit above the lowermost Grassy parasequence is non-marine coastal plain deposit, and the grey mud below S2.4 is the Mancos Shale. The Sunnyside Member is approximately 70 m thick at this locality.

The LST within this sequence is also located somewhere east of the study area, but this one has also not been identified in this field study. The TST is represented by the incised

valley fill exposed in Woodside Canyon and Long Canyon 2 (Chapter Four); no transgressive, shallow-marine unit has been identified in this sequence. S3 is bounded by a MFS, representing the transition into the overlying Grassy Member and the subsequent TST and HST of the same sequence (Figure 1.7 and Figure 1.6).

Both S2 and S3 also contain several high-frequency, fifth or sixth-order bedsets (Mitchum and Van Wagoner, 1991; Hampson and Storms, 2003; Howell et al., in review). S2 contains seven bedsets (S2.1-S2.7) stacked in an overall progradational pattern (see section 3.5.), where the uppermost four (S2.4-S2.7) are present in the study area (Figure 1.7). S3 is composed of another three bedsets, termed S3.1-S3.3, which are stacked in a similar progradational pattern. These bedsets are bounded by boundaries of non-deposition (described above) demonstrating a landward shift of facies (Howell et al., in review).

Throughout the thesis, the sequence stratigraphic terminology (defined above) of Mitchum (1977), Posamentier et al.(1988), Posamentier and Vail (1988), Van Wagoner et al.(1988), Van Wagoner (1990) and Mitchum and Van Wagoner (1991) will be used.

1.6 Previous Work

As the Blackhawk Formation is virtually unaffected by tectonism and faulting, and because of its excellent 3D exposure, it has become a type example of foreland basin deposition, ancient wave-dominated shorelines and high-resolution sequence stratigraphy. Thus, most of the studies conducted in the area are related to the identification of shallow-marine and marginal marine depositional environments and their position within the sequence stratigraphic hierarchy; this is especially true for the parasequence concepts (e.g. Kamola and Van Wagoner, 1995).

The area has also been thoroughly explored in the search for hydrocarbons, and the coastal plain deposits contains several thick commercial coal deposits which have been mined extensively throughout the past century; this is especially true for the "Sunnyside Coal". This industry has greatly increased our 3D understanding of the area through well logs and cores.

Regional mapping and correlation of the Blackhawk Formation, and the over and underlying stratigraphic units, was conducted in the 1920's to the 1950's, and a brief lithological interpretation of the Blackhawk Formation, including the Sunnyside Member, was complete by Spieker and Reeside (1925), Spieker (1946) and Young (1955). The detailed investigations on sedimentological and sequence stratigraphical aspects of the minor units,

initiated with examples from the Spring Canyon Member (Van Wagoner et al., 1990; Kamola and Van Wagoner, 1995), and has been followed by detailed interpretations of the Kenilworth Member (Pattison, 1995; Taylor et al., 1995; Hampson et al., 2001; Hampson and Storms, 2003), the Grassy Member (O'Byrne and Flint, 1995), and the Desert Member and the overlying Castlegate Sandstone (Van Wagoner, 1995). The Kenilworth Member has also been used as an analog for comparison between computer simulated, internal parasequences architecture, and outcrop examples, to identify potential mechanisms for bedset formation (Storms and Hampson, 2005). The sedimentology and sequence stratigraphy of the Sunnyside Member has been described in detail by Howell et al. (in review).

1.7 Methodology

A total of 25 sections were logged and measured in the study area; 16 in Woodside Canyon, 2 in Long Canyon 2, 1 in Jenny Canyon and 6 in Long Canyon 1 (Figure 1.8). The thickness of the sections varied between 8 and 132 m. The difference in thickness is related to the thickness of accessible outcrop, although most sections cover the entire Sunnyside Member. Some logs are restricted to the incised valley, and some also captures the lowermost part of the overlying Grassy parasequence. In addition, four logs (W1-W4) from the most proximal part of Woodside Canyon (Howell et al., in review), have been used to correlate west of the study area. See appendix for complete logs.

The logs used here have a resolution of 1:40 which gives a good representation of the relative homogenous shallow-marine deposits. Individual beds can usually be traced for tens to hundred of meters laterally and are usually thicker than 5 cm, which is the lowermost limit of unit thickness represented by the log. Incised valley strata are more heterolithic, therefore there are significant change in lithology within a few meters both laterally and vertically, making these deposits harder to represent within log-data.

The distances to the top of Grassy Parasequence 1 and 2 (G1 and G2) has also measured. The top of theseparasequences are bounded by gently (approximately 0.02°) basinward dipping flooding surfaces which represents a rise in relative sea level (Van Wagoner et al., 1990; O'Byrne and Flint, 1995; Hampson et al., 2001). These surfaces are used as datum as they are interpreted to be regional extensive and have a very gentle gradient. G1 bounding surface changes down-dip from foreshore and upper shoreface deposits in the western part, to lower shoreface and offshore transition zone in the eastern part of the study

area, resulting in a basinward increasing gradient (O'Byrne and Flint, 1995). G2 is represented by coastal plain deposition in the western part, and foreshore and upper shoreface strata in the eastern part of the study area. The easily recognizable, bleached foreshore and upper shoreface in G1 and G2 (O'Byrne and Flint, 1995), overlap in the central part of the study area and are both used as datum in the western and eastern part respectively.

Down-dip correlation diagrams were created from the measured log sections and positioned relative to the datum. Parasequence boundaries and bedset boundaries were walked out in the field for their lateral extent, providing good confidence of the correlations. Only in the proximal part of Woodside Canyon did the Sunnyside Member disappear into the subsurface at two locations, decreasing the potential for accurate correlation between log-sections. However, both Long Canyon 2 and the distal part of Woodside Canyon, along with the entire Long Canyon 1, were successfully correlated with a very high certainty, allowing for extrapolation along-strike. It is important to recognize that the three main cross-sections are positioned oblique to true dip, which is considered to be west-east (Howell and Flint, 2003; Howell et al., in review).

The main Woodside Canyon and Long Canyon 1 section represents a northwest-southeast profile, whereas Long Canyon 2 represents a southwest-northeast profile. The short Jenny Canyon cross-section represents a north northeast-south southwest, strike section.

Thicknesses and dip-gradients presented in this study are all based on the measured successions. The 1.5 m long Jacob's staff used during the field work has a potential for errors during logging and it is therefore important to measure the "true thickness" of the exposed succession. This is straight

Figure 1.8. The main study area in Woodside Canyon and Long Canyon 1. Log sections are marked by black dots. W1-W4 are from Howell et al. (in review).

forward in vertical, well exposed outcrops as the successions are undisturbed by tectonics etc. In poorly exposed outcrops, on the other hand, there is a potential for erroneous thicknesses,

especially if the outcrop is sloping and covered in scree and vegetation. In general, the uncertainties related to measuring and logging increase with the thickness of the succession and the decrease in outcrop quality. In some locations, especially in the proximal part, the Grassy Parasequence is very steep and inaccessible, and distances to the top of G1 and G2 have not been measured directly. In these locations, distances were calculated with the use of images and the known thicknesses calculated from the underlying S2 and S3.

In addition to uncertainties related to measurements, the estimated thicknesses and dip-gradient may deviate from true values due to post-depositional compaction and the nature of the oblique strike of the correlation panels. The amount of compaction is difficult to estimate and no evidence related to post-depositional compaction has been observed, but it is reasonable to believe that the muddy distal part has been more compacted than the more sandy proximal part. The overall effect of post-depositional compaction is to decrease the thickness of the stratigraphical units, and increase their dip-gradients. The effect of correlating oblique to dip has the opposite effect, resulting in too low dip-gradients. Combined, these effects may influence the overall stratigraphy differently as they cancel each other out or amplify each other.

Chapter Two – Facies association: Description and Interpretation

2.1 Introduction

This study of the Sunnyside Member along two (10-15 km long) down-dip sections involves correlation of shoreface-shelf and incised valley deposits on a relatively large scale. It is therefore appropriate to consider the deposits in the context of facies and facies associations (Reading and Levell, 1996). Within this study, the term facies association is used to describe sediments laid down in the same depositional environment. The aim of this study is not to give a detailed and careful description and interpretation of all sedimentary structures and the processes under which they were formed, but rather to group and interpret similar units which were deposited in similar settings and environments. Several of the interpreted facies associations comprise alternating sand and mud which have different properties (porosity, permeability etc.) and composition. These would under other circumstances be considered as separate facies, but since they reflect a given depositional environment and a set of depositional conditions, they are treated as facies associations.

The successions encountered in the Sunnyside Member have been divided into eleven facies associations FA1-11 (Table 2.1). FA1-6 reflects an upward shallowing and upward coarsening, progradational, highstand shoreface-shelf succession (Howell et al., in review) and constitutes the majority of described successions within the study area. FA7-10 have been interpreted to represent the filling of an incised valley by estuarine deposits during lowstand and transgression (Howell et al., in review). These facies associations are only present in the northern and most proximal part of the study area.

As described in Chapter One, the two shallow-marine parasequences represented in the study area are bounded by a SB and/or a PSB (Howell et al., in review). A SB is associated with a number of attributes which separates the surface from other erosional surfaces which are related to shallow and marginal marine environments (e.g. fluvial channels and delta mouth scouring during normal regression) (Van Wagoner et al., 1990). These include: distinct basinward shift of facies, abnormal subaerial exposure, truncation and incision, onlapping, and the presence of a *Glossifungites* firm-ground (Van Wagoner et al., 1990). An upward increase in marine influence reflecting a gradual landward shift of facies (during transgression) is also associated with SBs (Van Wagoner et al., 1990). In addition,

SBs have a more regional extent than fluvial channels. A detailed description of the internal geometries and the outline of the valley is given in Chapter Four.

Facies association	Interpretation	Description
1	Offshore	Grey mudstone with occasional thin sandstone beds
2	distal Offshore Transition Zone	Bioturbated mudstone with relatively thin, hummocky cross stratified, sandstone interbeds
3	proximal Offshore Transition Zone	Bioturbated mudstone with relatively thick, hummocky cross stratified, sandstone interbeds
4	Lower Shoreface	Amalgamated, hummocky cross stratified sandstone
5	Middle Shoreface	Heavily bioturbated, fine-grained sandstone
6	Upper Shoreface	Well sorted, planar- and trough cross stratified sandstone
7	Tidal reworked fluvial deposits	Structureless or trough cross-stratified, fine- to coarse-grained sandstone with abundant rip-up clasts
8	Tidally influenced meandering channel	Inclined heterolithic strata (IHS), interbedded, fine- to medium grained sandstone beds and grey siltstone beds
9	Tidal bars	Planar- and trough cross stratified (sometimes bidirectional), structureless, very fine- to medium-grained sandstone with rip-up clasts and rare root structures
10	Lagoonal and tidal flat deposit	Fine laminated mudstone with occasional fine- to coarse-grained sandstone interbeds
11	Transgressive lag	Poorly sorted, medium- to coarse grained sandstone with abundant shell fragments

Table 2.1. Summary of the eleven facies associations recognized in the study area.

2.2. Shoreface-shelf facies associations

The shoreface-shelf successions range in thickness from 1 to 20 meters and are laterally extensive over 10's km, allowing detailed correlation throughout most of the study area. This continuity combined with excellent outcrop exposure makes it possible to observe lateral and vertical changes between proximal and distal parts of the field area. The shoreface-shelf environments (Table 2.1) can be divided into six facies associations.

2.2.1 Facies association 1: Offshore deposits

Description: The most distal parts of this facies association commonly consist of bluish, light and dark grey mudstone. On a fresh surface the deposits are homogenous and massive, lacking sedimentary structures (Figure 2.1, A and B). In a weathered outcrop, the facies association usually looks more greyish and light brown and has a nodular texture (Figure 2.1,

C). The nodules do not seem to possess any noticeably changes in composition relative to the surrounding rocks. These distal, relatively massive mudstones do not contain any evidence of bioturbation.
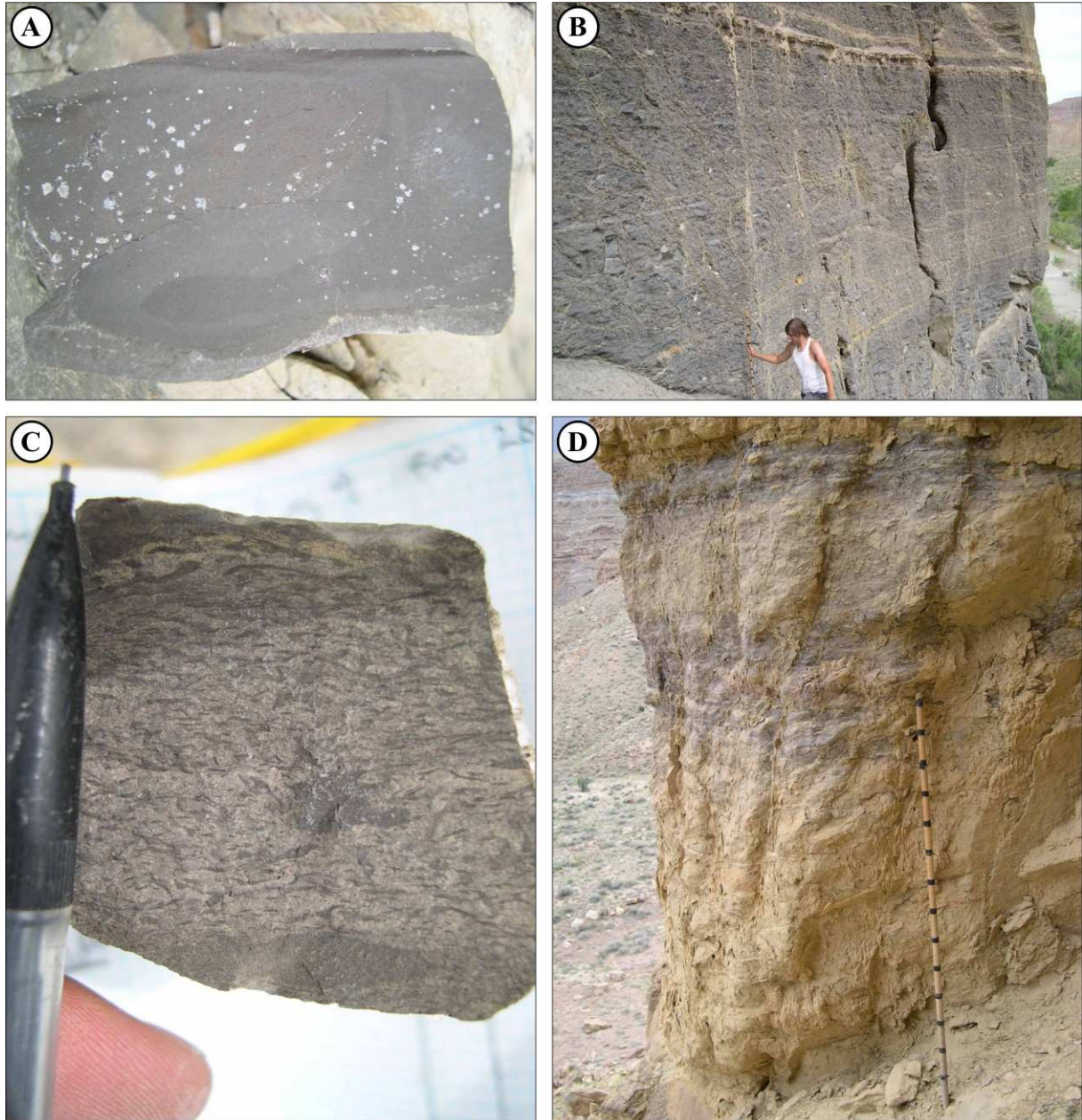
Figure 2.1. (A and B), Homogenous grey siltstone and mudstone of the distal parts of FA1. (C and D), very fine-grained, sandy and silty mudstone of the proximal parts of the FA1. (C) shows *Helminthopsis* bioturbation. Staff is 1.5 m long.

A typical succession becomes more silty and sandy upward. The lowest sands in the succession contain light grey and brown spots, thin lenses and discontinuous lamina (Figure 2.1, C). In contrast to the distal deposits described above, these silty mudstones are completely bioturbated (Taylor and Goldring, 1993). The amount of light grey silt and sand

increases upward but vary slightly locally within a succession. Burrows are generally small, a few mm wide with a dark lining, and filled with dark mud. Less bioturbated intervals may also contain very fine, planar and undulating lamination within the silt and mudstone. The amount of light brown, silt and sandstone interbeds is generally less than 5%, and where present, these beds are commonly heavily bioturbated but may contain vague planar and undulating lamination. The bed boundaries are usually very diffuse and disturbed by bioturbation and the sand is mixed with the surrounding mud.

The thickness of this facies association varies between 1 and 20 m, and it is only present in the lowermost parts of the logs, and in the eastern part of the study area. The deposits commonly overlie and are overlain by FA2, but in the proximal areas, they may overlie FA3 and FA4 and be overlain by FA3.

Interpretation: Thick, homogenous, upward coarsening mudstone units which indicates extensive marine bioturbation suggest deposition within an open marine environment below storm wave base (Walker and Plint, 1992). The gradual upward transition into wave influenced, sand- and mudstones of FA2 also support this interpretation.

During major, high-energy storm events, the nearshore area is eroded and reworked by waves (e.g. Inman and Bagnold, 1963; Niedoroda et al., 1984; Walker and Plint, 1992). Fine-grained material is transported seaward in suspension by waves and currents (e.g. geostrophic currents, longshore currents, rip-currents, delta plumes) (Figure 2.2). As these basinward directed currents loose their transport capacity, very fine-grained silt and sand is deposited as thin, sandy laminas or beds within the overall mud prone environment (Johnson and Baldwin, 1996). During fair-weather periods, this offshore environment receives pelagic and/or hemipelagic material from suspension (Stow et al., 1996). The offshore mudstones reflect relatively constant deposition over an extended period of time.

Lack of evidence for bioturbation in the lower (most distal) part of the facies association may relate to the homogenous, muddy nature of the deposits. The additional lack of lamination and stratification within the mudstones suggest intense burrowing and reworking of the muddy deposits, leaving no traces of the original sedimentary structures (Pemberton et al., 1992b). Evidence for high to intense burrowing becomes noticeable further up where the contrasts between brown silt and dark grey mud are very pronounced.

The coarsening upward succession reflects a gradual transition from a deep, quiet part of the shelf into shallower areas which were more influenced by storms induced as well as bottom currents. Although below storm wave base, currents are strong enough to produce planar-parallel and undulating lamination in the silty and sandy mudstone (Dott and

Bourgeois, 1982; Swift et al., 1983; Johnson and Baldwin, 1996). The boundary between FA1 and the overlying facies association is usually gradual and is picked at the lowermost sandstone bed showing hummocky cross-stratification.
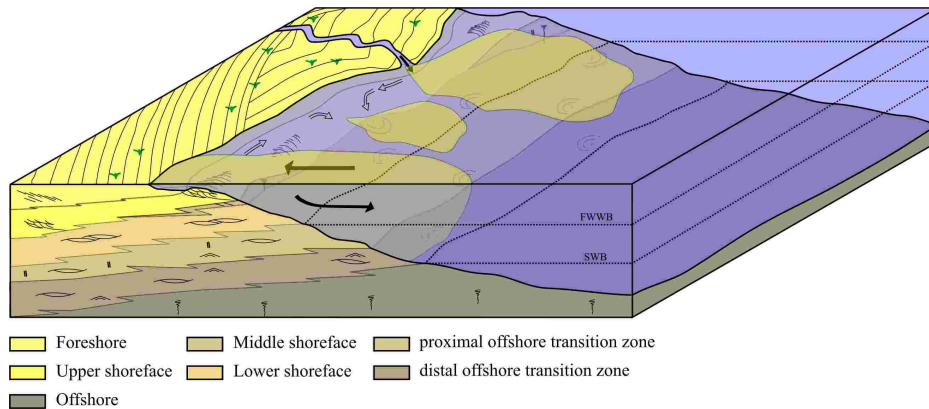
Figure 2.2. Sand and silt is transported to the shoreface-shelf by storm surges (thick black arrows), rip-currents (white arrows) or delta plumes (thin black arrow). Modified from Howell and Flint (2003).

2.2.2 Facies association 2: Distal offshore transition zone (dOTZ) deposits

Description: This facies is typically heterolithic containing interbedded sandstones and mudstone. Sandstones beds are fine-grained, 20-30 cm (maximum 70 cm) thick, with planar- and undulating lamination as well as hummocky cross-stratification (HCS) (Figure 2.3 and Figure 2.4). Wave ripples are common in the upper part (Figure 2.4, C). The boundary between the sandstone and mudstone beds may be disturbed and is not always sharp due to high to intense bioturbation (Figure 2.4, A). The thickness and frequency of sandstone beds increases upwards as the amount of bioturbation decrease. As a consequence, sandstone beds and boundaries between sandstone and mudstone become more pronounced upwards.

The thickness of the FA2 units varies between 1 and 20 m. In the distal (eastern) part of the study area, the succession commonly overlies muddy FA1 strata and is overlain by more sandy FA3 strata. In more proximal areas, the units may also overlie FA3 and FA4. The transition between the underlying FA1 and the overlying FA3 is gradual and there are no distinct boundaries between them. The base of FA2 is picked by the lowermost HCS bed, and the top where the amount of sandstone beds is generally above 25%.

The uppermost part of Log 11 – Log 17 and in Log 23 – Log 25, FA2 has a somewhat different expression. In these sections it is more fine-grained, has sparse to low bioturbation, and has better defined sandstone beds (Figure 2.5). This alternative expression of the facies occurs in units between 5 and 7 m thick within which each sandstone-mudstone interbed is between 0,5 and 20 cm thick. The silty and very fine-grained sandstones commonly display combined ripples (Figure 2.5, C) with crests going north-south and mm thick lamination ranging from being light and dark grey to black, green, red and brown (Figure 2.5, B). These deposits can be correlated with units belonging to FA3 when traced laterally in a palaeolandward direction (west).
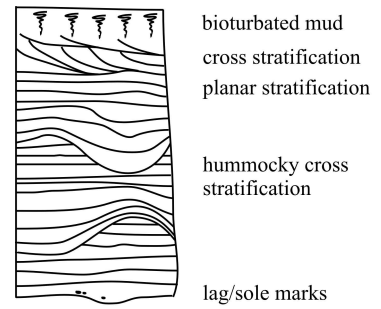
Figure 2.3. Idealized hummocky sequence. Modified from Dott and Bourgeois (1982).
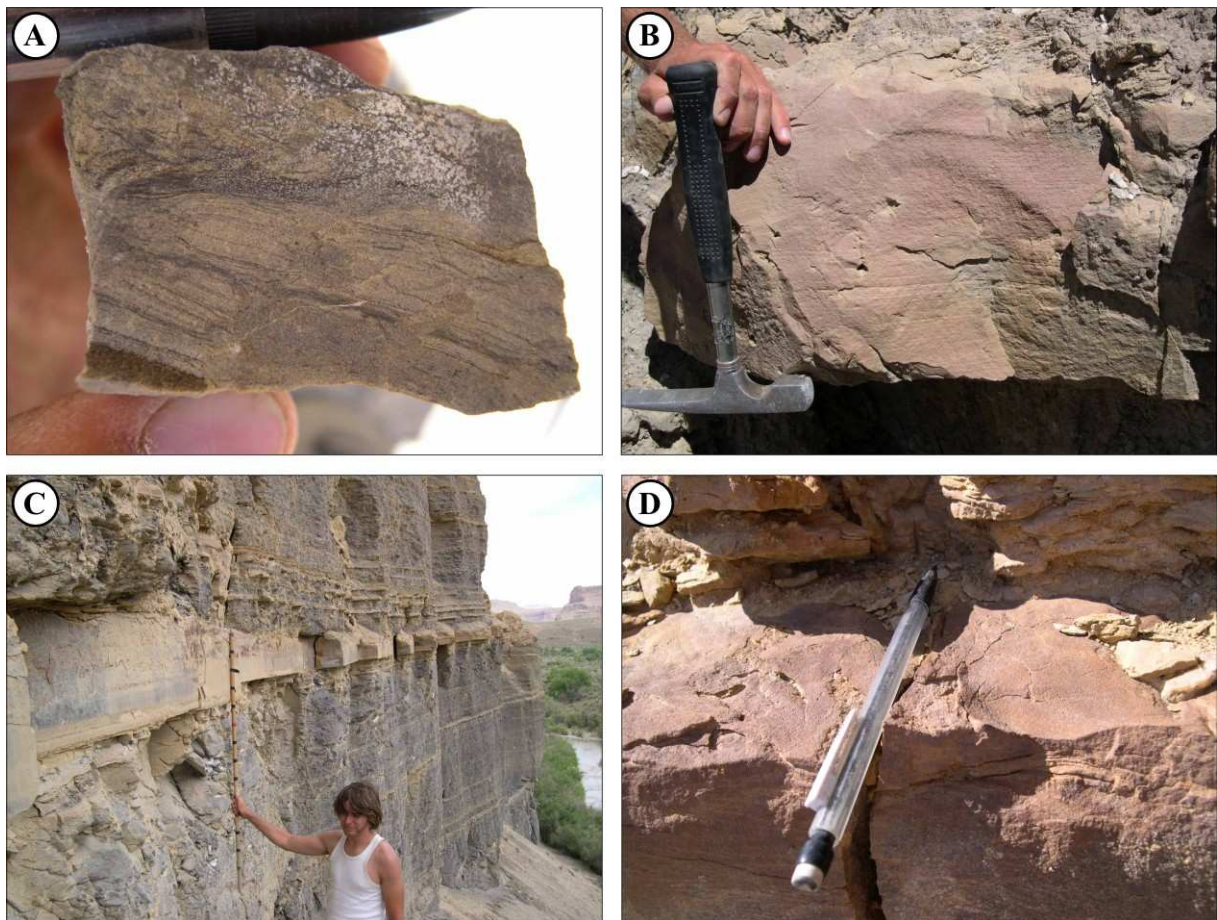
Figure 2.4. Interbedded, highly bioturbated (A), very fine-grained, HCS (B and D) sandstone and mudstone of FA2. Note large-scale wave ripples in the sandstone bed (C) and small, undulating "hummocks and swales" (D).

Interpretation: HCS sandstone in FA2 represents storm event beds in an overall muddy, distal offshore transition zone (dOTZ) environment, deposited between fair-weather wave base (FWWB) and storm wave base (SWB) (e.g. Dott and Bourgeois, 1982; Swift et al., 1983; Howell et al., in review). During fair-weather conditions, this area experience relatively quiet conditions with continuous deposition of mud from suspension.
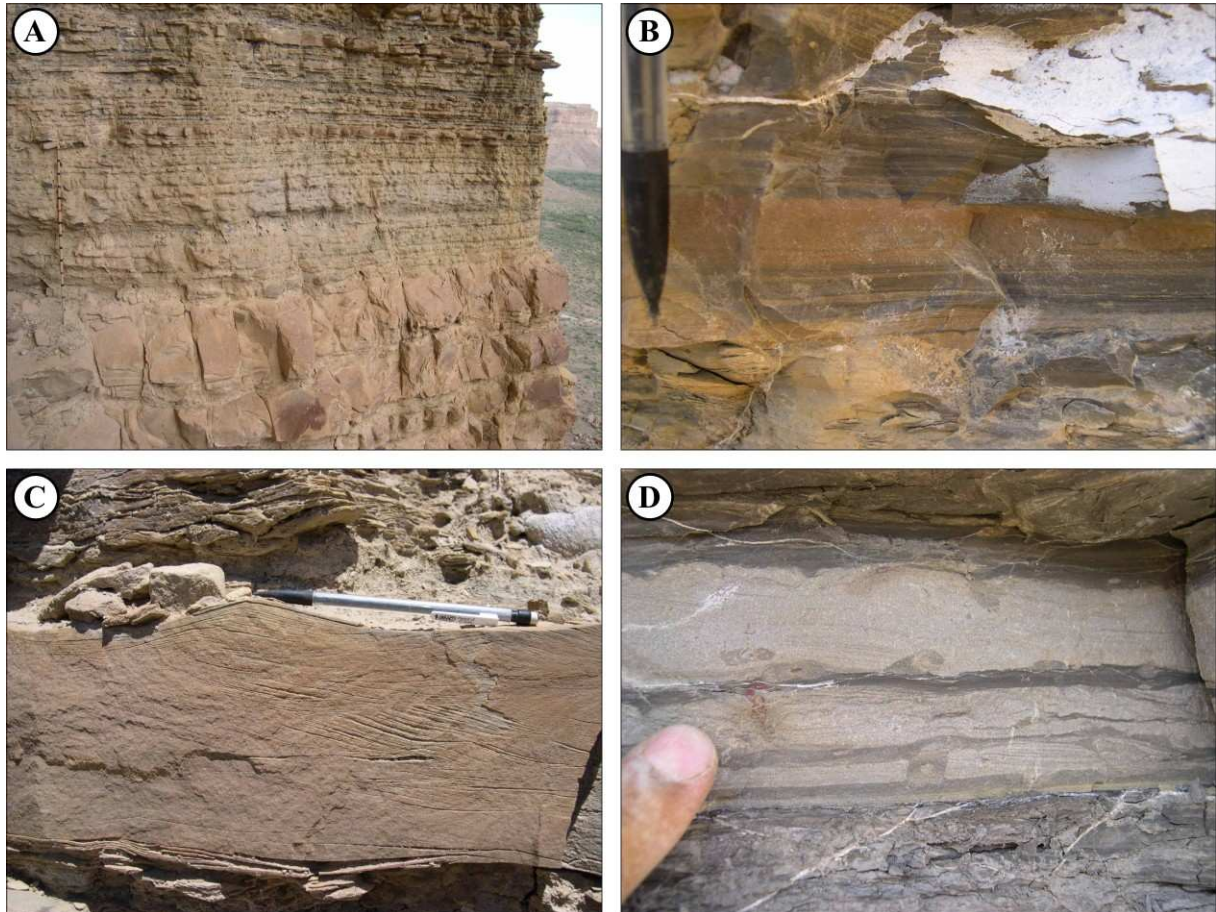
Figure 2.5. (A) Transition from FA3 and FA4 in the lower part into a compacted FA2 unit. Very fine laminated mudstone (B) is interbedded with many, closely spaced, very fine-grained sand- and silt beds with wave ripples and planar-lamination (C and D). Some of the sand- and mudbeds are mildly bioturbated. The symmetrical wave-ripples are oriented north-south. Staff is 1,5 m, pencil is 15 cm.

Periods of intense storm activity resulted in an abrupt increase in wave energy and the deposition of HCS, planar-laminated, and wave rippled sandbeds in an overall muddy environment. These event-beds represent less time than adjacent mudstone beds of similar thickness. As an effect of the relatively slow sedimentation rates, burrowing animals mixed the HCS sands with the hemipelagic muds, resulting in the diffuse boundaries between individual beds (Dott and Bourgeois, 1982; Taylor and Goldring, 1993). Differences in the

amounts of bioturbation and preserved sedimentary structures between sandstone beds may relate to the time and duration of event-bed deposition (Johnson and Baldwin, 1996; Taylor et al., 2003). Rapid deposition and high sediment inputs will result in better preservation of the primary sedimentary structures. The wave-rippled sandstones lacking prevalent HCS and bioturbation (Log 11 – Log 17 and Log 23- Log 25) have symmetrical crests reflecting oscillary waves as well as internal trough-cross-lamination, indicating unidirectional currents.

These sandbeds suggest primary deposition by currents during periods of high sediment input, followed by periods of more quiet conditions where the upper part of the sandbed became reworked by waves. This is characteristic for shallow-marine environments experiencing pulses of increased sediment input (Collinson and Thompson, 1989; Bhattacharya and Walker, 1992; Walker and Plint, 1992). A decrease in the amount of bioturbation and an increase in current induced sedimentary structures suggests more high-energy, hostile conditions for burrowing animals (Pemberton et al., 1992a; Taylor et al., 2003). Such changes indicate mixed wave and fluvial conditions in the offshore transitions zone, possibly related to increased proximity to a fluvial source. A north-south orientation of the wave ripples indicate wave action slightly oblique to the palaeoshoreline which is interpreted to be north-northeast (Balsely, 1980; Howell and Flint, 2003).

2.2.3 Facies association 3: Proximal offshore transition zone (pOTZ) deposits

Description: Like FA2, FA3 is also comprised of heterolithic and bioturbated sandstones and mudstones. The upward transition from FA2 to FA3 is gradual and arbitrarily picked at an increase in the proportion of sandstone beds to greater than 25%. The sandstone is very fine to fine-grained and contains HCS, wave-ripples, undulating and planar-lamination (Figure 2.6). The amount of bioturbation within the sandstone varies between moderate and intense, and includes *Ophiomorpha*r, *Thalassiniodes* and *Chondrites* of the Skolithos-Cruziana ichnofacies (Pemberton et al., 1992b). Many of the sandstone beds lack well defined boundaries (as in FA2) and are mixed with the surrounding, heterolithic sandy and silty mudstone. There is an upward increase in both sandstone thickness and in sandstone bed definition.

The facies association varies in thickness from 1 and 12 m, and it typically overlies FA2 and is overlain FA4 or FA2 deposits.
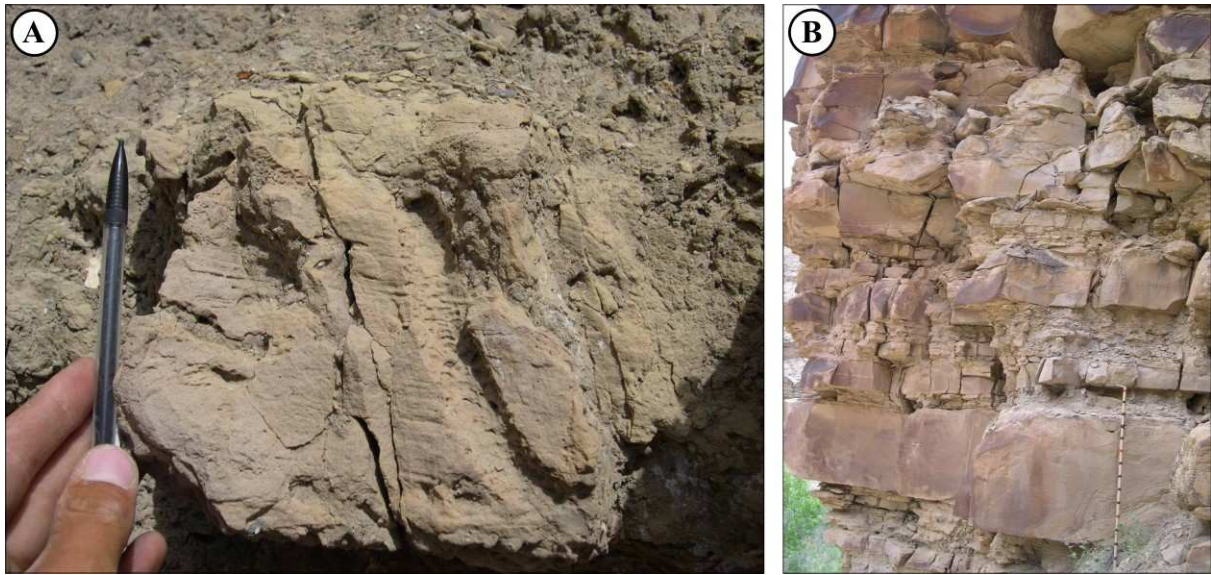
Figure 2.6. (A) HCS and *Ophiomorpha* burrow in fine-grained sandstone. (B) Well defined sandstone with relatively thin mudstone interbeds representing the upper part of FA3. The staff is 1.5 m.

Interpretation: FA3 was deposited between SWB and FWWB in the proximal part of the offshore transition zone (pOTZ). The depositional environment is related to the dOTZ and the transition between them is gradational. The depositional mechanisms are similar and the key difference is the higher proportion of sandstone, the greater sandstone bed thickness and the increased preservation of sedimentary structures, along with a decrease in bioturbation.

All of these observations indicate a transition into environments characterized by an increase in the effects of wave action which results in a lower preservation potential for mud deposited during fair-weather periods (e.g. Dott and Bourgeois, 1982; Walker and Plint, 1992; Howell and Flint, 2003). This increase in wave energy is attributed to a shallowing of the water depth.

2.2.4 Facies association 4: Lower shoreface (LSF) deposits

Description: FA4 consists of very fine- to fine-grained, 0,3 to 5 m thick, amalgamated HCS sandstone beds (Figure 2.7) with wave-ripples, planar-lamination and occasional undulating lamination (Figure 2.8). These relatively thick sandstone units are interbedded with relatively thin, fine laminated, very fine-grained sandstones, siltstones and mudstones that comprise less than 15% of the association. The laminated and low to moderately bioturbated, heterolithic

27

interbeds commonly pinch and swell, and are often laterally truncated by overlaying sandstone beds.

The heterolithic interbeds are burrowed with *Ophiomorpha, Chondrites* and *Thalassinoides* of the *Skolithos* ichnofacies (Pemberton et al., 1992b), in addition to unidentified burrows. The amalgamated sandstones are sparsely bioturbated with monotonous, sub-vertical *Ophiomorpha* burrows. Also *Teredolites* burrows and wood fragments/imprints were observed. The thick amalgamated sandstones beds are usually wave-rippled in the upper parts, but may also have zones of ripples and/or undulating lamination in the middle.
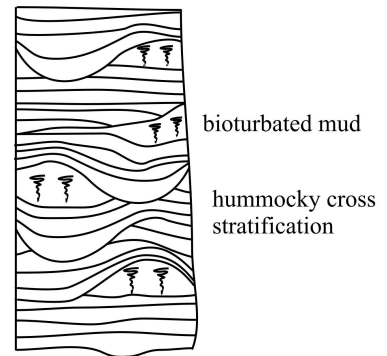
**Figure 2.7.** One common type of amalgamated HCS. Modified from Dott and Bourgeois (1982).

The extension of HCS varies between each sandstone bed. Some of the gently undulating laminas can be traced laterally several meters. Small scaled hummocks and swales less than 10 cm in length were also observed (Figure 2.4). Amalgamation surfaces were recognized where overlying beds erode and partially truncate the mud rich heterolithic unit. Such boundaries can also be recognized where opportunistic trace fossils are truncated by HCS beds. The transition from pOTZ to LSF is relatively sharp, going from overall muddy, heavily bioturbated, heterolithic sediments below, to more sandy, mildly bioturbated, and homogenous sediments above.
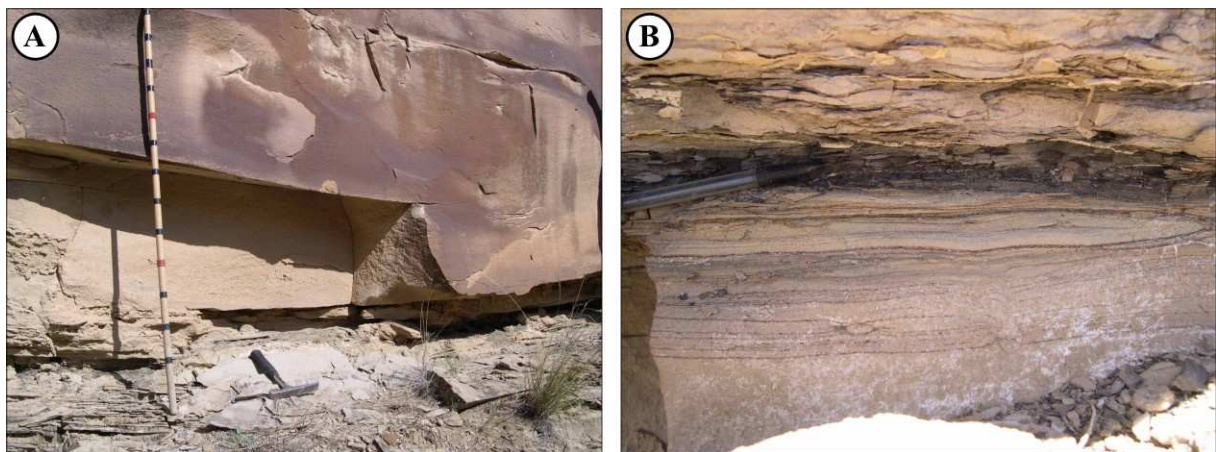
Figure 2.8. Amalgamated HCS sandstone (A) with laminated, mud- and sandstone interbeds (B). The heterolithic interbeds commonly pinch out laterally, suggesting varying degree of sandstone amalgamation. The staff is 1.5 m and the pencil is 15 cm.

The facies association commonly overlie pOTZ (FA3) and is overlain by middle or upper shoreface deposits of FA5 or FA6 (see description below). The units was traceable for several hundred meters in the proximal part of the study area (west), and pinch-out towards the east where they grade into deposits of the pOTZ.

Interpretation: The amalgamated HCS sandstones of FA4 were deposited above mean FWWB and represents deposition in the LSF which was frequently reworked by storm and fair-weather waves (e.g. Dott and Bourgeois, 1982; Walker and Plint, 1992; Howell et al., in review). Most of the fine-grained material deposited during quiet, fair-weather periods was eroded and reworked during storm periods and redeposited farther out in the basin (Niedoroda et al., 1984; Walker and Plint, 1992; Larson and Kraus, 1994; Reading and Collinson, 1996). This constant erosion and reworking resulted in amalgamation of well sorted HCS sandstone beds (Figure 2.7 and Figure 2.8). Heterolithic beds are the non-eroded fair-weather deposits. The low abundance of burrows indicates a higher energy environment than the underlying pOTZ (Pemberton et al., 1992b).

2.2.5 Facies association 5: Middle shoreface (MSF) deposits

Description: FA5 consists of lower fine-grained sandstone with vague planar-stratification and rare shell fragments (Figure 2.9). The unit is intensely to completely bioturbated, and only rare sedimentary structures and burrows are visible. The colour is more greenish grey than the overlying and underlying deposits. FA5 was only observed in Log 19 and Log 26 where it was

Figure 2.9. Intensely bioturbated, very fine-grained, green and grey sandstone of FA5. The staff is 1.5 m.

approximately 3 meters thick. In both localities the units overlie LSF amalgamated HCS sandstones and are overlain by FA6 deposits.

Interpretation: The stratigraphic occurrence of this facies between LSF, amalgamated HCS beds and upper shoreface trough cross-stratified sandstone (see below) indicates a

middle shoreface setting. The prevalent bioturbation and the lack of primary depositional structures indicates a locally sheltered setting, potentially in the lee side of large, low relief bar forms (Pemberton et al., 1992a; Howell and Flint, 2003)

2.2.6 Facies association 6: Upper shoreface (USF) deposits

Description: FA5 consists of fine to medium-grained, well sorted, trough- and tabular stratified sandstone, rare shell fragments and sparse to absent bioturbation (Figure 2.10). In the outcrops these units are often recognized by the distinctive light grey to white colour, but they may also be light brown. These deposits are only present in the proximal (west) part of the study area in the upper-

Figure 2.10. Trough, tabular- and planar-stratified sandstone of FA5. The exposed unit is approximately 5 m thick.

rmost parts of the measured succession where they have been traced for several hundred meters laterally.

Interpretation: Trough and tabular cross-stratification represent migration of dunes and bars along the shoreline due to littoral currents (rip currents, longshore currents etc.) in the upper shoreface (USF) (e.g. Clifton et al., 1971; Reineck and Singh, 1980; Collinson and Thompson, 1989; Howell et al., in review). The medium-grained sandstones along with the lack of bioturbation also suggest deposition within a high-energy environment (Pemberton et al., 1992a). The light grey and white color reflects bleaching of the sandstone by organic acids which originated from plant material once growing on top the beach (Collinson, 1996; Howell et al., in review).

2.3 Depositional environments within the mixed tidal and wave-dominated estuary

Facies association 7 to 11 (Table 2.1) are generally more heterolithic with a more complicated and more laterally restricted distribution than the shoreface deposits described above. Incised

valley strata are recognized in the proximal part of the study are in Woodside Canyon where the succession is up to 28 m thick (Howell and Flint, 2003). The unit then becomes thinner towards the east and disappears between Log 12 and Log 13.

2.3.1 Facies association 7: Partially reworked fluvial deposits

Description: FA7 is comprised of fine- to medium-grained, moderately to poorly sorted sandstone. The sandbed thickness varies between 30 and 300 cm. Examples commonly consist of several stacked sets of tabular and trough cross-stratified (Figure 2.11, B) sandstone with abundant bone fragments, wood fragments, clay and organic rip-up clasts. Clasts are especially concentrated in the lowermost part of the beds which also have erosive bases (Figure 2.11, A). Rarely, the lower beds also contain extra-basinal pebbles (up to 2 cm in diameter). The facies association is only present in the lowermost part of the incised valley, and in the most proximal part of the study area where it is underlain by the SB and overlain by FA8.
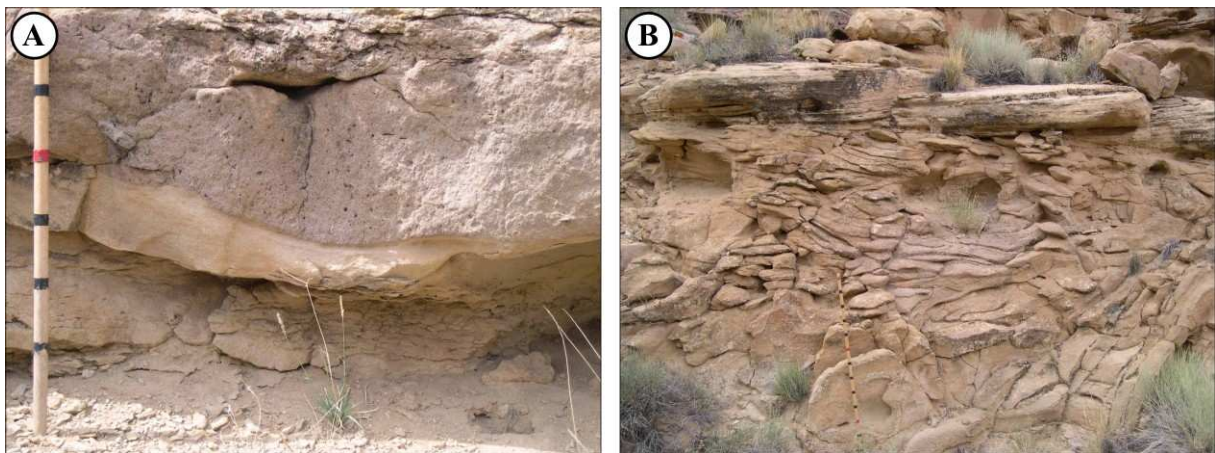
Figure 2.11. (A) Poorly sorted, medium- and coarse-grained sandstone with abundant rip-up clasts of FA7 erodes into well sorted, fine-grained planar and HCS sandstone of FA1 and 2. (B) Medium-grained, trough cross-bedded sandstone of FA7 overlain by IHS of FA8. The boundary between the two has been interpreted as a transgressive surface (see section 4.3). The staff is 1.5 m long.

Interpretation: The presence of trough cross-stratified and abundant rip-up clasts and rare pebbles suggests a fluvial origin (Figure 2.12) (Miall, 1992; Zaitlin et al., 1994; Collinson, 1996; Howell et al., in review). This is supported further by the palaeocurrent directions which indicate flow perpendicular or slightly oblique to the ancient shoreline (north-south), along with the position of the unit above the SB and below the overlying IHS

(FA8), representing an abrupt basinward shift of facies relative to the underlying shallow-marine deposits (Zaitlin et al., 1994). No distinct channel geometries were observed and some of the cross-bedded units are interpreted as minor bar forms positioned within a relatively wide channel system. However, double mud-drapes and shell fragments suggest that the deposits are not totally fluvial and that some of the sediments have been reworked by tidal currents (Thomas et al., 1987; Nio and Yang, 1991; Dalrymple, 1992), although the amount of reworking is hard to estimate.

Some of these tidally reworked fluvial deposits may also represent bars or dunes within the channel thalweg of a tidal influenced meandering river system (Thomas et al., 1987), and would then be associated with FA8. Tidal influences in channel-floor cross-bedding would be represented by shell fragments and double mud-drapes as describes above (Thomas et al., 1987). These deposits are discussed further in FA8.
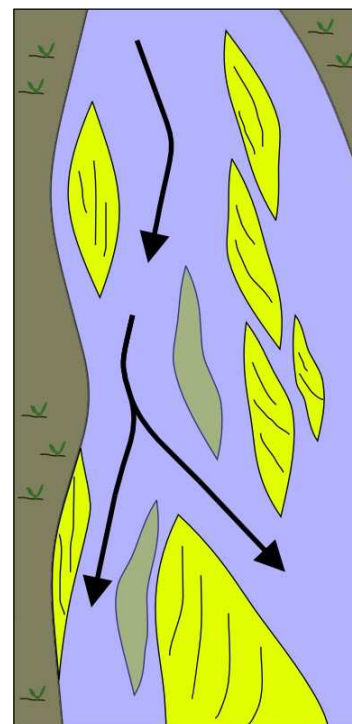
Figure 2.12. Braided river channels are characterized by numerous bars and islands reflecting high sediment transport, variable discharge and a generally high gradient (Miall, 1992).

2.3.2 Facies association 8: Tidal influenced meandering channel deposits (IHS)

Description: FA8 comprise inclined heterolithic strata which consist of lower very fine- to lower medium-grained sandstone and grey mudstone (Figure 2.13). The sandstone beds are generally between 5 and 100 cm thick and are inclined relative to the palaeo-horizontal. Some of the sandstone beds, generally the thickest ones, have a constant thickness and can be traced a few hundred meters laterally within the incised valley. The inclined sandstone beds are commonly truncated in the upper part by the flooding surface and downlap onto the sequence boundary in the lower part of the succession (Figure 2.13). The thin sandbeds are more discontinuous and have varying thickness laterally. They often pinch out or become truncated, both in an upward and downward direction.

There is a general fining upward trend within the IHS units, where the sandbeds become both thinner and more fine-grained upward. However, there are exceptions where the
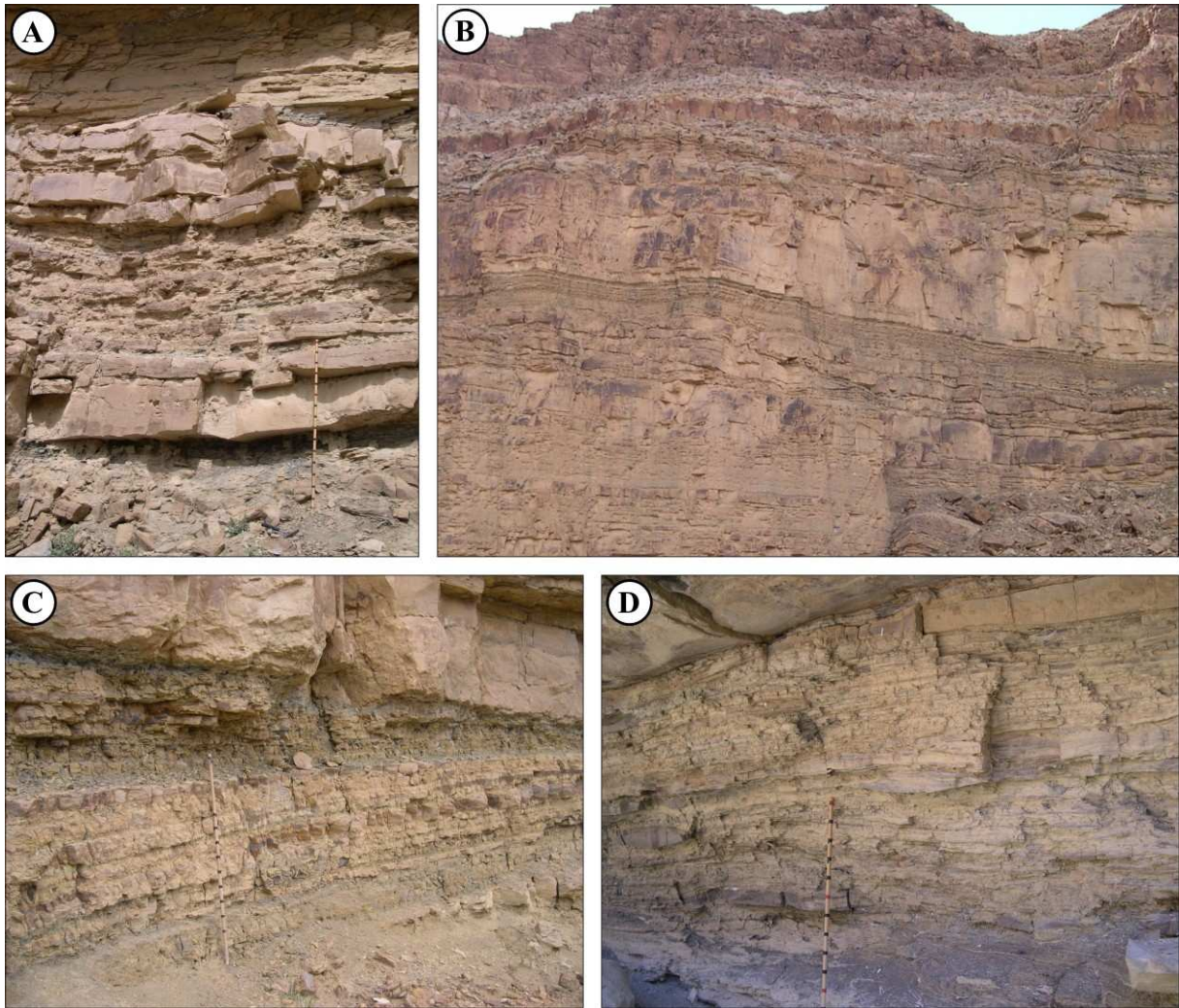
Figure 2.13. Different expressions of the IHS facies (FA8). (A) Interbedded mudbeds and sandbeds of various thickness. (B) Large, sandy inclined beds (middle of picture) underlain by S3 and overlain by mud of FA10 and G1. The inclined beds dip towards the right. IHS unit is approximately 8 m thick. (C) Muddy IHS truncated by G1b. The sandstone overlying the sub-horizontal flooding surface is the lowermost part of Grassy parasequence 1. (D) Discontinuous, interbedded sandstone and mudstone of varying thickness. The staff is 1.5 m long.

thickest and coarsest beds occur in the middle of the sets. Within individual sandstone beds there are generally no internal grading within each sandbed, although some beds demonstrate an upward decrease in grain-size (usually in the base of a sandstone unit), and others represents an upward coarsening. Sandstones are generally well sorted although some beds are poorly sorted and contains organic and clay rip-up clasts and shell fragments.

Sedimentary structures within the sandstone beds include trough cross-stratification (occasional bidirectional), wave ripple cross-stratification, planar-stratification, soft sediment deformation and water escape structures. Wave ripple orientation indicate wave approach from the northeast, whereas troughs suggest palaeocurrent mainly towards the north and the northeast, and bidirectional troughs indicates current towards north and south. Bioturbation is
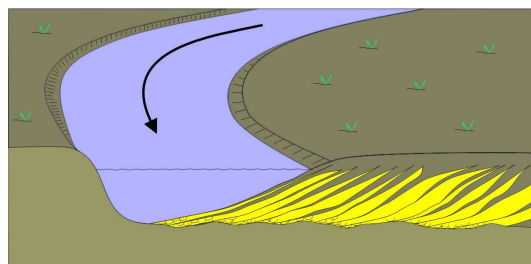
low to absent, but *Ophiomorpha* and *Teredolites* have been identified along with possible *Arenicolites*. Shell fragments have been observed in Log 4, 8, 11, 12, 19 and 26.

Dip-angle and progradation direction of the IHS varies between the localities. Dip generally increase with decreasing sandbed thickness and is commonly between 2 and 12°. Bar form migration direction of the inclined beds also varies greatly, especially in the proximal (western) part of the study area, where the direction shifts from northeast to southwest and back to northeast within a few kilometres. Farther basinwards, the main migration direction is toward the southeast and northeast.

Interbedded mudstone constitutes distinct beds of varying color and texture. Where the interbedded sandstones are thin and discontinuous, chaotic and unstratified mudstone fills the space around the sandstone lenses (Figure 2.13, D). These beds are commonly grey and brown and are either fine laminated or structureless. Locally, several meters in the upper part of an IHS unit are comprised entirely of inclined mud with thin sandy interbeds, thus resembling FA11 (Figure 2.13, C).

Interpretation: Inclined heterolithic strata is recognized in a variety of depositional environments, but the most common is as lateral accreted point-bars deposits of freshwater meandering rivers and intertidal meandering cannels (Figure 2.14) (Thomas et al., 1987). The main criteria used to differentiate tidal channels from freshwater ones is the presence of reversed flow (bidirectional current ripples, herring bone cross-stratification, reactivation surfaces), trace fossils, and rhythmic variations in thickness and the frequency of sand and mudbeds (Thomas et al., 1987).

Several of these criteria have been recognized in the IHS strata observed within the incised valley. Both *Ophiomorpha* and *Arenicolites* are associated with the Skolithos ichnofacies and are common in tidal and brackish environments (Pemberton et al., 1992b). In addition, *Teredolites* burrows indicate at least partially marine intrusion (Reineck and Singh, 1980; Bromley et al., 1984; Howell and Flint, 2003). This is further

Figure 2.14. Idealized tidal influenced meandering river. Migration of the point bar results in an overall fining upward unit, composed of trough cross-stratified sandstone in the base, overlain by IHS and mudstone. Increased rhythmic appearance suggest increased tidal influence. Modified from Thomas et al. (1987).

supported by the presence of shell fragments. Bidirectional ripples indicate reversed flow in at least some parts of the system.

Trough cross-stratification in the lowermost part of the facies association may represent minor bars or dunes migrating in the tidal influenced river channel (Miall, 1992). Where they are overlain by bidirectional cross-bedding and interbedded mudstones and sandstones further up, the succession is interpreted to represent a typical upward fining, tidal influenced meandering channel unit (Log 19 and Log 26,) (Thomas et al., 1987). The tidal range has been interpreted to be approximately 2 m, which is lower meso-tidal (Howell et al., in review).

Upward fining trends or proximal-distal fining trends within point bars are expected in a fluvial or tidal influenced meandering channel (Thomas et al., 1987). Such trends are evident in Log 19 and Log 26 where fine and medium-grained, trough cross-stratified sandstone fine upwards into fine-grained bidirectional cross-stratified sandstone, and further up into laminated siltstone and mudstone with sandstone interbeds. Upward fining successions are interpreted to reflect lateral point bar migration (Figure 2.15), bounded on top by coastal plain mud (Thomas et al., 1987; Dalrymple, 1992). The units may also represent lateral migration and abandonment of the active channel and its subsequent filling with mud and silt. Following abandonment, sand with shell fragments and rip-up clasts was washed in during major storms and flood events and became interbedded with the background mud and still what was otherwise deposited.

Trends related to the thickness and dip-angle of the inclined beds suggests that the thickest sandbeds have the lowest dip-angle and thus can be traced over longer distances than thinner, more mud-rich beds. These differences may be related to the original width and depth of the meandering channel, where the main channel(s) are expected to be sandier and have a lower dip-angle than muddy, more steeply inclined distributary channels. Variations in the dip of the inclined heteroliths may also relate to differences in the cohesive forces of sand and mud, allowing more steeply dipping mudbeds.
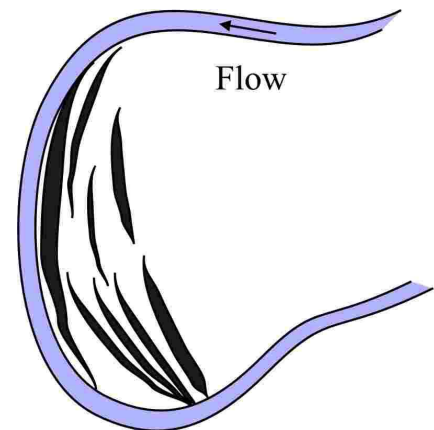
Figure 2.15. Various expressions of IHS along-strike. The dip-orientation of IHS indicates direction of point bar migration. Modified from Thomas et al. (1987).

2.3.3 Facies association 9: Tidal bars

Description: FA9 is comprised of lower fine to lower medium-grained, light brown to grey and white, planar and trough cross-stratified (sometimes bidirectional) sandstone (Figure 2.16). The sorting varies from poor to very good and generally improve upward within the succession. Individual sandstone bed thicknesses vary from a few tens of centimetres and up to several meters. The thick beds are commonly amalgamated and are comprised of several sets and cosets of trough and tabular cross-stratified sandstone, each set up to one meter in thickness. Some troughs have organic draped foresets (Figure 2.16, E).

Sedimentary structures include rare wave ripple cross-stratification and undulating lamination. Sets of trough cross-bedded sandstone are interbedded with discontinuous beds of grey mudstone and sandstone with mm thick organic lamination and mud-drapes, which are sometimes double. Orientation of trough cross-bedding indicates palaeocurrent in several directions; the most dominant is towards the west, southwest and northeast, although almost every direction is represented. The mudstone beds are generally structureless but some have minor lenses or laminas of fine-grained sandstone. Claystone rip-up clasts (up to 8 cm long), organic fragments and log imprints are also common.

In the area close to Log 5 and Log 6, the amalgamated, trough cross-stratified units are capped with a ca 50 cm thick unit of planar-stratified, bleached, well sorted sandstone with abundant root structures (Figure 2.16, B). In one locality, this grey and white sand unit is overlain by 30 cm of silty coal. Bioturbation is sparse to absent, and *Ophiomorpha* and *Teredolites* burrows have been observed.

In Log 6 (Figure 2.16, A and C), the lowermost 2 m is comprised of very poorly sorted and chaotic, coarse and fine to medium-grained, trough and planar cross-stratified sandstone. Coal fragments, clay rip-up clasts, pebbles, wood imprints, shell fragments, teeth and *Teredolites* burrows are abundant in the lower 30-50 cm, whereas rare clay rip-up clasts, organic fragments and organic drapes are observed in the upper, cross-stratified part. Troughs indicate palaeocurrent towards the northwest and southeast.

Interpretation: Large scale trough cross-bedding (up to one meter thick) containing evidence of intertidal and subtidal influence, suggests deposited as (sub)tidal bars and/or dunes (Figure 2.16 and Figure 2.17)(Reineck and Singh, 1980; Thomas et al., 1987; Nio and Yang, 1991; Dalrymple, 1992). *Teredolites* burrows also indicates that the depositional environment was at least periodically brackish (Bromley et al., 1984), and the presence of

coal and roots suggests that some of the units even were subaerially exposed for prolonged periods.
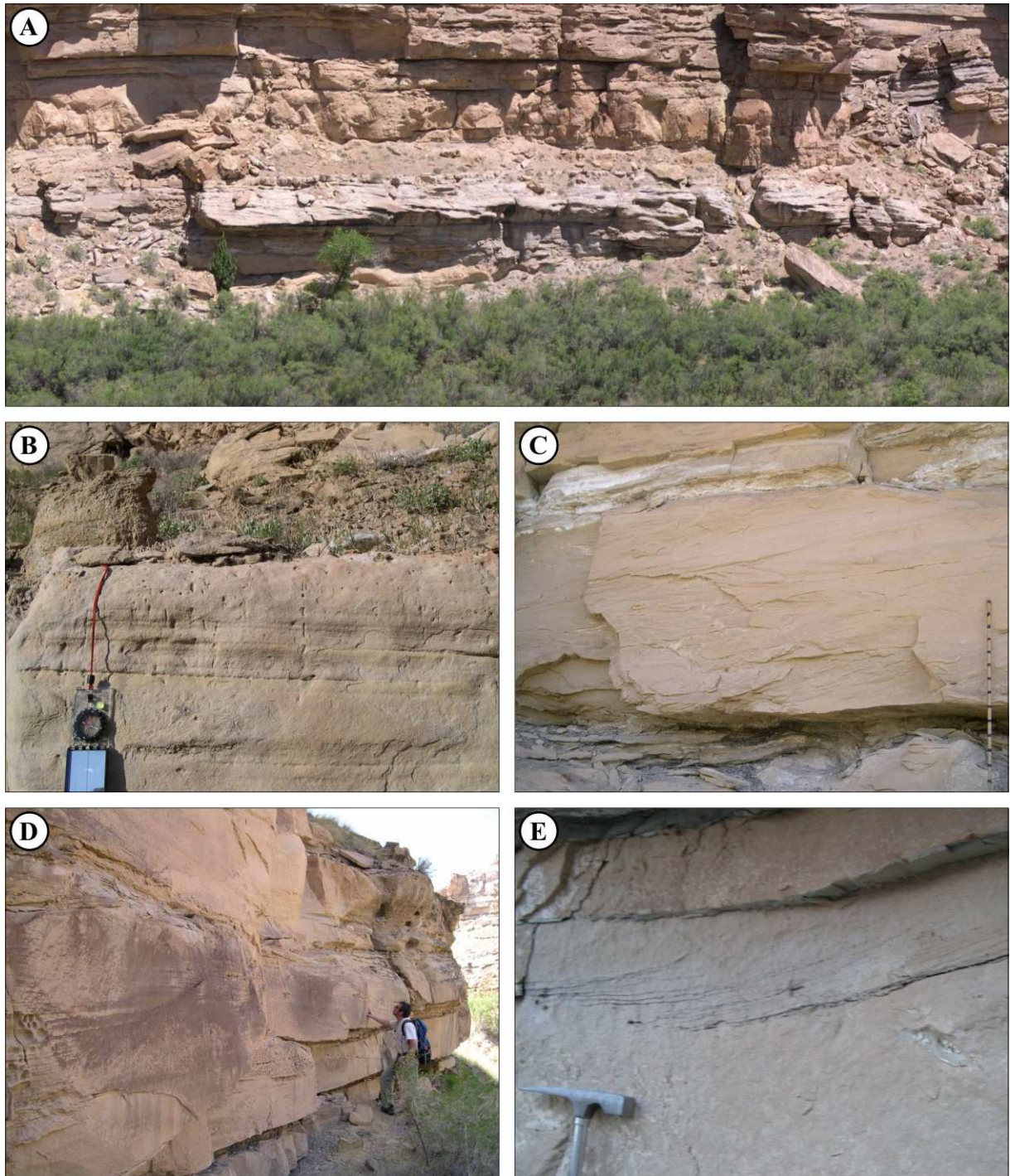
Figure 2.16. Different expressions of FA9. (A) Bleached, large scale, trough cross-bedded sandstone (white unit in the middle of the picture). Troughs indicate paleoflow towards the right. Unit is approximately 9 m thick. (B) Planar stratification and root structures in the upper part of the cross-beds in (A). (C and D) Large scale, commonly bidirectional cross-bedding with wood imprints, (E) rip-clasts and mud drapes.
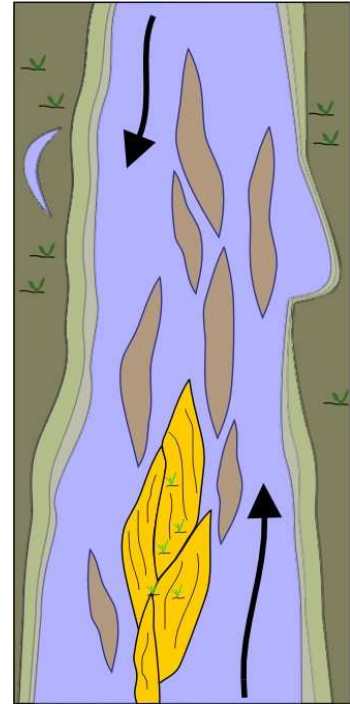
Large scale cross-bedding indicating palaeocurrent towards the west (Log 9 and Log 18) is interpreted to be of floodtidal origin (Figure 2.16, D and E), as they predict flow in a

palaeolandward direction. Abundant mud-drapes (including some doubles) indicate that at least some of these units were deposited in a subtidal environment (Thomas et al., 1987; Nio and Yang, 1991). The chaotic and coarse-grained unit in base of Log 6 (Figure 2.16, C) is interpreted to be the base of a tidal channel, as it demonstrates extensive erosional truncation of the underlying IHS deposits. The unit also contains very poorly sorted sandstone in the base overlain by bidirectional cross-stratification, indication deposition within a high-energy environment.

The area close to Log 5 and Log 6 (Figure 2.16, A) is more sandstone dominated than elsewhere in the incised valley complex, and it is interpreted to represents a very sandy part of the system, possible close to the main or to one of the main channels. The amalgamated trough cross-stratified sandbeds represent sandbars stacked into a sandwave within the tidal channel, indicating migration towards the northeast and southwest. Planar-stratified sandstone on top of the unit along with root structures and a poorly developed coal, indicate that the top set beds of the sandwave which became subaerially exposed for some time, allowing colonisation and vegetation. The facies observed in Log 5 and Log 6 may also represent a barrier complex, as the trough and planar-stratified white sand resembles a foreshore as seen elsewhere in the study area. However, such a feature should be regional extensive, and recognized in log sections and outcrops along-strike (Boyd et al., 1992; Reading and Collinson, 1996). Also a transgressive barrier island would separate marine deposits on the seaward side

Figure 2.17. Inter and subtidal bars and tidal flats. Tidal channels reflect varying depositional energy and are sourced from both the landward and basinward side. Mud is deposited in sheltered areas such as bays and abandoned channels.

from non-marine deposits in the landward side; immediately basinward of the unit is IHS, lagoonal and tidal flat deposits. Consequently as the unit is confined to the area surrounding Log 5 and Log 6 it is interpreted as an emergent bar in the middle of the tidal channel complex, rather than a continuous beach parallel to the palaeoshoreline.

2.3.4 Facies association 10: Restricted bay/lagoon and tidal flat deposits

Description: Facies association 10 consists of mixed parallel and planar-laminated, undulating and wavy-laminated, light and dark grey, brown, red, green and black mudstone with fine to medium-grained sandstone interbeds (Figure 2.18). The unit may appear very heterolithic or relatively homogenous depending upon the proportion of sandy interbeds. Internally, the mudstone is laminated, vaguely wave rippled, lenticular bedded or structureless. Bioturbation is absent. The sandstone beds display vague cross-stratification and contain abundant rip-up clasts, organic fragments, shell fragments and coal fragments. Some of these chaotic sandbeds can be traced laterally whereas others become truncated and eroded within few meters laterally. In Log 9, the interbedded sand is well sorted and thickens laterally into a meter thick unit of trough cross-stratified sandstone with rip-up clasts and organic drapes. The thickness of these mudstone units varies from two to eight meters and they are over and underlain by IHS and tidal bars of FA8 and FA9.
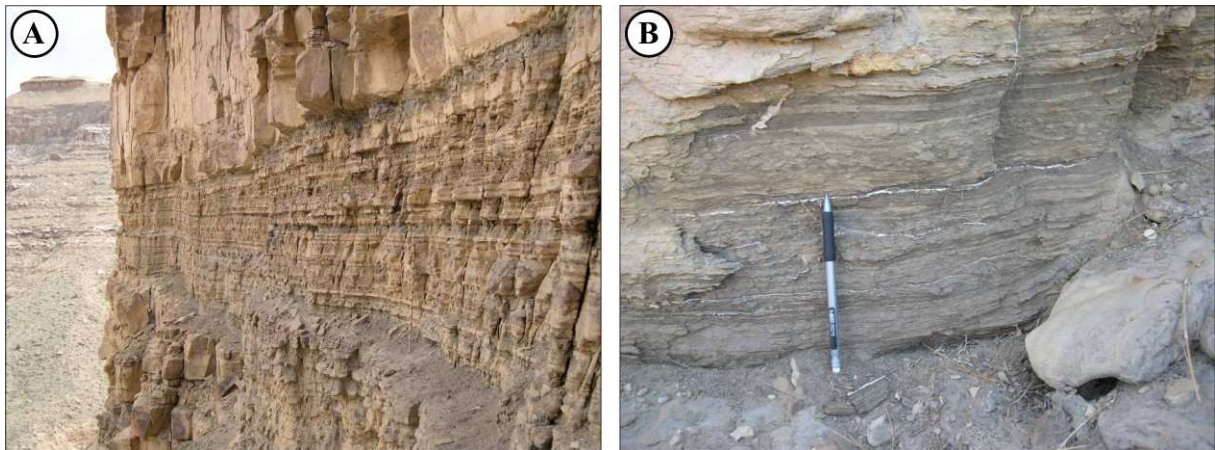

Figure 2.18. (A) Fine planar-laminated mudstone of FA10 onlapping IHS. Coarse-grained, chaotic sandstone bed in the middle. (B) Wavy and undulating lamination in mudstone and very fine-grained sandstone of FA10. The staff is 1.5 m and the pencil is 15 cm long.

Interpretation: Millimetre laminated, dark grey, brown and red muddy deposits indicate deposition within a quiet, low energy environment (Reineck and Singh, 1980; Nio and Yang, 1991; Dalrymple, 1992). The color, lack of rooting and bioturbation suggest that the conditions were anoxic or at least relatively inhospitable to burrowing animals and plants (Pemberton et al., 1992a). Undulating and vague wavy lamination and rare lenticular bedding indicates that the units have been deposited in a confined body of water, or somewhere away from high-energetic currents or waves; such as a inter estuarine lagoon or bay, or within the

intertidal zone where alternating mud and silty sand is deposited by everyday flood and ebb currents (Reineck and Singh, 1980; Collinson and Thompson, 1989; Dalrymple, 1992). This low-energy estuarine environment was disturbed by major flood or storm events, which deposited sandbeds throughout the area, and minor channels and creeks which deposited thin sandsheets in the intertidal ponds or lagoons.

2.3.5 Facies association 11: Transgressive lag deposits

Description: This facies association is between 10 and 50 cm thick and is composed of very poorly sorted, medium to coarse-grained sandstone with abundant shell fragments and sharks teeth (Figure 2.19). The unit is homogenous in the lower part, and sharply overlies sediments of FA8, FA9 or FA10 within the incised valley. The boundary is commonly associated with an abrupt increase in biogenic activity, demonstrating high to intense bioturbation. In the unit below, the presence of large, vertical and sub-vertical, unlined burrows filled with coarse sand from the unit above. *Arenicolites* and *Thalassinoides* burrows of the *Glossifungites* ichnofacies are abundant (Pemberton et al., 1992b; Pemberton, 1998). The sediments generally demonstrate increased sorting and fining upward into HCS, very fine and fine-grained sand or interbedded, bioturbated mud of FA3 and FA4. One succession also contain tabular cross-bedding in the lower part followed by a gradual transition into HCS further up. The facies association is only located in the upper part of S3, above the incised valley.
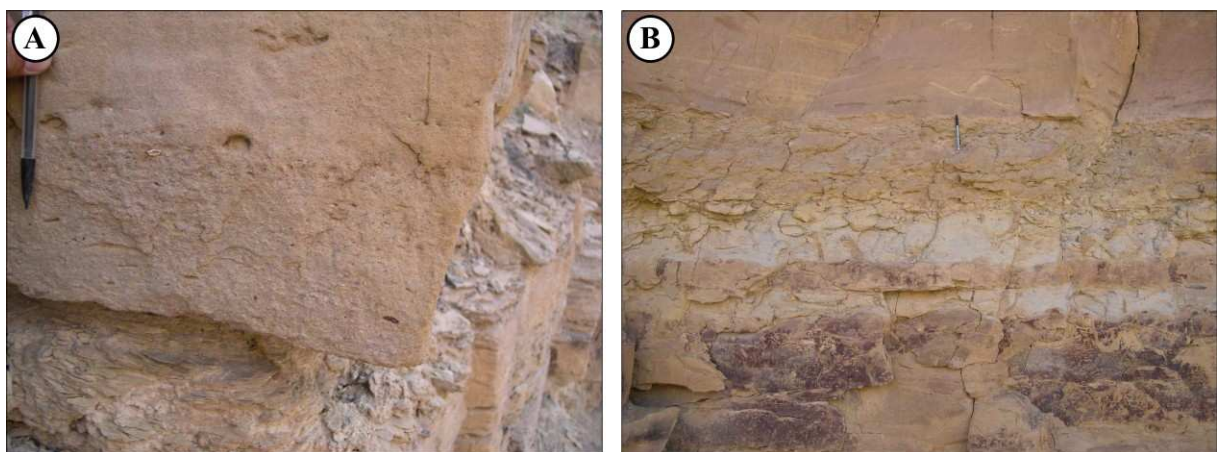
Figure 2.19. (A) Intensely bioturbated, medium-grained, poorly sorted sandstone of FA11 sharply overlying estuarine sand and mud of FA10. U-shaped burrows penetrate down into the muddy substrate and are filled with medium-grained sand from the overlying unit. Bioturbation decrease upward as sorting increase, and the unit gradually turns into HCS sand. (B) Sharp based, poorly sorted sandstone with abundant shell fragments and sharks teeth overlies FA8. The unit becomes better sorted upward and turns into HCS sand of FA3 within the Grassy Member. The pencil is 15 cm long.

Interpretation: Poorly sorted, medium- and coarse-grained sand with teeth and shell fragments suggests reworking within a high-energy environment (Van Wagoner et al., 1990). The *Glossifungites* ichnofacies is associated with firm-grounds and reflects erosion and exhumation of older, compacted and partially consolidated sediments (Pemberton et al., 1992b; Pemberton, 1998). The unit is interpreted as an erosional transgressive lag, deposited at the base of a high-energy upper shoreface (Van Wagoner et al., 1990). During the lowstand and early part of the transgressive systems tract, the old shoreface-shelf was subaerially exposed and the shoreline was located seaward of the study area (see section 3.7). As the shoreface migrated landwards during continuous sea level rise, the high-energy shoreface reworked some of the coarse-grained, estuarine sediments into a chaotic, discontinuous lag. The lag became gradually amalgamated with the overlying HCS sandstone as the sea level rose, and the specific area was positioned farther distally on the shoreface.

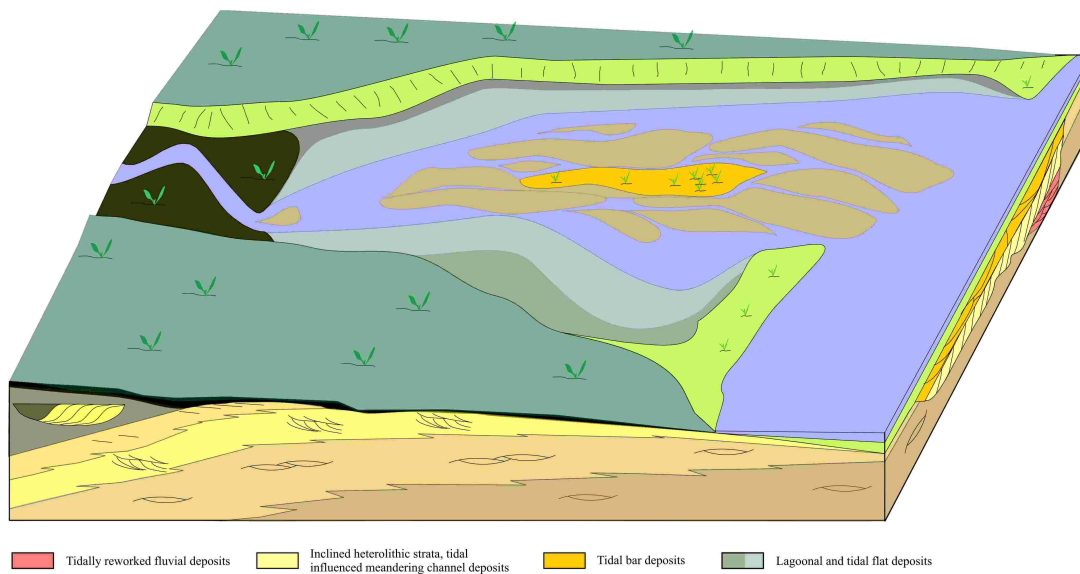## 2.4 Summary of depositional environments

Based on the interpretations of FA1-FA6, these stacked units represent successions of wave-dominated, shallow-marine sandstones and mudstones (Figure 2.20); deposited on a gently dipping shoreface-shelf (e.g. Bhattacharya and Giosan, 2003; Howell and Flint, 2003; Howell et al., in review). Combined wave and current induced sedimentary structures and an abrupt decrease in bioturbation is interpreted to reflect increased proximity to a fluvial source and a more stressed environment (e.g. Bhattacharya and Walker, 1992; Taylor et al., 2003). A detailed interpretation of these stratigraphical units will be given in Chapter Three.

Foreshore	Middle shoreface	proximal offshore transition zone	Offshore
Upper shoreface	Lower shoreface	distal offshore transition zone	
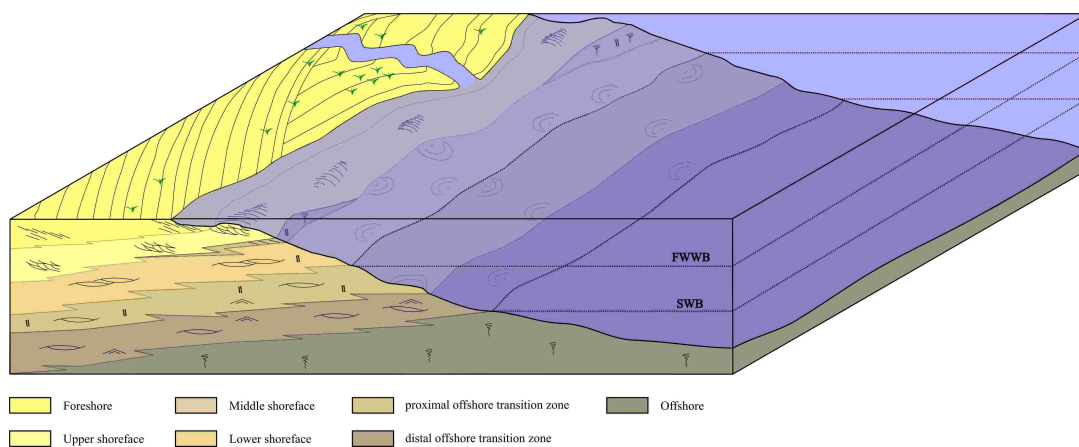
Figure 2.20. Shoreface-shelf depositional environment for facies association 1-6. See appendix for key. Modified from Howell and Flint (2003).

FA7-FA10 are interpreted to represent the filling of an incised valley by estuarine deposits (Figure 2.21)(Howell and Flint, 2003; Howell et al., in review). Tidal influenced fluvial deposits, IHS, tidal bars, lagoons and tidal flat deposits represent an abrupt basinward shift of facies unconformably overlying the shallow-marine sandstones and mudstones. This is followed by a gradual landward shift of estuarine deposits in response to the gradual filling and the landward dislocation of the shoreline (Dalrymple et al., 1992; Zaitlin et al., 1994). The depositional history of the incised valley will be discussed in Chapter Four.

| | Tidally reworked fluvial deposits | | Inclined heterolithic strata, tidal influenced meandering channel deposits | | Tidal bar deposits | | Lagoonal and tidal flat deposits |

Figure 2.21 Estuarine depositional environment for facies association 7-10. See appendix for key. Modified from Howell and Flint (2003).

Chapter Three – Internal Architecture and Palaeogeography of the Wave-dominated Sunnyside Shorelines

3.1 Introduction

A delta is defined as "a discrete shoreline protuberance formed at a point where a river enters an ocean or other large body of water" (Bhattacharya and Walker, 1992). A ternary diagram (Figure 3.1) is often used to classify such deltas, emphasizing the role off different depositional processes being diagnostic for each type (Boyd et al., 1992; Bhattacharya and Giosan, 2003). These three end members of these ternary systems are fluvial-dominated, tidal dominated and wave-dominated deltas. However, most deltas systems are influenced by a combination of these and both recent and ancient deltaic deposits contain evidence for a variety of depositional processes (Bhattacharya and Walker, 1992; Reading and Collinson, 1996).

Wave-dominated deltas, such as the Blackhawk Formation shorelines in the Book Cliffs are usually made up of several prograding beach ridge complexes which are nourished by littoral and fluvial sediments (Bhattacharya and Giosan, 2003).
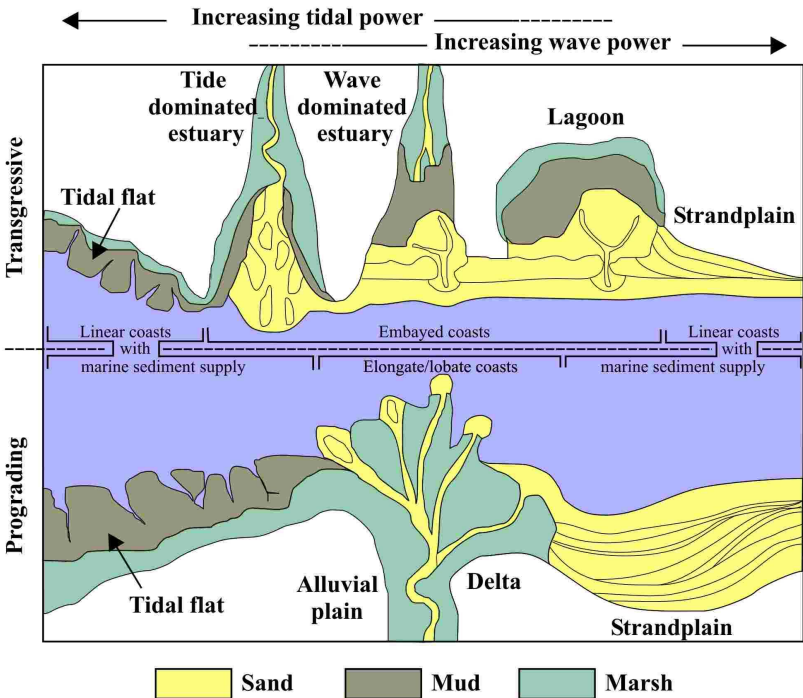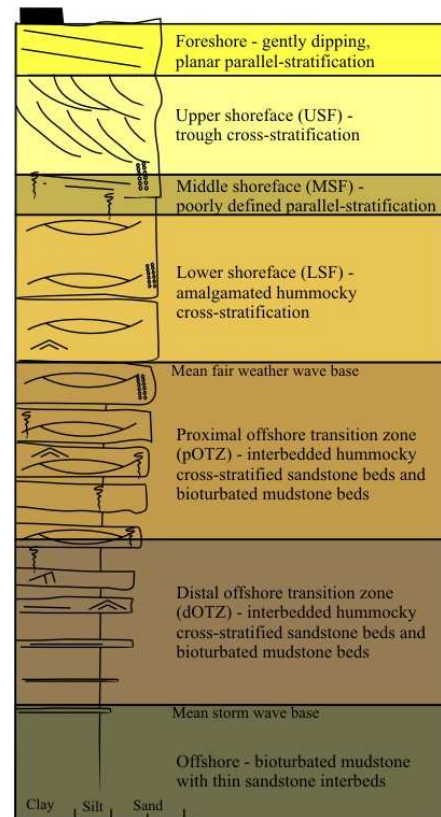

Figure 3.1

Classification of clastic coastal depositional systems, after Boyd (1992). Both transgressive and regressive systems are shown. Amount of tidal power increase towards the left and wave power increase towards the right. The regressive Sunnyside coastline is represented by the lower right part of the figure, whereas the transgressive estuary (Chapter Four) is represented by the central and upper part.

The degree of symmetry depends on the angle, strength and direction of incoming waves and the induced longshore current (Dominguez et al., 1987; Bhattacharya and Giosan, 2003). Processes and development of wave-dominated shorelines and deltas will be discussed further in Chapter Six.

In a vertical section, wave-dominated deltas are characterized by a relative continuous coarsening upward succession (Figure 3.2) recording the influence of wave and storm processes (e.g. Bhattacharya and Walker, 1992; Bhattacharya and Giosan, 2003). Mixed fluvial- and wave-dominated deltaic successions may in addition contain current ripples, soft sediment deformation and brackish water fauna close to the river outlet (Bhattacharya and Walker, 1992; Reading and Collinson, 1996). The amount of fluvial dominance will decrease up and down strike of the river mouth, indicating a transition from an environment characterized by varying and rapid deposition, to an environment dominated by storm reworking and more continuous deposition. Examples of modern wave-dominated deltas displaying various degrees of wave influence and symmetry, include the São Francisco, Rhone, Danube, Senegal and Paraíba do Sul deltas (Dominguez (Dominguez et al., 1987; Bhattacharya and Giosan, 2003).

Figure 3.2. Idealized log section through a wave-dominated deltaic shoreline See appendix for key. Modified from Howell and Flint (2003).

Strandplains are similar in geometry and internal structure to wave-dominated deltas and are commonly comprised of prograding beach-ridge sets. However, strandplains receive their sediments from marine sources whereas wave-dominated deltas are mainly fed by fluvial a source (Reading and Collinson, 1996). Strandplains (Figure 3.1) are characterised by wave and storm dominance, and a progradational unit typically consists of a continuous coarsening upward succession, similar to the ones of wave-dominated deltas. It may therefore very difficult in the rock record to differentiate between wave-dominated deltas and strandplains, particularly because the transition between the two may be gradual and the marine source of sediment to a strandplain may be longshore drift from a wave-dominated delta on the same

shoreline. This is occurring today in the modern Caravelas and the Nayarit strandplains (Curray et al., 1969; Dominguez et al., 1987). The wave-dominated, coarsening upward units studied in the Sunnyside Member are referred to as wave-dominated shorelines, as they feature evidence of both environments.

3.2 Internal geometry of Sunnyside Parasequence 2

Sunnyside Parasequence 1 (S1) pinches out approximately 60 km northwest of Woodside Canyon (Figure 3.3) (Hampson and Howell, 2005) and there is no trace of this unit in the study area. In the western and proximal part of Woodside Canyon, the lowermost part of the studied section is comprised of four coarsening upward units. These are 3,5 to 25 m thick and belong to Sunnyside Parasequence 2 (S2) (Figure 1.7) (Howell et al., in review). These units form "a relatively conformable succession of genetically related beds bounded by surfaces (called bedset surfaces) of erosion, non-deposition, or their correlative conformities", and are interpreted as bedsets (Van Wagoner et al., 1990; Howell et al., in review). These stacked bedsets also demonstrate an overall coarsening upward trend, where each bedset has a more basinward extension than the one below (Figure 3.4 and Figure 3.5). The identification of these upward shoaling units as bedset, rather than parasequences is important and will be discussed in detail later in this section.
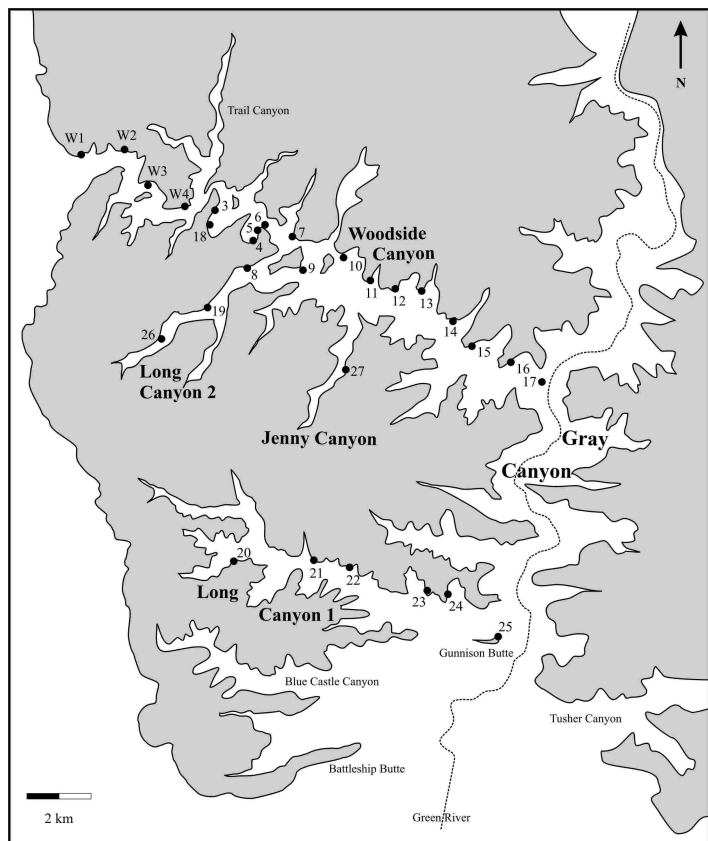

Figure 3.3. Map of the study area in the Beckwith Plateau, north of the town of Green River. Log sections are represented as black dots.

3.2.1 Sunnyside Bedset 2.4 (S2.4)

The lowermost bedset, S2.4, is up to 25 m thick and represents a transition from LSF deposits in the proximal part (Log W1, Figure 3.3)to dOTZ deposits in the eastern part (close to Log 9 in Woodside Canyon). The unit can also be traced in Long Canyon 2 where it is 15 m thick (Figure 3.4).

The base of S2.4 is a gradual transition from the underlying offshore deposits. The top of S2.4 is a non-depositional discontinuity surface which demonstrates an abrupt decrease in grain-size, sandbed thickness and frequency of HCS beds, along with an increase in the proportion of mudstone beds and the amount of bioturbation. This surface can be traced up depositional dip for several kilometres where it is lost in an amalgamated package of LSF deposits. The non-depositional discontinuity surface marking the top of the bedset (S2.5b) can be traced westwards from the study area for approximately 5 km (Howell and Flint, 2003) and eastwards for approximately 10 kilometres, to the area surrounding Jenny Canyon (Figure 3.3), where it gradually becomes thinner and pinches out. S2.5b has a gradient of 0.2° relative to the Grassy Parasequence 2 (G2) datum.
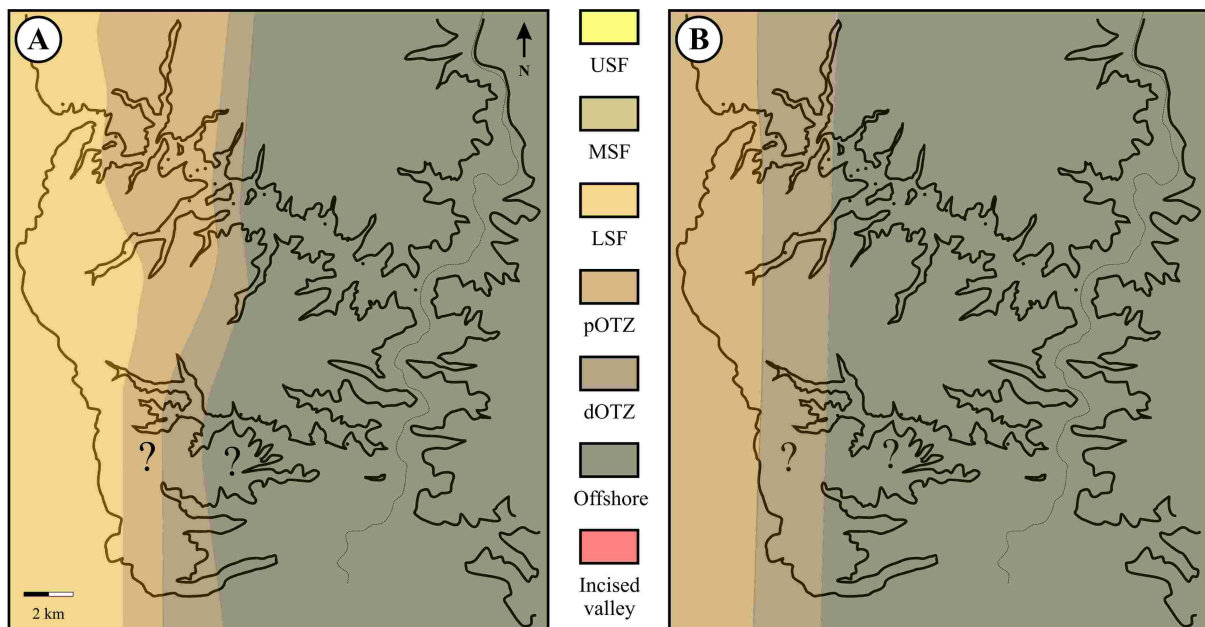
Figure 3.6. Orientation of the facies association belts at the time of formation of S2.5b. (A) The position was north-south prior to formation of the surface, with minor undulations of the facies belts. (B) A landward facies shift of approximately 5 km is associated with the bedset boundary, resulting in straight, north-south striking facies belts.

Farther south, in Long Canyon 1, the S2.4 is rarely exposed, but observations suggest that it is present some meters below S2.5, where it is locally visible as a light brown sandstone beds surrounded by grey mudstone (Figure 3.5).

Figure 3.6 illustrates a palaeogeographic map of the study area at the time of formation of S2.5b. The palaeogeography at the time immediately before the development of the discontinuity surface consisted of a set of north-south striking, undulating facies belts which indicates a minor basinward extension of the facies associations in Long Canyon 2. Immediately after the formation of the discontinuity surface, the facies belts shifted approximately 5 kilometres up-dip and had a relatively straight, north-south orientation.

3.2.2 Sunnyside Bedset 2.5 (S2.5)

Continued progradation of the shoreline resulted in the deposition of the next bedset (S2.5). S2.5 is thinner than the underlying bedset and has a thickness ranging between 17 m in the proximal part to 12 m in the distal part of Woodside Canyon. This bedset prograded slightly farther eastward than the previous one, and have been recognized 12 km down-dip, in the vicinity of Log 14 (Figure 3.4). In Long Canyon 1, the unit can be traced for approximately 5 km before it thins and become poorly exposed (Figure 3.4). S2.5 contains similar facies to S2.4, and represents a basinward transition from LSF deposits in the western part to dOTZ and offshore deposits towards the east.

The upper boundary of the bedset (S2.6b) amalgamates into the LSF facies near the entrance to Woodside Canyon (Log W1) (Howell et al., in review) This surface can be traced down-dip for approximately 14 km. In Long Canyon 1, the unit can be traced for approximately 8 km before it pinches out and becomes unexposed in the vicinity of Log 24 (Figure 3.4 and Figure 3.5). There are also some traces of the unit farther basinward, but because it has become so muddy and bioturbated, it is only visible as poorly defined, brown beds in the muddy slopes along the canyon walls. The dip-gradient of the bedset boundary is 0.16° and 0.21° in Woodside and Long Canyon 1 respectively. Figure 3.7 illustrates the distribution of the facies association belts at the time of formation of S2.6b. The situation is very similar to the one associated with S2.5b, however, S2.5 prograded farther basinward than S2.4. As with S2.4, there is still an undulating trend in the north-south striking facies belts prior to bedset formation with more basinward progradation in the northern part of the study area. During the formation of the discontinuity surface, the facies belts shifted up to 5 km

westwards in Woodside Canyon, whereas the shift in Long Canyon 1 seems to have been more subtle.
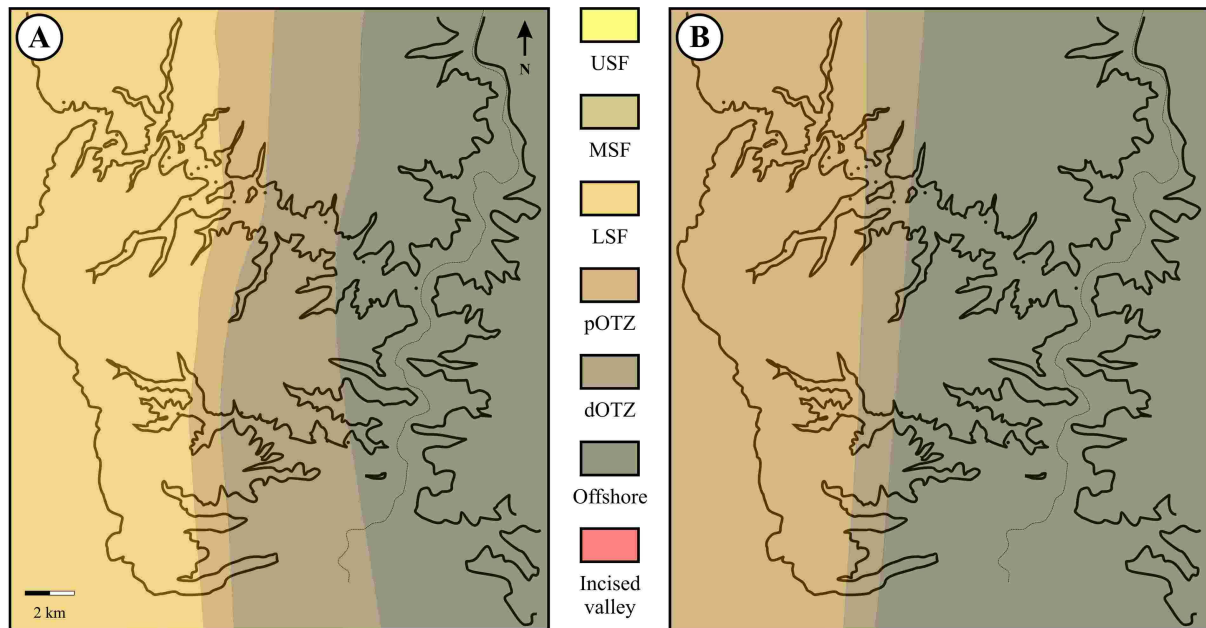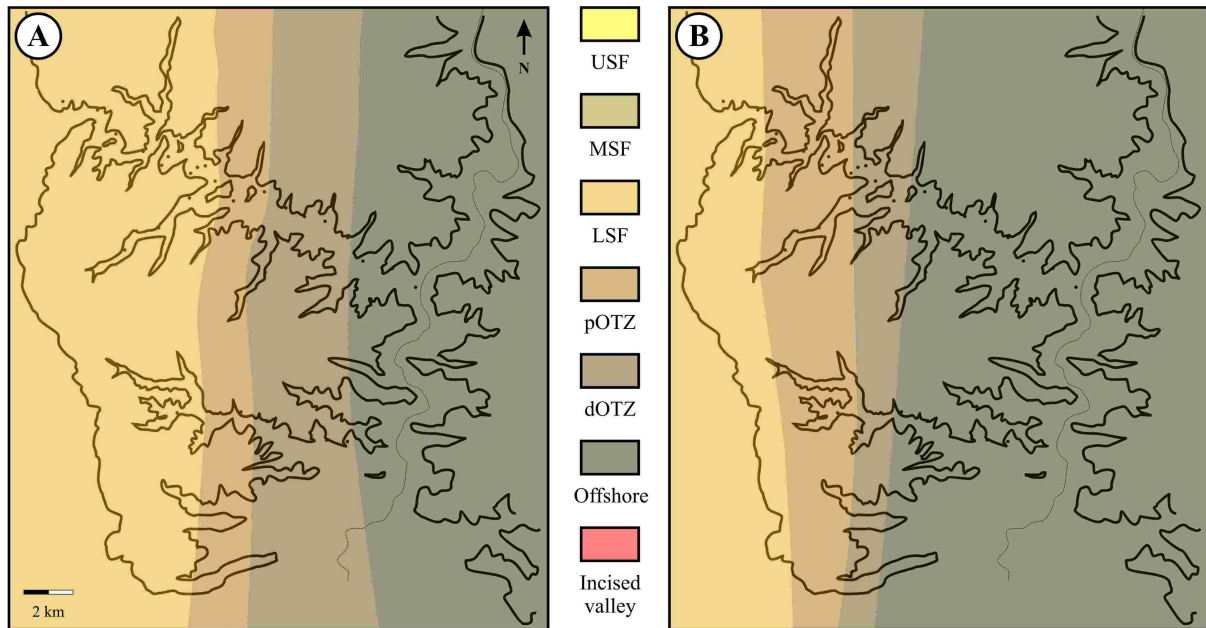

Figure 3.7. Orientation of the facies association belts at the time of formation of S2.6b. (A) Relatively straight, north-south trending LSF and OTZ facies belts deposited prior to the formation of the discontinuity surface (B). These are overlain by similar, parallel belts, reflecting a landward shift of facies of approximately 5 km.

3.2.3 Sunnyside Bedset 2.6 (S2.6)

S2.6 is also very similar to the previous bedsets (Figure 3.4 and Figure 3.5). This unit is between 4 and 9 m thick and increases in thickness in a down-dip direction in Woodside Canyon but remains constant in Long Canyon 1. Up-dip, this bedset amalgamates into the LSF in Log W1 at the entrance of Woodside Canyon (Howell et al., in review). Sunnyside bedset boundary 7 (S2.7b) can be traced for 8 km in the southern part of the area, and approximately 15 km in northern part of the study area, and has a dip relative to the datum of approximately 0.15° and 0.19° in Woodside and Long Canyon 1, respectively. The facies belts associated with the S2.7b are illustrated in Figure 3.8. These have a relatively straight north-south trend, very similar to that of the underlying units. A landward shift of facies of approximately 4 km is also consistent with the previous bedset boundaries.

Figure 3.8. Orientation of the facies association belts at the time of formation of S2.7b. The facies belts are relatively straight and parallel both before (A) and after (B) the formation of the discontinuity surface, reflecting a landward shift of facies of approximately 4 km.

3.2.4 Sunnyside Bedset 2.7 (S2.7)

The uppermost bedset in S2 (S2.7) has a thickness of approximately 3 m in the proximal part, where it amalgamates into the LSF near Log W1 (Howell et al., in review). This unit then increases to 12 m in Log W4, and decrease to 5 m farther basinwards of this location. Except for the thickening and thinning in the vicinity of Log W4, and a heavily to intensely bioturbated zone close to Log W2, there are no major lateral differences within the unit, and it is bounded by Sunnyside Parasequence boundary 3, which is described below.

3.2.5 Sunnyside Parasequence Boundary 3 (S3b)

The four bedsets described above are bounded by a major flooding surface which is identified by a decrease in grain-size and sandbed amalgamation and an increase in bioturbation. This surface is interpreted as a parasequence boundary, representing a rise in relative sea level and a landward dislocation of the shoreline (Figure 3.9); it is traceable landward of the foreshore and USF, and into the non-marine realm where the boundary is represented by a coal seem split (Howell and Flint, 2003; Davies et al., 2005; Howell et al., in review). In Woodside Canyon and Long Canyon 1 and 2, S3b represents a landward shift of facies of at least 6-8 km,

which is represented in the strata by OTZ deposits overlying LSF deposits (Figure 3.4). This flooding surface is laterally persistent and extends over the entire study area. The profile of the underlying S2 shoreface is revealed by studying the flooding surface. In the proximal part where the flooding surface sits on USF/LSF deposits, the surface has a dip between 0.26° and 0.36° whereas in the more distal OTZ and offshore, the surface dips more gentle between 0.13° and 0.15°.An average dip-gradient of 0.19° has been calculated for Woodside and Long Canyon 1 (relative to the datum).
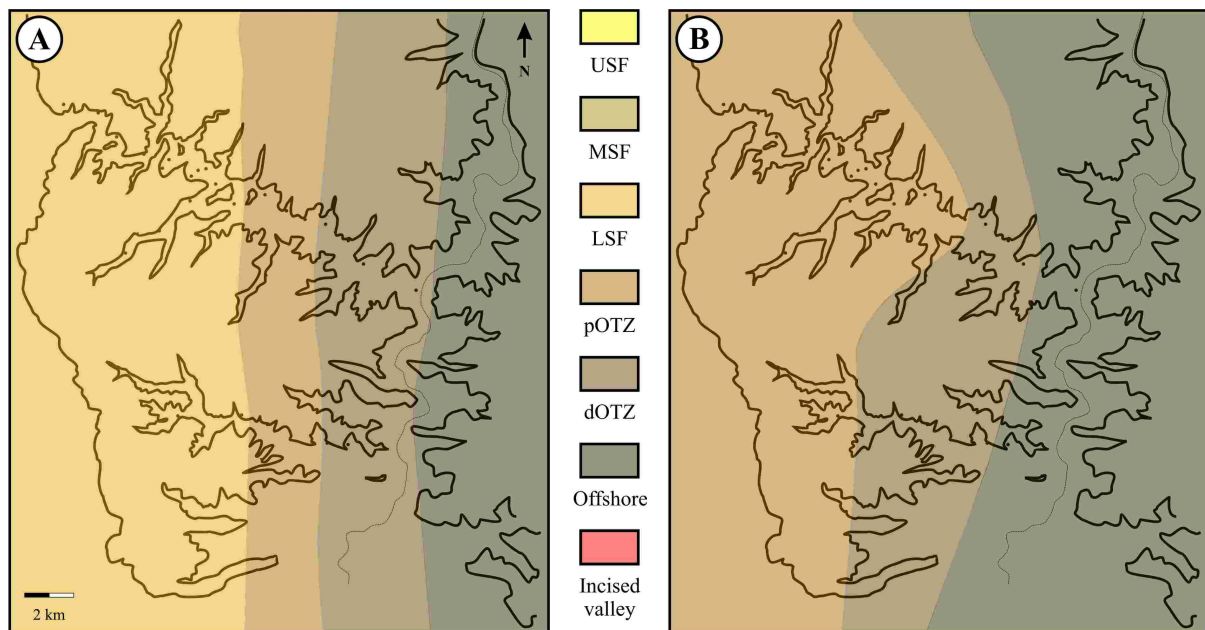
Figure 3.9. Orientation of the facies association belts at the time of formation of S3b. The parasequence boundary is related to a relative rise in sea level and a landward dislocation of the entire shoreline of at least 6-8 km. (A) The facies belts were parallel and north-south oriented prior to the sea level rise. (B) In the central part of Woodside Canyon, dOTZ deposits are overlain by more proximal strata of the pOTZ, indicating that this is also a sequence boundary and that the shoreline was situated farther basinwards of this point during lowstand. The repositioned facies belts are more undulating and indicate a basinward extension of the OTZ facies around Woodside Canyon (B).

In addition to being a flooding surface reflecting a rise in relative sea level, this boundary is also an interfluve sequence boundary and a transgressive surface (Van Wagoner et al., 1990; Howell and Flint, 2003; Davies et al., 2005). A fall in relative sea level ended the progradation of S2, resulting in incision into the shoreface-shelf unit a few tens kilometres northwest of the study area. During the incision and the following lowstand systems tract, the shoreface-shelf deposits in S2.7 became subaerial exposed, suggesting that this surface represents a considerable amount of time, equal to incision and transgressive infilling of the incised valley in the northwest of the study area. Very little direct evidence for this sequence

boundary was observed in the study area. The significance of this surface will be discussed in the forthcoming sections.

3.3 Internal geometry of Sunnyside Parasequence 3

Following the transgression and the landward dislocation of the shoreline (associated with S3b), the shoreface-shelf prograded eastward and seaward again as the rate of sediment input was higher than the rate of sea level rise. At the time of the onset of progradation, the shoreline was located approximately 15 km northwest of the study area (Hampson and Howell, 2005). Several upward fining units, up to 5 m thick, are present in the lowermost part of S3, directly above the parasequence boundary, where they consists of interbedded HCS sandstone and bioturbated mudstone. They will be discussed further in section 3.6.

### 3.3.1 Sunnyside Bedset 3.1 (S3.1)

As S2, S3 is also comprised of several upward coarsening units bounded by non-depositional discontinuity surfaces. The lowermost one (S3.1) is only present in Woodside Canyon, Long Canyon 2 and Jenny Canyon (Figure 3.3). The unit is absent in Long Canyon 1 to the south, and given the lack of exposure between the sections, the nature of the pinch-out there is unknown. The bedset thickens from 13 m in the proximal part (in the vicinity of Log 4), to approximately 20 m farther east, near Log 14, where its bounding surface becomes very poorly-defined and merges with the overlying unit (S3.2). The Sunnyside bedset boundary 3.2

Figure 3.10. Up-dip pinch-out of S3.2b close to Log 4. The discontinuity surface is represented by a thin, laminated sand and mud bed between amalgamated HCS LSF deposits. The canyon wall is approximately 200 m long. The location of bedset pinch-out is indicated on the map.

51

(S3.2b) can be traced proximally into the LSF where it becomes amalgamated and disappears. In Woodside Canyon, this amalgamation occur between Log 3 and Log 4 (Figure 3.10 and Figure 3.4). In Long Canyon 2 the amalgamation occurs between Log 19 and Log 8. The bedset boundary has an average dip-angle of 0.16° relative to the datum.

Figure 3.11 illustrates the distribution of facies belts at the time of formation of S3.2b. Prior to the formation of the boundary, the facies belts were relatively parallel in a north-south direction. A very bioturbated, middle shoreface unit is locally present in Long Canyon 2, (Log 19 and Log 26), and landward of the up-dip pinch-out of the bedset boundary. The westward and southern extension of this unit is unknown; however, it is not present in Long Canyon 1.
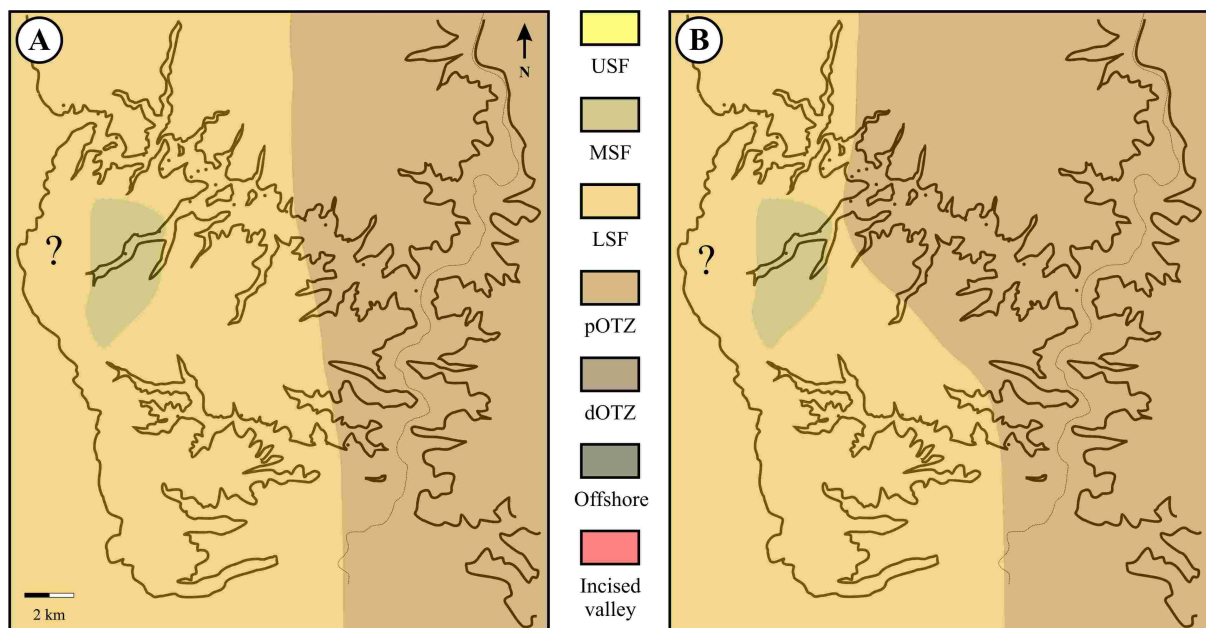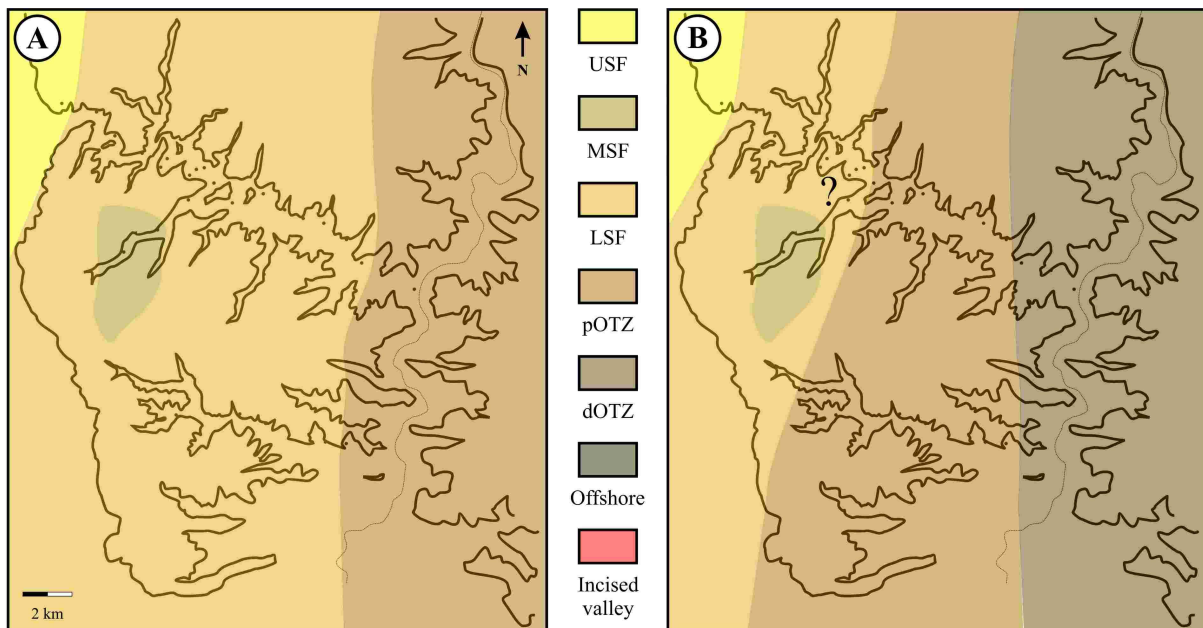

Figure 3.11. Orientation of the facies association belts at the time of formation of S3.2b. (A) Before the formation of S3.2b, the maximum seaward position of the LSF was near the central part of Woodside Canyon forming a relatively straight, parallel belt southwards to Long Canyon 1. (B) Localised relative deepening resulted in a landward shift of the facies in Woodside Canyon of approximately 5 km. Southwards, the boundary pinch out into S3.2 and the succession in Long Canyon is continuous at this level. Localised MSF deposits are present in Long Canyon 2, but the lateral extension of these are unknown.

As the bedset boundary is absent in Long Canyon 1, the position of the LSF is the same on either side of the boundary. In Woodside Canyon, the discontinuity surface is related to a 5 km landward shift of facies where the pOTZ overlies the LSF. This resulted in an asymmetry of the facies belts, indicating increased relative deepening, accompanied by a landward shift of facies in Woodside Canyon.

3.3.2 Sunnyside Bedset 3.2 (S3.2)

The overlying bedset, S3.2, is truncated by the incised valley in the central part of Woodside Canyon, and it is not possible to locate its up-dip amalgamation into the LSF (Figure 3.4). In Long Canyon 1 and 2, however, this unit is traceable throughout the entire area (Figure 3.5). The bedset is between 5 and 10 m thick and is relatively continuous down-dip without any major changes. In Long Canyon 1, the equivalent to S3.1 and S3.2 is a combined S3.2. Although S3.1 is not present in Long Canyon 1, the total thickness is between 12 and 29 m from east to west, indicating a continuous thickening basinward. For comparison, the thickness of S3.1 and S3.2 in Woodside Canyon varies less (between 15 and 26 m), indicating very similar thicknesses for both units. The discontinuity surface bounding the bedset has an average dip-gradient of 0.21° in Woodside Canyon, whereas the same surface in Long Canyon 1 only has a dip of 0.08° relative to the datum. In two locations (Log 11 and Log 27), this boundary is associated with nodules or concretions, resembling a lag deposit.

Figure 3.12. Orientation of the facies association belts at the time of formation of S3.3b. (A) Prior to the formation of the bedset boundary, the facies belts were relatively parallel and had a north-south strike . (B) The discontinuity surface is associated with a landward shift of the facies belts of approximately 7-8 km in Woodside Canyon and Long Canyon 1, leaving OTZ deposits on top of LSF deposits in the central parts of the

Figure 3.12 illustrates the position of the facies association belts below and above Sunnyside bedset boundary 3.3 (S3.3b). Immediately before the discontinuity surface was formed, the facies belts were oriented north-south. The time equivalent position of the

proximal facies is unknown because the incised valley has removed the uppermost 10-15 m of S3 in central parts of Woodside Canyon and Long Canyon 2. In the distal part of the study area, the bedset boundary is associated with a landward shift of faces of approximately 7 km in Woodside Canyon, and at least 8 km in Long Canyon 1, where pOTZ deposits overlie LSF deposits (Figure 3.13). There is a decreased amount of landward displacement of the shoreline in the north which has resulted in an oblique orientation of the pOTZ facies belts in this area.

Figure 3.13. S3.3b in Long Canyon 1 (Log 21). LSF deposits are overlain by OTZ deposits, indicating a landward shift of facies. Hammer for scale.

3.3.3 Sunnyside Bedset 3.3 (S3.3)

The uppermost bedset in Parasequence 3 (S3.3) is somewhat different from the others in S2 and S3 both in internal geometry and lithology. As described in Chapter Two, this unit is more compact and demonstrates both an increase in current induced structures and a decrease in the amount of bioturbation. In Woodside Canyon, the bedset is also truncated by the incised valley but reappears eastward as the valley becomes thinner between Log 9 and Log 11 (Figure 3.4 and Figure 3.5). In Long Canyon 1, the unit can be traced throughout the area, a distance of approximately 10 km at its maximum observed extent. In the proximal part, the bedset is similar to the other bedsets in S2 and S3, hence composed of interbedded HCS sandstone and bioturbated mudstone of the OTZ passing upward into the amalgamated HCS sandstone of the LSF facies association. The distal part of the bedset demonstrates an upward deepening trend, followed by an upward shallowing trend in both Woodside Canton and Long Canyon. This pattern is not, however, observed anywhere else in the study area. In addition, this uppermost bedset is the only bedset that becomes much thinner basinward and eastward; this unit's thickness also decreases from 14 m in the proximal part of Long Canyon 1 to 5 m in the distal part, near Gray Canyon. A similar decrease in thickness is also present in

Woodside Canyon. Figure 3.14 indicates the position of the facies belts associated with the uppermost discontinuity surface. As this unit is truncated by the incised valley in the central part of Woodside Canyon, the orientation remains unclear. The uppermost part of the bedset in Woodside Canyon is positioned more landwards relative to the southern Long Canyon 1, which gives a curved orientation to the facies belts.

I
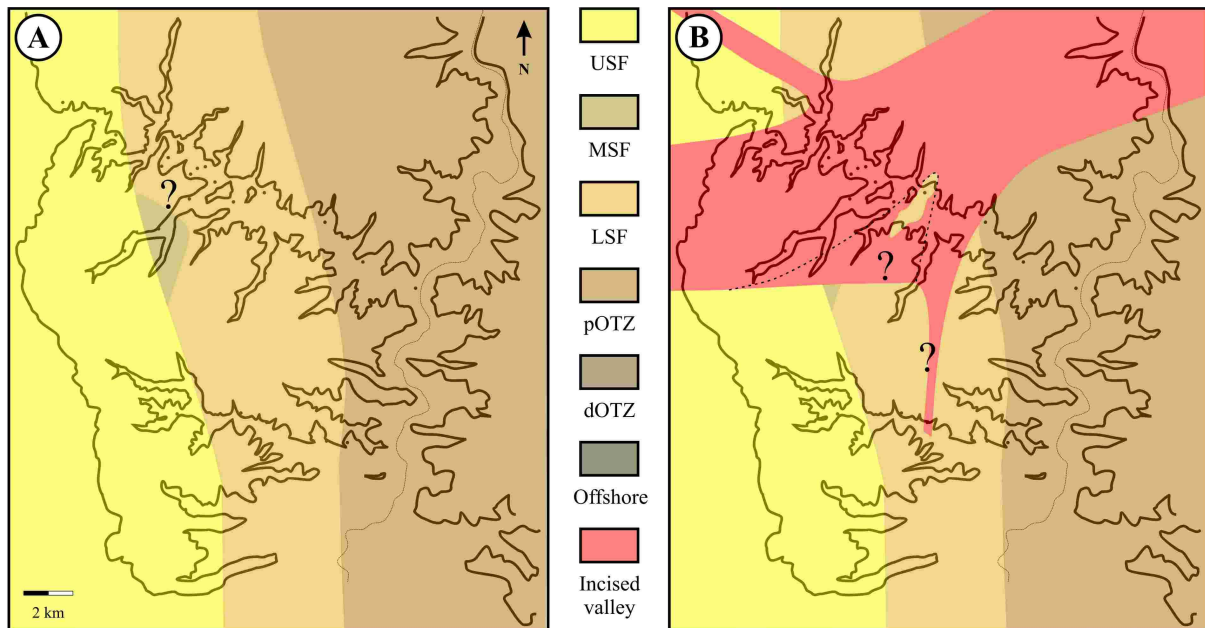
Figure 3.14. Position of the facies association belts at the time of falling sea level, incision and truncation of S3.3. (A) USF facies is located in the proximal part of Woodside Canyon and Long Canyon, suggesting a relatively straight north northwest-south southeast position of the shoreline. (B) As the sea level fell, at least two branches were cut into the underlying shoreface-shelf deposits and subsequently filled with transgressive, estuarine deposits.

3.3.4 Grassy Parasequence Boundary 1 (G1b)

The unconformity overlying S3.3 is interpreted as a combined parasequence boundary and a sequence boundary, representing a period with a fall in relative sea level, incision and subsequent transgression (Howell and Flint, 2003). As the relative sea level fell and the shoreline migrated basinwards, the shoreface-shelf deposits became subaerially exposed. The following relative sea level rise and transgression resulted in flooding of the incised valley. Wave ravinement associated with the transgression is interpreted to have removed all the evidence of subaerial exposure, as there are no signs of palaeosol formation on the interfluve sequence boundary in Woodside and Long Canyon 1 and 2. A coarse-grained transgressive lag is present in Woodside Canyon (close to and on the top of the incised valley), indicating

that at least some of the coarse-grained material was derived from the underlying estuarine deposits. As flooding continued, the shoreline migrated landwards and westwards of the study area, and a new shoreline was established. This shoreline is the lowermost parasequence in the Grassy Member termed G1 (GPS 1, O'Byrne and Flint, 1995) This surface and the associated transgressive erosion will be discussed later in more detail.

## 3.4 Depositional evolution of the Sunnyside Member

Figure 3.15 illustrates the stratigraphical development of S1, S2 and S3, as described by Howell and Flint (2003) and Hampson and Howell (2005). According to the studies, the maximum seaward position of the S1 shoreline is located around Bear Canyon, westward of the most basinward position of the underlying parasequence in the Kenilworth Member. The limited progradation of the Kenilworth TST (Pattison, 1995; Taylor et al., 1995) and the S1 left a considerable amount of accommodation in front of the prograding S2. This has resulted in S2 being unusually thick. Consequently, at least four bedsets were formed as S2 prograded basinwards. The shoreline of S2 prograded as far as Trail Canyon through normal regression. Deposition was then punctuated by a fall in relative sea level and incision into the underlying shoreface-shelf deposits (Howell et al., in review). The incised valleys associated with S2 are located to the north and west of the study area (Howell and Flint, 2003). As relative sea level rose, transgressive ravinement removed all evidence of subaerial erosion in both Woodside Canyon and Long Canyon 1. During the flooding, the transgressive shoreline migrated landwards of the maximum seaward position of the underlying S2 shoreline, resulting in an overall landward displacement of the shoreline. This landward displacement of the shoreline was limited by the position of a raised coal mire to the west (Howell and Flint, 2003; Davies et al., 2005). Similar processes were described from the Kaiparowits Plateau by (Shanley and Mccabe (1995). This transgression resulted in the OTZ deposits (which were associated with the transgressing shoreline) to become deposited above the LSF deposits of S2, represented by an upward fining unit. These relatively thin units are interpreted as being part of a transgressive unit and will also be discussed in more detail later in this section. Renewed progradation led to the deposition of S3, which is composed of three bedset. The maximum seaward position of S3's USF and foreshore deposits is located between Log 20 and Log 21 in Long Canyon 1 (Figure 3.3), indicating that during the maximum progradational extent, the highstand shoreline was located in this area. In Woodside Canyon, USF and foreshore

Progradation of parasequence 1
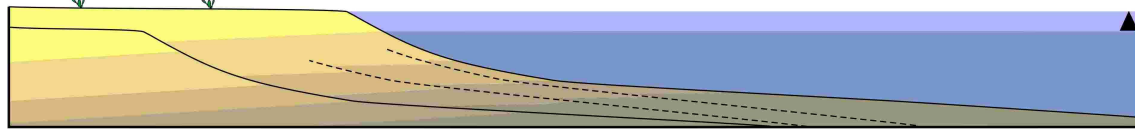
Regional flooding resulted in landward dislocation of the shoreline, followed by progradation of S2. As the parasequence prograded basinwards, four bedsets developed (S2.4-S2.7). The bedset boundaries represents a landward shift of the facies belts and can be traced into the lower shoreface. Maximum seaward position of the S2 shoreline is to the west of the study area.
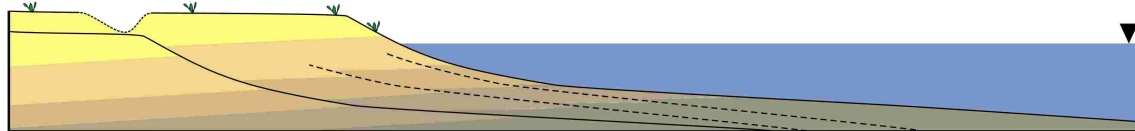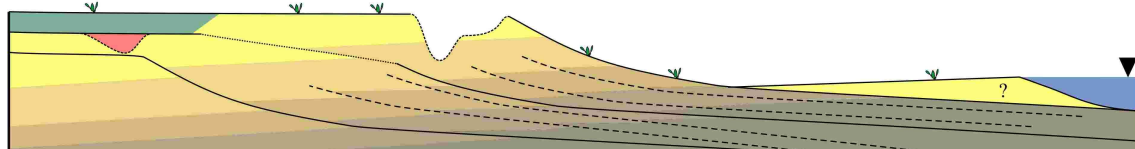
Sea level fall resulted in fluvial incision into the underlying shoreface-shelf deposits and a basinward dislocation of the shoreline. The incised valley is located farther to the north-west, and is not present the study area. In Woodside Canyon and Long Canyon, S2b is a combined parasequence boundary and a correlative sequence boundary which became subaerially exposed during lowstand.
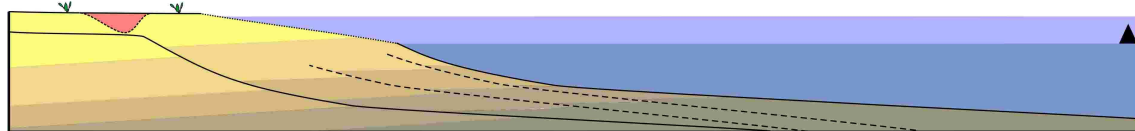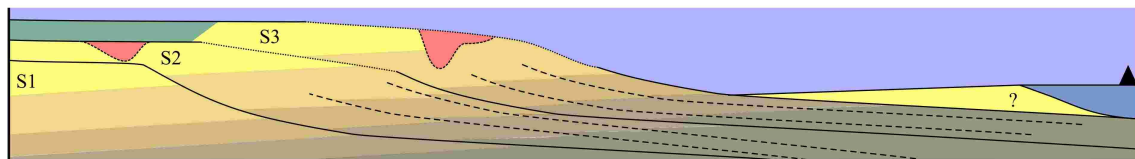
Renewed transgression led to filling of the incised valley as the shoreline migrated landwards. During transgression, the high-energy upper shoreface eroded the uppermost part of the old parasequence, removing all evidence of subaerial exposure.
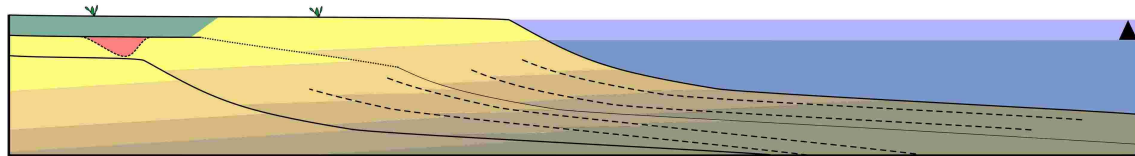
As the rate of relative sea level rise decreased, S3 prograded eastward to a maximun seaward position around the central part of Woodisde Canyon and Long Canyon 1. Similarly to S2, several bedsets (S3.1-S3.3) were formed as the parasequence prograded.

Sea level fall of about 28 m resulted in fluvial incision near the present day Woodside Canyon. The lowstand shoreline is not exposed, but it must have been positioned farther east, outside the study area. The sea level fall resulted in subaerial exposure of the S3 shoreface-shelf.

Renewed rise in relative sea level resulted in flooding and filling of the incised valley, and a landward shift of the shoreline. During transgression, high-energy upper shoreface environments eroded the uppper part of S3, creating a ravinement surface and an associated trnasgressive lag. Erosion also romoved all evidence of subaerial exposure. Subsequent progradation led to depositon of Grassy Parasequence 1.
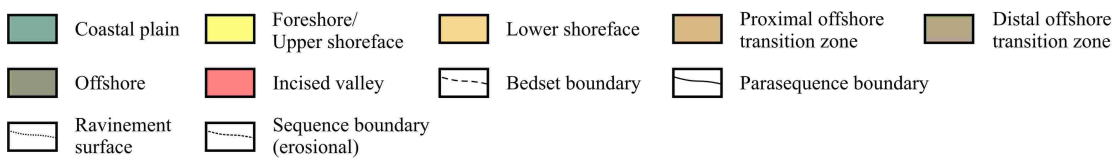
Figure 3.15. Conceptual sequence stratigraphic evolution of the Sunnyside Member. Modified from Howell et al. (in review).

deposits have been removed by a fall in relative sea level following the deposition of S3. This fall resulted in extensive fluvial incision in Woodside Canyon, eroding up to 28 m of stratigraphy and resulting in a seaward shift of the shoreline. The valley system fed sediments to a detached lowstand shoreline (sensu Ainsworth and Pattison, 1994) east of the study area, and the shoreface-shelf deposits of S3 were subaerially exposed. Details of the incised valley are discussed more thoroughly in Chapter Four. The nature of the lowstand shoreline would have depended on the duration of the stillstand which occurred after the sea level had stopped falling (Posamentier et al., 1992). As with the lower Sunnyside sequence boundary at the top of S2, transgressive erosion is interpreted to have removed all evidence of subaerial exposure on the interfluve. Sea level rise then flooded the entire shoreface-shelf and the incised valley, resulting in a renewed landward dislocation of the shoreline west of the study area which was followed by the progradation of G1.

3.5 Bedset stacking pattern and shoreline trajectories

In the northern part of the study area, the bedsets in S2 demonstrate a progradational trend in the lower part, followed by a more aggradational trend in the upper part. This is evident in both Woodside Canyon and Long Canyon 2, where the basinward extent of the LSF deposits in S2.5 are located between Log W2 and Log W3 and between Log 26 and Log 19 respectively (Figure 3.4 and Figure 3.3). The basinward extent of the LSF deposits in S2.5-S2.7 is located close to Log 7 in Woodside Canyon, approximately 5 km farther basinward of S2.4. This suggests an aggradational pattern of the lowermost bedset in S2, whereas S2.5-S2.7 in Long Canyon terminate somewhere between Log 20 and Log 21 (Figure 3.4), indicating a more progradational pattern in this area. The basinward termination of the uppermost bedset in S2 may also be related to the amount of transgressive ravinement during the subsequent sea level rise.

In S3, the bedsets display a continuous progradational stacking pattern in both Woodside Canyon and Long Canyon 1 (Figure 3.4). The pinch-out of the LSF deposits in S3.2 occurs 3-4 km east of the most basinward extension of the underlying S3.1 LSF deposits. The basinward extension of the uppermost bedset in S3 (S3.3) occurs at approximately the same place (or landwards of) S3.2 in Woodside Canyon and Long Canyon 1. This may be related to transgressive erosion and removal of the most basinward part of the bedset; similar to the situation in the uppermost part of S2.

According to the study of the Sunnyside Member completed by Howell et al. (in review), the four bedsets which are recognized within S2 (S2.4-S2.7) constitute only the most basinward half of the parasequence, and at least three bedset are present farther west of the study area. Recent models for the formation of parasequences in the Book Cliffs, based on the work by Kamola and Van Wagoner (1995), suggests that they may form with an initial phase of aggradation (relative steep shoreline trajectory sensu Helland-Hansen and Martinsen, 1996) followed by near horizontal progradation (Howell and Flint, 2003; Howell et al., in review). This overall pattern of a steep shoreline trajectory in the proximal part, west of the study area, followed by a gentler trajectory farther east, suggest that the minor variations observed in Woodside Canyon and Long Canyon are related to local changes in progradation rate, sediment supply or bathymetry rather than changes in sea level and accommodation space.

3.6 Transgressive deposition

Due to the landward shift of the shoreline associated with a rise in relative sea level and the presence of an incised valleys northwest of the study area, S3b is both a parasequence boundary and an interfluve sequence boundary (Figure 3.15 and Figure 3.5), indicating that a considerable amount of time is represented by this surface (Howell et al., in review). Following the progradation of S2, the relative sea level fell and an incised valley was cut into the underlying shoreface-shelf parasequence. Later, as sea level rose, the incised valleys that were located northwest of the study area were filled, and the "Sunnyside Sandstone" was deposited (Howell and Flint, 2003; Howell et al., in review). As the transgressive shoreline reached the most basinward position of the old S2 shoreline it continued to retreat, and the old S2 shoreface-shelf became flooded. The shoreface deposits of S2 were overlain by a set of OTZ deposits related to the landward migration of the S3 shoreline. These transgressive units are present in the central part of both Woodside Canyon (Log 10-Log 16) and Long Canyon 1 (Log 22 and Log 23), where they can be traced up to 6 km down-dip (Figure 3.16 and Figure 3.4). Towards the west (palaeolandwards), these units become thicker and more sandy, and pass into a continuous coarsening upward OTZ succession in the vicinity of Log 9 and Log 21. Eastwards, these transgressive units become thinner and more shaly, pinching out close to Log 16 and Log 23 in Woodside Canyon and Long Canyon 1, respectively. Although these upward fining units are present in both canyons, the thicknesses and distributions varies slightly. In Long Canyon 1, the transgressive unit is up to 3.5 m thick and can be traced for

approximately 3 km in a basinward direction, whereas in Woodside Canyon, the unit is up to 5 m thick and can be traced for at least 6 km. The unit is also more sandy and has thicker, and more pronounced, sandstone beds in Woodside Canyon.
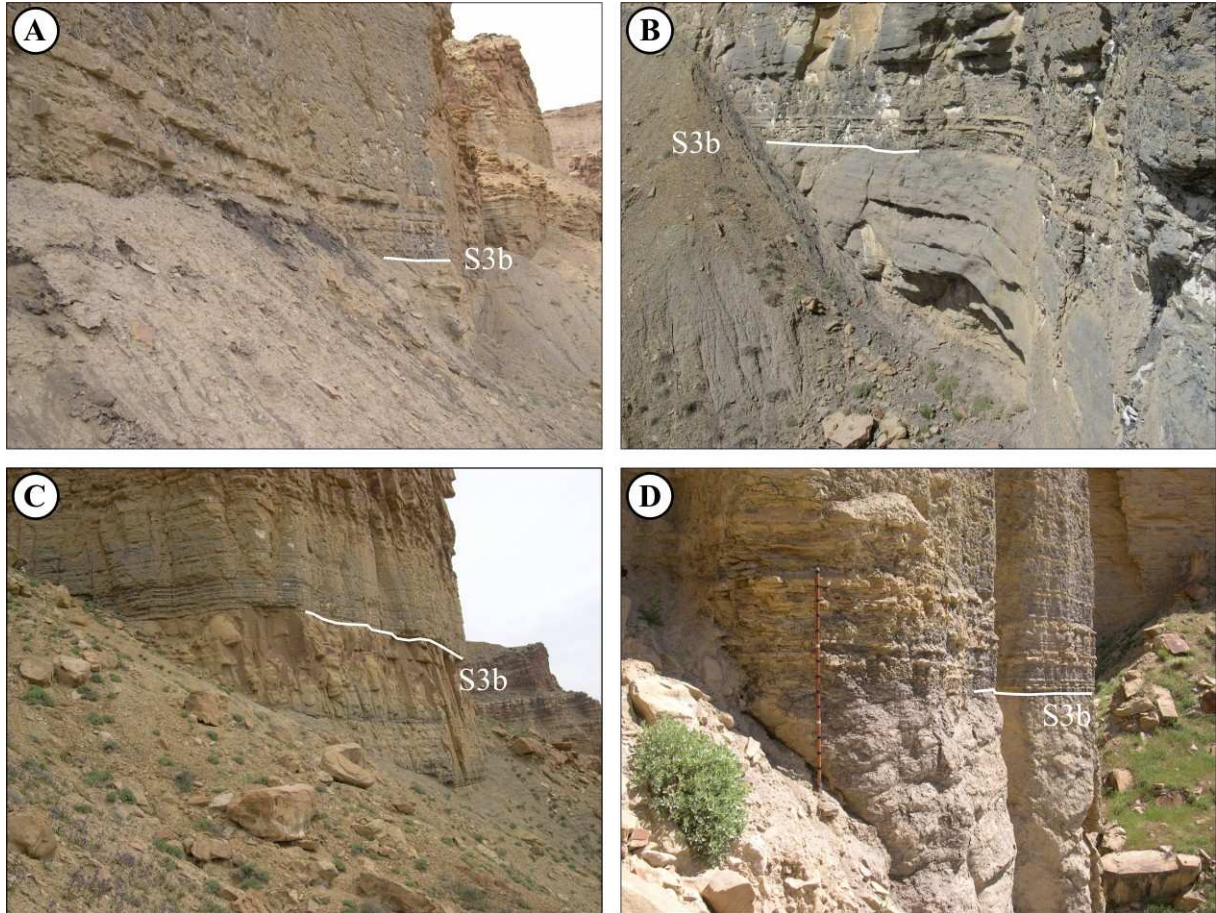
Figure 3.16. Minor upward fining units in Woodside Canyon are represented by a decrease in sandstone content and thickness of HCS beds between the (A) proximal near Log 13 and the (B) distal part close to Log 16. In Long Canyon 1, the unit is thinner and less sandy and the difference between (C) proximal and (D) distal is less pronounced compared to Woodside Canyon. Exposed units in A, B and C are approximately 15 m, 16 m and 20 m respectively. 1.5 m long staff for scale in D.

As the sea level continued to rise, more distal facies were deposited successively until the sediment input was higher than the sea level rise and the shoreline started to prograde basinwards again, resulting in the overall upward coarsening S3. Both the incised valley fill and the upward fining unit above the parasequence boundary are interpreted to belong to the transgressive package (Figure 3.17), whereas the underlying S2 and the following S3 belong to the highstand system tract (e.g. Van Wagoner et al., 1990; Howell et al., in review). The maximum flooding surface that represents the change from a retrogradational regime to a progradational regime, and which reflects the most landward position of the S3 shoreline, is

located in the uppermost part of the upward fining unit. The thickness variation between Woodside Canyon and Long Canyon 1 may be related to variations in sediment input as described on a larger scale from the Holocene of the Texas Gulf coast (Suter and Berryhill, 1984) thus indicating that the north of the study area was closer to the sediment source at the time of deposition, hence a more proximal deposit.

Figure 3.17. Transgressive unit exposed in the central parts of Long Canyon 1. S2.5-S2.7 are coarsening upward units within the overall upward shallowing S2. The parasequence constitutes a highstand systems tract (HST) which is bounded by a combined sequence boundary (SB) and a parasequence boundary representing relative fall and rise in sea level. Subsequent sea level rise resulted in deposition of a relatively thin, upward fining, transgressive unit, laying unconformably on the SB. The transition from transgressive conditions and relative deepening to regressive conditions and relative shallowing is marked by a maximum flooding surface (MFS, broken line) which represents the most landward position of the shoreline. The exposed section is approximately 20 m thick.

3.7 Transgressive erosion

There are several indications of transgressive erosion in the uppermost part of S2 and S3. These include: truncation of the incised valley deposits and variations in bedset thickness in Woodside Canyon. The lack of evidence of subaerial exposure, such as roots and soil profiles, and the lacking evidence for any lowstand shoreline are also indirect evidence for significant erosion. Transgressive ravinement surfaces are commonly accompanied by a firm ground, *Glossifungites* tracefossil suite (Pemberton, 1998) and transgressive lags (see section 2.3.5).

In the Sunnyside member, lag deposits were only observed on G1b in proximity of the incised valley, suggesting the reworking of fluvial and estuarine deposits. More regional mapping of S2 also suggest that the landward equivalents of the LSF, USF and the foreshore of S2.6 and of the entire succession of S2.7, has been eroded by transgressive erosion (Howell et al., in review). More detailed evidence for transgressive erosion is discussed below.

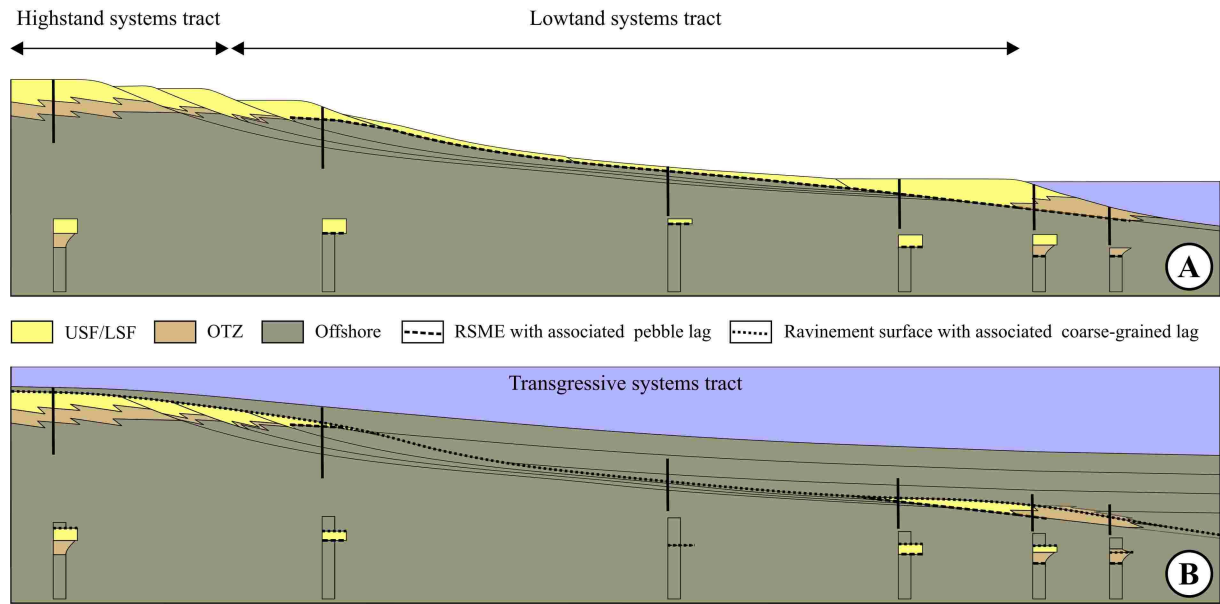*3.7.1 Subaerial exposure and transgressive erosion*

Estimates of sea level fall associated with the formation of the two sequence boundaries the Sunnyside Member are >20 m and >28 m for the lower and upper respectively. These estimates are taken from the thickness/depth of documented incised valleys (Howell and Flint, 2003). Using and average Sunnyside shoreface-shelf gradient of approximately 0.2° (which is the average dip-angle for S2.5b-S2.7b), a base level fall of 20 m will result in a basinward shift of the shoreline of 6 km. If the gradient is even gentler, for example 0.1°, the basinward shift of the shoreline will increase to 11 km. This gradient is representative for the proximal part of the Sunnyside shoreface-shelf profile, but the angle will probably decrease to approximately 0.01-0.03° in the offshore area, similar to what has been observed in the underlying Kenilworth Member (Hampson and Storms, 2003), resulting in an increased shift of the shoreline as the gradient decrease further. The position of the S3 shoreline prior to sea level fall was eastward of Log 20 in Long Canyon 1 Figure 3.3), and probably between Log W3 and Log W4 in Woodside Canyon. Assuming the average shoreface-shelf gradient was less than 0.1°, the position of the lowstand shoreline would be east of the study area, indicating that the entire G1b and at least parts of S3b was subaerial exposed during lowstand.

Given some time, subaerial exposure of the shoreface and shelf would have resulted in the formation of palaeosols (Collinson, 1996). Alteration of the sediments during the formation of a palaeosol includes chemical changes and discoloration, along with physical changes such as biogenic reworking and rooting (Collinson, 1996). None of these features have been recognized, neither along S3b or G1b. Instead, well developed trace fossils of the *Glossifungites* ichnofacies are associated with the boundaries, suggesting a degree of erosion at the surfaces within a shallow-marine realm (Pemberton, 1998). The absence of evidence for subaerial exposure can be explained in two ways, either the area was never exposed, or, more likely, the evidence has been removed by later erosion

Given the presence of the incised valleys and the stratal evidence for sea level fall, it is reasonable to assume that the lowstand shorelines was positioned east of the study area, and that the entire dip-section of S3b and G1b was subaerially exposed. The lack of evidence supporting subaerial exposure must be related to later erosion and the removal of a palaeosol. The presence of a locally developed transgressive lag in several of the logged sections, indicating erosion and reworking of the underlying unit during sea level rise, maybe as far east as Log 14 in Woodside Canyon. Such lag deposits usually coincide with sequence boundaries, and are composed of coarse-grained material, shell fragments and rip-up clasts derived from the underlying incised valley (Van Wagoner et al., 1990). Tracefossil assemblages consisting of *Diplocraterion* and *Thalassinoides* are related to the firmground Glossifungites ichnofacies (Pemberton, 1998) and with the erosional surface. Exhumation of partially compacted shoreface-shelf sediments along with the transgressive lag therefore indicates considerable transgressive ravinement, and may explain the total lack of evidence for subaerial exposure.

3.7.2 Attached/detached lowstand shorelines and transgressive erosion

An eastward dislocation of the shoreline during sea level fall would result in either an attached or a detached lowstand shoreline (Figure 3.18) (e.g. Posamentier et al., 1992; Ainsworth and Pattison, 1994). Forced regressive shorelines have previously been recognized in the underlying Kenilworth Member where they are associated with sharp-based, LSF successions bounded by regressive surfaces of marine erosion (Pattison, 1995; Storms and Hampson, 2005). These surfaces were formed as the facies belts shifted downwards and seawards as the sea level fell, successively eroding the underlying OTZ deposits. The sharp-based LSFs indicate that the sediment input was high enough to keep up with the rate of falling sea level, resulting in an accretionary forced regressive shoreline (Helland-Hansen and Martinsen, 1996). However, if the rate of sea level fall outpaced the amount sediment input, a detached, non-accretionary forced regressive shoreline would form, resulting in exposure of parts of the shoreface-shelf profile. Detached forced regression can also be formed by the transgressive erosion of part of a previously attached falling stage deposit (Ainsworth et al., 2000).

Highstand systems tract

Lowtand systems tract

USF/LSF OTZ Offshore ----- RSME with associated pebble lag .... Ravinement surface with associated coarse-grained lag

Transgressive systems tract

Figure 3.18. Cross-section of a wave-dominated shoreline during a cycle of relative sea level fall and rise. (A) Falling sea level results in forced regression during the late HST and the LST. The basinward stepping, lower shoreface erodes into underlying OTZ and offshore deposits, forming a regressive surface of marine erosion (RSME) which may be associated with a pebble lag. During deposition of the LST, the lowstand shoreline is attached, indicating that the sediment supply to the shoreline was high enough to keep-up with the falling sea level. If the sediment supply to the shoreline was insufficient to maintain a continuous falling shoreline, the lowstand would be detached. (B) Sea level rise results in transgressive erosion and the formation of a ravinement surface, removing parts of the lowstand shoreline and the evidence of attachment. The only indication of the lowstand is the presence of a transgressive lag which is over and underlain by offshore deposits. No RSME has been observed in the study area, and no transgressive lag has been observed in the offshore deposits, suggesting that the lowstand shoreline was detached, or that the transgressive erosion was very extensive and removed major parts of the late HST and the LST. Modified from (Walker and Plint, 1992).

The basinward extent of foreshore and USF deposits in S3 and S2 is located in the middle, and western part of the study area, respectively. None of the parasequences present any evidence of sharp-based shorefaces and all log sections suggests a continuous succession through dOTZ into LSF or USF deposits. This lack of evidence suggests a detached shoreline, which can be attributed to rapid sea level fall or detachment during extensive transgressive erosion. Subsequent detachment was discussed by Ainsworth et al (2000) and has been reported by Walker (1992) where transgressive ravinement separated an attached shoreline from a highstand shoreline, leaving a single lowstand sandstone unit encased in mudstone, tens of kilometres offshore. In that case, the only evidence suggesting extensive transgressive ravinement was a lag surrounded by offshore mudstone. A similar scenario has been described by Posamentier (1992), suggesting removal of up to 10-20 m of proximal shoreface-shelf deposits during transgression. As long as no such lag deposits have been observed seaward of the incised valley (east of Log 13), and no sharp-based LSFs have been observed, neither in Woodside Canyon or in Long Canyon 1, it is very difficult to determine the shoreline geometries associated with the lowstand; in this case it is most likely that

transgressive ravinement has removed all the evidence of such a process. However, total removal of an attached lowstand shoreline would imply a considerable amount of erosion as the entire foreshore, USF and sharp-based LSF succession would have to be removed. Erosion of a detached lowstand unit, reflecting a rapid fall in sea level followed by an abrupt basinward dislocation of the shoreline, on the other hand, would require much less erosion; making this a more likely scenario.

3.7.3 Incised valleys and transgressive erosion

Another indication of extensive transgressive erosion is the presence of a local exposure of incised valley strata in Log 22, located in Long Canyon 1 (Figure 3.4 and Figure 3.5). This unit is four meters thick and can be traced for approximately 50-100 m along the canyon wall. Except for this single cross-section, there is no sign of the unit along-strike or dip, and, as will be discussed in Chapter Four, the unit is interpreted to be a minor branch of the incised valley, associated with the G1 sequence boundary. The absence of this unit elsewhere in Long Canyon 1 may be related to transgressive erosion. Incised valley systems may have variable bottom relief due to differential erosion by the lowstand river (Schumm and Ethridge, 1994). Such changes have been recognized in the main valley system in Woodside Canyon, where the estuarine successions vary in thickness (Figure 3.4). A subsequent sea level rise and the associated transgressive erosion may have cut off the uppermost part of the valley fill succession and the subaerially exposed hinterland, only leaving behind the topographic low areas as "bowls" of estuarine deposits, which are encased in shallow-marine sandstones and mudstones.

3.7.4 Varying bedset thickness and transgressive erosion

Significant transgressive erosion may also explain some of the thickness variations in the underlying bedsets, especially in Woodside Canyon. In the area between Log W2 and Log 3, S2.7 demonstrates a considerable change in its thickness (from 2,5 m to 12 m and back to 7 m within 3 km down depositional dip, Figure 3.4). These thickness variations are not observed in Long Canyon 1 and may therefore be related to differential erosion during transgression. However, bathymetric variations along the shoreline, possibly associated with the presence of a river outlet, may have resulted in increased or decreased wave action and shoreface erosion.

Also, the uppermost bedset in S3 (S3.3) has an abnormal geometry as it becomes thinner basinwards. Although this bedset differs from all the others in terms of its internal composition and stacking of HCS beds, the basinward thinning of the unit in both Woodside Canyon and Long Canyon 1 may be related to transgressive ravinement at the time of flooding of S3. Except for the lack of evidence for subaerial exposure, there is no direct evidence that support this interpretation, and the difference between this bedset and the other bedsets in the Sunnyside Member may be related to other controlling factors. These will discussed below.

3.8 Bedsets and depositional environments

As described in Chapter Two, two different kinds of offshore transition zone deposits are recognized in the Sunnyside Member. The most common (type I) is composed of intensely bioturbated, interbedded HCS sandstone and mudstone, whereas the other kind (type II), is more compact, and is represented by reworked current ripples and sparse to low bioturbation. Bedsets with type I OTZ deposits (S2.4-S2.7 and S3.1-S3.2) have relatively continuous thickness basinwards, and are interpreted to represent a wave-dominated shoreface-shelf, where major storms reworked and redeposited sand into lateral extensive sandsheets across the basin floor (e.g. Niedoroda et al., 1984; Boyd et al., 1992; Howell, 2004). A decrease in the amount of bioturbation and the presence of current induced structures in the OTZ suggests increased fluvial influence and a closer proximity to a river mouth in S3.3 (Bhattacharya and Walker, 1992; Pemberton et al., 1992a; Reading and Collinson, 1996). This package also demonstrates considerable thinning in a down-dip direction. Palaeocurrent measurements suggest flow towards the northeast. The transition from wave dominance to a mixed energy environment may be related to changes in the depositional mechanisms, these include: increased/decreased fluvial discharge, delta lobe shifting or changing wave influence. Similar changes from wave-dominated shoreface deposits to fluvial-dominated delta front deposits have also been observed in the Spring Canyon Member (Kamola and Van Wagoner, 1995). Although these changes occurred laterally within the same parasequence, increased proximity to the river mouth is interpreted to be the main reason for the changes in the facies.

Combined ripples or wave-modified current ripples indicate relatively rapid deposition by currents followed by partially reworking by waves close to a river mouth. A major decrease in the amount of bioturbation indicates a change to poorer living conditions for the

burrowing animals (Pemberton et al., 1992a). Such changes may reflect a decrease in food supply, an increase in energy, or changes water salinity, all which can be related to the proximity of river outlets and brackish water. This is supported by the presence of syneresis cracks which suggests changes in salinity (Reineck and Singh, 1980). In addition, an erosional, channel-like unit with trough cross-stratification and rip-up clasts is present in S3.3 in Log 12 (Figure 3.19). This unit is interpreted as a storm scour or a minor distributing channel in the proximal part if the OTZ, suggesting a mixed fluvial and storm-dominated environment, influenced by short-time, high-energy events, such as storm scours or pulses of increased fluvial discharge along the shoreline.

Figure 3.19. Storm scour channel/distributary channel in the pOTZ. The channel is up to 2.5 m thick and approximately 10 m wide and truncates the underlying interbedded HCS sandstones and bioturbated mudstones. Note loading structures in the base of the sandstone unit. The exposed canyon wall is oriented approximately east-west. The staff is 1.5 m long.

The bedset boundary separating the fluvial influenced bedset from the wave influenced bedset below, is also somewhat different from the other bedset boundaries in the study area. Whereas the other discontinuity surfaces are very sharp, indicating an abrupt decrease in thickness and amount of HCS stormbeds and an increase in bioturbation, S3.3b is more gradual, displaying an upward coarsening in S3.2 and commonly an upward fining into S3.3, making the definition of the contact problematic (Figure 3.20). This difference in the bedset boundary expression might indicate that there are different mechanisms responsible for the formation of bedset, or that the transition from a wave-dominated to a mixed energy depositional environment (forming the bedsets) is related to other depositional processes. Mechanisms for formation of bedsets and bedset boundaries will be discussed further in Chapter Six.
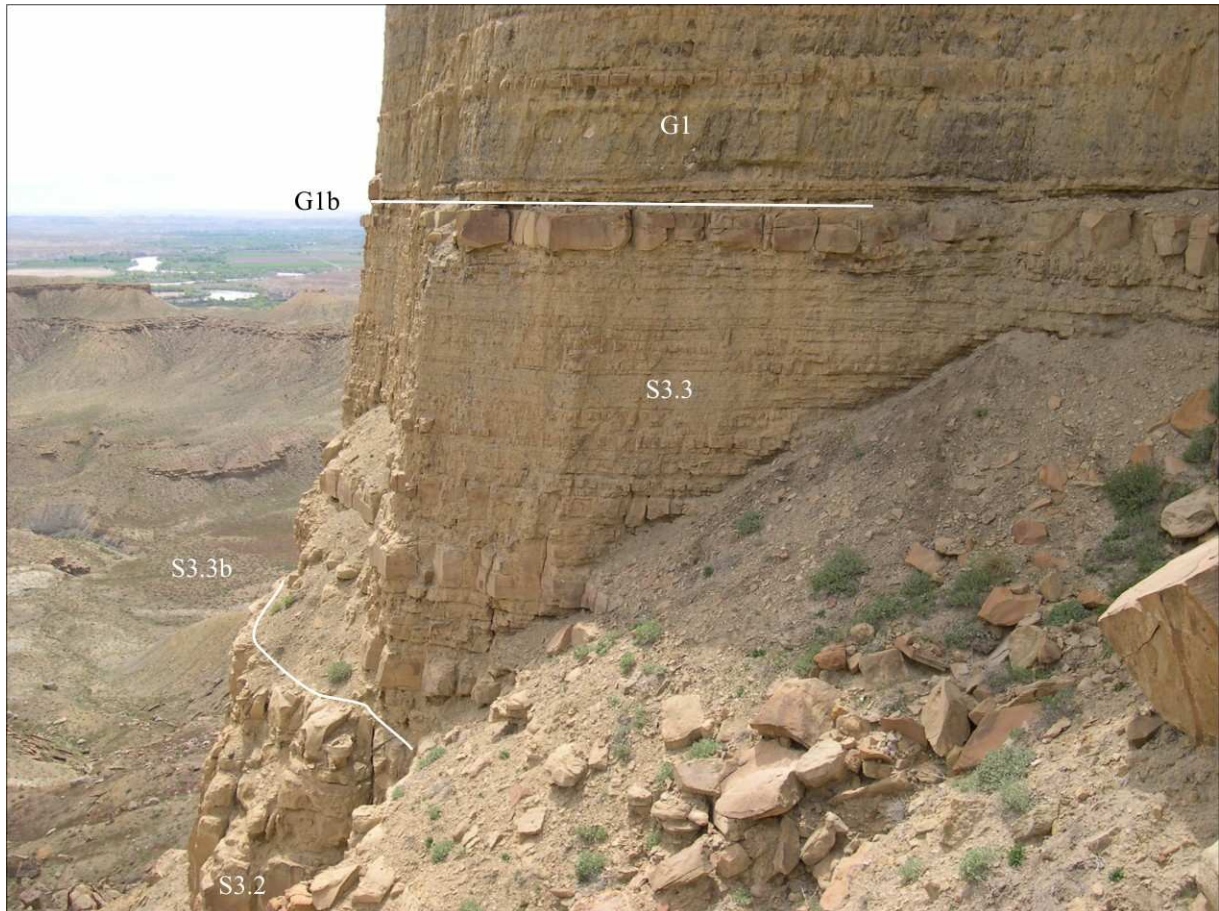
Figure 3.20. Gradual change from storm influenced S3.2 to the overlying, more fluvial influenced S3.3, close to Log 24 in Long Canyon 1. The expression of the bedset boundary is different from the other discontinuity surfaces in the study area which indicate a very abrupt decrease in amount and thickness of sandstone beds. S3.3 is bounded in the top by G1b marking flooding and the transition into the G1. S3.3 is 6 m thick at this location.

In contrast to the other bedsets in S2 and S3, S3.3 is the only bedset which demonstrates a distinct basinward thinning. In Long Canyon 1, this unit can be traced for approximately 9 km oblique to dip, where it also thins from 14.5 m in the proximal part to 5,5 m in the distal part; similar thinning is also observed in Woodside Canyon. Assuming a continuous sediment supply, such changes indicate that less material was transported to the offshore transition zone and the offshore area, and that more material was trapped close to shore. Where fresh water is mixed with sea water, the capacity needed for keeping sediments in suspension decreases rapidly, and sand is deposited relatively close to the river mouth, forming a basinward thinning sediment wedge (Wright, 1977; Bhattacharya and Walker, 1992; Reading and Collinson, 1996). The amount of fluvial influence will decrease along-strike resulting in dominating wave action, and more sediments will therefore be reworked and redeposited into deeper water. Modern studies of North American wave-dominated shorelines has demonstrated a similar basinward thinning of the sediment wedge close to the

river mouths, suggesting that the amount of sediment deposited by the river close to shore, exceeded the wave potential of reworking and redepositing sediments on the shoreface-shelf (Larson and Kraus, 1994).

3.9 Palaeogeography of the wave-dominated shoreface-shelf

The majority of shallow-marine systems in the study area were dominated by waves and are therefore represented by HCS in the LSF and OTZ deposits. The sub-parallel, north-south trending facies belts also suggests wave dominance by reworking and redepositing of sediments along the shoreline. This parallel alignment of facies, and the shape of the shoreline, depends on the amount of sediments deposited by the river, and also on the reworking potential of the waves (Bhattacharya and Walker, 1992; Bhattacharya and Giosan, 2003). If the waves are able to rework and redeposit all sediments introduced by the fluvial source, the shoreline and facies belts will be relatively straight. However, if they are not able to rework the sediments, the shoreline around the river mouth will be more cuspate, arcuate or lobate dependent on the amount of fluvial input (Reading and Collinson, 1996; Bhattacharya and Giosan, 2003). Furthermore, river mouth morphology is also dependent on the angle of the approaching waves (Dominguez, 1996). For example, if the wave approach is perpendicular to the shoreline a symmetrical wave-dominated delta will form as longshore currents, induced by the on-shore waves, are deflected and redeposit sediments along the shoreline on both sides of the river mouth. This situation is very rare and commonly the waves will approach the shoreline at an angle, resulting in a groyne effect in the updrift area where sediments transported by longshore currents becomes trapped close to the river mouth (Dominguez, 1996). In the modern São Francisco strandplain, the updrift part of the shoreline progrades as longshore driven sediments are incorporated into prograding beachridges (Dominguez, 1996). Downdrift of the river mouth, the shoreline progrades as reworked fluvial material, represented by mouth bars and spits, are accreted onto the shoreline, resulting in advancement.

Distribution of facies belts presented in sections 3.2-3.3 illustrates a relatively straight north-south orientation similar to what can be expected in a wave-dominated system. Despite this trend, the transition across most bedset boundaries is associated with minor undulations or bulges in the facies belts. These undulations may relate to geomorphological changes in the shoreline resulting from uneven distribution of sediments transported by the river and longshore drift. The pattern associated with S3b displays no differences along-strike, and

unlike the bedset boundaries, the parasequence boundary does not represent a palaeosurface on the shoreface-shelf as it has been reshaped by the transgressive ravinement (Van Wagoner et al., 1990; Howell et al., in review). The distributions of facies associations represented in Figure 3.9 demonstrates that the transgressive succession immediately overlying the parasequence boundary is better developed in Woodside Canyon, suggesting increased sediment input in this area. The changes associated with S3.2b (Figure 3.4 and Figure 3.5) represent a major difference from Woodside Canyon to Long Canyon 1, as the bedset boundary pinch out and disappears between the two locations. This indicates that the area in Woodside Canyon experienced a relative deepening and a landward shift of facies during the development of this surface, whereas in Long Canyon 1 the system continued to prograde. Moreover, this suggests that the area around Long Canyon 1 experienced continuous or increased sediment supply, whereas the supply was cut off to the area around Woodside Canyon. Possible mechanisms responsible for such changes include: high-frequency changes in climate, channel avulsion and delta lobe shifting, changes in wave climate and changes in sediment supply (Curray et al., 1969; Dominguez et al., 1987; Bhattacharya and Giosan, 2003; Hampson et al., in review; Rodriguez and Meyer, in review). These mechanisms are discussed further in Chapter Six.

At the time of formation of S3.2, the facies belts were again relatively parallel and north-south orientated, reflecting a straight shoreline. This bedset boundary is different from the other boundaries in that it is gradual rather than sharp. This also represents the transition into mixed fluvial and wave influenced deposits, suggesting a change in the deposition environment. The distribution of the facies belts prior to incision and relative sea level fall indicates a slightly more oblique shoreline orientation, although S3 is associated with significant transgressive ravinement, which may affect the present day distribution of facies belts, similar to S3b.

The orientation of wave ripples in S2 and S3 indicates a wave approach from east and northeast (Figure 3.21). The average orientation of facies association belts is north-south, indicating a similar orientation of the shoreline. Ripple orientations therefore suggests oblique wave approach and potential longshore current direction from the north. Within the 23 logged sections, there is only one shallow-marine unit that contains evidence of being deposited by currents (Log 8). This unit is composed of a locally restricted, tangential trough cross stratified sandstone which is truncated by HCS sandstone laterally (Figure 3.22).
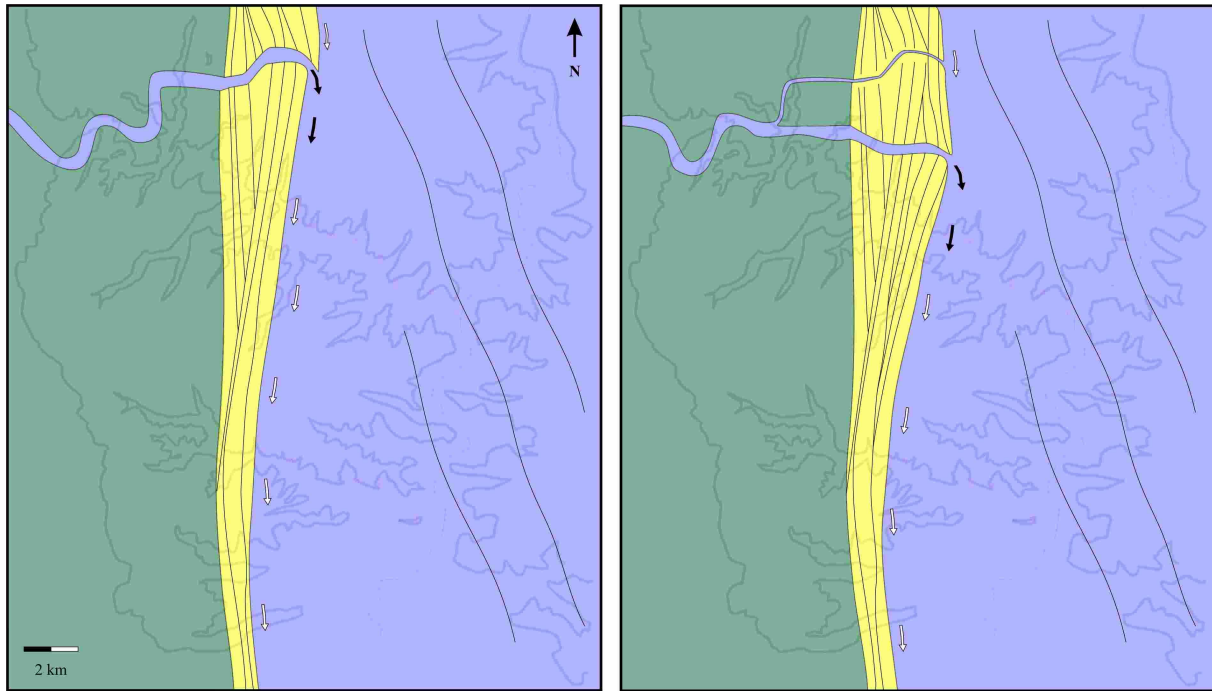
Figure 3.21. Palaeogeographical map of the late S3 shoreline and S3.3. The position of the incised valley along with palaeocurrent directions, thickness relationships between parasequences and bedsets suggests that the river mouth was positioned north of the study area and that longshore drift was towards the south. The appearance of S3.3 in Woodside Canyon and Long Canyon1 suggests that the river mouth shifted down-drift, resulting in increased current influence on the bedset in the study area. Black and white arrows indicate fluvial and longshore transported sediments respectively. Main wave approach is from the northwest.

The cross-stratification suggests a palaeocurrent direction towards the south. Although one measurement is insufficient to draw any conclusions concerning the palaeocurrent pattern, and the fact the cross bedding may not relate to longshore currents at all, the main flow direction fits well with the interpretation of a southerly directed sediment transport. A similar palaeocurrent direction has also been reported from the underlying Spring Canyon and Kenilworth Member (Hampson and Howell, 2005).

As can be seen in (Figure 3.14), the incised valley that is associated with S3 is mapped in the western and central part of the study area, suggesting an eastern and northeastern orientation of the estuary during deposition. At the time of incipient incision, rivers tend to follow the existing channels as lowering of the base level inhibits lateral erosion (Schumm and Ethridge, 1994).

In the western part of the study area, the valley is orientated relatively east-west. However, in the central and eastern part, the valley is deflected northwards into a northeastern direction. This suggests that the river had a similar course, going east and northeast, feeding a new shoreline north of the study area.

Changes in bedset and parasequence thicknesses along-strike are another indication of the proximity of a sediment source north of the study area. One would expect a parasequence to become thicker and more sandy towards the main sediment source, and to

Figure 3.22. Tangential cross bedding in Log 8. The bed is truncated laterally by amalgamated HCS sandstone. Direction of palaeoflow is towards the south.

thin along-strike as the amount of sandy material decreases. Although there are some measurements variations, such a thickness comparison between log sections positioned along-strike (north-south), suggests that S3 is slightly thicker in Woodside Canyon than it is in Long Canyon 1. This may be an indication of increased sediment input in the northern part, but could also reflect differential transgressive erosion or compaction (discussed above). There are also lateral thickness variations between the individual bedsets which indicate the same interpreted relationship.

Figure 3.23. Tabular (occasionally bidirectional) cross bedding in overlying Grassy Member (Log 9). The deposits are interpreted as fluvial and tidal influenced USF deposits, suggesting a nearby river mouth feeding the Grassy shoreline. Similar deposits have not been observed in the Sunnyside Member. The staff is 1.5 m long.

Although there is no direct evidence of a river mouth in, or north of the study area, there is clear evidence of such a fluvial system in the overlying G1, which lies stratigraphically above S3 in Woodside Canyon (Figure 1.7). In this parasequence, fluvial channels (represented by tabular and sometimes bidirectional cross-stratification) cut into the

shoreface indicating the proximity of a river mouth (Figure 3.23). These features are interpreted to be the remnants of a river feeding the younger Grassy shoreline. Similar features in the non-marine part of the Sunnyside Member are probably removed by the incised valley.

Chapter Four – Internal Facies Distribution and Palaeogeography of the Mixed Wave and Tidal-Dominated Sunnyside Estuary

4.1 Introduction

An estuary is defined as "the seaward portion of a drowned valley which receives sediment from both fluvial and marine sources, and which contains facies influenced by tide, wave and fluvial processes; the estuary is considered to extend from the landward limit of tidal facies at its head to the seaward limit of coastal facies at its mouth"(Figure 4.1) (Boyd et al., 1992; Dalrymple et al., 1992). The Sunnyside succession in Woodside Canyon includes an interval that has previously been interpreted as the estuarine fill of an incised valley (Howell and Flint, 2003). Within this present study, this interval has been mapped and logged east from the location of the work presented by Howell and Flint (2003) and their model has been critically assessed and expanded upon. Understanding the facies and distribution of the valley fill has important implications for understanding the sea-level history of the Sunnyside Member.

A typical wave-dominated estuarine succession is composed of fluvial sediments in the lower part, overlain by inter-valley fluvial deltas, muddy lagoons, flood deltas and barrier islands deposited as the estuary filled during transgression; demonstrating a distinct tripartite facies distribution (Dalrymple et al., 1992). In contrast, a typical tidal-dominated estuarine succession is composed of fluvial sediments in the lower part, overlain by tidal-influenced meandering channels, tidal bars, marshes and sandflats. Tidal-dominated estuaries lack the characteristic tripartite facies distribution which is characteristic of wave-dominated estuaries (Dalrymple et al., 1992). This is because tidal energy penetrates farther landward than wave energy, resulting in redistribution of sandy material along the estuarine dip-axis by tidal currents (Dalrymple et al., 1992). Figure 4.1 illustrates the idealized facies distribution in a tidal influenced estuary (Dalrymple et al., 1992). In the distal, marine dominated zone, sandflats and mudflats prevail along with large, shoreline perpendicular sandbars. Farther landwards, in the mixed energy zone, meandering channels, marshes and mudflats dominates. This represents the part of the estuary where tidal and fluvial forces are equivalent, and where the net energy is the lowest. A decrease in current energy results in a decrease of the transport capacity, deposition and meandering of which the river (Dalrymple, 1992; Dalrymple et al., 1992). In the most landward and fluvial-dominated part of the estuary, the idealistic facies

model predicts straight fluvial channels and marshes. The amount of tidal influence will decrease upward and landward in the estuary due to increased friction and fluvial energy.
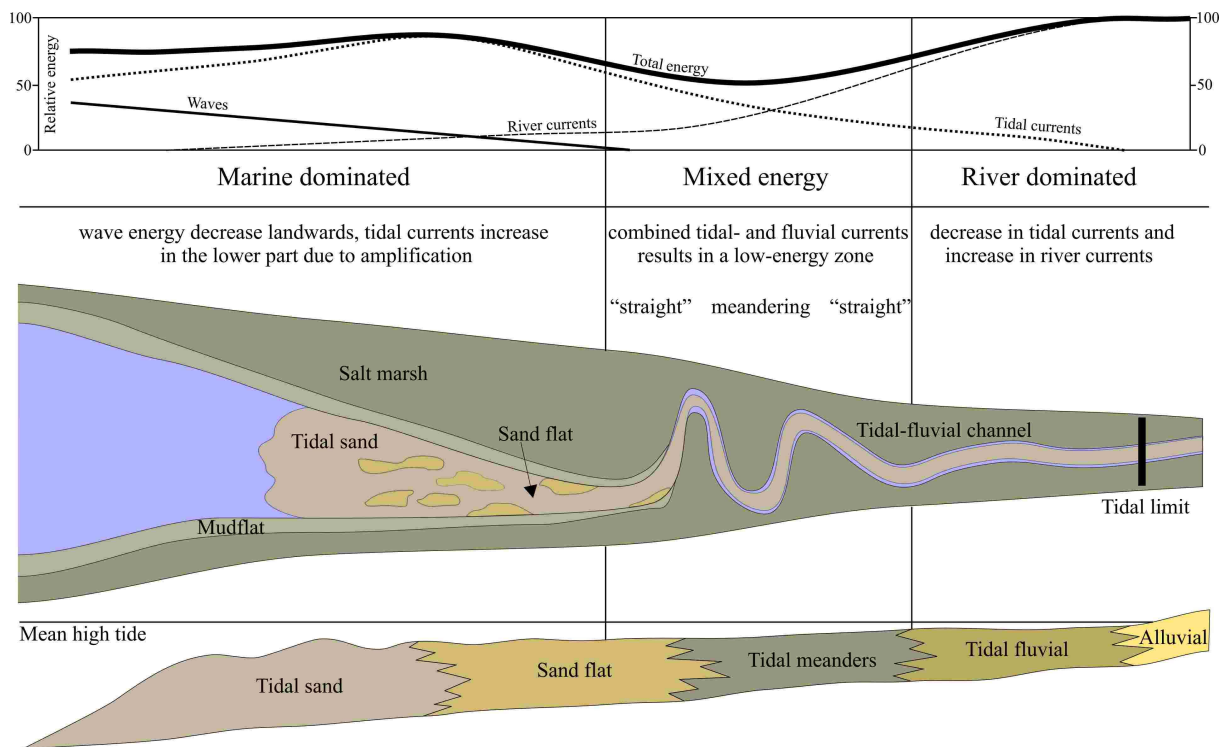

Figure 4.1. Idealized tidal-dominated estuary. The facies will be less tidal influenced and more fluvial influenced landwards, going from sandy bars and flats in the tidal-dominated zone, into heterolithic sand and mud in the mixed zone. In the upper part of the estuary, the facies will be sandy and dominated by river currents. Modified from (Dalrymple et al., 1992).

4.2 Internal geometries of the incised valley deposits

Figure 4.2 illustrates the distribution of estuarine facies which have been observed in the upper Sunnyside incised valley. The most proximal part of the section demonstrates an overall upward transition from tidal-influenced fluvial deposits into meandering channel deposits. Farther basinward, meandering channels also juxtapose tidal bar deposits, lagoonal and tidal

Figure 4.2. Correlation of logsections containing incised valley strata in Long Canyon 2 and Woodside Canyon. The facies distribution is relatively complicated, but there is a general trend of increased marine influence upward in the succession. Localized tidal influenced, fluvial deposits are present in the proximal part of Woodside Canyon overlying the SB. IHS dominates, but also large tidal bars are present. Subaerially exposed bars in the central part of the study area reflect a sandy and high-energy zone within the estuary. Lagoonal and tidal flat deposits commonly occupy the uppermost part of the valley fill, representing progradation, drowning and abandonment of the river channels. The valley fill is bounded in the upper part by a flooding surface (G1b) which represents a major landward dislocation of the shoreline, and the transition into the overlying Grassy Member. The flooding surface is commonly associated with a *Glossifungites* firmground and a transgressive lag, indicating significant erosion during sea level rise. See appendix for key and complete logs.
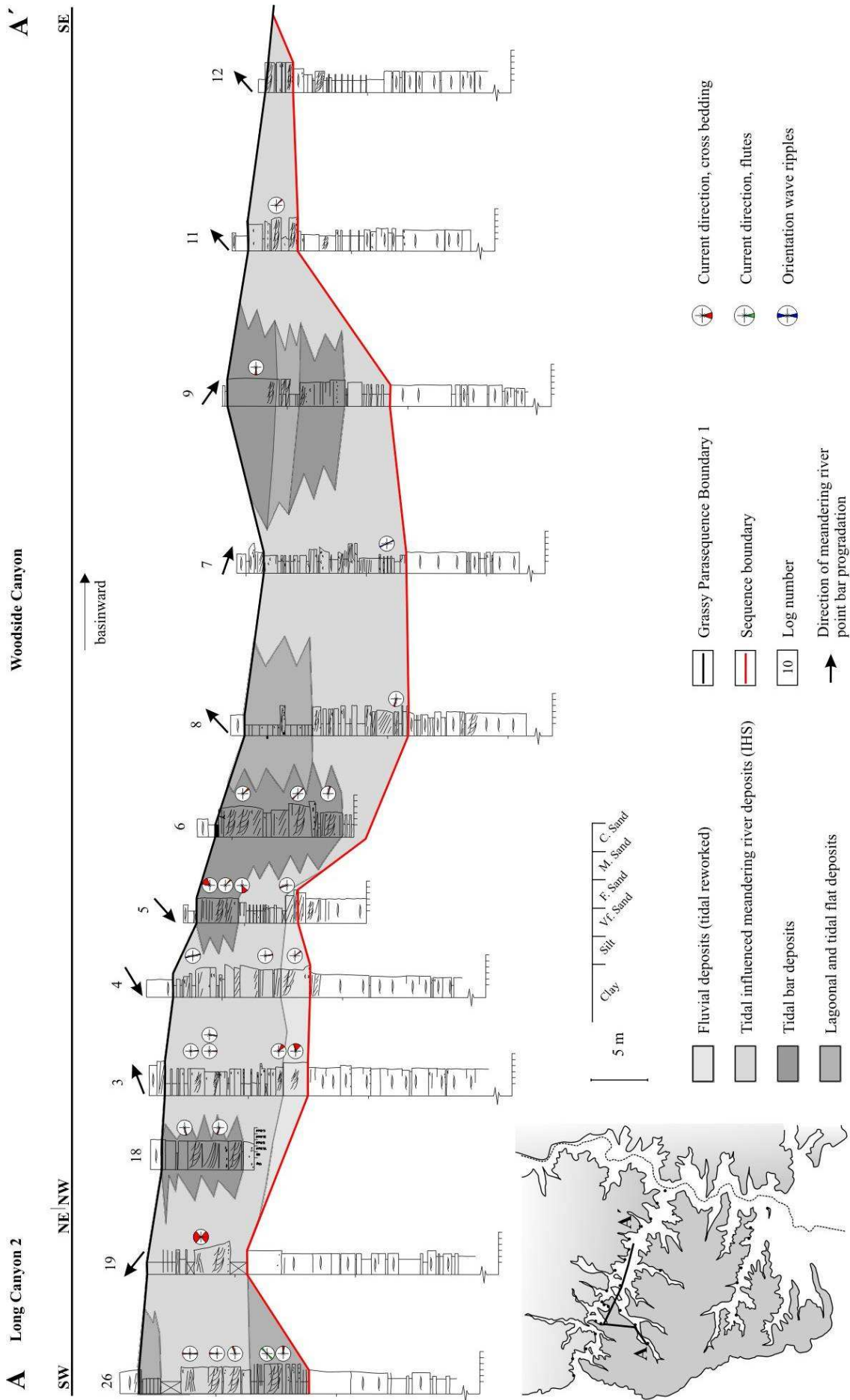
flat deposits (Figure 4.3). In the central part of the exposed valley fill (in the area close to Log 5 and Log 6, Figure 4.2), large tidal bars contain evidence of subaerial exposure. Several units within the tidal bar successions are bleached and white in color, containing sub-vertical root structures indicating colonization by plants. Low angle, planar parallel stratified sandstone resembling foreshore beach deposits also suggest subaerial exposure and wave reworking of the bars.
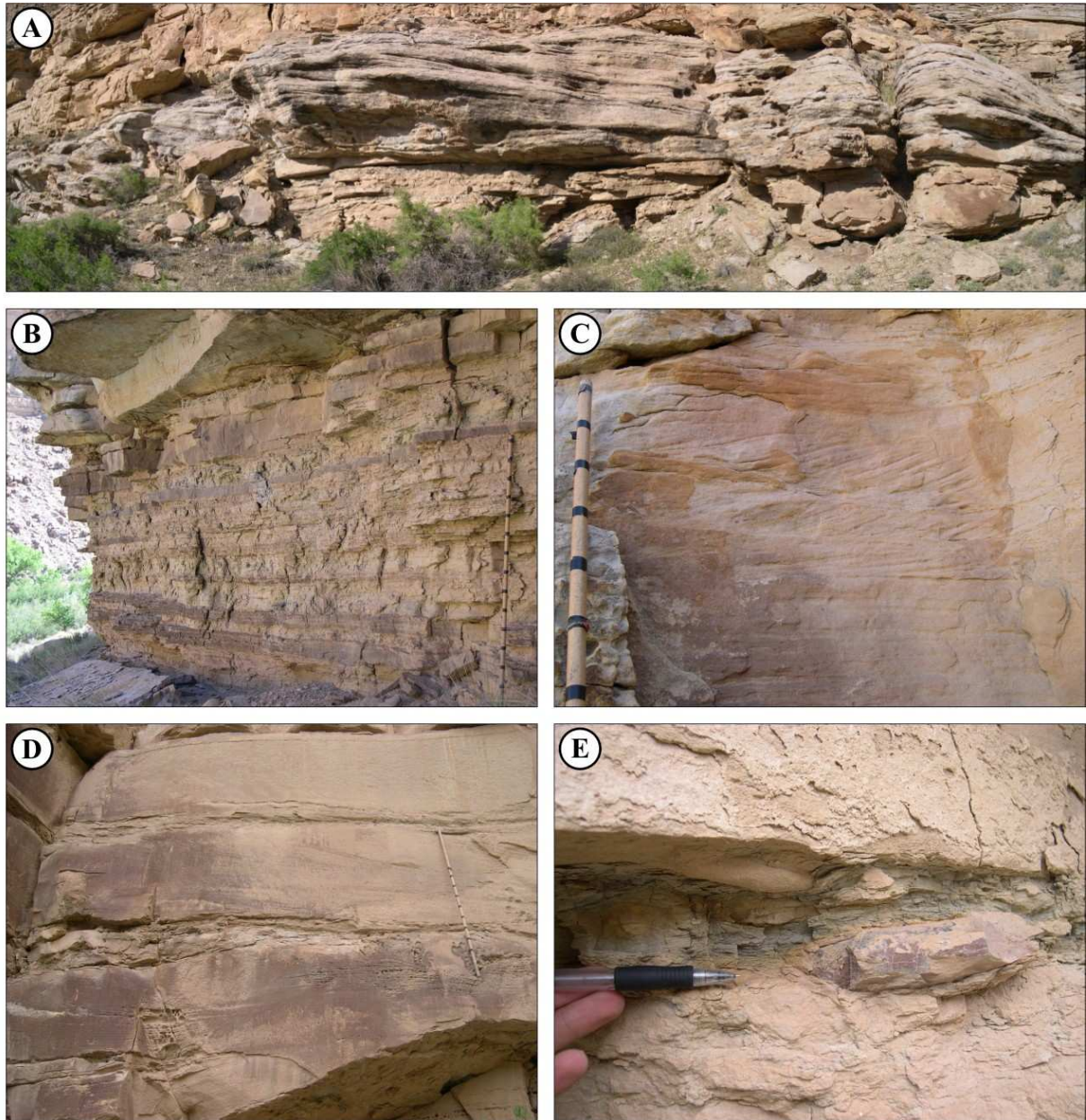
Figure 4.3. Estuarine deposits in the main incised valley section in Woodside Canyon. (A) Large, subaerially exposed tidal bars (approximately 8 m thick) truncates (B) underlying IHS. Main progradational direction is to the right, and out of the picture.(C) The bars also demonstrate small sets of (sometimes bidirectional) tabular and sigmoidal cross-stratification. (D) Several sets of large, subtidal bars are also locally present (flow is towards the right). Commonly, their bases contain mud-drapes and (E) large clay rip-up clasts. The staff is 1.5

Palaeocurrent measurements indicate a relatively complicated current pattern, where meandering channel deposits (IHS) indicate dominant flow towards the north and south, whereas bar deposits suggest flow towards the east and west.There are also significant variations in the orientation of the IHS, but most inclined beds reflects point bar migration
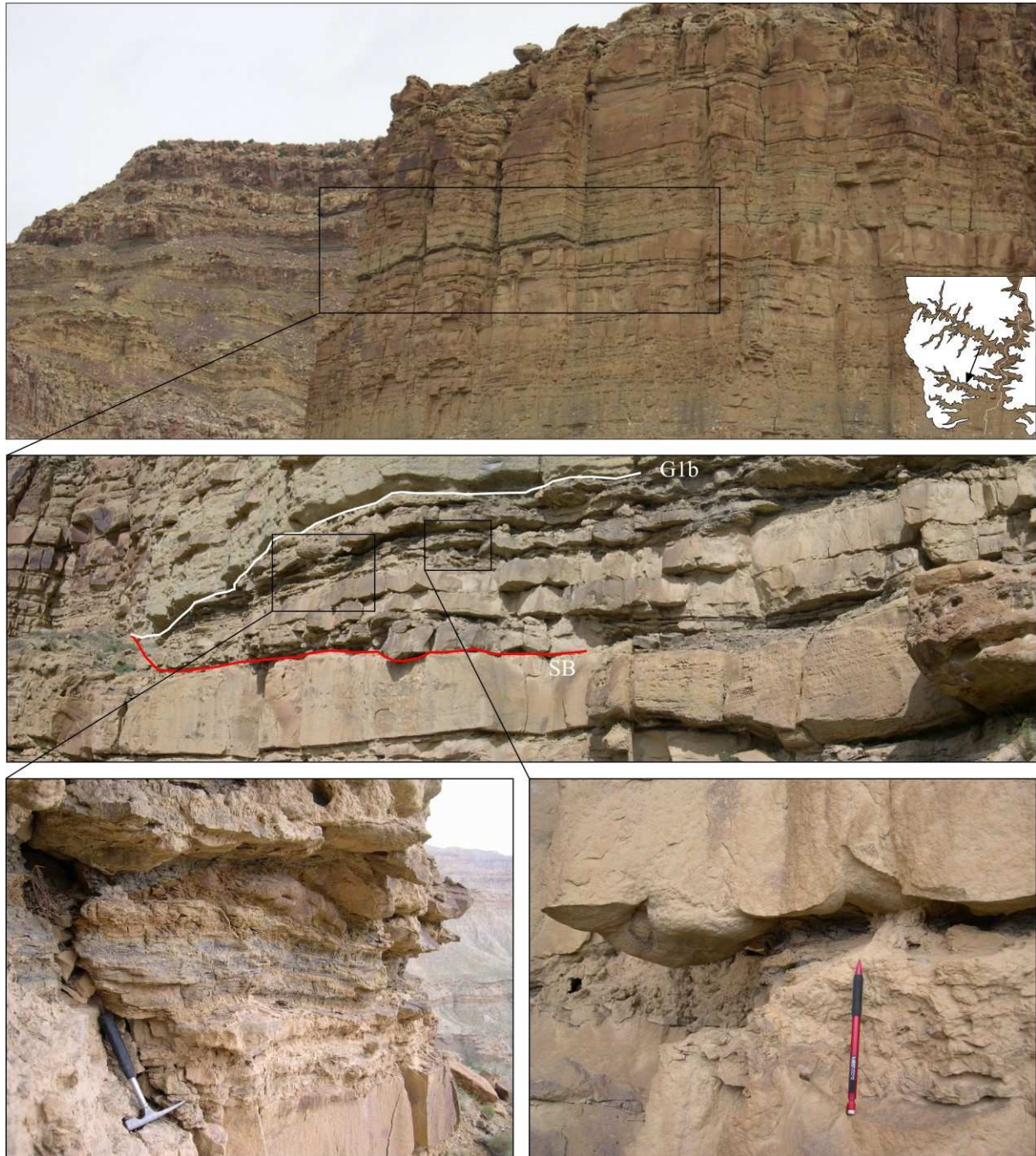
Figure 4.4. Incised valley deposits in Long Canyon 1 (Log 22). (A) The outcrop was traced for 50 m along the canyon wall, where the margin is marked by a distinct erosional surface. (B) The succession is upward fining and marked by three sandstone channels in the lower part, and (C) interbedded, heterolithic sandstone and mudstone in the upper part. Rip-up clasts and (D) load casts are abundant. The unit is up to 4 m thick. The pencil is 15 cm long.

towards the northeast, southwest and southeast (normal to the overall palaeocurrent directions in the area). Wave ripples are oriented in a similar direction as those observed in the shallow-marine deposits, suggesting wave approach from the east and northeast.

Incised valley strata are recognized in all proximal log-sections in Woodside Canyon, in Long Canyon 2, Jenny Canyon and in one section in Long Canyon 1 (Figure 4.2 and Figure 3.3). The thickness of the incised valley succession observed in the study varies between 0 and 16 m, and the general pattern is a continuous thinning basinwards and eastwards where the valley pinches out between Log 13 and Log 14 (Figure 4.2). The incised valley is close to 6 km wide in the western part of the Beckwith Plateau and widens eastward, approximately 8 km in the central part of the study area. The presence of estuarine deposits in Long Canyon 1 is restricted to one locality (Log 22, Figure 4.4). This section is 4 m thick and was traced laterally for approximately 50 m. No palaeocurrent readings were obtained, and the succession consists of interbedded sandstone and mudstone. The unit demonstrates a distinct upward fining trend represented by channel sandstones with abundant rip-up clasts in the lower part, and interbedded discontinuous sandstones and mudstones further up. Coal fragments, *Teredolites* burrows and loadcasts are abundant in the interbedded, heterolithic part of the succession (Reineck and Singh, 1980; Collinson and Thompson, 1989).

4.3 Palaeogeography of the mixed wave and tidal-dominated estuary

Trough cross-stratified sandstone of fluvial origin (FA7) has been observed in several locations within the study area (Figure 4.2) and are interpreted as falling stage, or early transgressive stage deposits (Dalrymple et al., 1992; Zaitlin et al., 1994). The sandstone is interpreted to be remnants of a braided river (Figure 2.11 and Figure 2.12) (Collinson, 1996) which has been preserved in low areas during periods when the incised valley was mainly bypassing sediment to the lowstand shoreline (Figure 4.5). Palaeocurrent measurements indicate flow towards the southeast, which is slightly oblique to the main dip-direction of the incised valley (west southwest-east northeast). Shell fragments and mud-drapes towards the top suggest that these fluvial deposits have been tidally reworked during later transgression. Because no distinct boundary separating purely fluvial from IHS deposits have been observed, it is difficult to recognize any transgressive surface within the estuarine deposits, although it should be located in the lowermost part of the succession (Zaitlin et al., 1994). The transgressive surface defines the transition from the LST to the overlying TST (Van Wagoner

et al., 1990). The lack of thick fluvial lowstand units in the base of the incised valley indicates that the time of lowstand progradation was relatively short.
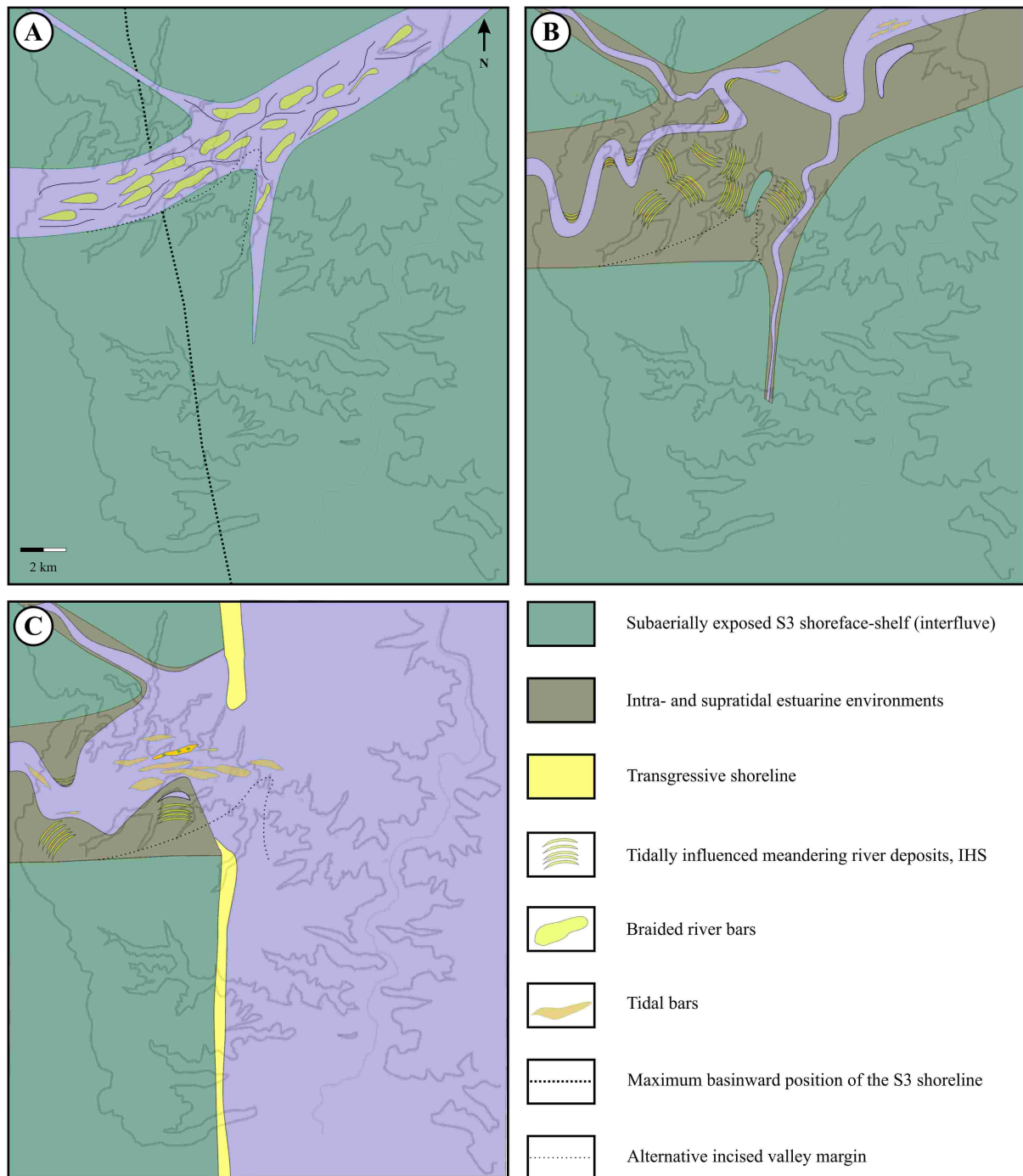
Figure 4.5. Palaeogeographic history of the incised valley in response to relative sea level change. (A) During the lowstand, the incised valley mainly experienced sediment bypass, although some fluvial sediments were preserved in low areas. (B) As sea level rose, these fluvial deposits became reworked by tidal currents and the estuary was filled with IHS deposits. The inclined heteroliths observed in the field (B) represents the approximate orientation and migration direction of the meandering pointbars. (C) Tidal bars were deposited in the meandering river, and as the shoreline migrated landwards, high-energy, sandy tidal channels (representative of the more distal and tidal-dominated part of the estuary) deposited large bars in the present day central part of Woodside Canyon. The interfluve and an alternative positioning of the valley margin is indicated close to Log 10 (see section 4.4 for further discussion).

A rise in relative sea level subsequent to the lowstand conditions resulted in rapid landward shoreline migration and marine intrusion into the incised valley. A sharp facies boundary between tidal influenced fluvial deposits and tidal influenced meandering deposits (of FA7 and FA8), is locally present. This boundary marks the transition from fluvial to estuarine deposits and is represented by the initial flooding surface (Zaitlin et al., 1994). As the sea level continued to rise, the distal part of the estuary was flooded and tidal influence extended up the meandering channels (Figure 4.5). This is evident from abundant *Teredolites* borings (Figure 4.6), suggesting partially marine influence (Bromley et al., 1984; Pemberton et al., 1992a). *Teredolites* are wood-boring bivalves which commonly occur in log jams and compacted organic material, such as peat (Bromley et al., 1984). In addition, *Arenicolites* burrows of the *Skolithos* inchnofacies, which are also common in intertidal environments (Pemberton et al., 1992b; Maceachern and Pemberton, 1994), have been observed in one section (Log 18, Figure 4.2).
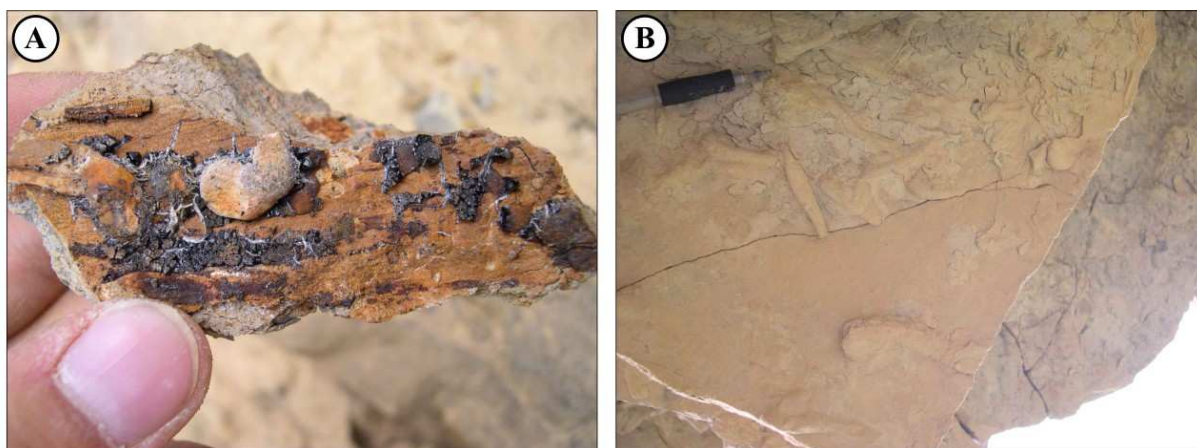
Figure 4.6. (A) *Teredolites* in coalified wood and (B) *Arenicolites* within the inclined heterlolithic deposits suggests brackish conditions.

The tidally influenced meandering channel deposits (FA 8) commonly overlie reworked fluvial deposits and represents an upward transition into a more distal facies association. This facies is normally very heterolithic, and variations in the sandstone and mudstone content along with differences in the dip of the inclined beds, probably reflect various types of channels within the estuary (Thomas et al., 1987). The successions represented by the IHS coincide with the mixed energy zone of a tidal-dominated estuary (Figure 4.1), as described by Dalrymple et al. (1992).

Figure 4.7 illustrates three different end-members of IHS observed in the study area. The muddiest unit (A) is inclined relative to the underlying beds which are truncated, and to

the overlaying flooding surface at the base of G1.These inclined beds have a dip-gradient up to 10-12°. This unit is interpreted to represent a low-energy, meandering, estuarine channel which was sheltered from high-energy flood events. Some of the units may also reflect abandonment and passive filling of the same channels. More heterolithic meandering deposits (B) are composed of alternating sandstones and mudstones, and indicate similar dip-gradients as the muddy units. As individual IHS beds were traced from the top of the incised valley to the valley floor, they demonstrated a decrease in the dip-angle towards the base, indicating flattening towards the channel thalweg as expected within a meandering channel point bar (Thomas et al., 1987; Collinson, 1996). The sand dominated IHS (C) contains more gently dipping sandstone beds (of approximately 2-10°), indicating deposition in a wider, more high-energy channel. Similarly to the muddy units, the dip-gradient of the inclined beds is also lower towards the base of the unit, suggesting a transition into deeper water (Thomas et al., 1987). Ideally, these meandering point bar deposits could be traced from the uppermost part of the point bar (and the subaerially exposed part of the estuary) to the middle part of the channel, demonstrating a sigmoidal shape (Thomas et al., 1987). But because the uppermost part of the IHS probably was removed by significant transgressive erosion during sea level rise, only the foresets and bottomsets have been preserved.

The dip-direction of IHS beds indicates point bar migration in a variety of directions, commonly normal or oblique to the palaeocurrent in the area (Figure 4.2). Both muddy and sandy meandering channel successions illustrate this pattern, suggesting that a variety of tidal influenced channels migrated back and forth within the estuary.

FA8, 9 and 10 are interpreted to be juxtaposed within the estuary, reflecting the heterolithic nature and variety of these depositional environments (Figure 4.2 and Figure 4.5). Tidal bars overlying IHS suggests deposition within the meandering channel. In the western part of the study area (Log 18, Figure 3.3) large scale, trough cross-bedding (FA9) shows landward directed palaeocurrents (west). Similar, large scale, landward directed cross-bedding with organic-draped foresets are also present farther east in the study area, indicating a dominant flood current towards the west. These units are interpreted to represent large tidal bars, laid down in a sandy, high-energy part of the estuarine channel.

In the central part of Woodside Canyon (close to Log 5 and Log 6, Figure 3.3), stacked sets of large scale, cross-stratified sandstone (FA9) indicate a different palaeocurrent direction, although a main component is directed towards the southeast, indicating dominating
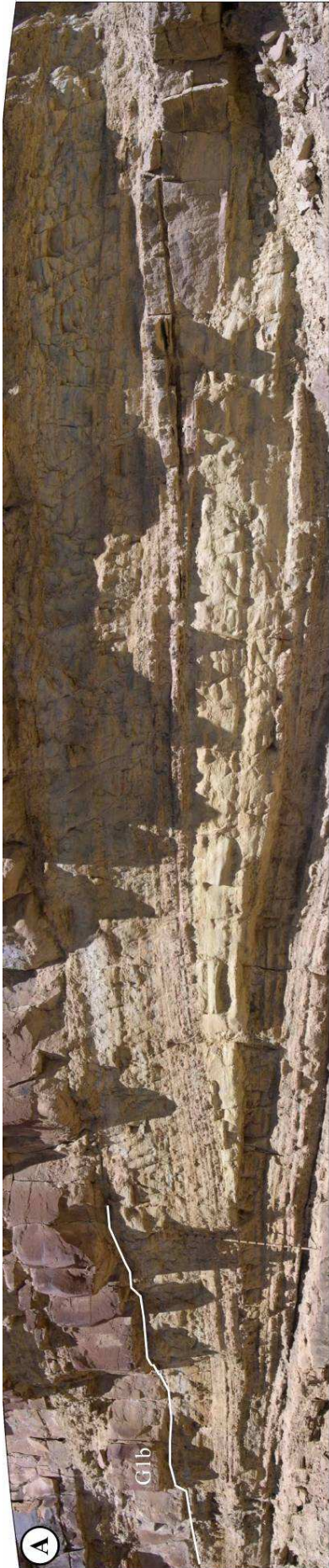
Figure 4.7. IHS within the study area has a variety of expressions, reflecting the diversity of depositional environments within the estuary. Muddy (A) and mixed muddy and sandy (B) units have generally steeper dipping beds compared to sandy units (C). The dip-angle and orientation of the IHS reflects the width and progradational direction of the meandering river, suggesting a complicated pattern of rivers within the estuary. Staff for scale in A and B is 1.5 m long. The exposed canyon wall in C is approximately 300 m long.

ebb currents. Chaotic and erosive based sandstone beds indicate deposition within a major channel (Figure 2.16, C). The upper part of the unit is bleached and penetrated by roots. A poorly developed coal is present on the uppermost part of the succession, suggesting that this sandy unit was subaerially exposed for a considerable amount of time (Miall, 1992; Collinson, 1996). This accumulation of sand is interpreted as a sandwave in the central part of the estuary, and a landward shift of the facies representing a transition into a higher-energy environment in the outer, marine influenced part of the estuary (Figure 4.5) (Dalrymple et al., 1992; Zaitlin et al., 1994). The partially subaerially exposed sandwave reflects high sediment input and possibly minor periods of paused sea level rise and stillstand.

The extensive tidal influence in this overall wave-dominated system is probably related to amplification of the lower meso-tidal (Howell et al., in review) environment within the estuary. The funnel-shaped estuary results in increased tidal currents landwards, as the width of the valley decreases. Farther up-dip, frictional forces and fluvial currents compensate and neutralize the landward directed tidal influence (Figure 4.1) (Dalrymple et al., 1992).

Muddy channels, tidal flats and small lagoons/ponds (FA10) reflect low-energy, inter and supra-tidal parts of the estuary. IHS is commonly overlain by very fine-laminated, mudstone successions indicating a decrease in current energy. Upward fining successions in Log 19 and Log 26 (Figure 4.2 and Figure 4.8) represents a typical transition from erosive, tidal influenced channel deposits in the lower part, into interbedded heteroliths and muddy channel deposits in the upper part, typical of a migrating point bar succession (Thomas et al., 1987). Log 8 (Figure 4.2) illustrates a similar transition from IHS to laminated mudstone deposits, reflecting abandonment and passive filling of the meandering channel. Coarse-grained beds containing shell fragments are interpreted to result from high-energy events, such as storms or major floods.

Although though the estuarine facies associations in the incised valley show a somewhat complicated distribution laterally, the successions demonstrate increased marine influence upwards. This reflects continuous sea level rise and flooding of the distal pars of the estuary (Figure 4.5). As the transgressive shoreline reached the position of the old S3 shoreline, the gradient decreased abruptly from the shoreface-shelf to the coastal plain. This

85

resulted in a rapid landward shift of the shoreline and drowning of the distal part of the estuary. The valley fill is overlain by G1 which represents renewed shoreline progradation.

Figure 4.8. Upward fining estuarine succession in Long Canyon 2 (Log 19). Lower half is composed of sandy, gently dipping IHS, whilst the upper part is muddy and dips more steeply. The sharp transition between the two units may represent partially channel abandonment during transgression and infilling of the estuary, a transition into more muddy point bar deposits, or, alternatively, truncation and amalgamation of two separate point bars. The incised valley succession is 8 m thick, and is bounded by a transgressive ravinement surface (G1b), and is overlain by G1.

.

4.4 Incised valley topography

Incised valley deposits have been observed in all logsections west of Log 13, except for Log 10 (Figure 4.2). Figure 4.9 illustrates a down-dip correlation of Log 9, 10 and 11 in the central part of Woodside Canyon. The most proximal section (Log 9) represents a 13,5 m thick succession of incised valley strata cutting into, and eroding the entire S3.3. In Log 10, S3.3 is fully preserved and displays wave influenced, locally intensely bioturbated OTZ deposits overlain by amalgamated HCS of the LSF; typical of the shoreface-shelf environment. Farther east (in Log 11), the same bedset is truncated by another, 4 m thick incised valley unit. The lack of incised valley strata in Log 10 may be explained by three scenarios: i) differential incision resulted in the area surrounding Log 10 being exposed as an island in the middle of the estuary, ii) the area near Log 10 was located outside the incised valley and was part of the interfluve during incision, or, iii) the area only experienced shallow incision and the valley fill was later removed by transgressive erosion.
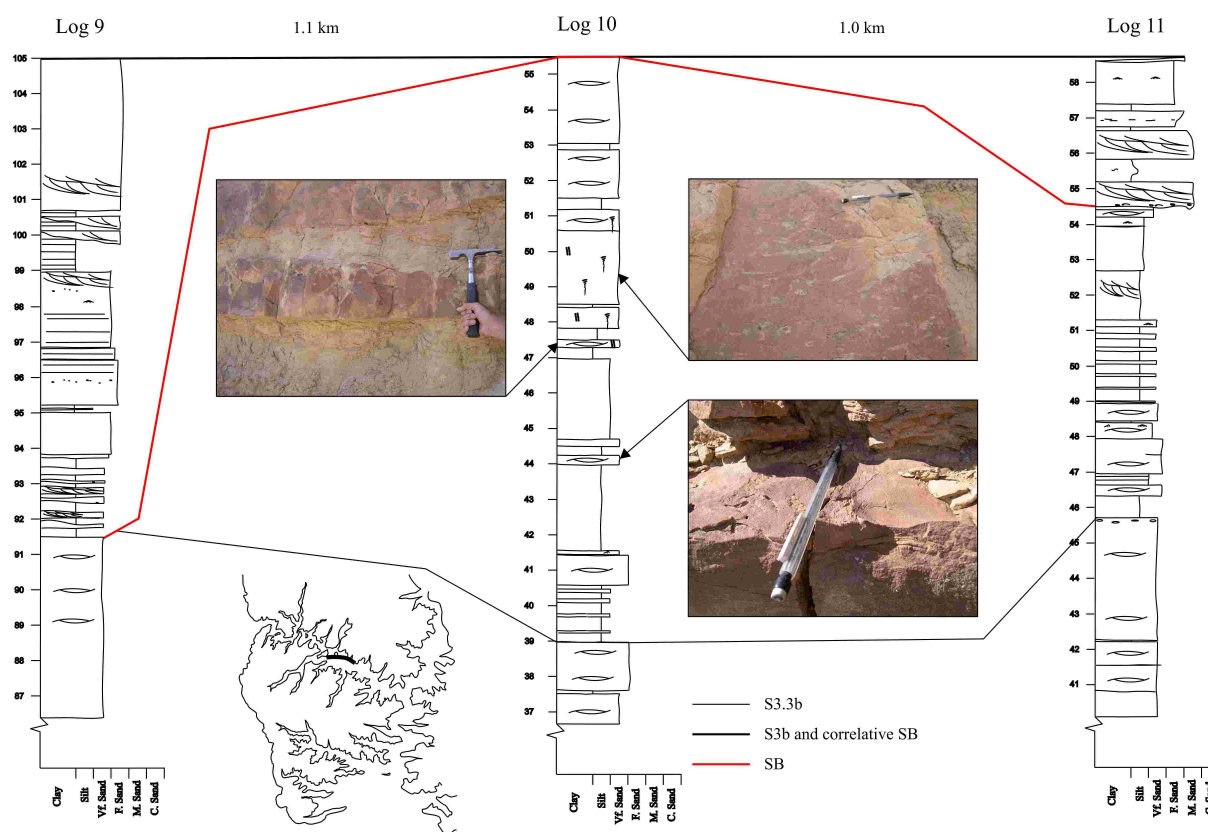
Figure 4.9. Log 9 is located 1,1 km west of Log 10 and represents approximately 14 m of incised valley strata cutting into S3.3 and LSF strata of S3.2. Between the two locations, the incised valley disappears, leaving Log 10 apparently unaffected by the incision, and the SB coincide with the G1b. At this location, S3.2 is overlain by S3.3 which represents interbedded HCS sandstone and commonly intensely bioturbated mudstone typical of the OTZ and LSF (pictures). No evidence of subaerial exposure has been observed in the section. Log 11 is located 1 km farther east, representing 4 m of valley fill cutting into fluvial and wave influenced OTZ deposits of S3.3. The correlated section is indicated in black on the map. See appendix for key, and Figure 3.4 for position in the down-dip correlation panel.

Intravalley highs have previously been reported from the overlying Grassy Member, where they are orientated parallel to the incised valley; being less than 1 km wide and approximately 4 km long (O'Byrne and Flint, 1995). Except for local occurrences of siderite nodules and roots, transgressive erosion has also removed all evidence for subaerial exposure in the this unit (O'Byrne and Flint, 1995).

Due to limited access to the outcrops near Log 10, it is not possible to trace the sequence boundary to the south side of the canyon, and it is therefore difficult to determine the lateral extension of the unaffected succession in Log 10. But assuming an intra valley high was orientated parallel to the incised valley, similar to the interfluves in the Grassy Member (O'Byrne and Flint, 1995), it may extend for several kilometres in this direction. The width of the interfluve, on the other hand, can not have been more than approximately 1 km, assuming

the valley margins terminate half way between Log 9 and 10, and between Log 10 and 11. In contrast to the interfluves reported from the Grassy Member, no nodules or roots have been observed in the upper part of Log 10, and there is no other evidence suggesting subaerial exposure; although these may have been removed by later erosion.

Alternatively, the area represented by Log 10 may have been part of the surrounding interfluve rather then an intra-valley high (Figure 4.10). In this case, a tributary valley may have connected with the main valley in the vicinity of Log 11 and Log 12, leaving the surrounding Log 10 squeezed between the tributary and the main valley. The interpretation of the estuarine valley fill located in Log 22 being a tributary, draining towards the north and northeast, supports this theory. However, because of the remote location of the incised valley fill (approximately 7 km south of Woodside Canyon, Figure 3.3) and its restricted lateral extent, no positive connection can be established between the two systems.
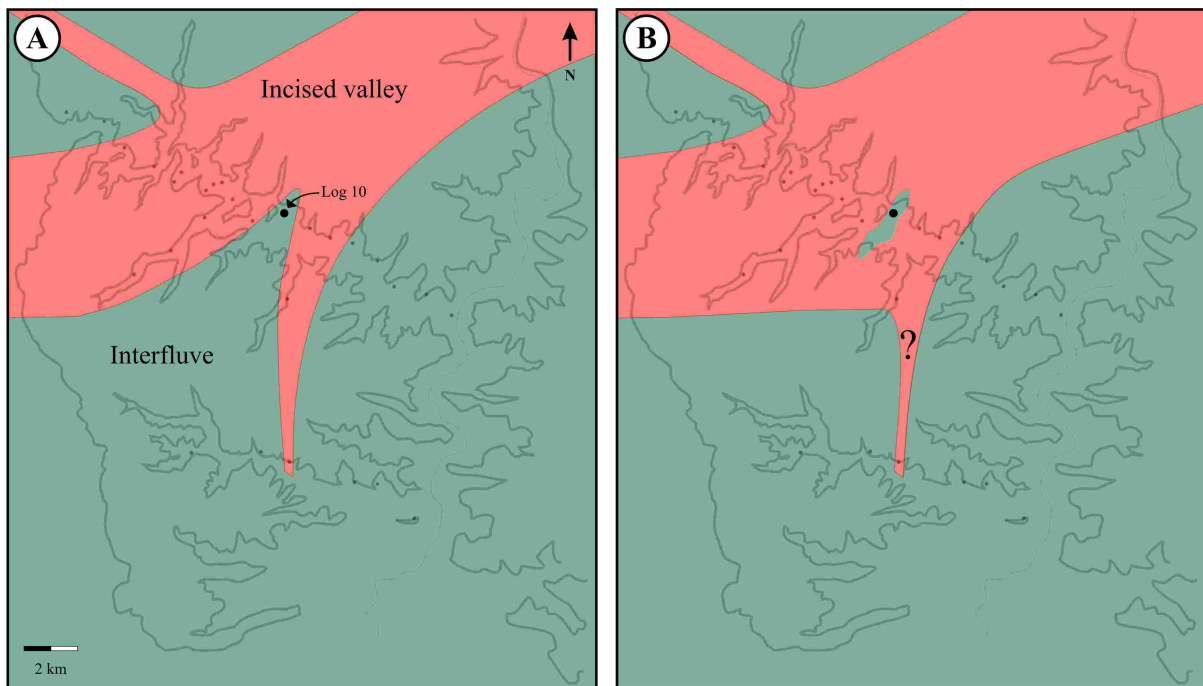
Figure 4.10. The lack of incised valley strata in Log 10 may relate to (A) a tributary draining from the south, which was connected with the laterally restricted incised valley unit present in Log 22, resulting in the area close to Log 10 being a part of the surrounding interfluve. Or, alternatively, (B) the area represented by Log 10 is an intra valley interfluve positioned parallel to the main incised valley. Lack of valley fill may also be explained by extensive transgressive erosion.

A third explanation for the relationships observed in Woodside Canyon, which would also explain the localized exposure of valley fill in Long Canyon 1, is removal of a significant amount of incised valley fill by transgressive erosion. Relatively thick transgressive lag deposits and well developed *Glossifungites* firmgrounds (Pemberton et al., 1992b;

Maceachern and Pemberton, 1994; Pemberton, 1998), together with the lack of evidence for lowstand shorelines and subaerial exposures, supports this interpretation (see section 3.7 for a more detailed discussion on transgressive erosion). Further detailed mapping of the valley fill and the sequence boundary close to Log 10 and on the south side of the canyon may reveal the true outline of the incised valley in this area.

4.5 Implications for the position of the lowstand shoreline

In the previous sections, it has been argued that the estuarine deposits which outcrops in Woodside Canyon represents the central and distal part of a mixed wave and tidal-dominated estuary, as described by Dalrymple et al. (1992), Zaitlin et al. (1994), Howell et al. (in review) and Howell and Flint (2003). According to this interpretation, a considerable amount of the estuary should be located basinward (east) of the area represented by Woodside Canyon, as the facies associations shift landwards during sea level rise and infilling of the estuary (Zaitlin et al., 1994). Woodside Canyon estuarine deposits represents tidal influenced meandering channels and tidal bars in the mixed-energy zone, indicating that the marine influenced, basinward part of the estuary (Dalrymple et al., 1992) was situated farther east of the study area. The gently thinning incised valley unit which pinch-out between Log 12 and 13 (Figure 4.2 and Figure 3.5) is therefore interpreted to represent the southern valley margin, and not its maximum basinward extent.
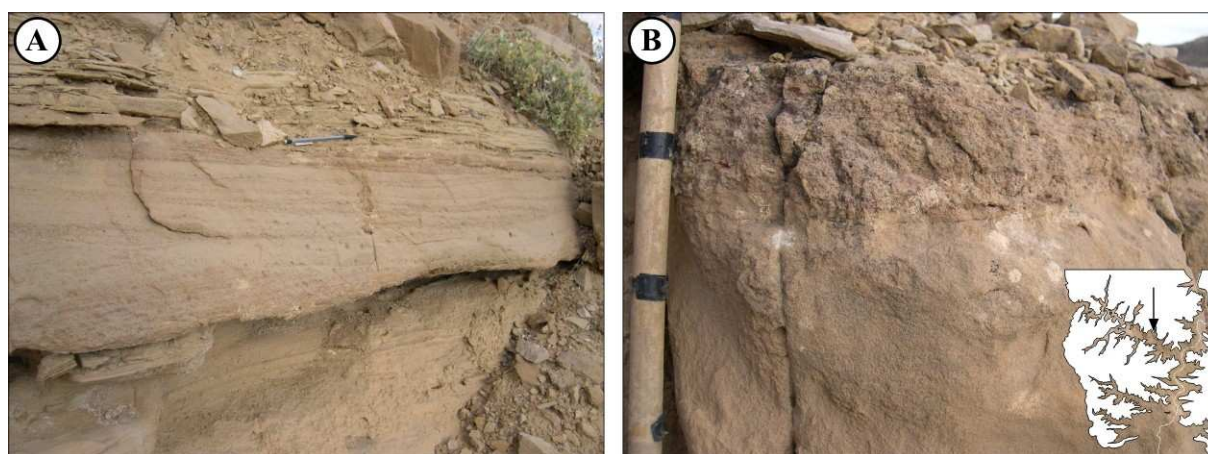
Figure 4.11. The pinch-out of the incised valley between Log 12 and Log 13 is represented by sandstone bar deposits (A) inside the valley, and a transgressive lag (B) a few hundred meters farther southeast, outside the valley. The pencil in A is 15 cm long. The spacing between tape measures is 10 cm.

This transition between the estuary and the interfluve was reworked during subsequent transgressive ravinement. This is evident from a partly erosive,10-40 cm thick, poorly sorted unit on top of S3.3, which has been interpreted as a transgressive lag (FA11), rather then a shallow part of the incised valley (Figure 4.11). This relationship suggests that the lowstand shoreline was situated farther towards the northeast, and that tidal channels and sandy tidal bar deposits of the most distal estuarine zone, was deposited somewhere between Woodside Canyon and the lowstand shoreline.

Chapter Five – 2D Modelling of Internal Shoreface – Shelf Parasequence Architecture

5.1 Introduction

Numerical modelling of shallow-marine depositional environments presents an excellent opportunity to study the development and distribution of intra parasequence architecture within a prograding shoreface-shelf unit, and the output data provided by this type of simulations may be used directly for comparison with field observations (Storms and Hampson, 2005). The data also presents information concerning the origin and relationship between observed stratigraphic units (such as bedsets) and their bounding surfaces. An event-based stratigraphic modelling software (BARSIM, Storms, 2003) was used to obtain such data, and the model was subsequently applied as a comparison to the internal geometries observed in the Sunnyside Member. The main aim with this 2D modelling was to investigate the effects of changing depositional conditions within the shoreface-shelf, and search for connections between annual deposition rates, profile curvatures and the formation of non-depositional discontinuity surfaces.

Process-response models are dynamic models which are based on simplified rules of sediment transport and distribution over long time intervals, and will thus give an approximate representation of the depositional system (Storms, 2003). BARSIM is a two-dimensional modelling software which simulates shoreface-shelf progradation during specific depositional conditions. Because the wave-dominated shoreface-shelf environments is characterized by alternating depositional energy, this model distinguishes between fair-weather and storm deposits stochastically to provide a more realistic representation of the shallow-marine system (Storms, 2003). In the model, erosion varies with depth and is restricted to the area basinward of the shoreline and landward of the wave base (Figure 5.1). All the eroded sediments are redeposited according to the principle of mass conservation (Storms et al., 2002; Storms, 2003; Storms and Swift, 2003). Deposition, on the other hand, is dependent on the grain-size and event magnitude, and occurs along the entire profile, including the back barrier area and the shelf below wave base (Storms and Swift, 2003). All initial modelling conditions, such as shoreface-shelf gradient, fair-weather wave base, grain-size distribution, as well as time varying parameters like sediment input and sea level, can be

changed to meet specific depositional conditions (Storms et al., 2002; Storms, 2003; Storms and Swift, 2003). Output data includes lithologic cross-sections, lithologic wells, annual deposition rates and shoreface-shelf profiles.
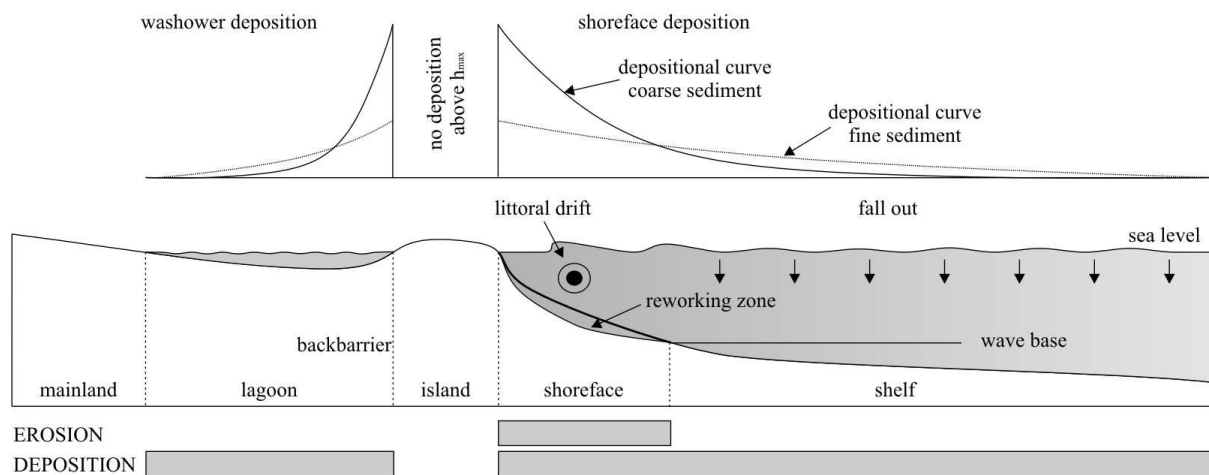
Figure 5.1. Schematic cross-section of a wave-dominated coastal system as used in BARSIM. Erosion is restricted to the shoreface whereas deposition may occur in the backbarrier area as well as along the entire shoreface-shelf profile. From Storms and Swift (2003).

The shoreface-shelf profile is considered to be an equilibrium profile within geological time scales (>10^3 years), and will adapt to changes in sea level, sediment input and wave base (Bruun, 1962; Storms et al., 2002). However, the profile will not respond to imposed short-time changes in the depositional conditions by a simple translation of the profile, as postulated by the Bruun Rule (Bruun, 1962), but rather by a long-time interaction between the proximal and distal parts of the profile (e.g. Larson and Kraus, 1994; Stive and De Vriend, 1995; Hampson and Storms, 2003). In contrast to the assumptions used to validate the Bruun Rule (e.g. closed depositional system), BARSIM models sediment loss and gain to both the backshore area and the area seaward of the "closure depth" (storm wave base) (Storms et al., 2002; Storms, 2003). In addition, longshore drift is simulated as sediment influx, thus allowing net sediment gain and loss by littoral currents (Storms et al., 2002).

A limited amount of input variables accompanied by short computer running time makes this software suitable for modelling high-frequency changes in the depositional environment similar to those observed in the Sunnyside Member. Although modelling tools may be very useful in predicting and increasing our understanding of intra parasequence architecture and discontinuity surfaces, such information should be used with care as it only provides a simplified representation of the depositional system.

See Storms et al (2002), Storms (2003) and Storms and Swift (2003) for a detailed description of BARSIM, including its assumptions and limitations.

5.2 Previous 2D modelling of discontinuity surfaces in the Blackhawk Formation

Storms and Hampson (2005) presents a study on the (underlying) wave-dominated Kenilworth Parasequence 4 (K4, Figure 1.6), which shares many similarities with S2. Both parasequences are considered to be unusual thick reflecting considerable accommodation space due to limited basinward progradation of the previous and underlying parasequences (Howell et al., in review). The two units can also be closely compared in terms of depositional environment, both reflecting a relatively straight, north-south oriented shoreline along a ramp margin basin. The most striking difference between the two parasequences is the depositional history and their internal architecture. The Sunnyside parasequences are interpreted to reflect relatively simple progradation within a normal regressive system (Howell et al., in review). The bedset boundaries encountered in the Sunnyside Member are therefore non-depositional discontinuity surfaces reflecting normal regression with a sub-horizontal shoreline trajectory (Helland-Hansen and Martinsen, 1996; Hampson, 2000; Howell et al., in review). The depositional history of the K4 is more complicated, suggesting both "positive" and "negative" shoreline trajectories (sensu Helland-Hansen and Martinsen, 1996) throughout its progradational history, reflecting periods of both normal regression and forced regression (Pattison, 1995; Hampson, 2000; Hampson and Storms, 2003). The study performed by Storms and Hampson (2005) suggests that whereas non-depositional discontinuity surfaces are related to periods of normal regression and relative sea level rise (similar to S2 and S3), erosional discontinuity surfaces are commonly related to periods of forced regression. This implies that the S2 and S3 only can be directly compared to the normally regressive part of the K4.

The non-depositional discontinuity surfaces in the K4 have similar properties to the ones observed in S2 and S3, representing upward coarsening units with thicknesses between 1 and 18 m, which demonstrates an upward increase in thickness and amalgamation of HCS event beds (Hampson, 2000). The bedset boundaries have been traced for 0.8 to 6 km down-dip where they slope between 0.02° and 0.58° (Hampson, 2000), which is comparable the ones in the Sunnyside Member (having an average slope of 0.21°). Storms and Hampson

(2005) performed several simulations using the BARSIM process-response model where they differentiated between the proposed mechanisms for bedset boundary formation (changes in sea level, sediment input and wave climate) by presenting several end-member scenarios. Fall and rise in relative sea level resulted in the formation of erosional and non-depositional discontinuity surfaces close to the LSF which were accompanied by a basinward and landward shift of facies respectively; these erosional surfaces were interpreted as regressive surfaces of marine erosion (RSME) (Storms and Hampson, 2005). Changes in wave climate also resulted in the formation of discontinuity surfaces close to the LSF. Differences in deposition rate along the entire profile suggested that these changes affected the entire shoreface and the inner part of the shelf (Storms and Hampson, 2005). A decrease in wave regime was accompanied by a 2 km landward shift of facies, which was of similar magnitude across the entire shoreface-shelf. According to the study, gradual changes in sediment supply also resulted in the formation of discontinuity surfaces when the rate of progradation was low, but in contrast to changes in wave climate, the surfaces were not associated with a landward shift of facies or distinct changes in amount of amalgamated event beds (Storms and Hampson, 2005). Instead, low sediment supply resulted in increased reworking and sorting of the sediments, and a steepening of the shoreface-shelf profile. Neither abrupt changes in sedimentation rate produced well developed discontinuity surfaces, because a continuous fall-out of fine-grained sediments compensated for periods of low sediment input, resulting in a relatively uniform deposition rate in the distal part of the shoreface-shelf (Storms and Hampson, 2005). The study concluded that discontinuity surfaces are formed as sea level falls, as sediment supply decreases, and when wave climate changes, but only the latter produce discontinuity surfaces which are associated with a distinct landwards shift of facies (Storms and Hampson, 2005).

5.3 Input variables and modelling conditions

The basic input variables for the simulations were the same as for the K4 study described above (Storms and Hampson, 2005) as they are interpreted to be representative for modern storm-dominated shorelines, and as the K4 is comparable to any of the Sunnyside parasequences. Four grain-size classes were used: 10 µm (15 %), 100 µm (25%), 200 µm (35 %), 350 µm (25%), in addition to a simulated fall-out, or background sedimentation (10 µm) rate of 0.2 mm/y. A minimum fair-weather period of 10 years, and a wave height of 4 m were

also assumed during each simulation, which was set to last for 25 ky. The initial shoreface-shelf slope was set to 0.09° (Storms and Hampson, 2005).

The grain-size classes correspond to the following spectrum of mud and sand: <62.5 µm - mud, 62.5-125 µm - very fine (vf) sand, 125-250 µm - fine (f) sand and >250 µm - medium (m) sand (Boggs, 2001). By using the granulometric facies diagram presented in Storms and Hampson (2005, their Figure 9) plotting the mean and standard variation of grain-sizes within a 1 m vertical interval, and by examining the physical characteristics of the grain-size variations in the wells, three facies associations were recognized: Amalgamated mud (AM) has been defined as successions demonstrating an average grain-size less than 62.5 µm and a low standard deviation (Storms and Hampson, 2005). This facies has been interpreted to represent background deposition of mud from suspension, occasionally interbedded by thin sandbeds below storm wave base, and is therefore equivalent to the offshore facies association in the Sunnyside Member (Storms and Hampson, 2005; Howell et al., in review). An interbedded sand and mud facies association (ISM) is represented by high grain-size variety, ranging between 62.5 and 125 µm (Storms and Hampson, 2005). The variety in grain-size and standard deviation is interpreted to represent interbedded storm event beds and fair-weather beds (equivalent to the OTZ) positioned between the storm wave base and the fair-weather wave base (Storms and Hampson, 2005; Howell et al., in review). Amalgamated sand (AS) facies association is represented by a variety of grain-sizes classes (between 62.5 and 300 µm), and a low standard deviation (Storms and Hampson, 2005). The facies has been interpreted as amalgamated sand, equivalent to LSF, USF and foreshore deposits in the Sunnyside Member. The AS facies represents deposition above fair-weather wave base where every day waves continuously rework sediments and prevents preservation of fair-weather deposits (Storms and Hampson, 2005; Howell et al., in review).

Figure 5.2 presents the "base case" shoreface-shelf cross-section after 25 ky of progradation. The steep proximal part of the profile (red) is equivalent to the high-energy USF and foreshore. In the panels illustrating the annual deposition rate (Figure 5.4), this zone is commonly represented by an abrupt decrease in deposition rate, seen as a (sometimes negative) peak which represents the surf-zone (Storms, personal communication, 2005). Farther basinwards, a negative "bump" in the profile (yellow and green, Figure 5.2) represents the LSF, which is characterised by fair-weather and storm scour (Storms and Hampson, 2005). In the annual deposition rate panels, this is represented by the low in deposition positioned 6 km offshore. Even farther basinwards, deposition is higher due to decreased erosion seaward of the LSF and the wave base (Storms and Hampson, 2005). This increased deposition is

represented by the minor positive "bump" in both the cross-section (light and dark blue, Figure 5.2) and in the annual deposition rate panel (approximately 9 km from the shoreline). The dark blue in the most distal part represents the offshore which only experience steady fall-out sedimentation.

5.4 Base Case

To simulate continuous, normal progradation of a wave-dominated shoreline, constant sediment supply, sea level and wave base was imposed on the shoreface-shelf. During 25 ky of progradation with a sediment supply of 15m²/y, this reference shoreline migrates approximately 12 km basinwards (Figure 5.2), with an average progradation rate of ca 0.5 m/y. Well A and B are positioned 15 and 20 km off the shoreline during incipient progradation, respectively (Figure 5.3), and represents a continuous upward coarsening unit containing interbedded sand and mud in the lower and distal part, and amalgamated sand in the upper part.
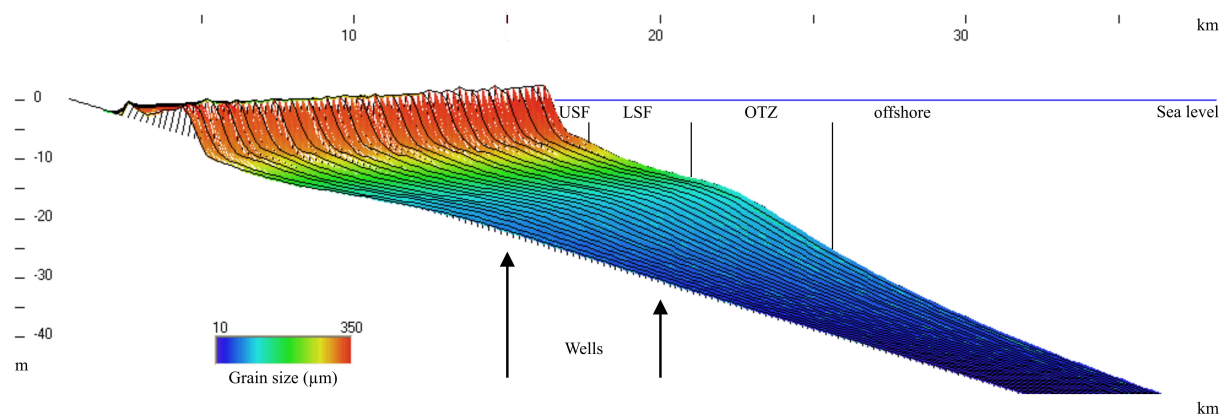
Figure 5.2. Litholigic, shoreface-shelf cross-section, representing 25 ky of simulated progradation with continuous sediment supply, sea level and wave base. Approximate positions of the main depositional environments are indicated. Wells A and B are positioned 15 and 20 km basinward of the original shoreline, respectively.

During progradation, the shoreface-shelf profile steepenes from 0.09° to 0.14° as the shoreline progrades into deeper water (Figure 5.4). This steepening of the profile is only noticeable basinwards of the LSF, where it continuously increases basinwards. The effect of increased accommodation is therefore not detectable in the foreshore and USF. This permanent configuration of the proximal part of the profile suggests that wave action is the
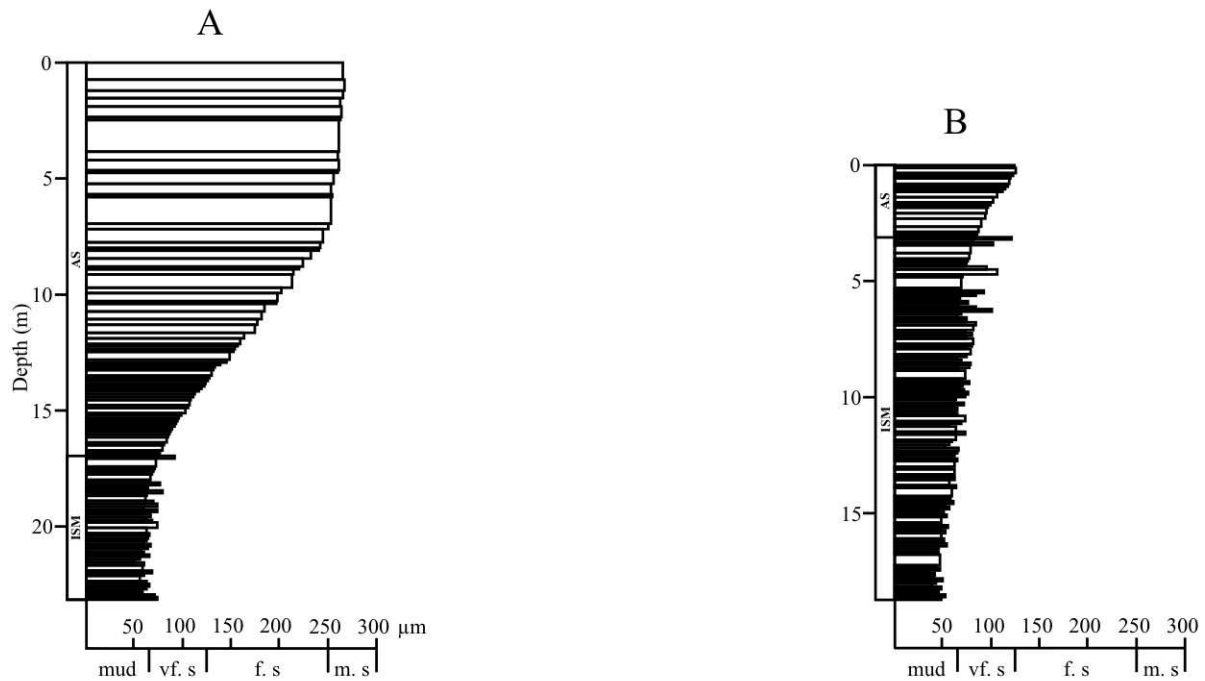
Figure 5.3. Well A and B illustrate a relatively continuous, upward coarsening unit characterized by an upward increase in grain-size and sandbed thickness. The facies are comprised of interbedded mud and silt and amalgamated sand.

main dominant force shaping this part of the shoreface-shelf. Deepening of the distal parts of the profile results in a slight compression of the facies belts as the wave base moves closer to the shoreline. During the onset of progradation, the wave base is situated approximately 14 km basinwards of the shoreline whereas the wave base is located only 10 km from the shoreline in the end of the 25 ky period.
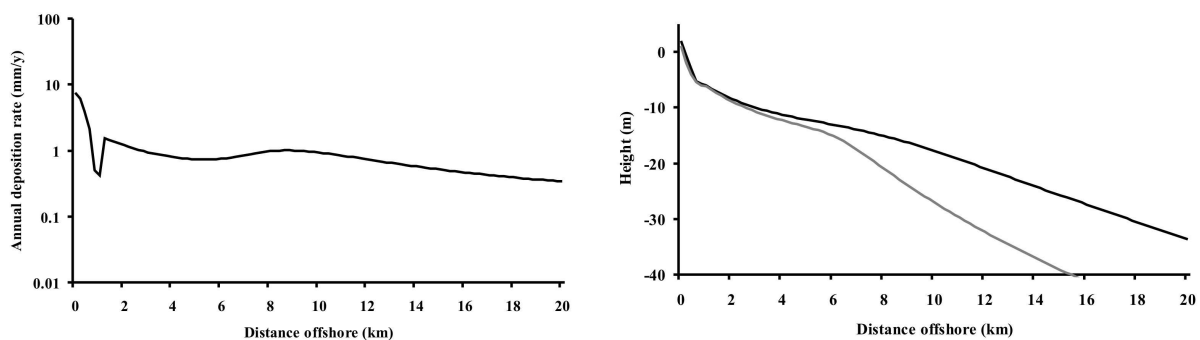
Figure 5.4. Left panel: Annual deposition rate along the shoreface-shelf profile during normal progradation. The low in deposition after 1 km represents the surfzone. A low in deposition is located approximately 6 km offshore where wave erosion is high relative to deposition. This is equivalent to the position of the LSF. Farther basinward, the deposition rate increases as wave erosion decrease. Right panel: The distal part of the shoreface-shelf profile increase as the shoreline progrades into deeper water and the accommodation space increases. The black line represents the shoreface-shelf during incipient progradation whereas the grey line represents the profile after 25 ky of progradation.

The annual sediment supply rate varies along the shoreface-shelf profile during progradation (Figure 5.4). In the upper part of the foreshore, deposition is approximately 7.5 mm²/y. The annual sediment supply decreases relatively rapidly towards 1 mm²/y, ca 6 km offshore (close to the fair-weather wave base and the LSF). Farther basinwards, the sediment supply increases in the OTZ, ca 8-12 km offshore, before it decreases basinwards of the storm wave base and approaches the fall out rate of 0.2 mm²/y.

5.5 Changes in sea level

To simulate high-frequency changes in sea level, 2 m cycles of eustatic sea level rise and fall was imposed on the prograding shoreline. The length of one cycle was 8300 years, resulting in two periods of simulated forced regression and transgression. Sediment supply and wave base was kept continuous throughout the simulation. The shoreline progrades approximately 10 km basinward during the 25 ky interval, 4 km less than the base case scenario.

Progradation occurs exclusively during periods of relative sea level fall (Figure 5.7). This indicates that the sediments which are continuously added to the shoreface-shelf are accumulated and stored in the non-marine realm during transgression, and that little or no sediments are added to the distal parts of the profile at the time.

Well A and B (Figure 5.6), indicate that the distal part of the prograding shoreface-shelf is composed of three upward coarsening units which are bounded by non-depositional
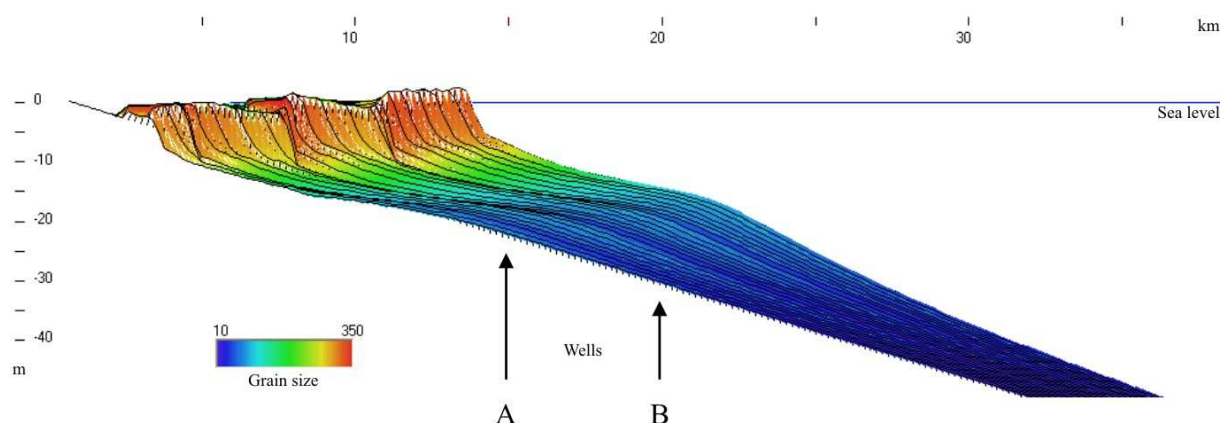
Figure 5.5. Lithologic, shoreface-shelf cross-section representing 25 ky of simulated progradation with continuous sediment supply and wave base, and cyclic changes in relative sea level of 2 m. Amalgamation of timelines indicates discontinuity surfaces. Well A and B are positioned 15 and 20 km from the original shoreline respectively.

discontinuity surfaces (represented by amalgamated time lines), indicating a decrease in sediment supply and relative deepening. When traced landwards, the two lowermost surfaces correlate with two similar surfaces which are marked by a decrease in grain-size and sand bed amalgamation. The uppermost discontinuity surface correlates landward with an erosional surface, suggesting truncation of the surface during subsequent sea level fall and erosion of the LSF. This indicates that the distinct, upward coarsening units which are associated with changes in sea level are formed during a decrease in sediment supply accompanied by a relative deepening of the profile, and that they are most pronounced in the distal parts of the shoreface-shelf profile.

The discontinuity surfaces are also associated with a landward shift of facies, resulting in offshore deposits overlying OTZ deposits (Figure 5.5 and Figure 5.6). Landwards of the LSF, the discontinuity surfaces are truncated by more proximal strata deposited during subsequent periods of sea level fall. This shift of facies (of approximately 2 km) is related to a landward dislocation of the shoreline.
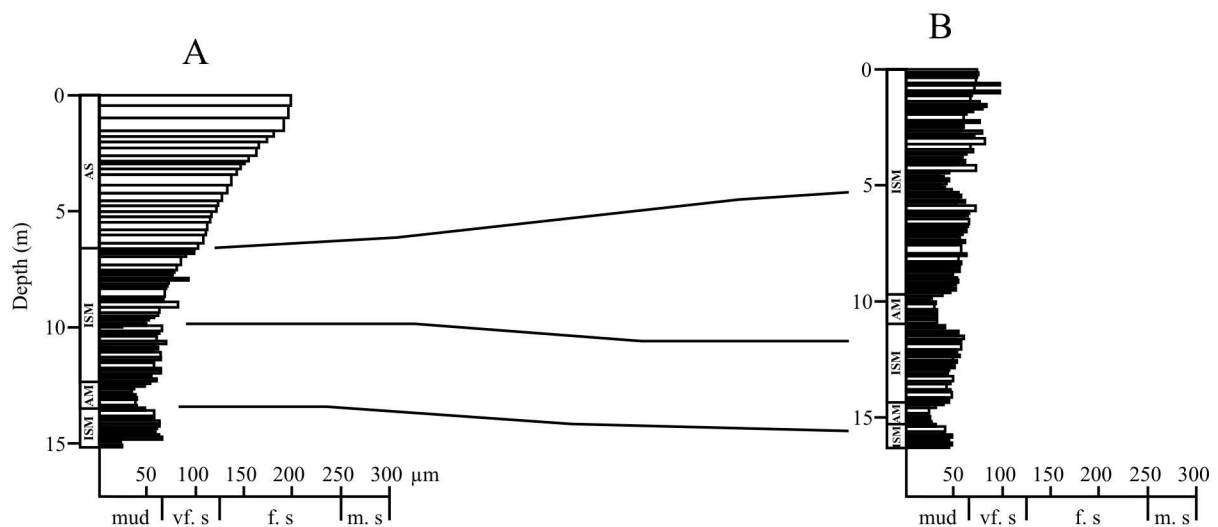
Figure 5.6. Cyclic changes in relative sea level results in the formation of both erosional and non-depositional discontinuity surfaces in Well A and B. The erosional surfaces are only present in the proximal part where they truncate the underlying non-depositional discontinuities. The surfaces represent an abrupt increase in grain-size and sandbed amalgamation, and are associated with a basinward shift of facies. Non-depositional discontinuity surfaces represent a relatively abrupt decrease in grain-size and sandbed amalgamation, and are associated with a landward shift in facies (and the shoreline).

Falling sea level results in forced regression and flattening of the shoreface-shelf profile as the both the proximal and distal part becomes shallower (Figure 5.8). This effect is most prominent in the proximal part, landward of the LSF. The effect of relative sea level rise,

99

on the other hand, is an overall deepening of the profile accompanied by increased curvature as both the proximal and distal parts become steeper.

Mean annual deposition rates during transgression reflect low sediment supply to the shoreface-shelf as most of the material is deposited in the backshore area (Figure 5.8). The deposition rate decreases continuously with a low at 8 km (close to the position of the fair-weather wave base). In contrast, during sea level rise the average sediment supply is higher as no accommodation space is available in the backshore area. However, net erosion occurs between 5 and 11 km as the LSF
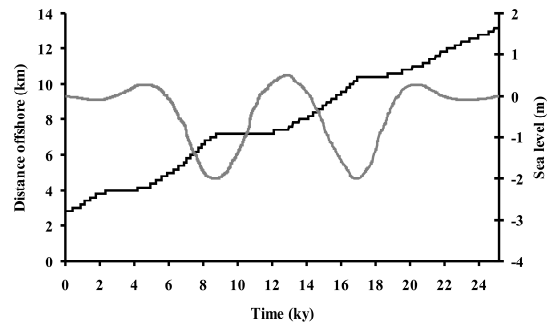
Figure 5.7. Cyclic changes in relative sea level (grey line) results in a stepwise shoreline migration (black line). During relative sea level rise, most the sediment is trapped in the backshore area and the shoreface-shelf is sediment starved.

erodes underlying deposits during forced regression. Basinward of the LSF, deposition increases as erosion only occurs during occasional storm events. Farther seawards, the deposition rate decreases towards the fall out rate as waves and currents are less capable of transporting sediments. Annual deposition rates during rise and fall in relative sea level are different across the entire shoreface-shelf profile, suggesting that the discontinuity surfaces which are associated with the rise in sea level should be distinguished across the entire profile.
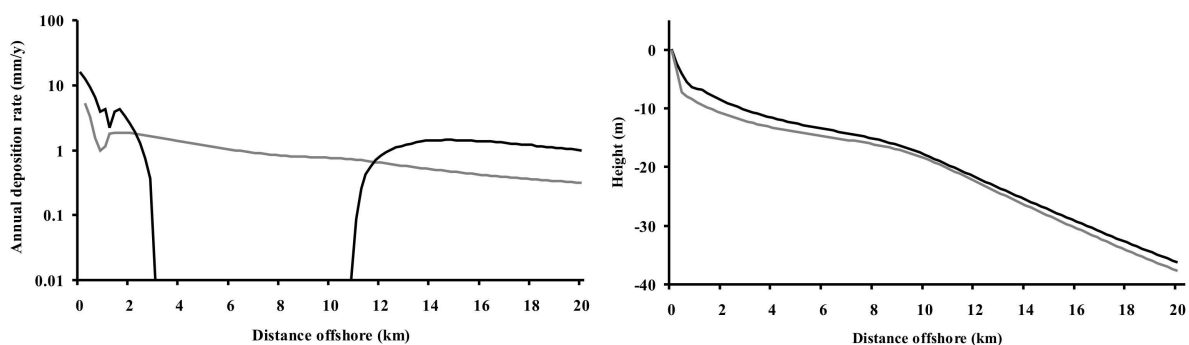
Figure 5.8. Left panel: The annual deposition rate suggests erosion in the USF and LSF during sea level fall (black line). Basinward of the average wave base (which is located at approximately 12 km), deposition increases as wave erosion decreases. During rising relative sea level, annual deposition is low and relatively continuous across the entire shoreface-shelf as most sediments are trapped in the backshore area. Right panel: The effect of relative sea level fall is steepening of the shoreface-shelf profile as the proximal part becomes shallower and the distal part becomes deeper (black line). Relative sea level rise has the opposite effect (grey line).

5.6 Changes in wave climate

To simulate high-frequency changes in wave climate due to changes in wind direction, shoreline topography, bathymetry etc, mean fair-weather wave height was set to 4 m with imposed amplitude of 0.75 m (Figure 5.9 and Figure 5.11). This forces the mean fair-weather wave base to change 1.5 m, (between 3.25 and 4.75 m), in an 8300 year cycle. Deepening of the mean fair-weather wave base results in increasing LSF erosion and the formation of erosional discontinuity surfaces (Figure 5.9 and Figure 5.10). These surfaces can be traced from the USF where they are marked by an abrupt increase in grain-size and sandbeds thicknesses, to the OTZ where they are marked by a more gradual increase in grain-size and the amount of sandbeds. The discontinuity surface becomes less pronounced seaward and seems to disappear in the distal parts of the OTZ.
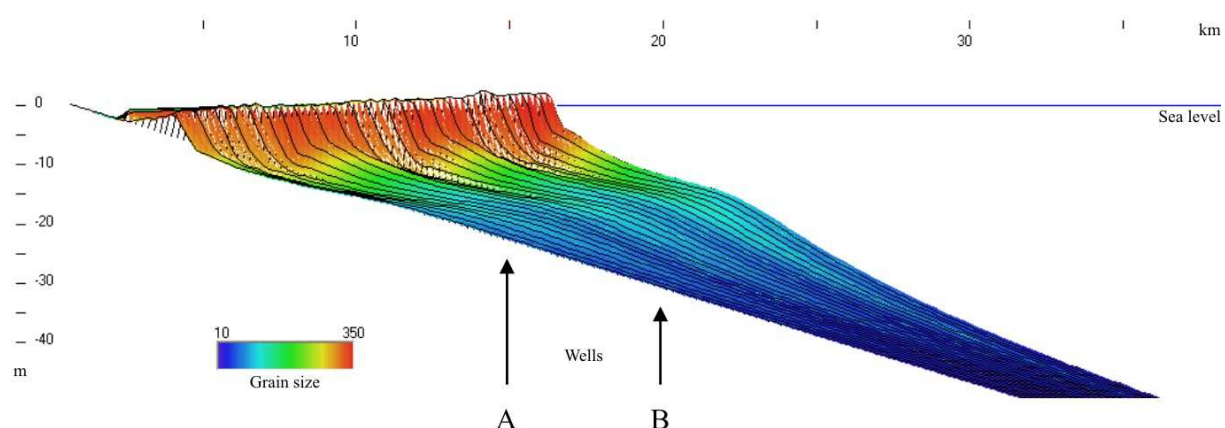
Figure 5.9. Litholigic, shoreface-shelf cross-section representing 25 ky of simulated progradation with continuous sediment supply and sea level, with cyclic changes in wave climate of 1.5 m. Facies shifts are most pronounced during periods of increased wave climate. Amalgamation of timelines indicates discontinuity surfaces. Well A and B are positioned 15 and 20 km from the original shoreline respectively.

The erosional discontinuity surfaces are also associated with a 2-3 km basinward shift of facies (Figure 5.9). Similar to the discontinuity surfaces, these shifts of facies are most pronounced in the proximal part of the shoreface-shelf, and are less distinct farther basinwards. Beyond the OTZ, there are no apparent facies shifts, indicating that the effect of changes in wave base decreases continuously seawards. Similar landward shifts of facies are recognized during shallowing of the wave base, but these are not associated with any distinct discontinuity surfaces in the wells (Figure 5.10).
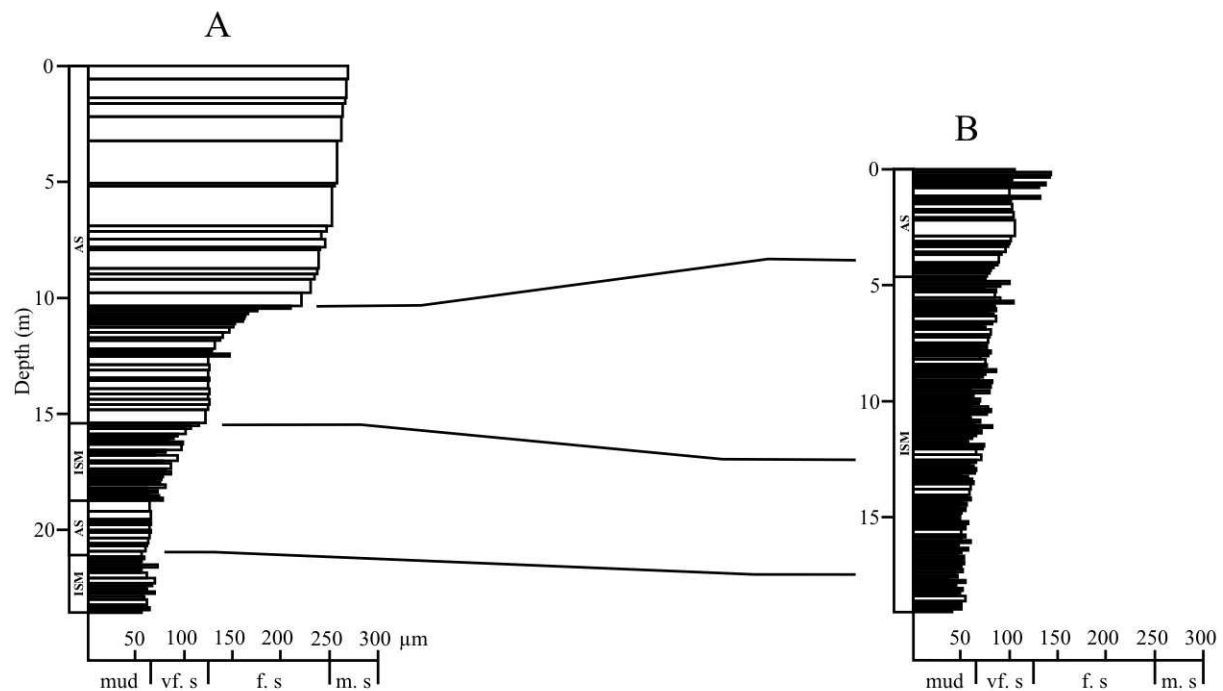
Figure 5.10. Changes in wave climate results in the formation of erosional discontinuity surfaces which are represented by an abrupt increase in grain-size and sand bed amalgamation in Well A and B. These surfaces can be correlated basinward into more poorly developed discontinuity surfaces illustrating the same facies relationships. No distinct discontinuity surfaces are formed during decreasing wave climate. Change in wave climate is also associated with shifts of facies of at least 2-3 km.

During 25 ky of simulation, the shoreline progrades approximately 12 km basinwards. Progradation does not occur linearly but increases and decreases relative to the fair-weather wave height (Figure 5.11). During periods of rapid progradation and high wave climate, the annual sediment supply rate decreases rapidly in the LSF, close to the position of the fair-weather wave base, which is positioned approximately 6 km off the shoreline (Figure 5.12). Basinward of the average wave base and the LSF, the deposition rate increases as erosion decrease, and the high annual deposition rate basinward of the LSF indicate that more material was transported to the distal parts of the basin during periods of increased wave climate. During periods of increasing, decreasing or more constant low fair-weather wave climate, shoreline progradation is relatively slow. The annual deposition rate is relatively linear suggesting less erosion in the LSF (close to the fair-weather wave base) compared to periods of high wave climate.

Comparison between annual deposition rates during alternating periods of changing wave base demonstrates minor differences in the OTZ and offshore area, suggesting that associated discontinuity surfaces are formed in the proximal part of the profile where the

curves deviate (Figure 5.12). Basinward of the wave base, the effect of changes in wave climate decreases continuously.

The shoreface-shelf gradient also varies between periods of high and low wave climate (Figure 5.12). Low energy conditions result in steepening of the profile as the proximal part becomes shallower and the distal part becomes deeper. During high-energy conditions, on the other hand, the proximal part is deeper and the distal part is shallower resulting in flattening of the profile.
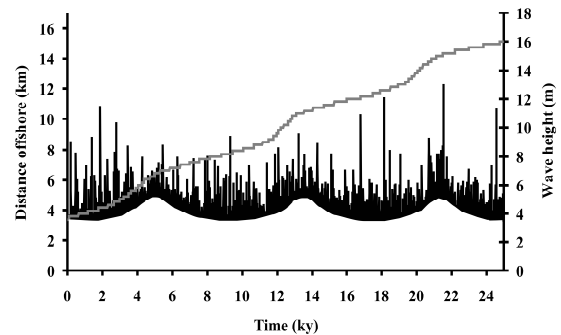
Figure 5.11. Shoreline progradation is governed by wave climate. Rapid migration (grey line) occurs during high wave climate (black line), whereas the shoreline migrates more slowly during periods of low wave climate.
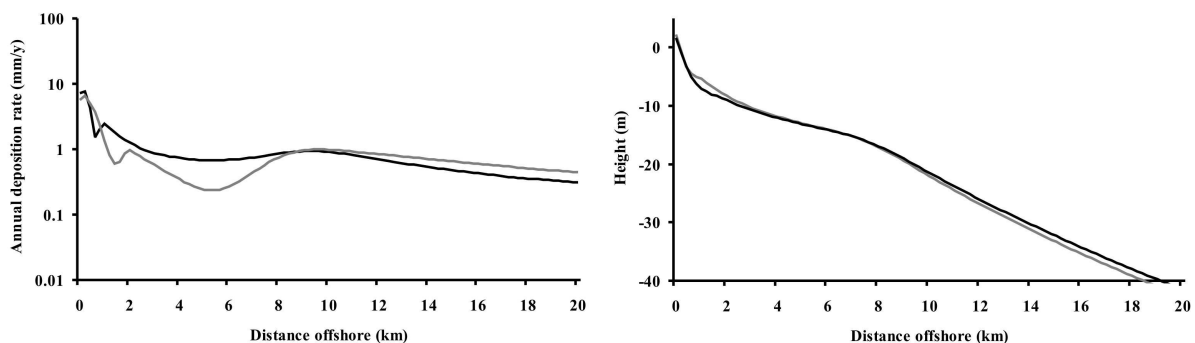
Figure 5.12. Left panel: Annual deposition rates during high wave climate (grey line) suggest a distinct low close to 6 km (at the position of the average wave base and the LSF). High wave climate also results in increased deposition in the OTZ due to increased storm induced currents. During low wave climate deposition is more continuous even though a low is recognized at 6 km, close to the wave base. A decrease in wave climate also results in less deposition basinward of the LSF compared to periods of high wave climate conditions (black line). Right panel: High wave climate results in flattening of the shoreface-shelf profile as sediment are eroded from the USF and foreshore and redeposited in the OTZ (black line). Low wave climate results in increased curvature and steepening of the profile as the net sediment transport direction is landwards (grey line).

5.7 Abrupt change in sediment supply

To simulate abrupt changes in sediment supply in response to e.g. delta lobe shifts, the sediment supply was varied abruptly between 15 m²/y and 0 m²/y in cycles of 8300 years. These abrupt changes results in the formation of discontinuity surfaces which are marked by a pause in deposition and amalgamation of time lines across the entire shoreface-shelf profile (Figure 5.13 and Figure 5.15). Subsequent rapid increase in sediment supply results in the
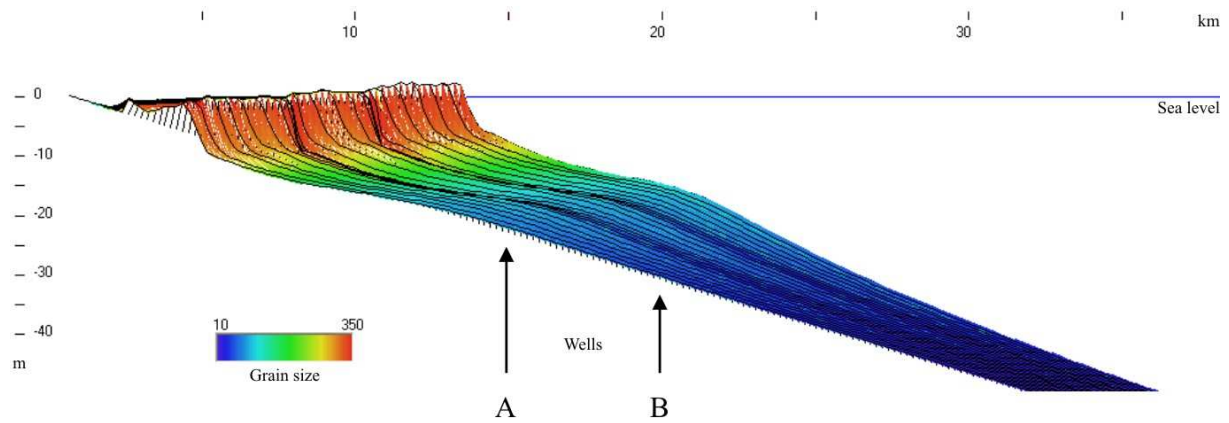
103

Figure 5.13. Litholigic, shoreface-shelf cross-section representing 25 ky of simulated progradation with continuous wave base and sea level, and abrupt changes in sediment supply between 0 and 15 mm/y. Amalgamation of timelines indicates discontinuity surfaces. Well A and B are positioned 15 and 20 km from the original shoreline respectively.

formation of an erosional discontinuity surfaces in the proximal area, which truncates the underlying non-depositional discontinuity surface approximately 5 km down-dip. The non-depositional discontinuity surfaces are not as distinct as those formed by changes in sea level. However, they are recognized by a relatively rapid decrease in grain-size and amalgamation of storm event beds (Figure 5.14). The discontinuity surfaces that form during abrupt decrease in sediment supply are not associated with a landward shift of facies.
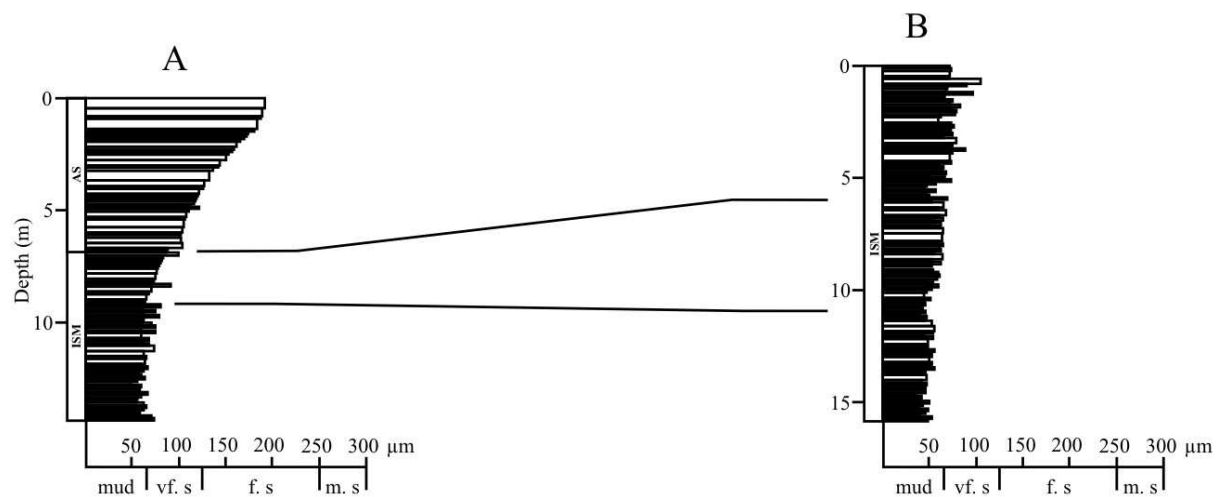
Figure 5.14. Abrupt changes in sediment supply results in the formation of non-depositional discontinuity surface in the distal part of the shoreface-shelf profile, whereas erosional discontinuity surfaces are formed in the proximal part. The non-depositional surfaces which are formed in response to low sediment supply are marked by a decrease in grain-size and sandbed amalgamation, but they are not associated with a distinct shift of facies.

During 25 ky of progradation, the shoreline migrates approximately 9 km basinwards. Periods of high sediment input results in rapid progradation, whereas periods of no sediment supply prevents the shoreline from migrating (Figure 5.15). The cyclic pattern of decreasing and increasing progradation is somewhat similar to the pattern formed by changes in relative sea level, although more gradual.

Annual deposition rates across the shoreface-shelf during periods of low sediment input indicates erosion in the most proximal part as waves rework the older sediments, followed by a gradual increase towards the position of the average wave base (approximately 10 km offshore, Figure 5.16). During peri-ods of high sediment input, the average deposition rate decreases slowly basinwards with a low close to the fair-weather wave base.Even farther basinwards (in the OTZ), the deposition rate decreases towards the fallout rate in the same rate as during low sediment input.This indicates that the depositional pattern is very similar seawards of the LSF during periods of alternating sediment supply, and that the distribution is only
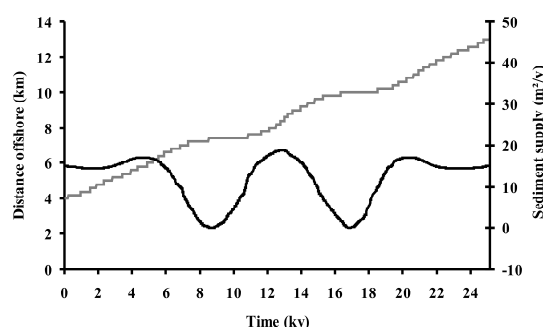
Figure 5.15. Changes in sediment supply (black line) results in stepwise progradation of the shoreline (grey line). Rapid progradation occurs during periods of high sediment supply, whereas migration decreases as the sediment input is reduced.
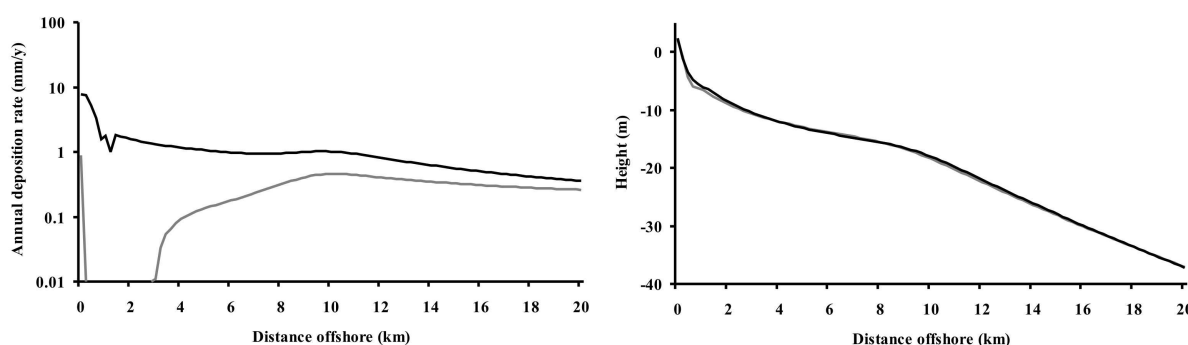
Figure 5.16. Left panel: Annual deposition rates during periods of low sediment supply (grey line) suggest erosion of the proximal part of the shoreface-shelf profile and redeposition in the distal part. The sedimentation rate during increasing sediment supply (black line) suggests more continuous deposition across the entire profile. The separation between the curves suggests that the non-depositional discontinuity surfaces can be correlated along most of the profile, although they becomes less pronounced basinwards. Right panel: The effect of low sediment supply is a marginal flattening of the shoreface-shelf profile as the proximal part deepens and the distal part becomes shallower (grey line). The effect of increased sediment supply is a marginal steepening of the profile (black line).

related to the amount of sediment supply. This variation in deposition rate suggests that the non-depositional discontinuity surfaces can be recognized across most of the shoreface-shelf profile.

A decrease in sediment supply forces the shoreface-shelf profile to flatten as the proximal part deepens and the distal part becomes shallower (Figure 5.16). High sediment input has the opposite effect, forcing the profile to steepen as the proximal part becomes shallower and the distal part becomes deeper. This relationship is similar to the one formed by changes in relative sea level, only more pronounced.

5.8 Gradual and asymmetrical change in sediment supply

To simulate long-term, allocyclic changes in sediment supply due to alterations in the current patterns, fluvial drainage area, climate etc, the sediment supply was changed gradually and asymmetrically between 5 and 15 m²/y. These changes result in relatively continuous shoreline progradation, although the rate varies with the amount of available sediments (Figure 5.17 and Figure 5.19). As a result, poorly defined discontinuity surfaces are formed both in the proximal and the distal part of the shoreface-shelf profile (Figure 5.18). These surfaces are similar to those formed during abrupt changes in sediment supply, although less pronounced. Periods of high sediment supply are associated with the formation of erosional discontinuity surfaces in the proximal part of the shoreface.
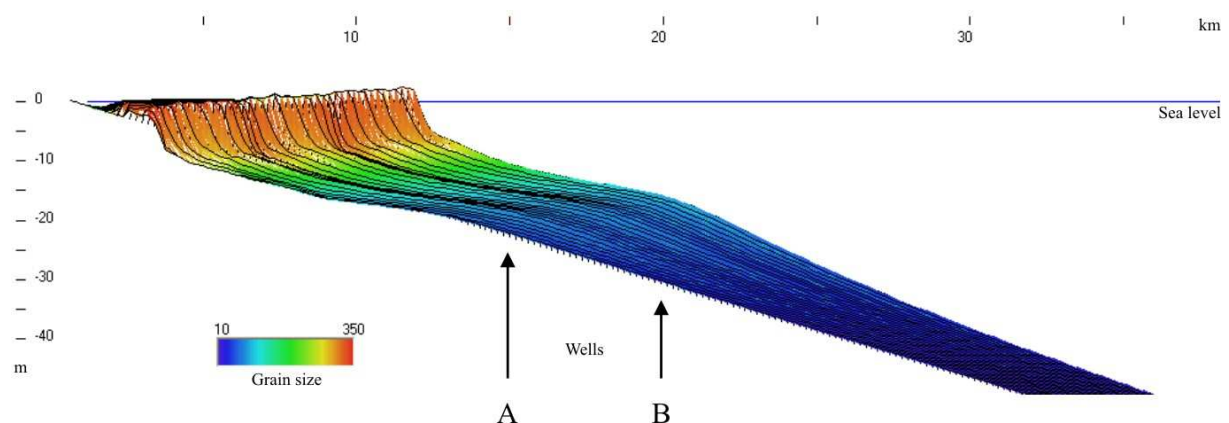

Figure 5.17. Litholigic, shoreface-shelf cross-section representing 25 ky of simulated progradation with continuous wave base and sea level, and gradual, asymmetric changes in sediment supply between 5 and 15 mm/y. Amalgamation of timelines indicate discontinuity surfaces. Well A and B are positioned 15 and 20 km from the original shoreline respectively.

Periods of low sediment supply are represented by zones of lower grain-size and sand bed frequency; however, they are not associated with sharp boundaries in the wells. No distinct shifts in facies are recognized across the discontinuity surfaces, and the distal succession (Well B) represents varying types of interbedded sand and mud, typical of the OTZ.
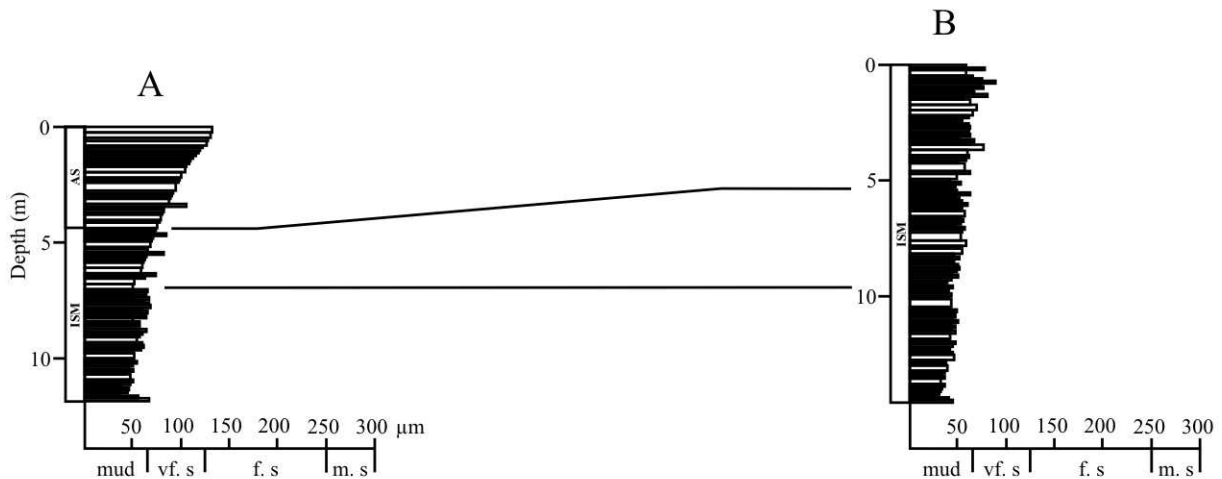
Figure 5.18. Gradual, asymmetric changes in sediment supply results in the formation of poorly pronounced discontinuity surfaces, similar to the ones associated with abrupt changes in sediment supply. The boundaries are marked by a decrease in grain-size and sandbed amalgamation. Up-dip, the surfaces are truncated by erosional discontinuity surfaces formed during increasing sediment supply.

The discontinuity surfaces associated with gradual and asymmetrical changes in sediment supply are more restricted down-dip compared to those formed during abrupt changes in sediment supply. Time-lines are only amalgamated in the LSF, and both the foreshore and offshore area demonstrates relatively continuous progradation. Low sediment supply result in low annual deposition rate in the USF and LSF (Figure 5.20), followed by an increase basin- ward of the fair-weather wave base (approximately 10 km offshore). During periods of high sediment input, deposition is high in the LSF, and decreases relatively continuously basinwards. Seaward of the LSF, both curves are relatively equal, suggesting no major differences in deposition rate during alternating sediment supply.
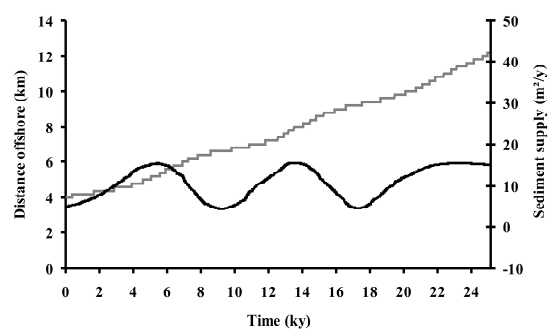
Figure 5.19. Gradual changes in sediment supply (black line) results in relatively continuous shoreline progradation (grey line). Progradation rate increases as the sediment input increases.

The shoreface-shelf response to gradual changes in the sediment supply is a marginal (Figure 5.20), flattening the profile as the sediment supply decreases (similar to the effects of abrupt changes). This is represented by shallowing of the proximal and distal part, although the most proximal USF and foreshore is continuous. During increased sedimentation, the curvature increase as both the proximal and the distal part becomes marginally deeper.
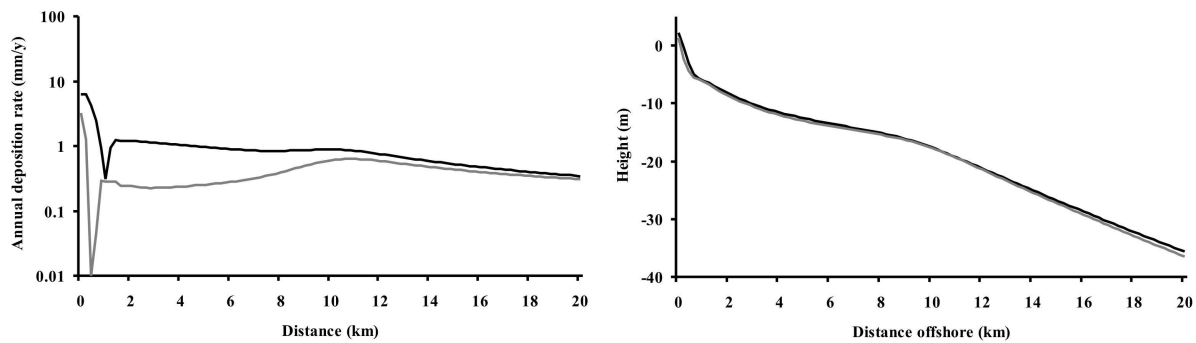
Figure 5.20. Left panel: Annual deposition rate during periods of low sediment supply (grey line) suggest gradually increasing deposition in the LSF. Maximum deposition occur approximately 10-12 km offshore (basinward of the LSF and the position of the average wave bases). Deposition is higher in the proximal part of the profile during periods of high sediment supply. Basinwards of the LSF, the deposition rate is the same as during low sediment supply, suggesting that changes in sediment supply will not affect deposition basinward of the LSF. Right panel: The effect of gradual decrease in sediment supply is the same as for abrupt changes, resulting in marginal flattening of the profile (grey line). Increased sediment supply has the opposite effect (black line).

5.9 Combined changes in wave climate and sediment supply

To simulate the combined effects of changes in sediment supply and wave climate due to high-frequency alterations in wind pattern, topography/bathymetry etc., 8300 year cycles of changing sediment supply and wave base was imposed on the prograding shoreline. As a result, both erosional and non-depositional discontinuity surfaces are formed (Figure 5.21 and Figure 5.22). An increase in sediment supply combined with an increase in wave base results in the formation of erosional discontinuity surfaces in the proximal part of the shoreface shelf profile which truncates underlying non-deposition discontinuity surfaces. Basinwards, these surfaces become less pronounced as wave action decreases. The distinct non-depositional discontinuity surfaces in the distal part of the profile are marked by a decrease in grain-size and sandbed amalgamation.
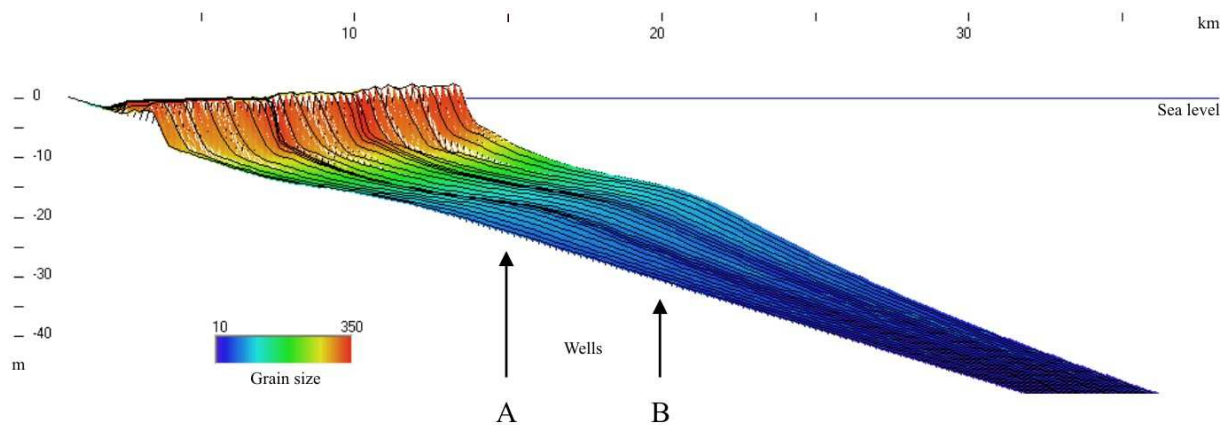
Figure 5.21. Litholigic, shoreface-shelf cross-section representing 25 ky of simulated progradation with continuous sea level and cyclic changes in both sediment supply and wave base. Two zones of dark blue offshore and OTZ deposit pinch-out into the LSF. No facies shifts are recognized farther landwards. Amalgamation of timelines indicates discontinuity surfaces. Well A and B are positioned 15 and 20 km from the original shoreline respectively.

The combination of low and high sediment supply and wave base results in lateral shifts in the position of the average wave base of approximately 3 km. These shifts in facies seem to be most pronounced in the distal part of the profile, and decrease up-dip as the surfaces disappear close to the USF.
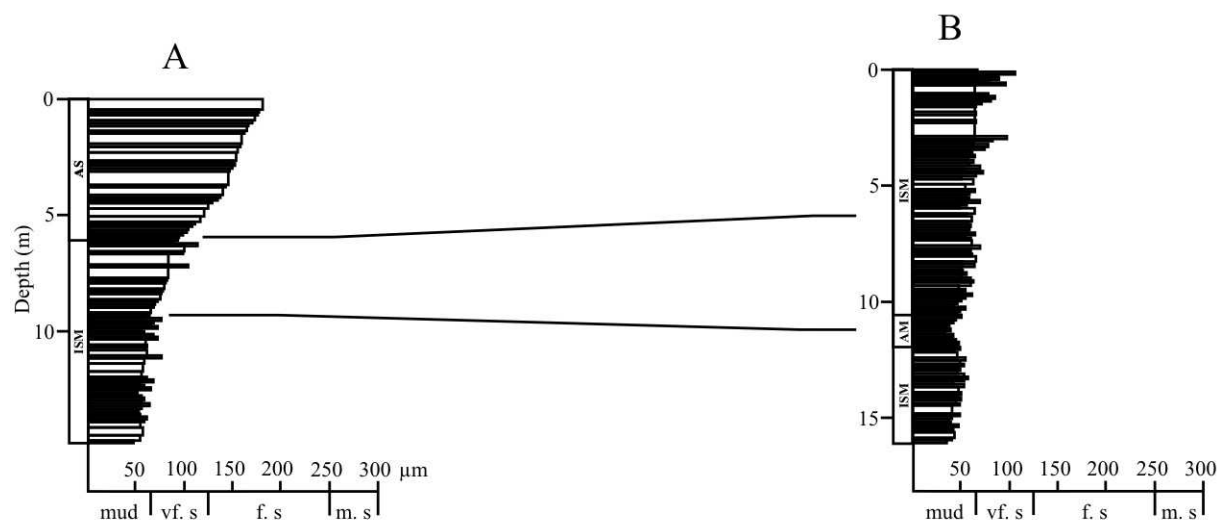
Figure 5.22. Cyclic changes in both sediment supply and wave base results in the formation of non-depositional discontinuity surfaces and erosional discontinuities in Well A and B. The non-depositional discontinuities are formed as sediment supply decreases and wave climate decreases, and are marked by a decrease in grain-size and amalgamation of sandbeds. The surface are also associated with a landward shift of facies of at least 3 km. Poorly developed discontinuity surfaces are formed in the proximal part as sediment supply increases. These truncate underlying non-depositional surfaces and becomes less pronounced basinwards.

During periods of low sediment supply and wave climate, the proximal part of the shoreface-shelf experience erosion as waves rework the shoreface-shelf. This forces shoreline progradation to stop for a period of time as the sediment supply and wave climate is at its lowest (Figure 5.23). At the time, deposition only occur basinward of the LSF (and the mean wave base) where less wave scouring favors preservation of storm event beds (Figure 5.24).

During subsequent periods of high sediment supply and wave base, deposition is relatively high in the proximal part, and decreases towards the mean wave base as wave erosion increases. Basinwards of the LSF (which is positioned approximately 6 km offshore), the deposition rate increases slightly towards the OTZ. The annual deposition rate during periods of high sediment supply and wave base is noticeably higher compared to low periods, suggesting that the discontinuity surfaces are present throughout most of the profile.
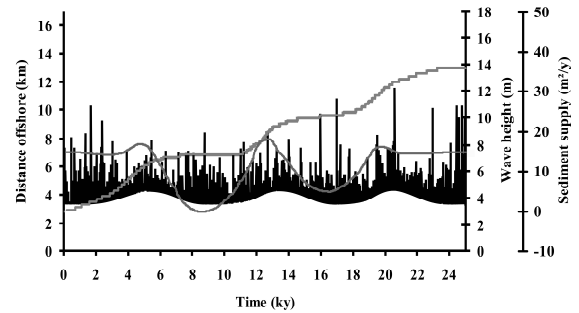
Figure 5.23. Changes in sediment supply (dark grey line) and wave base (black line) results in stepwise progradation of the shoreline (light grey line). During periods of low sediment supply and wave base, progradation is reduced to a minimum. As sediment supply and wave base increases, the shoreline progrades rapidly.

The effect of decreasing sediment supply and wave climate is flattening of the LSF and a marginal deepening of the distal part of the profile (Figure 5.24). An increase in sediment supply and wave climate has the opposite effect, resulting in deepening of the proximal part along with marginal shallowing of the distal part. There are no changes if the profile curvature proximal of the LSF, or in the most distal part (basinward of 20 km).
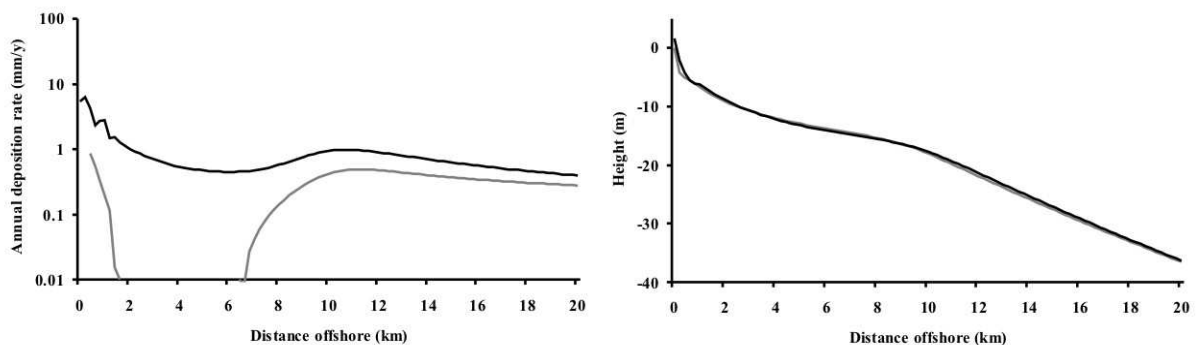
Figure 5.24. Left panel. A combination of low sediment supply and low wave base results in net erosion of the proximal part of the shoreface-shelf profile and relatively low, continuous deposition in the OTZ (grey line). During subsequent periods of high sediment supply and wave base, the annual deposition rate is higher across the entire profile (black line). A low is present close to the LSF and the deposition rate decreases towards the fall out rate. Right panel. The effect of decreasing sediment supply and wave base is an overall flattening of the profile curvature as the proximal part deepens and the distal part becomes shallower (grey line). The effect of increased sediment supply and wave base is the opposite (black line).

Chapter Six – Potential Mechanism for the Formation of Non-Depositional Discontinuity Surface: Comparison between Model Results and Field Observations

6.1 Introduction

The shoreface-shelf profile is commonly interpreted to be an equilibrium profile which gradually adapts to continuous changes in relative sea level (Bruun, 1962). This theory, known as the Bruun Rule, states that during a sea level rise, the shoreface-shelf profile shifts upwards and landwards, resulting in erosion of the USF and foreshore, and deposition in the LSF and OTZ as accommodation space is being created (Figure 6.1) (Bruun, 1962). This theory assumes that all sediments on the shoreface-shelf are transported by waves, and that no sediments will be transported seaward of the "closure depth", which is the basinward limit of wave influence. The theory also assumes a closed system, where no sediments are lost to the backshore area, and where no sediments are lost or gained by longshore drift processes in the littoral zone. Although this rule is originally thought off as a general approximation to predict the erosional effects of sea level rise within a relatively short time interval (hundreds of years) (Bruun, 1962), it has also been applied to various types of transgressive and regressive systems to explain coastal behaviour and evolution of the shoreface-shelf profile within longer-term (geological) time-scales (e.g. Dominguez and Wanless, 1991; Thorne and Swift, 1991a; Nummedal et al., 1993; Zhang et al., 2004). However, other studies claim that the Bruun Rule has limited validity because of its restricted applicability to modern and ancient shoreline systems, and that various parts of the shoreface-shelf profile will respond differently to changes in the depositional environment (Niedoroda et al., 1995; Stive and De Vriend, 1995; Hampson and Storms, 2003; Cooper and Pilkey, 2004).

There are several reasons why this simple equilibrium model cannot be adapted as basis for the study of discontinuity surfaces in the Sunnyside Member. The discontinuity surfaces (bedset boundaries) in the study area are interpreted to be palaeosurfaces of the ancient shoreface-shelf (Hampson, 2000), that amalgamate into the LSF and indicate that the system was in disequilibrium at the time of, or immediately after, the formation of the boundaries, as predicted by Stive and De Vriend (1995). This amalgamation suggest that the
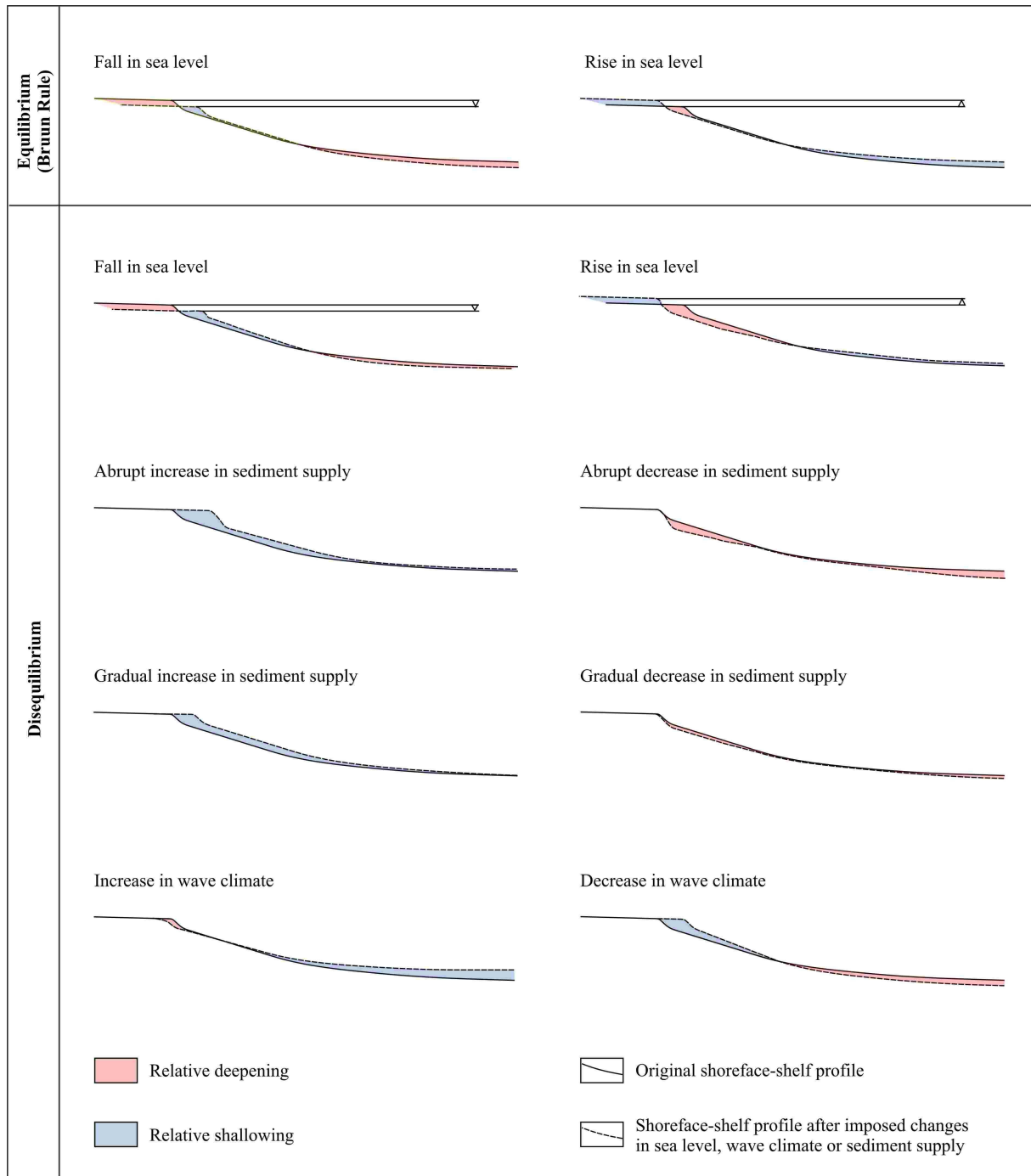
Figure 6.1. Theoretical shoreface-shelf profile response to changes in relative sea level, sediment supply and wave climate. The Bruun Rule predicts an upward and landward displacement of this profile in response to sea level rise and a similar down stepping in response to sea level fall. However, modelling suggests disequilibrium and flattening of the shoreface-shelf profil during sea level fall, resulting in a landward dislocation of the shoreline which is associated with parasequence boundaries (not bedset boundaries). Abrupt (autocyclic) decreases in sediment input due to shifts in delta lobe or fluvial discharge will result in a relative deepening in the distal parts of the profile, whereas the proximal part adapt to the imposed changes more rapidly. A gradual decrease (allocyclic) will result in a more continuous deepening across the profile. Also, the distal parts of the profile have time to adapt as sediment input gradually decreases. The flexible USF and foreshore changes continuously as the sediment input decreases. A decrease in wave climate will result in steepening of the entire profile as more material is added close to the shoreline by net landward sediment transport. The distal part of the profile will experience relative deepening.

proximal part of the profile (the USF and the foreshore) reacts more quickly to the imposed changes than the distal part, where there is a time lag for the profile to adapt (Stive and De Vriend, 1995). Imposed changes in depositional environment along the shoreline will have different effects on the shoreface-shelf profile (as described in Chapter Five) and the feedback time, the time it will take for the profile to achieve renewed equilibrium to a new set of depositional conditions, will also vary. Seasonal variations produced by, for instance, a major winter storm, may only result in disequilibrium for a few years until renewed equilibrium is attained (Larson and Kraus, 1994), whereas long-term changes in wave climate may result in disequilibrium ranging over geological time scales ($>10^3$ years)(Hampson and Storms, 2003). If changes in depositional environment occur more frequently than the shoreface-shelf profile can adapt, the profile may be in constant disequilibrium. As a result, the shoreface-shelf is interpreted not to respond similarly across the entire profile, but rather (given enough time) imposed changes will gradually adjust the profile into that of a long-term equilibrium profile. Imposed mechanisms which may affect the profile curvature include changes in relative sea level, changes in wave climate and sediment supply (O'Byrne and Flint, 1995; Storms and Hampson, 2005; Howell et al., in review). These effects will be discussed in the following sections in addition to output data derived from modelling, where they are compared to observations from the Sunnyside Member.

6.2 The effect of changes in relative sea level

Changes in relative sea level force the formation of a prograding shoreline through alternating cycles of accretionary forced regressions and transgressions, assuming continuous sedimentation (Helland-Hansen and Martinsen, 1996). The results from modelling indicate that the LSF progressively erodes the underlying shoreface-shelf sediments during forced regression, creating an erosional discontinuity surface; resulting in an overall steepening of the profile (Figure 6.1). This discontinuity becomes less distinct basinward of the LSF and is interpreted to represent a RSME (Storms and Hampson, 2005). Subsequent sea level rise results in the formation of non-depositional discontinuity surfaces and amalgamation of time-lines as new accommodation space is created in the proximal part, and the majority of sediments are trapped in the backshore area. This period is also associated with flattening of the shoreface-shelf profile (Figure 6.1). The surface represents a landward dislocation of the shoreline and is interpreted as a marine flooding surface (parasequence boundary) (Van

Wagoner et al., 1988; 1990). This relationship is different from the one observed in the Sunnyside Member, where the discontinuity surfaces are most distinct basinward of the LSF. However, the lateral extension down-dip of approximately 10 km is in the same order if magnitude, although marginally higher than the ones observed in study area, which can be correlated up to 7 km in a down-dip direction.

The three upward coarsening units represented by Well A (Figure 5.6) are similar to those observed in the Sunnyside Member, illustrating the same distinct decrease in grain-size and sandbed amalgamation, and the same lateral shifts in facies. However, when traced up-dip to Well B (Figure 5.6), distinct erosional discontinuity surfaces are present, indicated by an abrupt increase in grain-size and amount of sandbed amalgamation. These features are not observed in the Sunnyside Member, instead the non-depositional discontinuities amalgamate into the LSF without any distinct changes in lithology, neither above nor below these surfaces. Even farther landwards, the simulated discontinuities are associated with a landward dislocation of the shoreline, representing rise in relative sea level. In the Sunnyside, such dislocation of the shoreline is associated with parasequence boundaries rather than bedset boundaries (Howell et al., in review). Differences in annual deposition rates suggest that changes in sea level will affect most of the profile in a down-dip direction. This corresponds to the field observations of this study where parasequence boundaries can be traced from the non-marine realm (Howell et al., in review) and basinwards for at least 15 km. Changes in relative sea level is therefore not considered as the main driving mechanism for the formation of non-depositional discontinuity surfaces in the Sunnyside Member, even though PSBs have similar characteristics in the distal part of the profile. PSBs will be difficult to distinguish from those which are not associated with a landward shift of the shoreline, and only by tracing the surfaces up-dip can the distinction be made, enabling one to separate landward amalgamated bedsets from landward displaced parasequences.

6.3 The effect of changes in wave climate

Wave climate (height, wave length, frequency) is related to a variety of factors, such as: alongshore topography, offshore bathymetry and wind strength, duration and direction. Topography and bathymetry determine whether the shoreline is reflective or dissipative (Wright et al., 1979) and how much wave energy which is redirected along the shoreline as longshore currents (Inman and Bagnold, 1963). During major storm events, low pressure and

winds may result in the local sea level rising by several tens of centimetres and a subsequent build-up of water along the shoreline (Inman and Bagnold, 1963; Walker and Plint, 1992; Larson and Kraus, 1994). This pile-up of water results in down-welling and a basinward directed gradient, forcing the water back into the basin as the storm weakens (Figure 6.2). The sediments which are eroded at the shoreface during the high-energy period will be transported basinwards by this storm induced geostrophic current or storm surge, and redeposited farther out on the shoreface and the OTZ, where the wave and current energy is below the threshold for sediment transport (Dott and Bourgeois, 1982; Swift et al., 1983; Walker and Plint, 1992). During fair-weather periods, shallow waves transport sediments landwards, resulting in a net sediment transport towards the shoreline (Inman and Bagnold, 1963; Walker and Plint, 1992; Larson and Kraus, 1994). Such changes in the wave climate may occur at different time spans, ranging from days during individual storms, to seasonal (increased winter storm intensity), or within geological time spans (Larson and Kraus, 1994). Figure 6.1 illustrates how changes in wave climate will affect the shoreface-shelf profile. A long-time increase in wave energy results in erosion of the proximal part and deposition in the distal part of the shoreface-shelf, leading to a flattening and shallowing of the profile (Inman and Bagnold, 1963; Walker and Plint, 1992; Larson and Kraus, 1994; Niedoroda et al., 1995). This is supported by the difference in shoreface-shelf profiles during simulated periods of changing wave climate (Figure 5.12). Short-time changes on the other hand, ranging from hours to seasonal, have similar effects, but reestablishment of pre-storm profiles commonly occurs within years (Leatherman, 2001; Zhang et al., 2004). Similarly, a decrease in wave base results in a net landward sediment transport and an increased profile curvature due to steepening of the USF and deepening of the OTZ (Figure 6.1)(Inman and Bagnold, 1963; Larson and Kraus, 1994; Niedoroda et al., 1995). Again, this is confirmed by the change in shoreface-shelf profile during a simulated decrease in wave climate. The lowering of storm and fair-weather wave base also results in a basinward displacement or extension of the facies belts (basinward of the USF). The amount of displacement depends on the shoreface-shelf gradient and a decrease in dip-angle during high-energy periods may amplify this displacement. In contrary, a decrease in wave energy results in elevation of the fair and storm weather wave base, and a landward displacement or shortening of the facies belts will occur as a reduced amount of the seabed is affected by the oscillating waves. A consequence of this is that the facies belts overlying a non-depositional discontinuity surfaces, formed during decreasing wave climate, should be narrower than the ones below as less surface area is influenced by wave action. This is evident from some of the palaeogeographical maps presented in Chapter Three (Figure

3.7and Figure 3.8) demonstrating more confined OTZ facies belts above the discontinuity surfaces; however, this trend is not conclusive.

Low wave climate   High wave climate
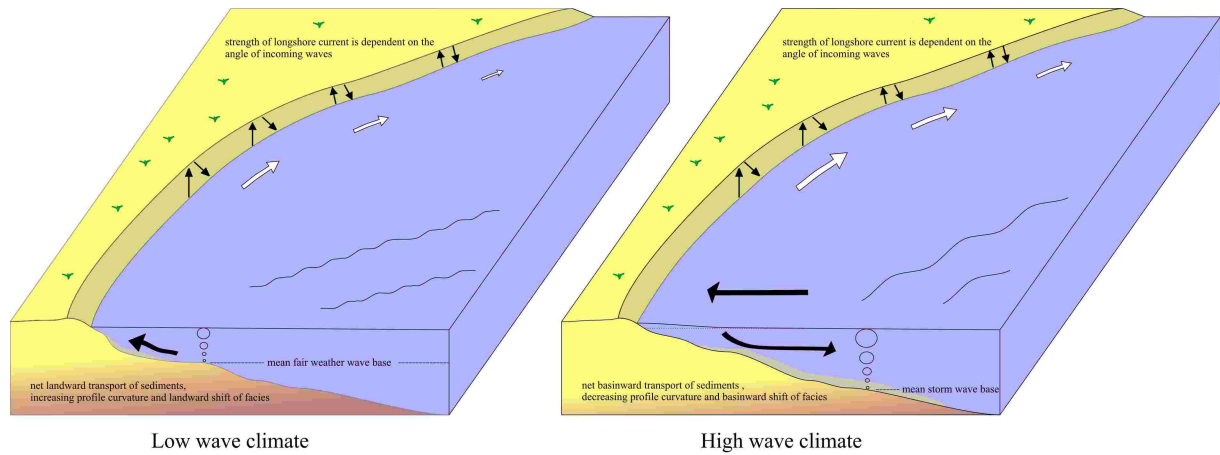
Figure 6.2. Both short and long-term changes in wave climate may affect the shoreface-shelf profile, shoreline morphology and sediment distribution. Low wave climate results in an increased profile curvature, landward transport of sediments, and landward shift of facies. High wave climate results in flattening of the profile curvature, net basinward sediment transport and basinward shift of facies. Strength and direction of longshore drift depends on the direction and energy of incoming waves.

Simulated changes in wave climate have been shown to result in the formation of discontinuity surfaces which are primarily associated with erosion (Storms and Hampson, 2005). Amalgamation of time lines suggests that the discontinuity surfaces are primarily confined to the LSF. This observation is similar to those observed in the Sunnyside which can be correlated for approximately 7 km down-dip. The major difference between the simulated discontinuity surfaces and those encountered in the Sunnyside Member is that the ones observed in the field are exclusively non-depositional. In addition, the discontinuities associated with change in wave climate are most pronounced in the LSF and the USF where they are associated with facies shifts of at least 2-3 km, whereas the non-depositional surfaces in the Sunnyside Member are most pronounced in the distal part of the LSF and the OTZ, and are associated with landward facies shifts of up to 5 km. Therefore, an increase in wave climate results in the formation of erosional discontinuity surfaces, the equivalents of which have not been observed in the study area. A decrease in wave climate results in poorly developed, coarsening upward successions overlain by units reflecting gradual decrease in grain-size and sandbed amalgamation, together with a minor landward shift of facies; these are usually considerably less distinct than those observed in the field.

116

6.4 The effect of autocyclic and allocyclic changes in sediment supply

Wave-dominated shorelines are generally fed by two different sediment sources: dip-sources, represented by river mouths, and strike-sources, represented by longshore drift and reworking of shoreface-shelf material (Rodriguez et al., 2001). These two supply mechanisms have very different influence on the shoreface-shelf profile. Extensive dip-feeding close to a river mouth forces the profile to be convex, due to the amount of sediments added, compared to the reworking potential of waves and currents in the USF (Larson and Kraus, 1994). Strike feeding on the other hand, will result in a relatively continuous sediment supply along the shoreface-shelf, allowing progradation without changing the profile from its original concave shape (Rodriguez et al., 2001).

Figure 6.1 illustrates how the shoreface-shelf profile will respond to changes in sediment supply. Although the dip-fed shorelines will be different from strike-fed shorelines, the general response to an increase in sediment supply is elevation and increased curvature of the profile (Niedoroda et al., 1995; Rodriguez et al., 2001). In the case of abrupt changes in sediment supply, increased input will result in progradation of the foreshore and the upper part of the shoreface, and an overall shallowing of the profile. This will again increase the profile's curvature as the sediments can not be distributed quickly enough to maintain the original shoreface-shelf slope (Rodriguez et al., 2001). Similarly, an abrupt decrease in sediment input will result in flattening of the shoreface profile as less material is added to the proximal part. These internal changes of the shoreface-shelf profile are less distinctive than those associated with changes in relative sea level and wave climate (Niedoroda et al., 1995). This is supported by modelling results, which demonstrates that the prograding shoreline experiences both abrupt and gradual changes in sediment supply. An abrupt increase therefore results in slight steepening of the proximal part of the profile whereas the distal part becomes slightly deeper. During simulations completed in this study, the profile never obtained a convex shape, as have been reported elsewhere outside river mouths in modern wave-dominated systems (Rodriguez et al., 2001). This is probably related to the relationship between the sedimentation rate and the wave reworking potential.

Gradual changes in sediment supply (Figure 6.1) will have similar effects to those mentioned above. A long-time increase will provide waves and currents with more time to distribute sediments more evenly, resulting in a progradational, shallowing profile (Rodriguez et al., 2001). Unlike the case of abrupt increase in sediment supply, these gradual changes will force the profile to step seaward without any major changes in the profile's curvature. A slow

decrease in sediment supply would similarly lead to gradual deepening of the shoreline as the sediments available are trapped close to the shore. This is also supported by simulations, where gradual changes in sediment supply have even less influence on the profile than abrupt changes, resulting only in minor variations of the curvature during progradation.

Changes in sediment supply are related to several depositional mechanisms of both autocyclic and allocyclic origin (e.g. Dominguez et al., 1987; Bhattacharya and Giosan, 2003). Allocyclic controls on sedimentation are related to alterations in: e.g. climate, tectonics or subsidence, and are associated with long-term and regional changes in sediment input. Abrupt, autocyclic changes in sediment supply are related to internally-derived forced alterations, possibly triggered by allocyclic processes, such as channel avulsion and delta lobe shifting (Figure 6.3) (Dominguez, 1996). Channel avulsion is induced by either changes in relative sea level, variable fluvial discharge, or by the progradation and subsequent abandonment of channels due to decreased transport capacity (Dominguez et al., 1987; 1996). Studies of Quaternary, wave-dominated shorelines suggests that the most important driving mechanism for delta lobe shifting is high-frequency changes in relative sea level, resulting in flooding of the river mouth and a decrease in the rivers transport capacity (Dominguez et al., 1987; 1996). Such abrupt changes in the position of the river mouth will affect the sediment supply at a given point along the shoreline, and the areas up- or down-drift of the abandoned part will then experience a decrease in sediment input, along with subsidence and compaction (Dominguez, 1996).

Channel avulsion and delta lobe shifts are generally considered to be autocyclic events and are related to variations in the fluvial gradient, which determines the rivers transport capacity (Beerbower, 1966; Dominguez et al., 1987; Dominguez and Wanless, 1991; Thorne and Swift, 1991b). Generally, a systems transport capacity decreases as the topographic slope decreases and visa versa, assuming no other controlling factors (Thorne and Swift, 1991b). Such decrease in fluvial transport capacity is the main mechanism for crevassing and channel migration, and it is most commonly obtained by progradation and the over-extension of the river's course (Dominguez and Wanless, 1991); although it can be triggered by various high-frequency autocyclic and allocyclic processes (Beerbower, 1966). Both an increase in sediment supply and a decrease in fluvial discharge, results in decreased transport capacity and the increased probability of channel avulsion (Beerbower, 1966). In modern systems, allocyclic processes such as tectonics (Goodbred and Kuehl, 2000) and eustasy (Dominguez et al., 1987; Dominguez and Wanless, 1991; Dominguez, 1996) have also proven to affect the alluvial slope, transport capacity and subsequent channel avulsion. Other allocyclic changes

are related to high-frequency climate changes which have resulted in reversal of the littoral drift, and which have been studied along the Holocene Nayarit strandplain (Curray et al., 1969). This resulted in erosion, channel avulsion, truncation and the rearranging of the beach-ridge sets along with the entire coastline. A similar relationship is observed in the Danube delta, where lobe shifts and increased wave climate resulted in erosion and increased longshore drift (Bhattacharya and Giosan, 2003).
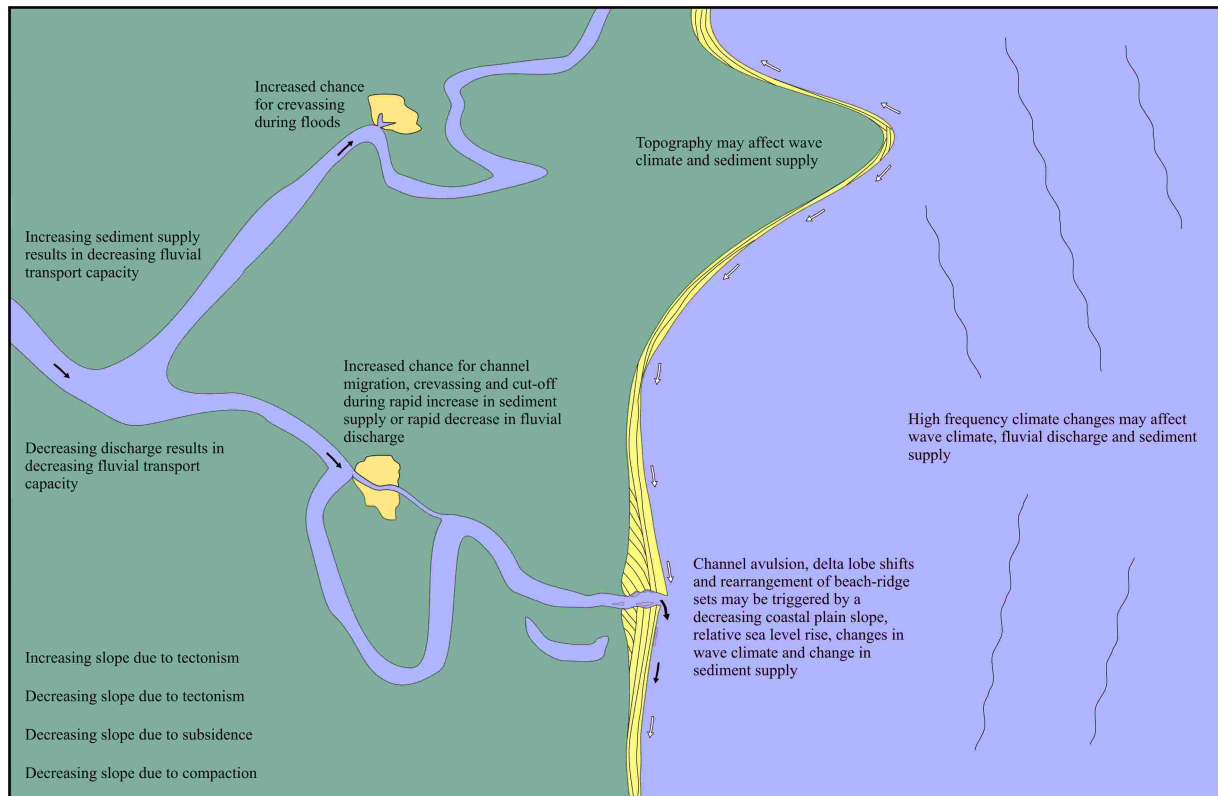
Figure 6.3. Summary of autocyclic and allocyclic processes and mechanisms which may affect and trigger channel avulsion and associated delta lobe shifts. White and black arrows represent longshore drift and fluvial discharge respectively.

Variations in fluvial discharge may also affect the morphology of a wave-dominated shoreline (Dominguez, 1996). Figure 6.4 illustrates how the river mouth may act as barrier for longshore drift when fluvial discharge is high, and how it is forced down-drift during subsequent periods of low discharge (Dominguez, 1996). During periods of increased fluvial input, longshore driven sediments will accumulate up-drift of the river mouth, resulting in progradation as beach-ridges accrete along the shoreline. This is because high fluvial discharge will act as a groyne, decreasing the longshore drift. This is accompanied by high deposition directly in front of the river mouth, as waves and currents are not able to redeposit the high amount of sediments introduced to the shoreline. This effect is also recognized in the

present day Brazos delta, where a major channel mouth bar was created during a flood-event in 1965 (Rodriguez et al., 2000). In periods of low discharge, the model predicts that less longshore driven sediments accumulate around the river mouth, and the updrift part of the shoreline is eroded and reworked by waves into a spit. This spit will partly close off the river mouth and force the river to deflect downdrift. During this period, the sediment previously deposited in front of the river mouth is redeposited along the shoreline by longshore currents, and may accrete to form a new shoreline farther down drift (Rodriguez et al., 2000; Bhattacharya and Giosan, 2003). This is the present day situation in the Brazos delta, where the 1965 mouth bar has been attached to the shoreline down drift, and constitutes the present day shoreline. Subsequent increase in fluvial discharge resulted in entrapment of river borne sediments updrift of the river mouth, and the shoreline therefore prograded basinward of the previously truncated beachridges. This mechanism is not directly related to channel avulsion and the effects are less important, but it can still result in relocation of the river mouth and changes of the sediment supply along the shoreline (Dominguez, 1996).

Simulation studies of progradational shorelines which are exposed to abrupt changes in sediment supply suggests that discontinuity surfaces are formed during periods of decreased sediment supply, and that they extend across most of the shoreface-shelf. Up-dip (in the USF), the non-depositional discontinuity surfaces are truncated by erosional surfaces which formed during subsequent periods of an abrupt increase in sediment supply. This relationship is similar to what can be observed in the Sunnyside Member where pronounced, non-depositional discontinuity surfaces pinch-out landwards. Although there are no signs of erosional truncation associated with the pinch out of the discontinuity surfaces into the LSF, it cannot be excluded. The lateral extension of the simulated discontinuity surfaces is hard to determine, but these surfaces seem to gradually pinch-out basinward as storm event deposition decrease. In contrast to the discontinuity surfaces which are associated with changes in sea level and wave base, these surfaces are mainly restricted to the LSF and the OTZ, similar to the ones observed in the Sunnyside Member. However, the most distinct difference between the non-depositional discontinuity surfaces in the simulated succession and the ones in the Sunnyside Member, is the absence of a landward dislocation of the facies in the modelled succession. This is because changes in sediment supply alone cannot change the position of the wave base; sediment supply can only determine the amount of sediments supplied to the wave base and not its reworking potential.

High discharge   Low discharge   High discharge
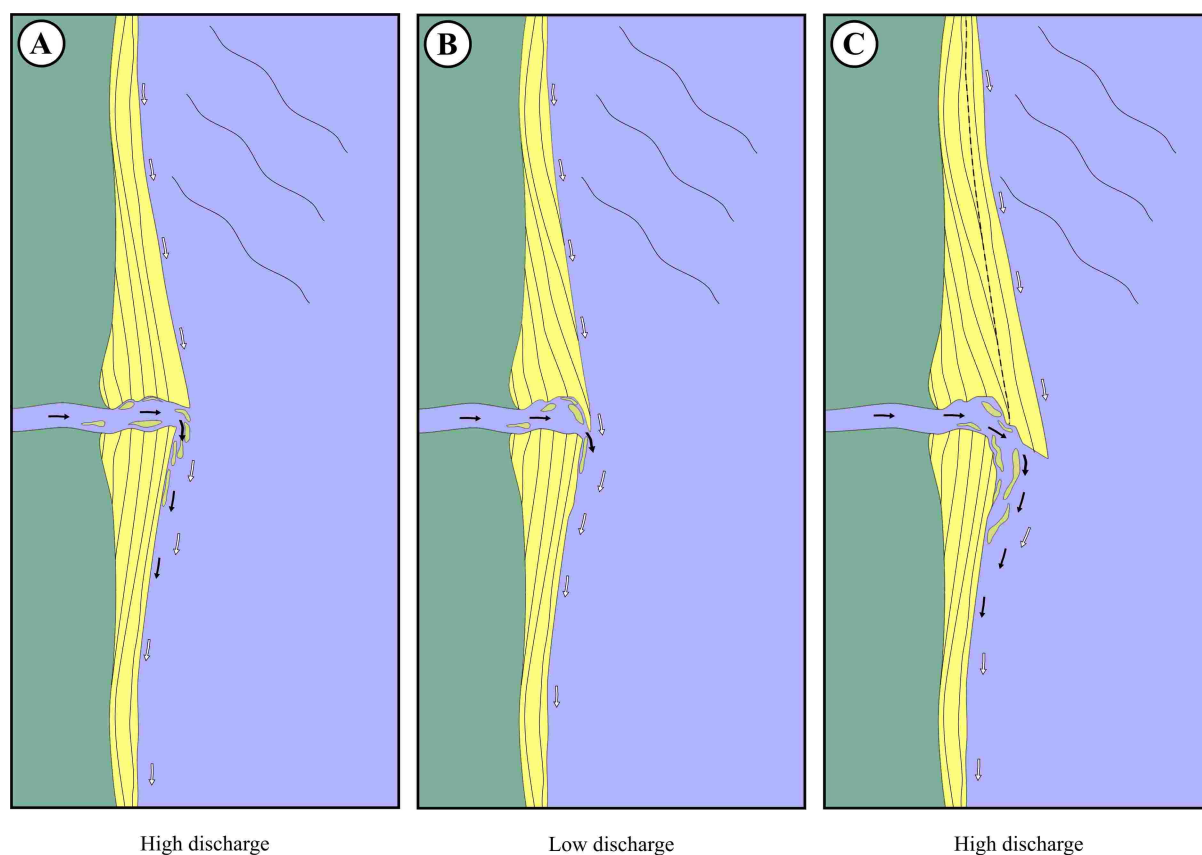
Figure 6.4. Model for downdrift migration of the river mouth in response to changes in fluvial discharge. High fluvial discharge (A) result in entrapment and progradation of longshore driven sediments updrift the river mouth. As the fluvial discharge is low (B), longshore driven sediments are no longer trapped around the river mouth and the updrift shoreline experience erosion. A spit is formed as sediments are redeposited close to the outlet, forcing the river to a path further downdrift. Renewed high discharge (C) results in progradation of the updrift part as sediments are trapped. Black and white arrows indicate fluvial and longshore transported sediments respectively. Modified from (Dominguez, 1996).

The simulated effects of gradual and asymmetric changes in sediment supply are somewhat similar to those related to abrupt changes, only less distinct. The discontinuity surfaces formed in the distal parts of the profile (Well A, Figure 5.18), are less pronounced and less comparable to the ones observed in the Sunnyside Member. In addition, the amalgamation of time lines is restricted to the LSF and OTZ, suggesting that no major discontinuities were formed in the USF or in the offshore zone. The simulated surfaces can be correlated for approximately 5-10 km down-dip, a distance which is directly comparable to the ones measured in the Sunnyside Member which are traceable for approximately 7 km down-dip. The major difference between the two sections is the lack of a landward shift of facies (in the simulated unit), which is similar to the effects of abrupt decrease in sediment supply, as described above.

6.5 The combined effect of changes in sediment supply and wave climate

A combined decrease in wave climate and sediment supply may occur in response to a variety of changes in the alongshore topography, bathymetry and climate (see sections above). The induced longshore transport of material, which is determined by the angle of the approaching waves and their interaction with the shoreline (Inman and Bagnold, 1963; Bittencourt et al., 2002), is considered to be a very important sediment source along wave-dominated shorelines (Dominguez et al., 1987; Dominguez, 1996; Bhattacharya and Giosan, 2003). As a consequence, changes in wave climate may also affect the sediment supply along-strike, so that decreasing wave climate might be accompanied by decreasing sediment supply.

Modelling of the progradational shoreline suggests that cyclic changes in both wave climate and sediment supply will force the shoreface-shelf profile to experience periods of disequilibrium as it is readapting to the new depositional conditions. The result is a slightly increased profile curvature as the distal part (OTZ) becomes deeper and the most proximal part (USF) becomes slightly deeper during periods of low wave climate and sediment supply. At the time of subsequent high wave climate and sediment supply, the effect is opposite, decreasing the profile curvature. These alterations in the shoreface-shelf profile are very similar to those formed during periods of changing relative sea level, and to those resulting from abrupt changes in sediment supply alone.

Well A and B (Figure 5.22) suggest that distinct upward coarsening successions are formed in the distal part of the prograding unit. These are bounded by a discontinuity surface representing a decrease in grain-size and sandbed amalgamation. This is similar to what has been observed in the Sunnyside Member, where thick HCS sandbeds of the pOTZ are abruptly overlain by interbedded sandstone beds and mudstone beds of the dOTZ, or by offshore deposits. In addition, the simulated succession indicates a relatively distinct landward shift of facies, which is also one of the main characteristics of the discontinuity surfaces observed in the study area. The distal well (Well B, Figure 5.22) is therefore highly comparable to the sections observed in the Sunnyside Member. When correlated up-dip, these simulated surfaces correlate with discontinuity surfaces displaying interbedded sand and mudbeds overlying amalgamated sandbeds, resembling pOTZ deposits overlying LSF deposits. Even farther up-dip, the discontinuities disappear into amalgamated sandbeds, representing the LSF. Although the timelines amalgamate in the USF and foreshore, there are no distinct shifts of facies related to the surfaces landward of the LSF. This relationship is also observed in the Sunnyside Member, where OTZ deposits commonly overlie LSF deposits,

demonstrating a landward shift of the facies belts (Figure 6.5). This indicates that discontinuity surfaces, which are associated with a distinct shift in facies, are also associated with changes in the profile curvature, whereas the ones representing no facies shifts, reflect a continuous shoreface-shelf curvatures during changes in depositional environment. The exact pinch-out style of the non-depositional discontinuity surfaces is neither observed in Woodside Canyon or in Long Canyon, as the outcrops disappears into the subsurface in the particular area. Other discontinuity surfaces have been removed during later sea level fall and associated fluvial incision. The lateral extent of the non-depositional discontinuity surfaces formed during simulation of changing wave base and wave climate, is in the order of 5-10 km (considering the distance of time-line amalgamation down-dip). The surfaces are also confined to the LSF and OTZ, and are therefore highly comparable to the ones observed in the Sunnyside Member which have a similar extent and position in the shoreface-shelf profile (see Chapter Three).

Figure 6.5. S3.3b in the proximal part of Long Canyon 1 (Log 20). LSF deposits is overlain by OTZ deposits, indicating a landward shift of facies and wave base. The OTZ unit is approximately 2 m thick.

Non-depositional discontinuity surfaces have also been described in the Grassy Member, Kenilworth Member and Spring Canyon Member, where they are marked by moderately to intense bioturbation and sometimes carbonate cemented as they pinch out into the LSF (O'Byrne and Flint, 1995; Pattison, 1995; Hampson and Storms, 2003). In the Spring Canyon Member, some of these surfaces can also be traced even farther landwards into correlative, unusually thick, USF and foreshore deposits (Figure 6.6) where they may be marked by rooted surfaces (Hampson and Storms, 2003).
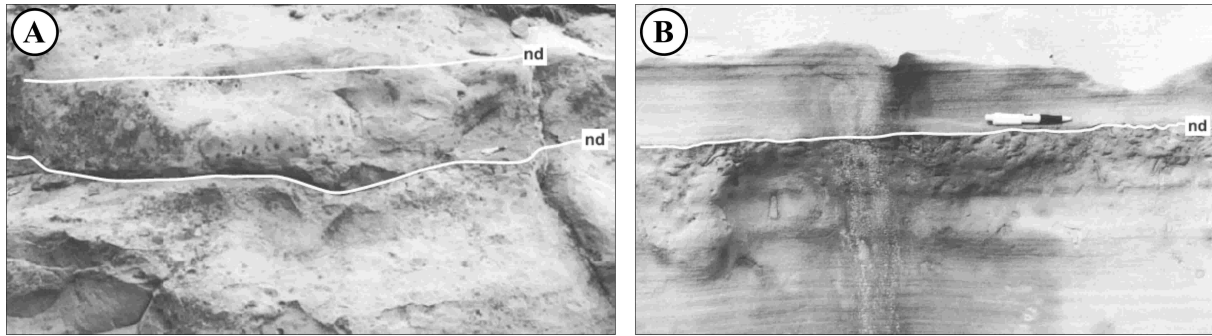
Figure 6.6. Up-dip expression of non-depositional (nd) discontinuity surfaces in the (A) foreshore and (B) lower shoreface, Kenilworth Member. The discontinuities pinch-out into unusually thick foreshore and USF deposits. The pictures are from Hampson et al. (in review, their Figure 6).

6.6 Formation of bedsets

The lateral extension of discontinuity surfaces will vary as different mechanisms affect the shoreline in different ways. Changes in wave climate and sea level will influence various parts of the shoreline similarly and simultaneously as the formative mechanisms most likely are of allocyclic origin (e.g. regional topography or high-frequency climate changes), whereas (autocyclic) changes in sediment supply may affect a more restricted part of the shoreline. In the Sunnyside Member, most of the discontinuity surfaces have been traced for at least 10 km along-strike (between Woodside Canyon and Long Canyon 1) without changing in thickness or internal architecture (except for S3.2b which pinch-out towards the south). The same have been observed in the overlying Grassy Member, where bedsets may be continuous for over 20 km along-strike (O'Byrne and Flint, 1995). This implies that the mechanism(s) responsible for bedset boundary formation are consistent for at least 10-20 km along-strike. In dip-direction, the bedsets in the Sunnyside Member have been traced for at least 8-14 km, whereas non-depositional discontinuity surfaces in the Kenilworth Member have been traced for 0.8-6 km (Hampson, 2000) and 0.5-9 km down-dip (Pattison, 1995). The formative mechanism(s) must therefore affect a relatively extensive part of the shoreface-shelf, both along-strike and down-dip.

According to Hampson and Howell (2005), the most landward position of S2 USF and foreshore deposits is located to the northwest of the study area (between Rock and Bear Canyon), whereas the basinward pinch-out of the same deposits is situated between Jeep Trail and Woodside Canyon, approximately 15 km farther to the east (Hampson and Howell, 2005). Similarly, the most landward position of S3 USF and foreshore deposits is found between South Lila Canyon and Woodside Canyon, whereas the basinward pinch-out can be observed

in the vicinity of Blue Castle Canyon, a distance of approximately 10 km farther to the east (Hampson and Howell, 2005). Between these localities, seven or eight bedsets have been recognized in S2 (Howell et al., in review), and three have been recognized in S3. This suggests that each bedset represent approximately 2-3 km of shoreline progradation. A similar pattern has also been interpreted from the underlying Kenilworth Member, which is indicating that each parasequence is comprised of 1-5 bedsets, each representing roughly 2-4 km of shoreline progradation (Hampson, 2000, their Figure 3 and Figure 6). Modern wave-dominated deltas demonstrate an average progradation rate of approximately 20 km for the last 5000 years (including several high-frequency sea level changes) (Dominguez et al., 1987; Dominguez, 1996). Assuming similar progradation rates for the ancient Sunnyside and Kenilworth shorelines, this (although very simplistic) comparison indicates that each bedset represent approximately 500-1000 years of progradation. Even though this not a fully quantitative estimation, this does indicate that bedsets are features which occupy a considerable amount of space and time, and that they were relatively sparse in numbers and comprised a substantial amount of the ancient prograding strandplain/delta system.

Hampson et al. (in review) suggested a close connection between individual beach-ridges and bedsets, beach-ridge sets and bedset stacking patterns, and progradational shorelines and parasequences. According to this study, beach-ridges (which are tens of meters wide, and tens of kilometres along-strike) can be traced into the subsurface where they correlated with basinward dipping clinoforms, which are interpreted to result from increased storm activity and/or high sediment reworking from longshore currents (Rodriguez and Meyer, in review). Beach-ridge sets (which are hundred of meters to several kilometres wide, and tens of kilometres along-strike) are bounded by erosional surfaces undistinguishable from the ones associated with individual beach-ridges, and do not correlate with distinct breaks in lithology (Rodriguez and Meyer, in review). Rather, these surfaces are angular discordant in plan view and mark the boundary of beach-ridge sets which indicate variations in shoreline trajectory (Hampson et al., in review). Beach-ridge sets have been interpreted to represent relocation of the river mouth in response to changes in sediment supply and wave climate, along with superimposed high-frequency changes in sea level (Hampson et al., in review; Rodriguez and Meyer, in review).

The main problem with connecting individual beach-ridges with individual bedsets, and beach-ridge sets with zones of different shoreline trajectories, is the variance in width and the time of formation. If each bedset in the prograding S3 was equivalent to one beach-ridge, each ridge would be several kilometres wide and the entire progradational shoreline would

125

have been composed of only 7-8 beach-ridges. For comparison, up to 280 beach ridges (one every 50 m) have been counted in four beach-ridge sets on the modern Nayarit strandplain in western Mexico (Curray et al., 1969). This indicates that modern beach-ridges occupy far less space, and that they are significantly more numerous than ancient bedsets in the Sunnyside Member (assuming similar dimensions of ancient and modern beach ridges).

The formation of beach-ridges is widely discussed, but there is a general agreement that sandy beach-ridges either originate as berms, or as alongshore amalgamation of mouth bars and spits (Bird, 2000; Otvos, 2000; Rodriguez et al., 2000; Bhattacharya and Giosan, 2003). The timing of beach-ridge formation is also debated, but an average of 30-150 years has been suggested by Otvos (2000), whereas Curray (1969) calculated that one beach-ridge was formed every 12-16 years during the Holocene progradation of the Nayarit strandplain. Rodriguez et al. (2000) suggested that ridges were created by alongshore migration of mouth bars, which may have formed within decades. However, both the preservation potential, and spacing of beach-ridges, are highly dependent on the sediment supply and amount of shoreline progradation (Bird, 2000). This suggests that the timing of beach-ridge formation in modern deltas and strandplains are at least one order of magnitude higher than bedsets in ancient shallow-marine systems.

Hampson et al. (in review) along with Rodriguez and Meyer (in review) have also suggested that individual beach-ridges can be traced into the subsurface, by using ground penetrating radar profiles, where they correlate with reflectors representing truncation of underlying strata. Although such erosional features may explain the presence of erosional discontinuity surfaces, they can not explain non-depositional discontinuities, as they are characterized by a decrease in sedimentation basinward of the LSF. Erosional scouring of the shoreface-shelf profile is likely to have occurred during increased wave climate, increased sediment supply or relative sea level fall, all of which increase sedimentation in the distal parts of the basin rather than decreasing it. Relative sea level fall and increasing wave base is also associated with a basinward shift of facies, instead of a landward shift of facies, which is characteristic for the bedset boundaries in the Sunnyside Member.

Beach-ridge sets, on the other hand, display more similarities to bedsets in both size and timing. They are considered to be up to several kilometres wide and are thought of as being deposited within several thousand years (Curray et al., 1969; Dominguez et al., 1987; Dominguez and Wanless, 1991; Dominguez, 1996; Hampson et al., in review). Some of the mechanisms associated with reorganization of beach-ridges (Figure 6.3) are related to changes in the wave climate (Rodriguez and Meyer, in review) or delta lobe sifting (Curray et al.,

1969), and even possibly with high-frequency changes in sea level (Dominguez et al., 1987; Dominguez and Wanless, 1991; Dominguez, 1996; Bhattacharya and Giosan, 2003; Rodriguez and Meyer, in review). As mentioned previously, internal parasequence architecture in the Sunnyside Member is characterized by non-depositional discontinuity surfaces in the LSF and OTZ, indicating decreasing wave climate. Observations from the study area suggest that the up-dip pinch-out of the surfaces occurs in the LSF where they become difficult to trace. In addition to this, core samples taken across truncating beach-ridge set boundaries demonstrates that there is no major change in lithology associated with the erosional surfaces (Rodriguez and Meyer, in review). This indicates that the bedset boundaries in the Sunnyside Member (along with those observed elsewhere in the Blackhawk Formation) may be related to similar erosional surfaces in the USF (and proximal LSF), which are not associated with changes in lithology. Moreover, Hampson and Storms (2003) also reported on unusual thick USF deposits associated with the landward pinch-out of bedset boundaries. Similar thick beach successions have also been observed on modern strandplains, where they occur along erosional boundaries and truncate beach-ridge sets (Curray et al., 1969). These observations further support a connection between bedsets and beach-ridge sets.

Figure 6.7 describes a theoretical model for development of non-depositional discontinuity surfaces (bedsets), as observed in the Sunnyside Member. As a delta lobe shifts due to for example channel avulsion, alternations in wave climate or high-frequency changes in sea level, the entire coastal system is rearranging, resulting in truncation of old beach-ridges, beach-ridge systems and repositioning of the river mouth (Curray et al., 1969; Dominguez, 1996; Bhattacharya and Giosan, 2003; Rodriguez and Meyer, in review). Topographic changes along the coastline, in response to repositioning of the river mouth, may result in alterations in the local wave climate as the abandoned part of the coastline becomes more sheltered. Changing height and direction of incoming waves will also affect the strength of the longshore currents, resulting in decreasing transport capacity and sediment supply (Figure 6.2) (Inman and Bagnold, 1963). Sediment supply may also decrease as the proximity to the river mouth and the fluvial discharge decreases. In addition, progradation of beach-ridge systems is dependent on wave climate and the amount of available sediments (Bird, 2000; Otvos, 2000; Rodriguez and Meyer, in review), and erosion occurs if the amount of sediments removed down-drift by longshore currents exceed the amount added from up-drift. As parts of the shoreline become abandoned, waves and currents rework the proximal part of the shoreface and transports sediments down-drift, rather than to the OTZ and offshore zone, which itself becomes sediment starved. In addition, the abandoned part of the shoreline may

experience localized compaction and subsidence due to loading, as well as a high-frequency, low-amplitude rises in sea level (Dominguez, 1996), which will only contribute further to this effect, storing all available sediments along the shoreline and the backshore area where accommodation space is being created. This may result in the formation of an erosional surface in the foreshore, USF and the most proximal part of the LSF as the profile adapts to the renewed depositional conditions (Figure 6.8). Because the distal part of the LSF and the OTZ only receives an insignificant amount of sediment during this period, the erosional surface correlates with a surface marked by non-deposition farther basinwards. This will explain the non-depositional discontinuity surfaces in the study area which are truncated in the LSF. As the newly established coastline progrades, an increasing amount of sediments will be distributed along the shoreline, and the abandoned part of the strandplain/delta will receive more material and eventually the whole system will start to prograde.
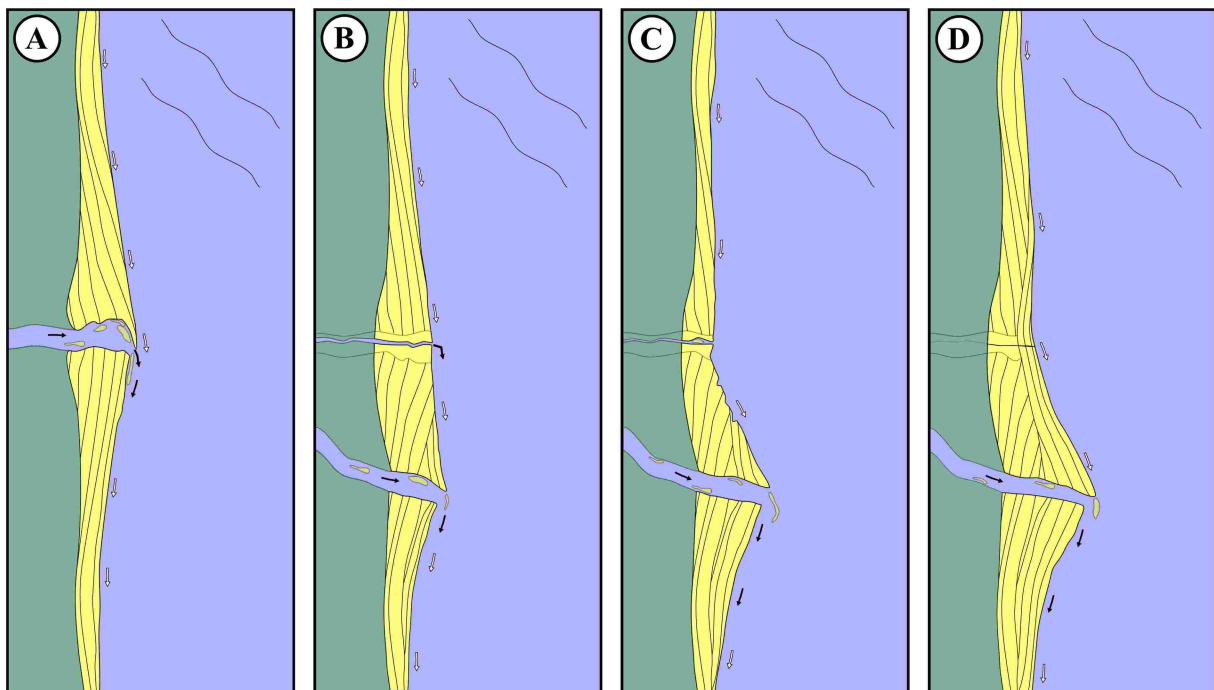
Figure 6.7.   (A and B) Bedsets may form in response to channel avulsion and delta lobe shifts. (B) Reorganization of the shoreline may result in a local decrease in longshore current and/or wave climate and sediment supply. (C) The proximal part of the abandoned shoreline is eroded and experience compaction and subsidence, whereas the distal part becomes sediment starved. (D) As the shoreline progrades, sediments are transported down-drift to the abandoned part of the shoreline which undergoes renewed progradation.

A relationship between the formation of bedsets and river mouth migration along progradational shorelines implies that the surfaces form during periods of normal regression with a horizontal to positively inclined shoreline trajectory (0°-90°) (Helland-Hansen and

Martinsen, 1996). A positively inclined shoreline trajectory indicates that accommodation space is being created in the non-marine realm, resulting in unstable distributary channels in coastal plain which are prone to avulsion. During periods of sea level fall and forced regression, on the other hand, no accommodation space is being created in the coastal plain or in the shallow-marine environment, and the distributary channels tend to be fixed within their pre-existing courses (Schumm and Ethridge, 1994). A similar relationship has also been described from the Kenilworth Member, where non-depositional discontinuity surfaces are interpreted to have been formed during normal regression, and where erosional discontinuities were formed during periods of falling sea level and forced regression (Hampson, 2000). The discontinuity surfaces in the Sunnyside Member have been interpreted to represent periods of a sub-horizontal shoreline trajectory (as discussed in Chapter Three) (Howell et al., in review), and reflects periods of relatively continuous accommodation space in the coastal plain. Non-depositional discontinuities surfaces similar to those which have been observed in the study area therefore interpreted to form during normal regression only, as forced regression inhibits lateral channel migration.
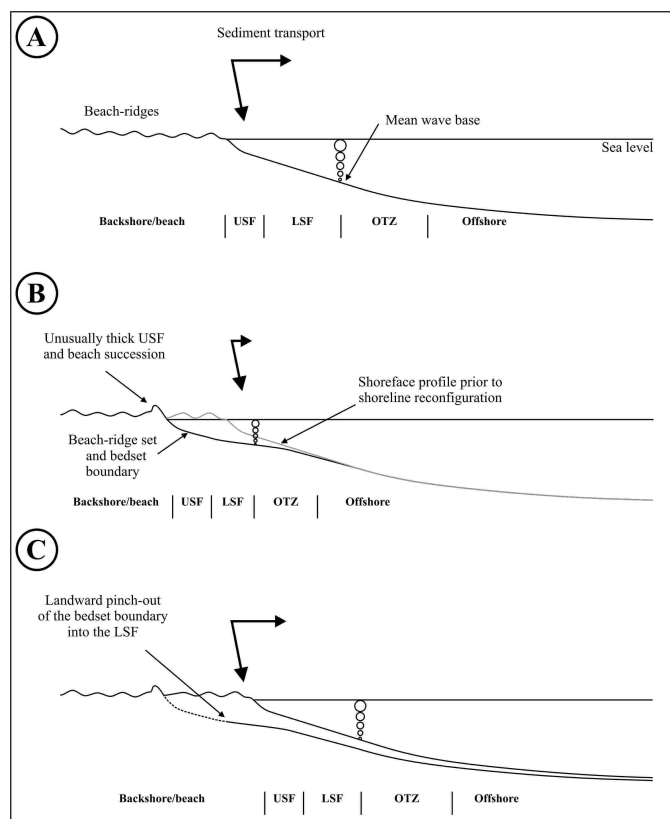
Figure 6.8. Model for formation of bedset boundaries and a beach-ridge set boundaries. (A) Normal progradation of a wave-dominated shoreline. Sediments are transported both basinwards (horizontal arrow) and along the shoreline by longshore drift (vertical arrow). (B) During periods of delta lobe shift and rearrangement of the shoreline topography, the foreshore, USF and the proximal parts of the LSF is eroded as the disequilibrium profile adapts to the new depositional setting. A decrease in wave climate and sediment supply to the distal parts of the shorefaces-shelf profile, results in the formation of a non-depositional discontinuity surfaces and a landward shift of facies. The landward extent of the bedset boundary marks the beach-ridge set boundary, which may be represented by a unusual thick USF and beach succession. (C) Reestablishment of the equilibrium profile results in renewed progradation of the shoreline.

Assuming a close connection between bedsets and beach-ridge sets (as suggested in the previous sections), these packages should reflect similar morphological patterns as beach

ridges along modern shorelines. The transition from S3.2 to S3.3 is associated with an abrupt change from an exclusively wave-dominated to a mixed wave and current-dominated bedset. Although the discontinuity surface bounding S3.3 (S3.3b) is less pronounced compared to the other bedset boundaries in the Sunnyside Member, the change in depositional environment that occurs across this surface is striking. This bedset in particular, supports the hypothesis of shifting delta lobes, positioning the ancient river mouth closer to the area represented by Woodside Canyon and Long Canyon 1.
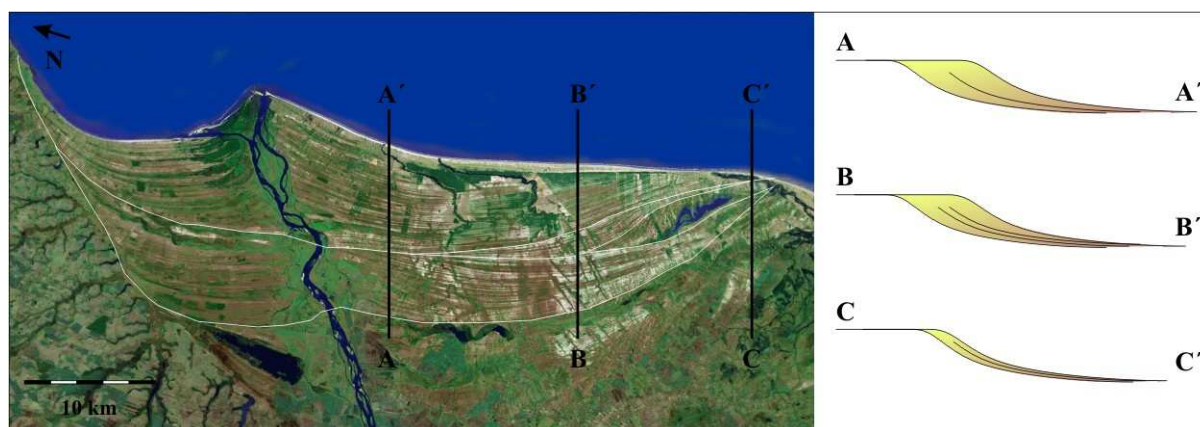
Figure 6.9. The Paraíba do Sul delta (Brazil) is composed of three discrete beach-ridge sets (bounded by white lines). Their cross-cutting relationship represents periods of delta lobe shifts and coastal reorganization during Holocene progradation. Cross-sections (A-C) represent different theoretical down-dip profiles through the delta, and indicate the variation in number and thickness of bedsets which may occur along-strike, assuming a close relationship between beach-ridge sets and bedsets. Bedsets may be lateral extensive along-strike but may also experience rapid truncation without leaving distinct erosional surfaces. The entire deltaic system is interpreted to correspond to a parasequence (Hampson et al., in review). Picture from Google Earth.

Another similarity between ancient bedsets in the Sunnyside Member and modern wave-dominated systems is apparent when one compares these to the modern day Paraíba do Sul delta in Brazil, which is composed of beach-ridge sets of different scales and sizes (Figure 6.9). Three main beach-ridge sets are recognized on the delta plain, representing episodes of delta lobe shifts and coastal reorganization during the Late Holocene (Dominguez et al., 1987). The width of beach-ridge sets varies along-strike as they are truncated by other ridge sets, or as they reach the delta plain margin. Interpreted cross-sections through the delta plain (based on the shapes and sizes of the beach-ridge sets) suggest that bedsets may vary in length along-strike and down-dip as they are truncated. Some bedsets (cross-section B) are laterally restricted when compared to others, as they are truncated along-strike. Such truncation of bedsets is comparable to the observations in the Sunnyside Member, where S3.1 and S3.2 in Woodside Canyon amalgamates into S3.2 towards the south, in Long Canyon 1 (Figure 3.4

and Figure 3.5). No erosional surface is observed in S3.2 (in Long Canyon 1) as anticipated by Rodriguez and Meyer (in review), indicating that beach-ridge set boundaries not are represented by changes in lithology. This interpretation also implies that beach-ridges should become thinner along-strike and eventually pinch-out or become truncated by another bedset. The pinch-out style is unpredictable, although observations of modern beach ridges (e.g. the Paraíba do Sul strandplain) suggest that they may be truncated within some hundred meters, which could be difficult to recognize in outcrop.

6.7 Petroleum and exploration potential of the Sunnyside Member

Reservoir properties within a wave-dominated highstand shoreline (such as one of the Sunnyside parasequences), will depend on good internal connectivity between sandstone bodies, both along-strike and down-dip. Parasequence boundaries are regional flooding surfaces which also have a continental component, reflecting a landward dislocation of the shoreline (Van Wagoner et al., 1990). Bedset boundaries, on the other hand, are more local and are not associated with a landwards shift of the shoreline. A good understanding of the reservoir will also depend on confident interpretation of bedset boundaries and parasequence boundaries, as they are associated with important geometrical differences (Hampson et al., in review). Intra parasequence connectivity between sandstone bodies will be related to pinch-out styles of bedsets and bedset boundaries, and it is therefore important to understand how they were formed in order to be able to predict their subsurface expression. The interpretation presented in this study suggests that besets similar to the ones observed in the Sunnyside Member will pinch out along-strike within some tens of kilometres, where they commonly becomes truncated by another bedset (beach ridge set). As observed between S3.1 and S3.2 in the field area, and between modern day beach ridge sets (Rodriguez and Meyer, in review), these truncational boundaries are associated with a sand-sand contact, resulting in good connectivity between successive sandstone bedsets along-strike (Figure 6.10). Consequently, the reservoir is characterized by an internal structure where most internal sandstone bodies are separated by a low permeable heterolithic unit vertically, but which are connected both up-dip, and along-strike, providing relatively good horizontal permeability.

From a reservoir perspective, the recognition of the incised valley complex, and an associated detached or attached lowstand shoreline, will also be of great importance.
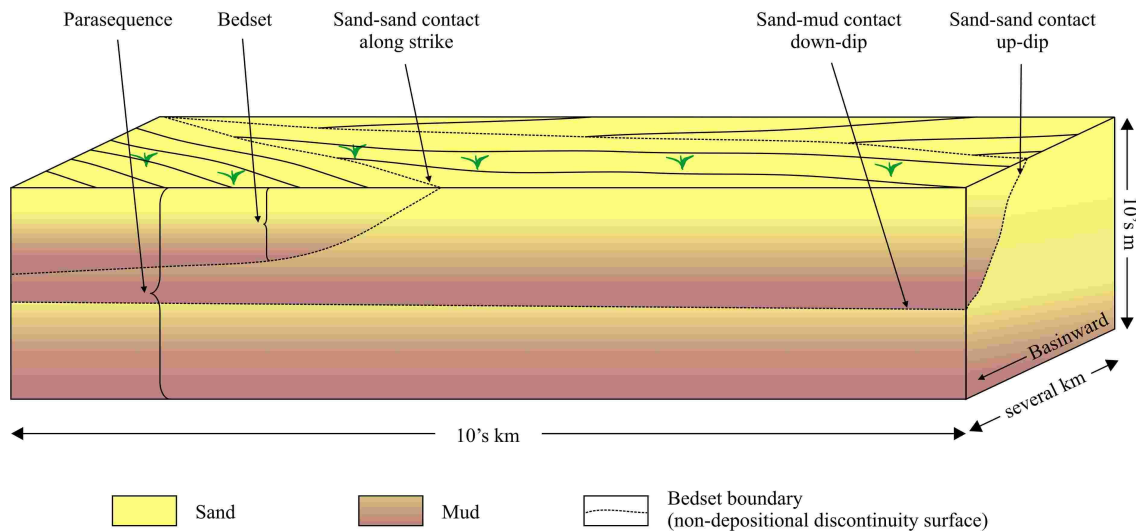
Figure 6.10. Bedset pinch-out style along-strike and down-dip. The parasequence is composed of three bedsets and represents a prograding wave-dominated shoreline. Bedset boundaries may form during truncation of beach ridge sets, and are associated with a sand-sand contact in the proximal part, and a sand-mud contact in the distal part. This results in good connectivity between the adjacent sandstone bodies. The figure is based on the features observed in the Sunnyside Member.

The sequence stratigraphic model for a foreland, ramp margin sequence (Figure 1.5) predicts deposition of a relatively sandy lowstand shoreline, whereas the model for shelf-break margin predicts relatively muddy submarine fans and slope fans (Van Wagoner et al., 1990). These lowstand fans are likely to be detached from the highstand shoreline if the sea level falls below the shelf break. The lowstand shoreline in a ramp margin (such as the Sunnyside shoreline) will probably be connected with the highstand shoreline through the incised valley, unless it is removed by transgressive erosion (Van Wagoner et al., 1990). In the Sunnyside Member, no lowstand shorelines have been observed and neither has the basinward pinch-out of the incised valley. As discussed in Chapter Three, this may relate to extensive transgressive erosion. The recognition of incised valleys and transgressive erosion is therefore important in predicting lowstand sandstones and down-dip connection between the HST and the LST, allowing fluid flow between potential reservoirs. In the Sunnyside Member, identification of an incised valley would be relatively straight forward in the proximal parts of Woodside Canyon, but very problematic distally and in Long Canyon 1, along the correlative SB. The only indication of an incised valley and an associated lowstand shoreline is the local presence of a coarse-grained transgressive lag, which is interpreted to be partly derived from the valley fill (Van Wagoner et al., 1990). No lag is present in Long Canyon 1, suggesting that the lag will disappear away from the incised valley, making the correlative SB hard to differentiate from a PSB which has similar expressions.

Chapter Seven – Summary and Conclusions

7.1 Summary and Conclusions

The Sunnyside Member was deposited on the western margin of the Late Cretaceous, Western Interior Seaway, and it is composed of three sandstone tongues which are separated by Mancos shale (Young, 1955). The three sandstone units are defined as wave-dominated, fifth-order parasequences, and comprise parts of three high-frequency sequences together with the underlying Kenilworth Member and the overlying Grassy Member (Young, 1955; Van Wagoner et al., 1990; Howell and Flint, 2003; Howell et al., in review). A number of sixth-order cycles (bedsets) are also superimposed on these parasequences, reflecting alternations in the shallow-marine depositional environment (Mitchum and Van Wagoner, 1991; Hampson and Storms, 2003; Howell et al., in review). Discontinuity surfaces bounding bedsets and parasequences may easily be misinterpreted in laterally restricted outcrops as their expression in the rock record is very similar, both marking units which are represented by an upward increase in grain-size and sandstone bed amalgamation. These surfaces indicate an abrupt decrease in sedimentation and an increase in bioturbation. The discontinuity surfaces can only be distinguished by tracing them up-dip, where bedset boundaries commonly disappear into the lower shoreface (indicating a landward shift of facies, not the shoreline), and where the parasequence boundary extend into the non-marine realm, suggesting marine flooding and a landward dislocation of the shoreline (Van Wagoner et al., 1990; Howell et al., in review).

Observations in Woodside Canyon and Long Canyon 1, suggest a progradational stacking pattern for the bedsets. The discontinuity surfaces allow correlation throughout most of the study area, and have been traced for 5-10 km down-dip, and commonly for more than 10 km along-strike, where they are associated with only minor changes in thickness and lithology (Figure 3.4 and Figure 3.5). All bedsets are characterized by an apparent landward shift of facies of a few kilometers. However, one bedset pinches-out laterally and amalgamates into the time-equivalent bedset farther south, leaving no trace of the discontinuity surface bounding it. Further, the uppermost bedset in S3 has a different expression then the remaining units, containing mixed wave and current induced sedimentary structures and low bioturbation (Figure 2.5). The unit also displays an abnormal pinch-out geometry and represents a basinward thinning wedge. This uppermost bedset is therefore

interpreted to result from an abrupt change in the depositional environment, and lateral shifts of the river mouth. Sea level fall subsequent to the deposition of this bedset led to extensive transgressive erosion of the uppermost part of the unit (Howell et al., in review). This is evident from a well developed Glossifungites firm-ground which is associated with the bounding PSB, and the removal of a considerable amount of proximal LSF, USF and foreshore deposits in and west of the study area.

Estuarine deposits in the proximal and central part of Woodside Canyon are interpreted as an incised valley fill, reflecting relative sea level rise (Howell et al., in review). This valley fill is very heterolithic and witness of a variety of depositional environments within the estuary (e.g. Figure 4.2)(Howell et al., in review). The general trend is a localized unit of tidal influenced fluvial deposits in the lower part of the valley, representing deposition during lowstand and early transgression (Dalrymple et al., 1992; Zaitlin et al., 1994). This unit is commonly overlain by IHS deposits, indicating a landward shift of facies, increased accommodation space, and decreasing down-dip gradient. The IHS has different expression and lithology throughout the study area, indicating varying types of tidal channels (Figure 4.7). Large, supra, intra and subtidal bar deposits are located within the channel sandstones, and commonly overlie the IHS. Locally, these are overlain by lagoonal and tidal flat interbedded mudstones and sandstone deposits, reflecting an upward transition into a more low- energy part of the estuary.

The absence of incised valley deposits in Log 10 suggests that this particular area was located outside the incised valley during sea level fall, or that the area represented an intra valley high at the time of formation (Figure 4.10). Alternatively, the absence of these deposits may relate to extensive transgressive erosion, as observed elsewhere in the field area (Howell et al., in review). The valley margin located between Log 12 and 13 (Figure 4.2) is interpreted to represent the southern margin of the estuary, and not its maximum basinward extent.

2D process-response modelling (BARSIM, Storms et al., 2002) suggests that discontinuity surfaces are formed within a variety of depositional environments (Storms and Hampson, 2005). Sea level rise results in the formation of distinct non-depositional discontinuity surfaces as most sediment is trapped in the nearshore and backshore area, and the entire shoreface-shelf experiences sediment starvation. The formation of these surfaces is associated with a deepening of the profile, both in the proximal and distal part, and a landward shift of facies and the shoreline. A (significant) rise in sea level gives rise to features which are characteristic of parasequences, not bedsets (Van Wagoner et al., 1990),

and are therefore not considered as an important driving mechanism for bedset (boundary) formation in the Sunnyside Member.

Changes in wave climate result mainly in the formation of erosional discontinuity surfaces in the proximal part of the shoreface-shelf and are accompanied with a basinward shift of facies (Storms and Hampson, 2005). Only minor discontinuities surfaces and facies shifts are associated with decreasing wave climate, which is also associated with deepening of the distal part of the shoreface-shelf profile. The discontinuity surfaces formed by changes in wave climate alone, are therefore not comparable to the ones observed in the field.

An abrupt decrease in sediment supply results in the formation of discontinuity surfaces extending across most of the shoreface-shelf. Such decrease is also associated with a marginal deepening of the distal part of the profile and a marginal shallowing of the proximal part. In contrast to changes in sea level and wave base, varying the sediment supply will not affect the position of the wave base, and the decrease in grain-size and amalgamation of sandstone beds is only dependent on the amount of sediments which are transported to the shoreface-shelf. Abrupt increase in sediment supply results in erosional surfaces which are restricted to the proximal part of the shoreface. Because of the lack of landward shift of facies, abrupt changes in sediment supply alone is not considered to be the main driving force for the formation of bedset boundaries observed in the field. Gradual, asymmetric changes in sediment supply have similar effects as those of abrupt changes, only less pronounced. Neither do these produce discontinuities which are comparable to the ones observed. The discontinuities which are associated with shifts in facies are also associated with changes of the shorefaces-shelf profile, whereas the ones not representing any facies shifts reflect a continuous profile curvature.

When the prograding shoreline is introduced to combined changes in wave climate and sediment supply, both erosional and non-depositional discontinuity surfaces are formed. Non-depositional surfaces are formed during periods when the shoreface-shelf is sediment starved, and when the wave base is dislocated landwards; this is associated with a minor deepening of the distal part of the shoreface-shelf profile. The discontinuity surfaces are truncated in the lower shoreface by erosional surfaces of restricted lateral extent. Even though the wells (A and B, Figure 5.22) do not display equally distinct coarsening upward units as those observed in the Sunnyside Member, the surfaces are associated with both a decrease in grain-size and sandbed amalgamation and a landward shift of facies, which makes them directly comparable to the ones observed in the field.

135

The bedsets in the Sunnyside Member are interpreted to result from shifting of delta lobes in response to for example changing fluvial discharge, over-extension of the river's course, high-frequency climate changes and/or, possibly, low-amplitude, high-frequency changes in relative sea level. A relatively abrupt relocation of the river mouth will affect the sediment supply down-drift. Such relocations may also be directly associated with changes in wave climate, either as a result, or as a consequence of the renewed coastline topography. The relationship between wave energy and topography also determine the strength and direction of the longshore current, which is an important sediment transport mechanism along wave-dominated coastlines (e.g. Inman and Bagnold, 1963; Dominguez et al., 1987). Delta lobe shifts may therefore be associated with a contemporary decrease in sediment supply and wave climate, resulting in sediment starvation and a landward shift of facies along the abandoned part of the coastline (Figure 6.3 and Figure 6.8). This effect may be further amplified by compaction, subsidence and low-amplitude, high-frequency changes in sea level.

A close connection between bedsets and beach-ridge sets is a result of this interpretation of bedset formation. Modern studies have suggested that beach ridge sets are formed as the river changes its course and rearranges the coastal morphology (e.g. Curray et al., 1969). This implies that bedsets in the subsurface will have similar geometries and aerial extent as the beach-ridge sets observed along modern coastlines. Core samples from modern strandplains indicates that the erosional boundaries defining each beach-ridge set not are associated with any change in lithology (Rodriguez and Meyer, in review). This will explain why bedset boundaries are hard to detect landward of the lower shoreface. Furthermore, unusual thick upper shoreface and foreshore deposits have been reported from the landward pinch-out of ancient bedset boundaries (Hampson and Storms, 2003). Similar, thick, beach ridge units have also been observed in modern stranplains where they occur along erosional boundaries truncating beach ridge sets (Curray et al., 1969). This relationship supports the interpretation of connection between bedsets and beach ridge sets.

The pinch-out geometry of bedsets both along-strike and down-dip is of great importance in a petroleum exploration perspective. Sand body connectivity is poor in the distal parts of the unit where thin sandstone tongues are interbedded with more muddy, distal deposits (Figure 6.10). Up-dip (landward of the lower shoreface), the transition between individual bedsets will be represented by a sand-sand contact, allowing fluid flow between the units. The erosional surfaces will also be connected by a sand-sand contact along-strike, favoring lateral connectivity between adjacent bedsets.

7.2 Further Work

Good control on the incised valley stratigraphy depends on detailed studies of the estuarine successions both in Woodside Canyon and in Long Canyon 2. Several valley margins should be present in these areas, but the detection of these will require careful tracing of the SB throughout the exposed cliff faces. The remote location of valley fill in Long Canyon 1 might be traced and exposed in outcrops on the southern side of the canyon. However, the unit is very thin and an identification will rely on detailed correlation of the G1b. Similarly, the outline of the incised valley in the area close to Log 10 might be identified by close inspections and tracing of surfaces in the relatively inaccessible cliffs.

The interpretation of bedset and bedset boundary formation presented in this study may be further strengthened by more close investigations both in the up-dip part and along-strike of the shallow-marine unit. If bedsets results from delta lobe shifts, they should pinch-out along-strike and/or be truncated by another bedset. Down-dip wells and core samples from modern analogs, extending from the backshore and into the offshore transition zone would identify non-depositional discontinuity surfaces along with their up-dip expression (erosion, rooting, cementing etc). In ancient outcrops, bedset boundaries should be traced to their most landward extent. If the uppermost, amalgamated part is a result from truncation and erosion during delta lobe shifts, the surface may be identified by a *Glossifungites* firm-ground, reflecting exhumation of the older shallow-marine sediments. The identification of unusual thick USF deposits will also indicate reorientation of beach ridge sets and lateral shifts of the river mouth (Curray et al., 1969).

References:

AINSWORTH, R.B., BOSSCHER, H. and M.J., N. 2000. Forward stratigraphic modelling of forced regressions; evidence for the genesis of attached and detached lowstand systems. In: *Sedimentary responses to forced regressions* (Eds D. Hunt and R.L. Gawthorpe), *Special Publication*, **172**, pp. 163. Geological Society.

AINSWORTH, R.B. and PATTISON, S.A.J. 1994. Where have all the lowstands gone? Evidence for attached lowstand systems tracts in the Western Interior of North America. *Geology*, **22**: 415.

BALSELY, J. 1980. Cretaceous wave dominated delta systems, Book Cliffs, East Central Utah. American Association of Petroleum Geologists field guide.

BEERBOWER, J.R. 1966. Cyclothems and cyclic depositional mechanisms in alluvial plain sedimentation. Symposium on cyclic sedimentation. *Bulletin*, **1**: 31.

BHATTACHARYA, J.P. and GIOSAN, L. 2003. Wave-influenced deltas: geomorphological implications for facies reconstruction. *Sedimentology*, **50**: 187.

BHATTACHARYA, J.P. and WALKER, R.G. 1992. Deltas. In: *Facies Models: Response to Sea-Level Change* (Eds R.G. Walker and N.P. James), pp. 157. Geological Association of Canada.

BIRD, E. 2000. *Coastal Geomorphology - An Introduction*. John Wiley & Sons Ltd, 340 pp.

BITTENCOURT, A.C.S.P., MARTIN, L., DOMINGUEZ, J.M.L., SILVA, I.R. and SOUSA, D.L. 2002. A significant longshore transport divergence zone at the Northeastern Brazilian coast: implications on coastal Quaternary evolution. *Anais Da Academia Brasileira De Ciencias*, **74**: 505.

BOGGS, S., JR. 2001. *Principles of sedimentology and stratigraphy*. Merrill Publ. Co. Columbus, OH, United States., 784 pp.

BOYD, R., DALRYMPLE, R. and ZAITLIN, B.A. 1992. Classification of Clastic Coastal Depositional-Environments. *Sedimentary Geology*, **80**: 139.

BROMLEY, R.G., PEMBERTON, S.G. and RAHMANI, R.A. 1984. A Cretaceous Woodground - the Teredolites Ichnofacies. *Journal of Paleontology*, **58**: 488.

BRUUN, P. 1962. Sea-level rise as a cause of shore erosion. *Proceedings of the American Society of Civil Engineers.*, **88**: 117.

BURCHFIEL, B.C. and DAVIS, G.A. 1975. Nature and Controls of Cordilleran Orogenesis, Western United-States - Extensions of an Earlier Synthesis. *American Journal of Science*, **A275**: 363.

CLIFTON, H.E., PHILLIPS, R.L. and HUNTER, R.E. 1971. Depositional structures and processes in the non-barred high-energy nearshore. *Journal of Sedimentary Petrology*, **41**: 651.

COLLINSON, J.D. 1996. Alluvial sediments. In: *Sedimentary Environments: Processes, Facies and Stratigraphy* (Ed H.G. Reading), pp. 37.

COLLINSON, J.D. and THOMPSON, D.B. 1989. *Sedimentary Structures*. Unwin Hyman Ltd, 207 pp.

COOPER, J.A.G. and PILKEY, O.H. 2004. Sea-level rise and shoreline retreat: time to abandon the Bruun Rule. *Global and Planetary Change*, **43**: 157.

CURRAY, J.R., EMMEL, F.J. and CRAMPTON, P.J.S. 1969. Holocene history of a strand plain, lagoonal coast, Nayarit, Mexico. In: *Lagunas costeras, un simposio-Coastal lagoons, a symposium.* (Eds C.A. Ayala and F.B. Phleger), pp. 63. Mex., Univ. Nac. Auton.

DALRYMPLE, R. 1992. Tidal depositional systems. In: *Facies Models: Response to Sea-Level Change* (Eds R.G. Walker and N.P. James), pp. 195. Geological Association of Canada.

DALRYMPLE, R.W., ZAITLIN, B.A. and BOYD, R. 1992. Estuarine facies models - conceptual basis and stratigraphic implications. *Journal of Sedimentary Petrology*, **62**: 1130.

DAVIES, R., DIESSEL, C., HOWELL, J., FLINT, S. and BOYD, R. 2005. Vertical and lateral variation in the petrography of the Upper Cretaceous Sunnyside coal of eastern Utah, USA - implications for the recognition of high-resolution accommodation changes in paralic coal seams. *International Journal of Coal Geology*, **61**: 13.

DECELLES, P.G. and GILES, K.A. 1996. Foreland basin systems. *Basin Research*, **8**: 105.

DOMINGUEZ, J.M.L. 1996. The Sao Francisco Strandplain; a paradigm for wave-dominated deltas? In: *Geology of siliciclastic shelf seas*, *Geological Society Special Publication*, **117**, pp. 217.

DOMINGUEZ, J.M.L., MARTIN, M. and BITTENCOURT, A. 1987. Sea-level history and Quaternary evolution of river mouth-associated beach-ridge plains along the East-Southeast Brazilian coast; a summary. In: *Sea-level fluctuation and coastal evolution* (Eds D. Nummedal, O.H. Pilkey and J.D. Howard), *Special Publication*, **41**, pp. 115. Society of Economic Paleontologists and Mineralogists.

DOMINGUEZ, J.M.L. and WANLESS, H.R. 1991. Facies architecture of a falling sea-level strandplain; Doce River coast, Brazil. In: *Shelf sand and sandstone bodies; geometry, facies and sequence stratigraphy* (Eds D.J.P. Swift, G.F. Oertel, R.W. Tillman and J.A. Thorne), *Special Publication*, **14**, pp. 259. International Association of Sedimentologists.

DOTT, R.H. and BOURGEOIS, J. 1982. Hummocky stratification - significance of its variable bedding sequences. *Geological Society of America Bulletin*, **93**: 663.

GOODBRED, S.L. and KUEHL, S.A. 2000. The significance of large sediment supply, active tectonism, and eustasy on margin sequence development: Late Quaternary stratigraphy and evolution of the Ganges-Brahmaputra delta. *Sedimentary Geology*, **133**: 227.

HAMPSON, G.J. 2000. Discontinuity surfaces, clinoforms, and facies architecture in a wave-dominated, shoreface-shelf parasequence. *Journal of Sedimentary Research*, **70**: 325.

HAMPSON, G.J., BURGESS, P.M. and HOWELL, J.A. 2001. Shoreface tongue geometry constrains history of relative sea-level fall: examples from Late Cretaceous strata in the Book Cliffs area, Utah. *Terra Nova*, **13**: 188.

HAMPSON, G.J. and HOWELL, J.A. 2005. Sedimentologic and geomorphic characterization of ancient wave-dominated deltaic shorelines: Late Cretaceous Blackhawk Formation, Book Cliffs, Utah. In: *River Deltas - Consepts, Models and Examples* (Eds L. Giosan and J.P. Bhattacharya), *Special Publication*, **83**. Society for Sedimentary Geology.

HAMPSON, G.J., RODRIGUEZ, A.B., STORMS, J.E.A., HOWARD, D., JOHNSON, H.D. and MEYER, C.T. in review. Geomorphology and high-resolution stratigraphy of wave-dominated shoreline deposits: impact on reservoir-scale facies architecture.

HAMPSON, G.J. and STORMS, J.E.A. 2003. Geomorphological and sequence stratigraphic variability in wave-dominated, shoreface-shelf parasequences. *Sedimentology*, **50**: 667.

HAQ, B.U., HARDENBOL, J. and VAIL, P.R. 1988. Mesozoic and Cenozoic chronostratigraphy and cycles of sea-level change. In: *Sea-level changes; an integrated approach* (Eds C.K. Wilgus et al.), *Special Publication*, **42**, pp. 72. Society of Economic Paleontologists and Mineralogists.

HELLAND-HANSEN, W. and MARTINSEN, O.J. 1996. Shoreline trajectories and sequences: Description of variable depositional-dip scenarios. *Journal of Sedimentary Research*, **66**: 670.

HINTZE, L.F. 1988. *Geologic history of Utah*. Geology Studies. Special Publication. 7. Brigham Young University. Provo, UT, United States, 202 pp.

HOWELL, J.A. 2004. Shoreface and shallow marine deposits. In: *Encyclopedia of Geology* (Eds R.C. Selley, L.R.M. Cocks and I.R. Plimmer), pp. 570.

HOWELL, J.A. and FLINT, S. 2003. Sedimentology and sequence stratigraphy of the Book Cliffs. In: *The Sedimentary record of sea-level change* (Ed G. Bearman), pp. 135. The Open University.

HOWELL, J.A., KAMOLA, D.L. and FLINT, S. in review. Sedimentology and Stratigraphy of the Sunnyside Member of the Blackhawk Formation, Book Cliffs, Eastern Utah.

HUNT, D. and TUCKER, M.E. 1992. Stranded Parasequences and the Forced Regressive Wedge Systems Tract - Deposition during Base-Level Fall. *Sedimentary Geology*, **81**: 1.

INMAN, D.L. and BAGNOLD, R.A. 1963. Beach and nearshore processes. In: *The sea-Ideas and observations on progress in the study of the seas* (Ed M.N. Hill), pp. 529.

JERVEY, M.T. 1988. Quantitative geological modeling of siliciclastic rock sequences and their seismic expression. In: *Sea-level changes; an integrated approach* (Eds C.K. Wilgus et al.), *Special Publication*, **42**, pp. 47. Society of Economic Paleontologists and Mineralogists.

JOHNSON, H.D. and BALDWIN, C.T. 1996. Shallow clastic seas. In: *Sedimentary Environments: Processes, Facies and Stratigraphy* (Ed H.G. Reading), pp. 232.

KAMOLA, D.L. and VAN WAGONER, J.C. 1995. Stratigraphy and facies architecture of parasequences with examples from the Spring Canyon. In: *Sequence stratigraphy of foreland basin deposits* (Eds J.C. Van Wagoner and G.T. Bertram), *Memoir*, **64**, pp. 27. American Association of Petroleum Geologists.

KAUFFMAN, E.G. 1984. Paleobiogeography and evolutionary response dynamic in the Cretaceous Western Interior seaway of North America. In: *Jurassic-Cretaceous biochronology and biogeography of North America* (Ed G.E.G. Westermann), *Special Paper*, **27**, pp. 273. Geological Association of Canada.

KRYSTINIK, L.F. and DEJARNETT, B.B. 1995. Lateral variability of sequence stratigraphic framework in the Campanian and lower Maastrichtian of the Western Interior Seaway. In: *Sequence stratigraphy of foreland basin deposits* (Eds J.C. Van Wagoner and G.T. Bertram), *Memoir*, **64**, pp. 11. American Association of Petroleum Geologists.

LARSON, M. and KRAUS, N.C. 1994. Temporal and Spatial Scales of Beach Profile Change, Duck, North-Carolina. *Marine Geology*, **117**: 75.

LEATHERMAN, S. 2001. Social and economic costs of sea level rise. In: *Sea level rise; history and consequences* (Eds B.C. Douglas, M.S. Kearney and S.P. Leatherman), *International geophysics series*, **75**, pp. 181.

MACEACHERN, J.A. and PEMBERTON, G.S. 1994. Ichnological aspects of incised-valley fill systems from the Viking Formation of the Western Canada sedimentary basin, Alberta, Canada. In: *Incised-valley systems; origin and sedimentary sequences* (Eds R. Dalrymple, R. Boyd and B.A. Zaitlin), *Special Publication*, **51**, pp. 11. Society for Sedimentary Geology.

MIALL, A.D. 1992. Alluvial deposits. In: *Facies Models: Response to Sea-Level Change* (Eds R.G. Walker and N.P. James), pp. 119. Geological Association of Canada.

MITCHUM, R.M. 1977. Seismic stratigraphy and global changes of sea level; Part 11, Glossary of terms used in seismic stratigraphy. Seismic stratigraphy; applications to hydrocarbon exploration. In: *Seismic stratigraphy; applications to hydrocarbon exploration* (Ed C.E. Payton), *Memoir*, **26**, pp. 205. American Association of Petroleum Geologists.

MITCHUM, R.M. and VAN WAGONER, J.C. 1991. High-Frequency Sequences and Their Stacking Patterns - Sequence-Stratigraphic Evidence of High-Frequency Eustatic Cycles. *Sedimentary Geology*, **70**: 131.

NIEDORODA, A.W., REED, C.W., SWIFT, D.J.P., ARATO, H. and HOYANAGI, K. 1995. Modeling Shore-Normal Large-Scale Coastal Evolution. *Marine Geology*, **126**: 181.

NIEDORODA, A.W., SWIFT, D.J.P., HOPKINS, T.S. and MA, C.M. 1984. Shoreface Morphodynamics on Wave-Dominated Coasts. *Marine Geology*, **60**: 331.

NIO, S.D. and YANG, C.S. 1991. Diagnostic attributes of clastic tidal deposits; a review. In: *Clastic tidal sedimentology* (Eds D.G. Smith, B.A. Zaitlin, G.E. Reinson and R.A. Rahmani), *Memoir*, **16**, pp. 3. Canadian Society of Petroleum Geologists.

NUMMEDAL, D., RILEY, G.W. and TEMPLETT, P.L. 1993. High-resolution sequence architecture; a chronostratigraphic model based on equilibrium profile studies. In: *Sequence stratigraphy and facies associations* (Eds H.W. Posamentier, C.P. Summerhayes, B.U. Haq and G.P. Allen), *Special Publication*, **18**, pp. 55. International Association of Sedimentologists.

O'Byrne, C.J. and FLINT, S. 1995. Sequence, parasequence and intraparasequence architecture of the Grassy Member, Blackhawk Formation, Book Cliffs, Utah. In: *Sequence stratigraphy of foreland basin deposits* (Eds J.C. Van Wagoner and G.T. Bertram), *Memoir*, **64**, pp. 225. American Association of Petroleum Geologists.

OBRADOVICH, J.D. 1993. A Cretaceous time scale. In: *Evolution of the Western Interior Basin* (Eds W.G.E. Caldwell and E.G. Kauffman), *Special Paper*, **39**, pp. 379. Geological Association of Canada.

OTVOS, E.G. 2000. Beach ridges - definitions and significance. *Geomorphology*, **32**: 83.

PATTISON, S.A.J. 1995. Sequence stratigraphic significance of sharp-based lowstand shoreface deposits, Kenilworth Member, Book-Cliffs, Utah. *American Association of Petroleum Geologists Bulletin*, **79**: 444.

PEMBERTON, S.G. 1998. Stratigraphic applications of the Glossifungites ichnofacies: Delineating discontinuities in the rock record. *American Association of Petroleum Geologists Bulletin, Distinguished Lecturers; Abstracts.*, **82**: 2155.

PEMBERTON, S.G., MACEACHERN, J.A. and FREY, R.W. 1992a. Trace fossil facies models; environmental and allostratigraphic significance. In: *Facies models; response to sea level change* (Eds R.G. Walker and D.P. James), pp. 47. Geological Association of Canada.

PEMBERTON, S.G., VAN WAGONER, J.C. and WACH, G.D. 1992b. Ichnofacies of a wave-dominated shoreline. In: *Applications of Ichnology to Petroleum Exploration: A Core Workshop* (Ed S.G. Pemberton), **17**, pp. 339. Society for Sedimentary Geology.

POSAMENTIER, H.W., ALLEN, G.P., JAMES, D.P. and TESSON, M. 1992. Forced Regressions in a Sequence Stratigraphic Framework - Concepts, Examples, and Exploration Significance. *American Association of Petroleum Geologists Bulletin*, **76**: 1687.

POSAMENTIER, H.W., JERVEY, M.T. and VAIL, P.R. 1988. Eustatic controls on clastic deposition; I, Conceptual framework. In: *Sea-level changes; an integrated approach* (Eds C.K. Wilgus et al.), *Special Publication*, **42**, pp. 109. Society of Economic Paleontologists and Mineralogists.

POSAMENTIER, H.W. and VAIL, P.R. 1988. Eustatic controls on clastic deposition; II, Sequence and systems tract models. In: *Sea-level changes; an integrated approach* (Eds C.K. Wilgus et al.), *Special Publication*, **42**, pp. 125. Society of Economic Paleontologists and Mineralogists.

READING, H.G. and COLLINSON, J.D. 1996. Clastic Coasts. In: *Sedimentary Environments: Processes, Facies and Stratigraphy* (Ed H.G. Reading) Third edn, pp. 154.

READING, H.G. and LEVELL, B.K. 1996. Controls on the sedimentary rock record. In: *Sedimentary Environments: Processes, Facies and Stratigraphy* (Ed H.G. Reading), pp. 5.

REINECK, H.E. and SINGH, I.B. 1980. *Depositional sedimentary environments*. Berlin, Heidelberg, New York, Springer Verlag, 549 pp.

RODRIGUEZ, A.B., FASSELL, M.L. and ANDERSON, J.B. 2001. Variations in shoreface progradation and ravinement along the Texas coast, Gulf of Mexico. *Sedimentology*, **48**: 837.

RODRIGUEZ, A.B., HAMILTON, M.D. and ANDERSON, J.B. 2000. Facies and evolution of the modern Brazos Delta, Texas: wave versus flood influence. *Journal of Sedimentary Research*, **70**: 283.

RODRIGUEZ, A.B. and MEYER, C.T. in review. Sea-level variations during the Holocene deduced from the morphologic and stratigraphic evolution of Morgan Peninsul, Alabama, USA.

SCHUMM, S.A. and ETHRIDGE, F.G. 1994. Origin, evolution and morphology of fluvial valleys. In: *Incised-valley systems; origin and sedimentary sequences.* (Eds R. Dalrymple, R. Boyd and B.A. Zaitlin), *Special Publication*, **51**, pp. 11. Society for Sedimentary Geology.

SHANLEY, K.W. and MCCABE, P.J. 1995. Sequence stratigraphy of Turonian-Santonian strata, Kaiparowits Plateau, southern Utah, U.S.A.; implications for regional correlation and foreland basin evolution. In: *Sequence stratigraphy of foreland basin deposits* (Eds J.C. Van Wagoner and G.T. Bertram), *Memoir*, **64**, pp. 103. American Association of Petroleum Geologists.

SPIEKER, E.M. 1946. Late Mesozoic and early Cenozoic history of central Utah. *U.S. Geological Survey Professional Paper*117.

SPIEKER, E.M. and REESIDE, J.B.J. 1925. Cretaceous and Tertiary formations of the Wasatch Plateau, Utah. *Geological Society of America Bulletin*, **36**: 435.

STIVE, M.J.F. and DE VRIEND, H.J. 1995. Modeling Shoreface Profile Evolution. *Marine Geology*, **126**: 235.

STORMS, J.E.A. 2003. Event-based stratigraphic simulation of wave-dominated shallow-marine environments. *Marine Geology*, **199**: 83.

STORMS, J.E.A. and HAMPSON, G.J. 2005. Mechanisms for forming discontinuity surfaces within shoreface-shelf parasequences: Sea level, sediment supply, or wave regime? *Journal of Sedimentary Research*, **75**: 67.

STORMS, J.E.A. and SWIFT, D.J.P. 2003. Shallow-marine sequences as the building blocks of stratigraphy: insights from numerical modelling. *Basin Research*, **15**: 287.

STORMS, J.E.A., WELTJE, G.J., VAN DIJKE, J.J., GEEL, C.R. and KROONENBERG, S.B. 2002. Process-response modeling of wave-dominated coastal systems: Simulating evolution and stratigraphy on geological timescales. *Journal of Sedimentary Research*, **72**: 226.

STOW, D.A.V., READING, H.G. and COLLINSON, J.D. 1996. Deep seas. In: *Sedimentary Environments: Processes, Facies and Stratigraphy* (Ed H.G. Reading).

SUTER, J.R. and BERRYHILL, H.L. 1984. Late Quaternary shelf margin deltas, Northwest Gulf of Mexico.AAPG annual convention with divisions; SEPM/ EMD/ DPA. *American Association of Petroleum Geologists Bulletin*, **68**: 532.

SWIFT, D.J.P., FIGUEIREDO, A.G., FREELAND, G.L. and OERTEL, G.F. 1983. Hummocky cross-stratification and megaripples - a geological double-standard. *Journal of Sedimentary Petrology*, **53**: 1295.

TAYLOR, A., GOLDRING, R. and GOWLAND, S. 2003. Analysis and application of ichnofabrics. *Earth-Science Reviews*, **60**: 227.

TAYLOR, A.M. and GOLDRING, R. 1993. Description and Analysis of Bioturbation and Ichnofabric. *Journal of the Geological Society*, **150**: 141.

TAYLOR, D., LOVELL, R. and RICHARD, W.W. 1995. High-frequency sequence stratigraphy and paleogeography of the Kenilworth Member, Blackhawk Formation, Book Cliffs, Utah, U.S.A. In: *Sequence stratigraphy of foreland basin deposits* (Eds J.C. Van Wagoner and G.T. Bertram), *Memoir*, **64**, pp. 257. American Association of Petroleum Geologists.

THOMAS, R.G., SMITH, D.G., WOOD, J.M., VISSER, J., CALVERLEYRANGE, E.A. and KOSTER, E.H. 1987. Inclined heterolithic stratification - terminology, description, interpretation and significance. *Sedimentary Geology*, **53**: 123.

THORNE, J.A. and SWIFT, D.J.P. 1991a. Sedimentation on continental margins; II, Application of the regime concept. In: *Shelf sand and sandstone bodies; geometry, facies and sequence stratigraphy* (Eds D.J.P. Swift, G.F. Oertel, R.W. Tillman and J.A. Thorne), *Special Publication*, **14**, pp. 33. International Association of Sedimentologists.

THORNE, J.A. and SWIFT, D.J.P. 1991b. Sedimentation on continental margins; VI, A regime model for depositional sequences, their component systems tracts, and bounding surfaces. In: *Shelf sand and sandstone bodies; geometry, facies and sequence stratigraphy* (Eds D.J.P. Swift, G.F. Oertel, R.W. Tillman and J.A. Thorne), *Special Publication*, **14**, pp. 189. International Association of Sedimentologists.

VAN WAGONER, J.C. 1995. Sequence stratigraphy and marine to non-marine facies architecture of foreland basin strata, Book Cliffs, Utah, U.S.A. In: *Sequence stratigraphy of foreland basin deposits* (Eds J.C. Van Wagoner and G.T. Bertram), *Memoir*, **64**, pp. 137. American Association of Petroleum Geologists.

VAN WAGONER, J.C., MITCHUM, R.M., CAMPION, K.M. and RAHMANIAN, V.D. 1990. *Siliciclastic sequence stratigraphy in well logs, cores, and outcrops; concepts for high-resolution correlation of time and facies*. Methods in Exploration Series, **7**. American Association of Petroleum Geologists, 55 pp.

VAN WAGONER, J.C., POSAMENTIER, H.W., MITCHUM, R.M., VAIL, P.R., SARG, J.F., LOUITT, T.S. and HARDENBOL, J. 1988. An overview of the fundamentals of sequence stratigraphy and key definitions. In: *Sea-level changes; an integrated approach* (Eds C.K. Wilgus et al.), *Special Publication*, **42**, pp. 39. Society of Economic Paleontologists and Mineralogists.

WALKER, R.G. and PLINT, A.G. 1992. Wave- and Storm-Dominated Shallow Marine Systems. In: *Facies Models: Response to Sea-Level Change* (Eds R.G. Walker and D.P. James), pp. 219. Geological Association of Canada.

WEIMER, R.J. 1988. Record of relative sea-level changes; Cretaceous of Western Interior, USA. In: *Sea-level changes; an integrated approach* (Eds C.K. Wilgus et al.), *Special Publication*, **42**, pp. 285. Society of Economic Paleontologists and Mineralogists.

WRIGHT, L.D. 1977. Sediment Transport and Deposition at River Mouths - Synthesis. *Geological Society of America Bulletin*, **88**: 857.

WRIGHT, L.D., CHAPPELL, J., THOM, B.G., BRADSHAW, M.P. and COWELL, P. 1979. Morphodynamics of Reflective and Dissipative Beach and Inshore Systems - Southeastern Australia. *Marine Geology*, **32**: 105.

YOUNG, R.G. 1955. Sedimentary Facies and Intertonguing in the Upper Cretaceous of the Book Cliffs, Utah-Colorado. *Geological Society of America Bulletin*, **66**: 177.

ZAITLIN, B.A., DALRYMPLE, R.W. and BOYD, R. 1994. The stratigraphic organization of incised-valley systems associated with relative sea-level change. In: *Incised-valley systems; origin and sedimentary sequences.* (Eds R. Dalrymple, R. Boyd and B.A. Zaitlin), *Special Publication*, **51**, pp. 45. Society for Sedimentary Geology.

ZHANG, K.Q., DOUGLAS, B.C. and LEATHERMAN, S.P. 2004. Global warming and coastal erosion. *Climatic Change*, **64**: 41.

Appendix:

Sedimentological logs and facies associations

Log 3 to Log 27

Trail Canyon
W1
W2
W3
W4
3
26
18
4
6
10
9
11
Woodside
Canyon
12 13
8
19
14
26
15
27
16
17
Long
Canyon 2
Jenny Canyon
Gray
Canyon
20
Long
21 22
23 24
Canyon 1
25
Gunnison Butte
Blue Castle Canyon
N
Tusher Canyon
2 km
Battleship Butte
Green River
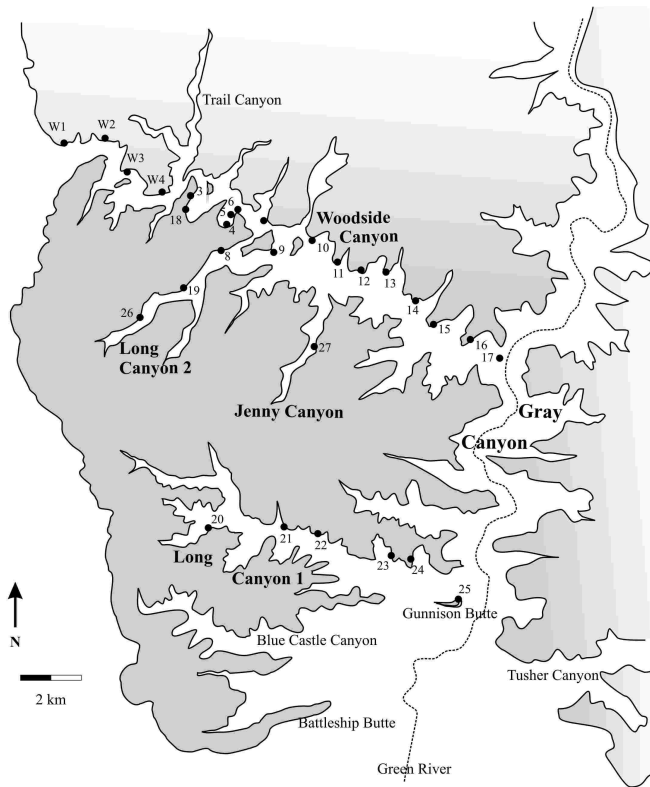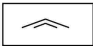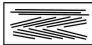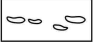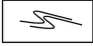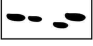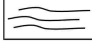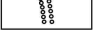
Bounding surfaces:

G3b — Grassy parasequence boundary 3

G2b — Grassy parasequence boundary 2

G1.1b — Grassy bedset boundary 1.1

G1b — Grassy parasequence boundary 1
(locally also interfluve sequence boundary)

SB — Sequence boundary

S3.3b — Sunnyside bedset boundary 3.3

S3.2b — Sunnyside bedset boundary 3.2

S3.1b — Sunnyside bedset boundary 3.1

S3b — Sunnyside parasequence boundary 3
(interfluve sequence boundary)

S2.7b — Sunnyside bedset boundary 2.7

S2.6b — Sunnyside bedset boundary 2.6

S2.5b — Sunnyside bedset boundary 2.5

S2.4b — Sunnyside bedset boundary 2.4

Facies associations:

Upper shoreface (USF)

Lower shoreface (LSF)

Distal offshore
transition zone (dOTZ)

Middle shoreface (MSF)

Proximal offshore
transition zone (pOTZ)

Offshore

Incised valley
(marginal marine)

Log key:

Trough cross-stratification

Wave ripples

Teeth

Tabular cross-stratification

Current ripples

Mud rip-up clasts

Planar stratification

Soft sediment deformation

Pebbles

Undulating stratification

Roots

Concretions/nodules

Flaser/lenticular/wavy bedding

Wood/log imprint

High-intense bioturbation
typical of the *Cruziana*
ichnofacies

Hummocky cross-stratification

Bone fragments

Low to moderate bioturbation
typical of the *Skolithos*
ichnofacies

Shell fragments

Glossifungites ichnofacies

Log 3
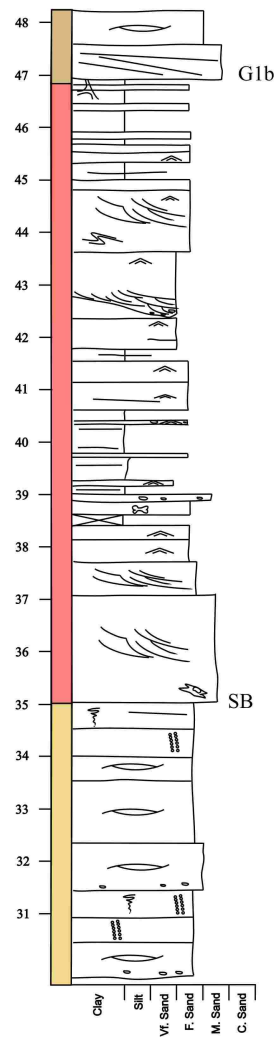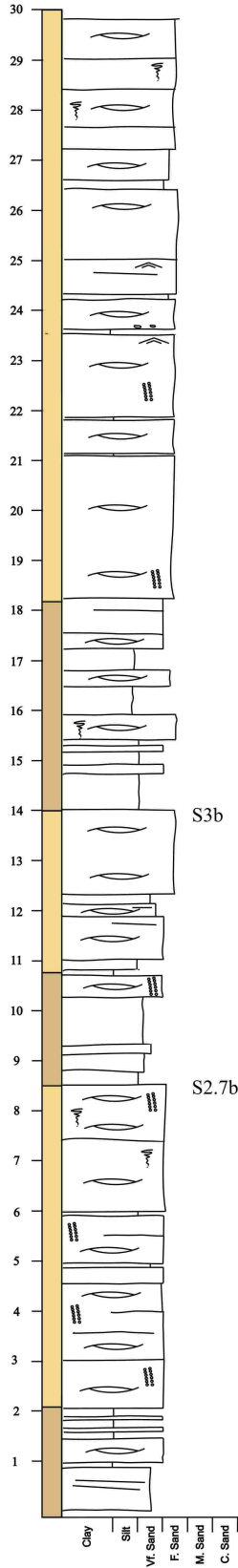
Log 4
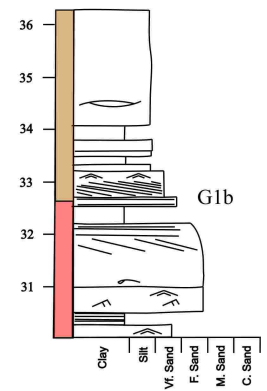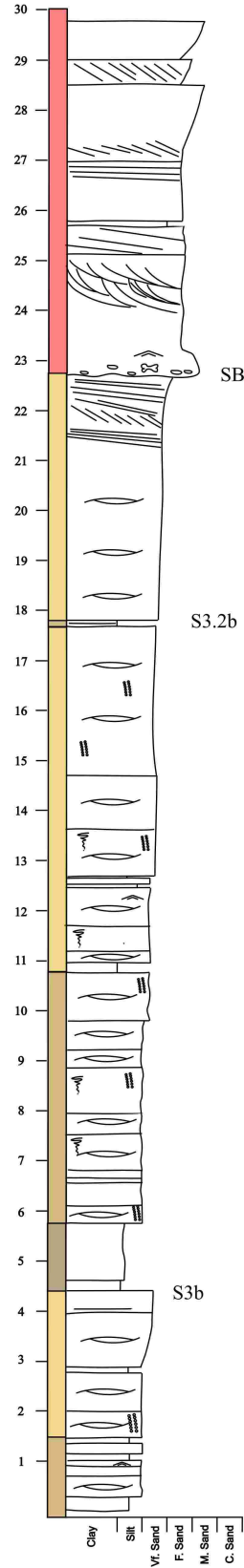
Log 5
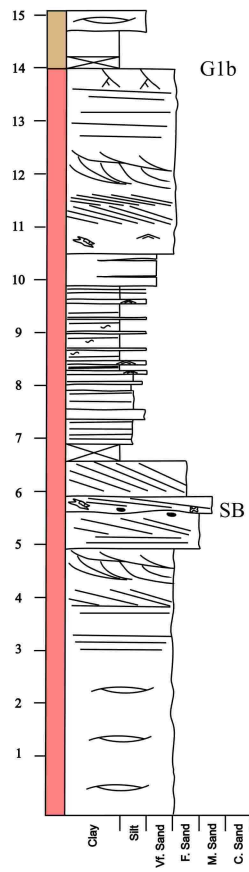
Log 6
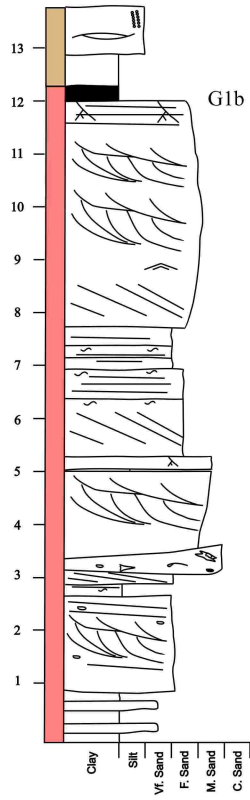
Log 18
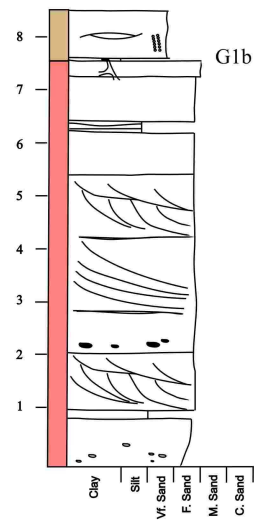
Log 7
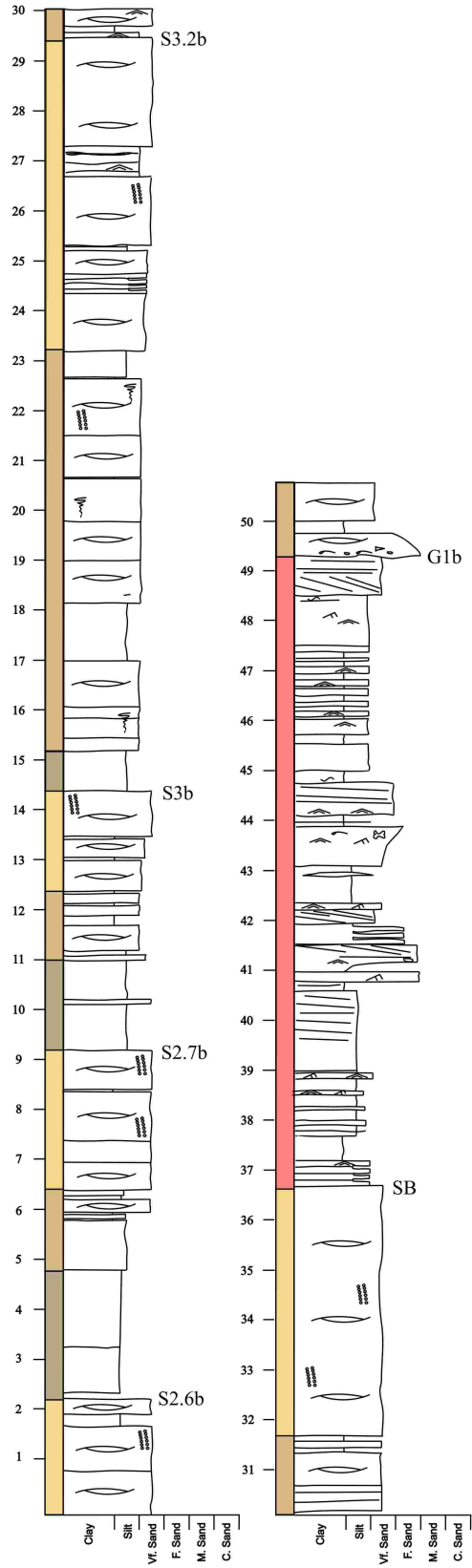
Log 8
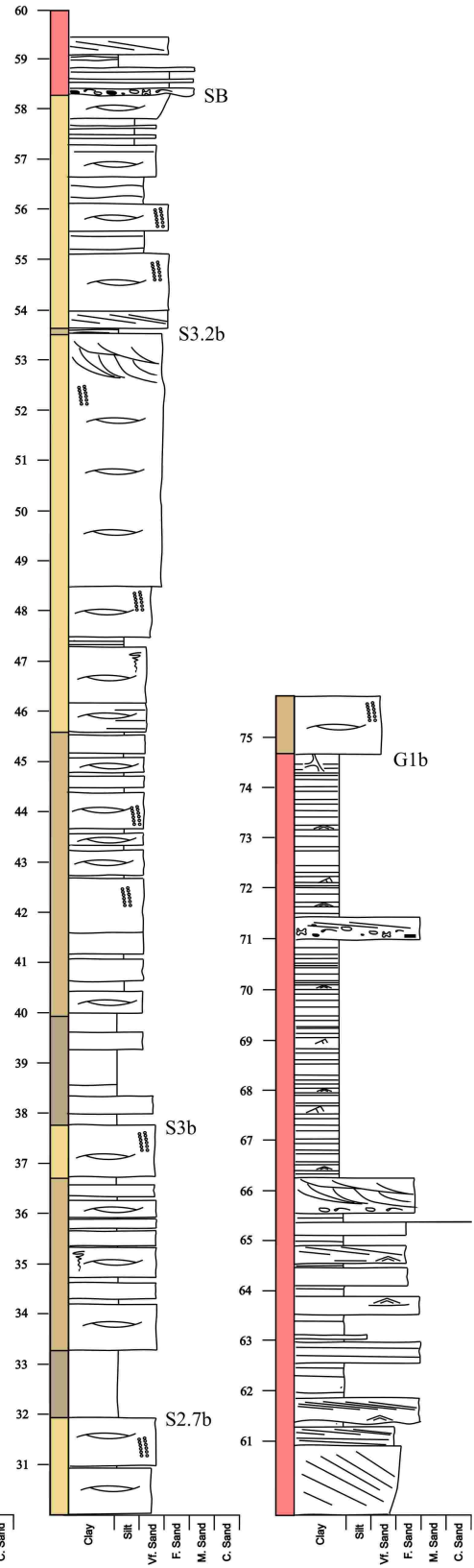
Log 9
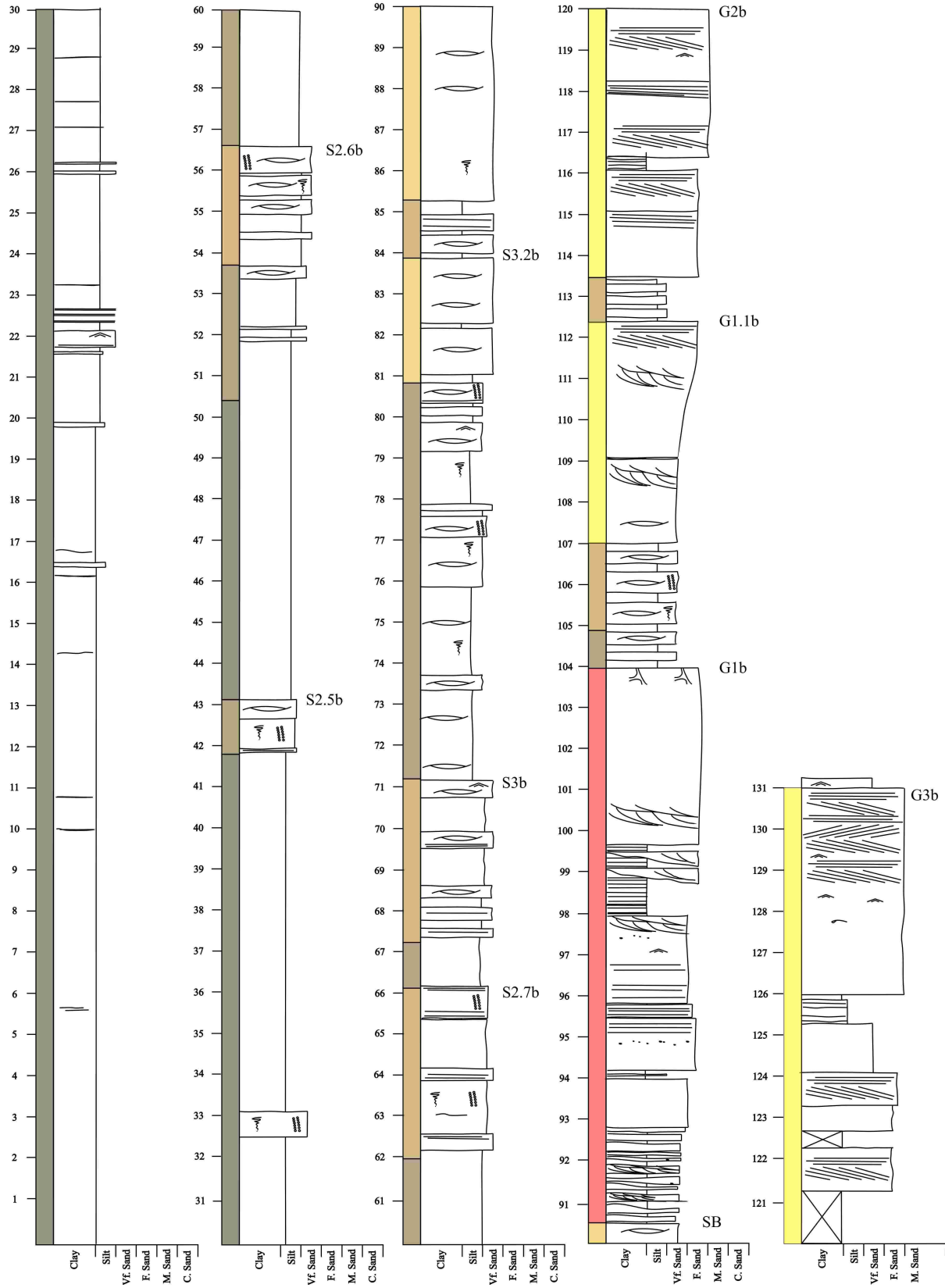
Log 10
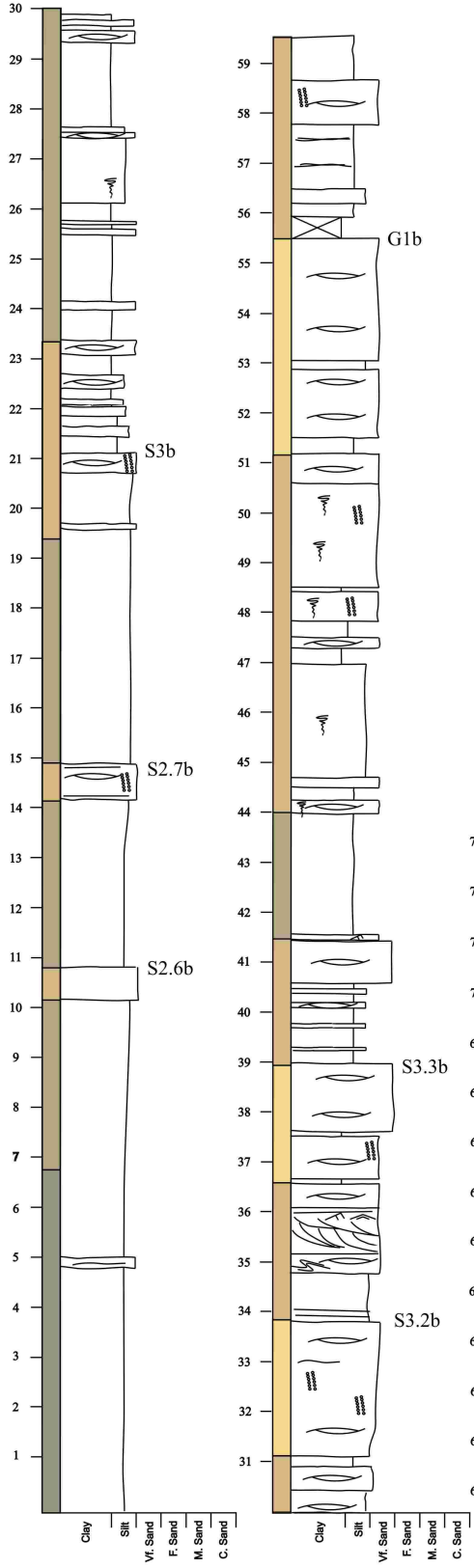
Log 11
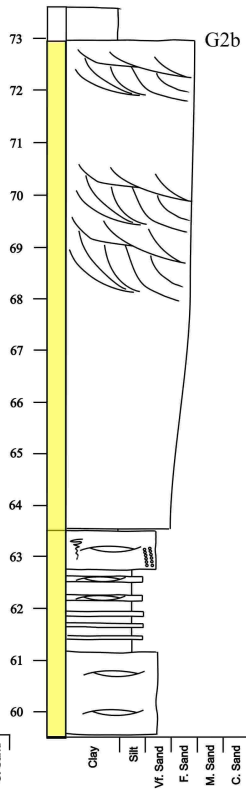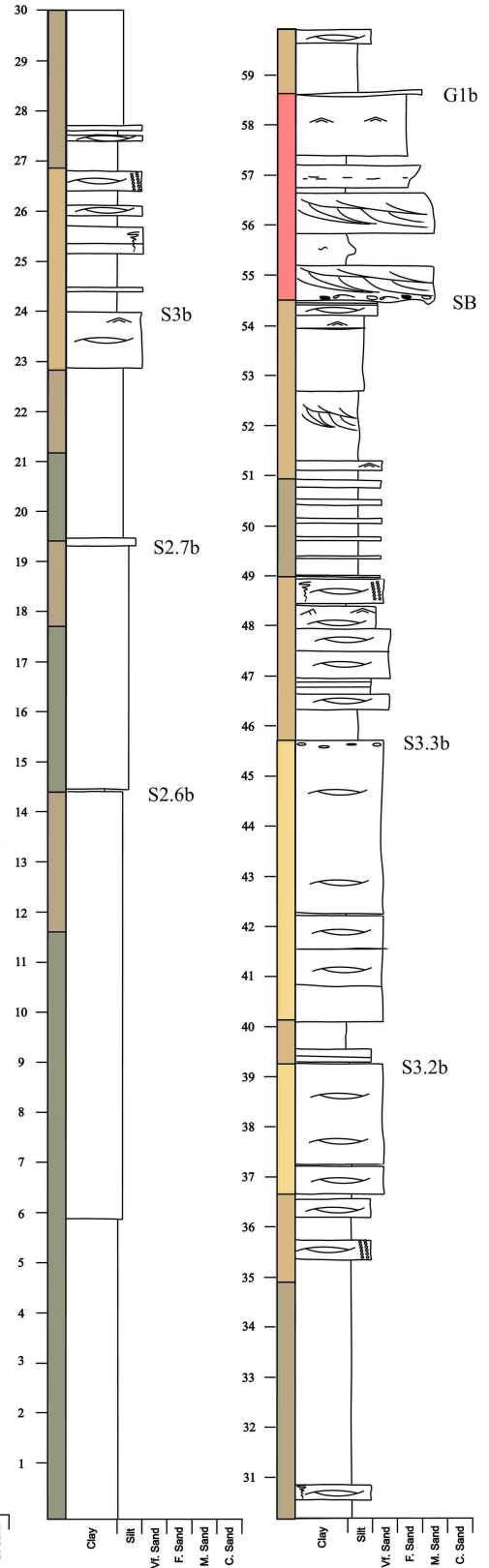
Log 12
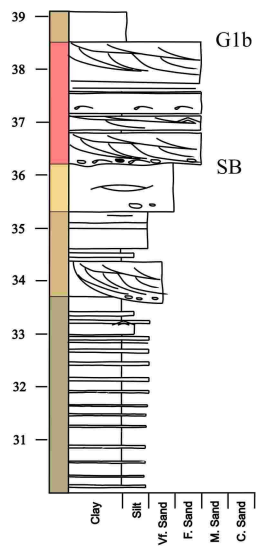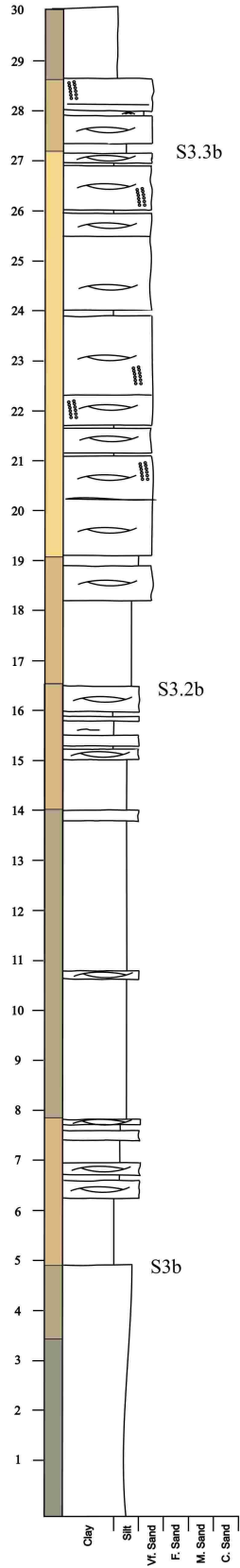
Log 13
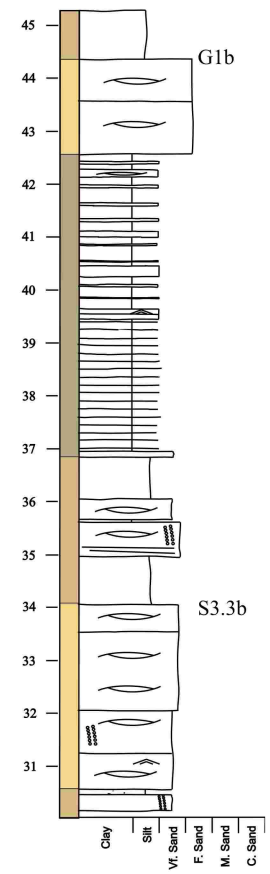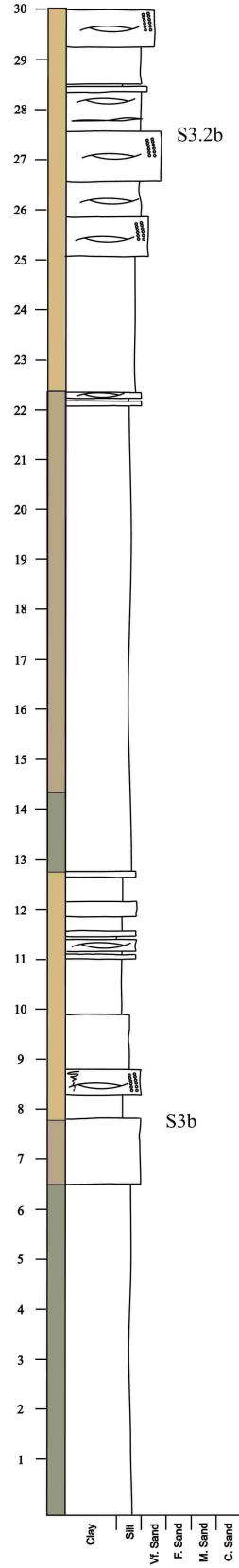
Log 14
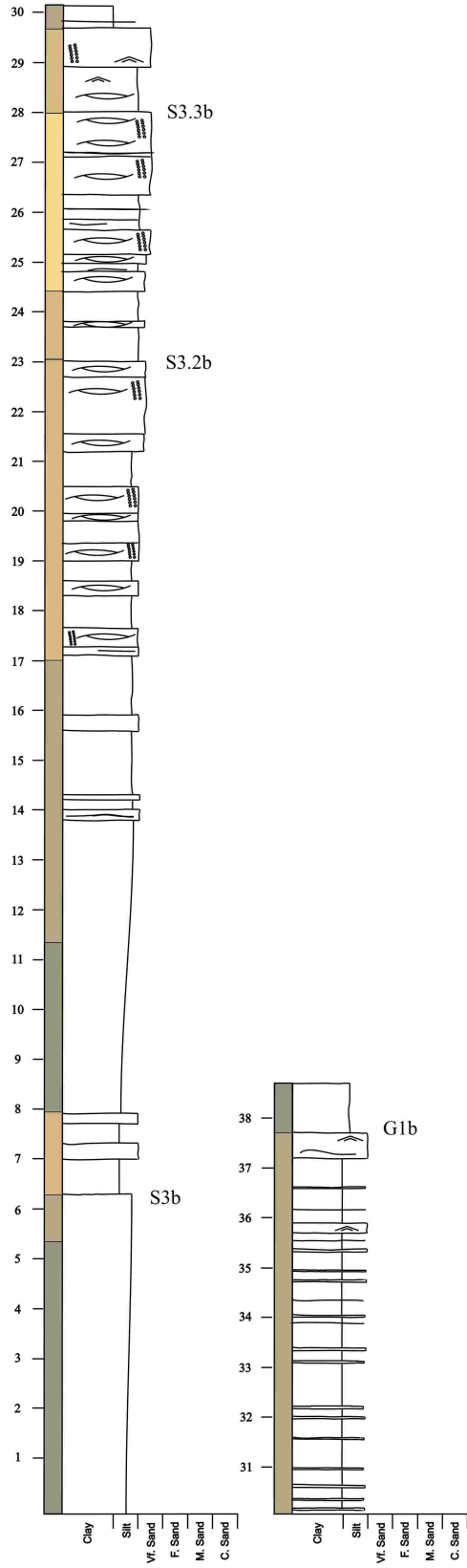
Log 15
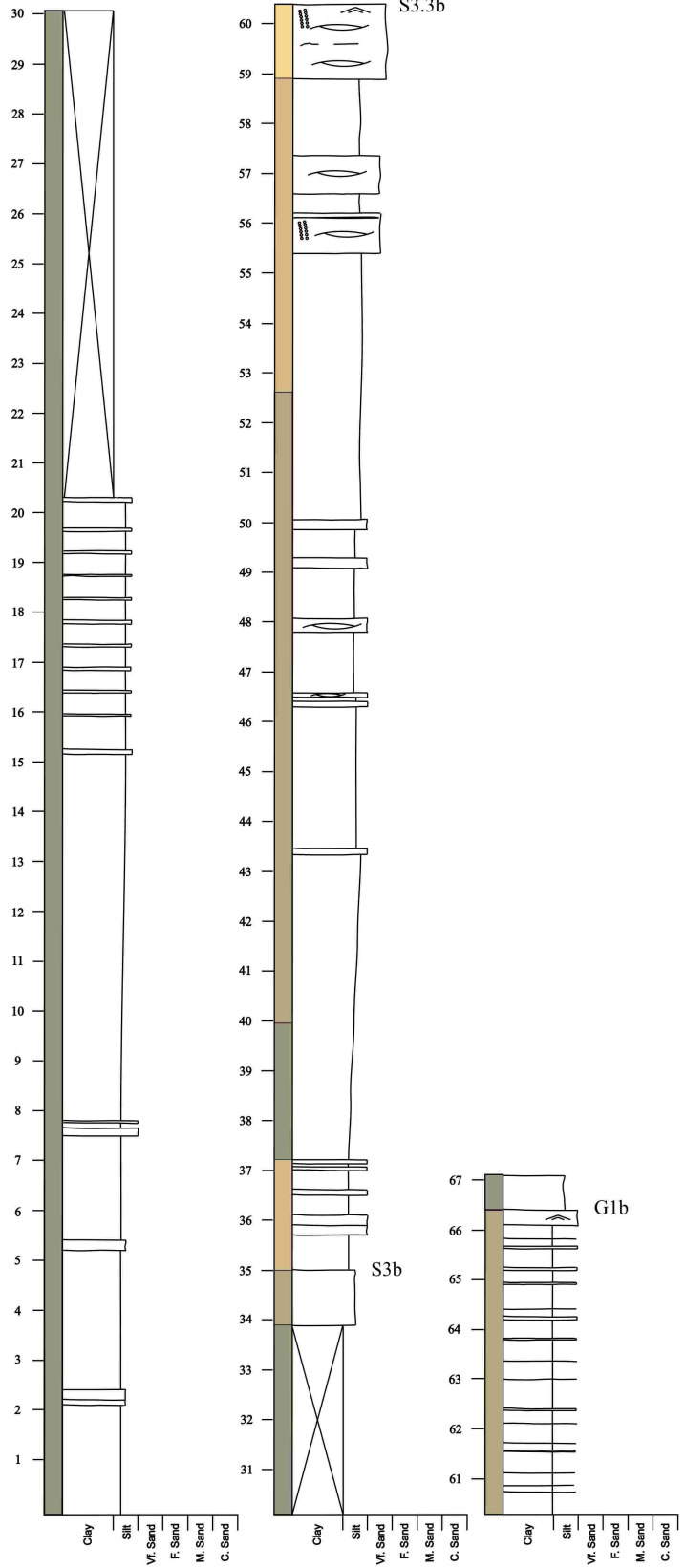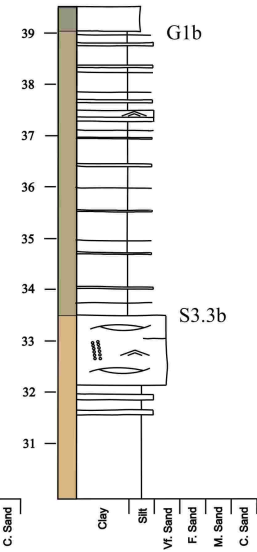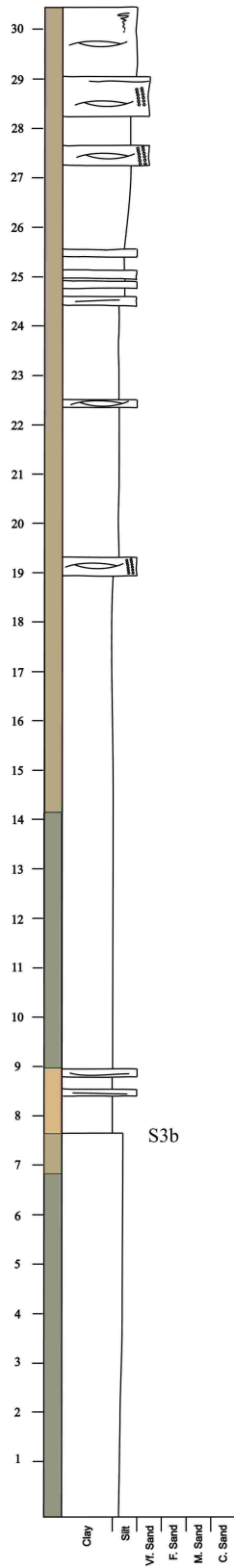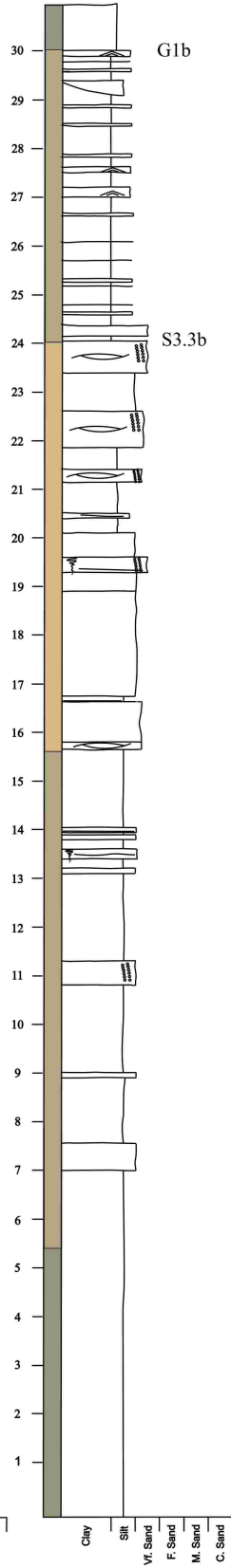
Log 16   Log 17   Log 27

Log 20

Log 21

Log 22

Log 23

S3b

S2.7b

S2.6b

G1b

SB

S3.3b

S3b

S2.7b

G1b

S3.3b

Log 24

Log 25

G1b

S3b

S2.7b

S2.6b

S3.3b

G1b

S3.3b
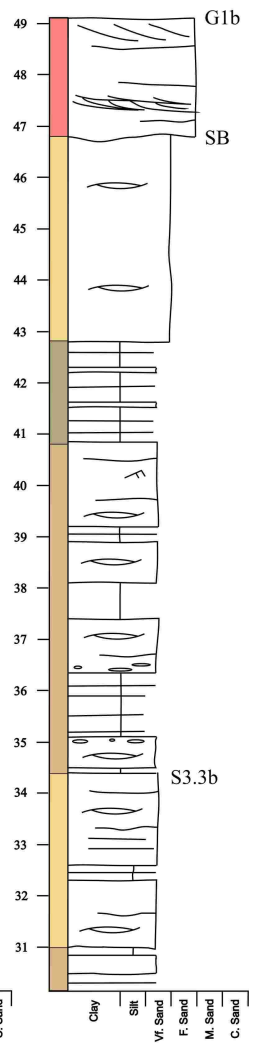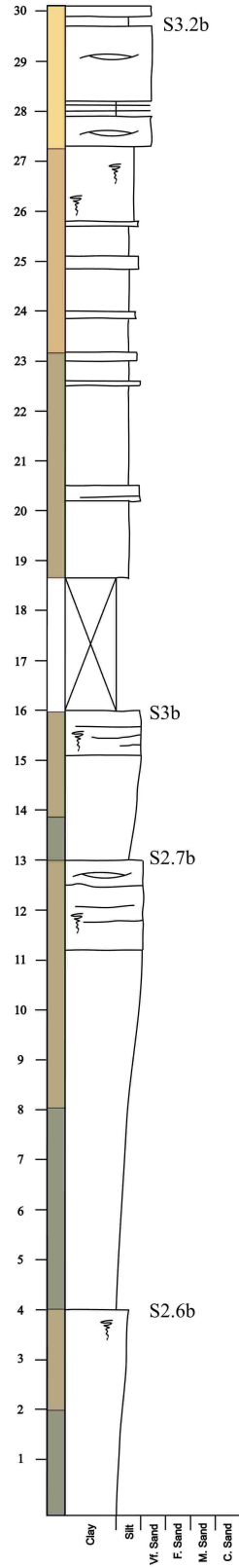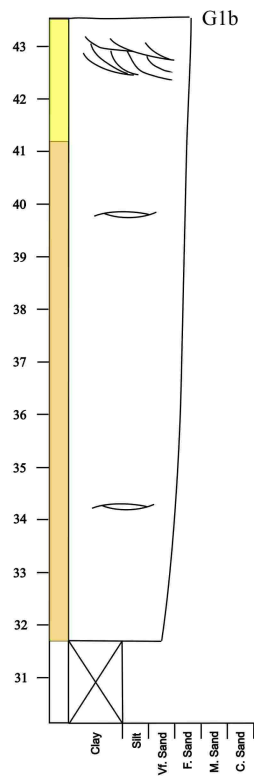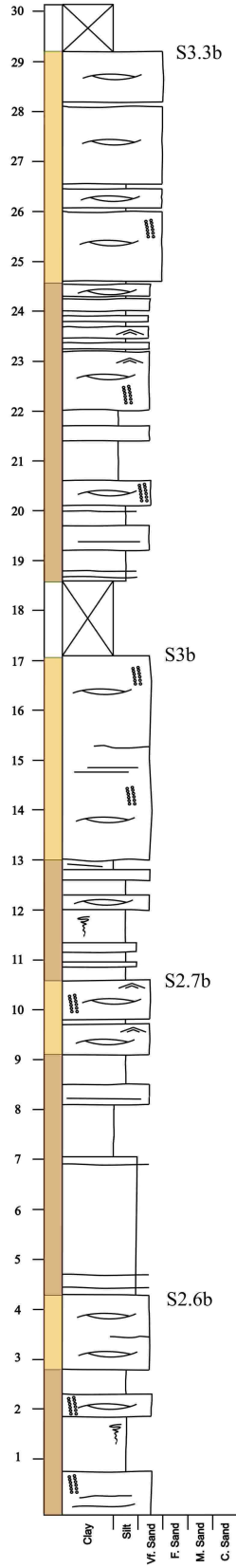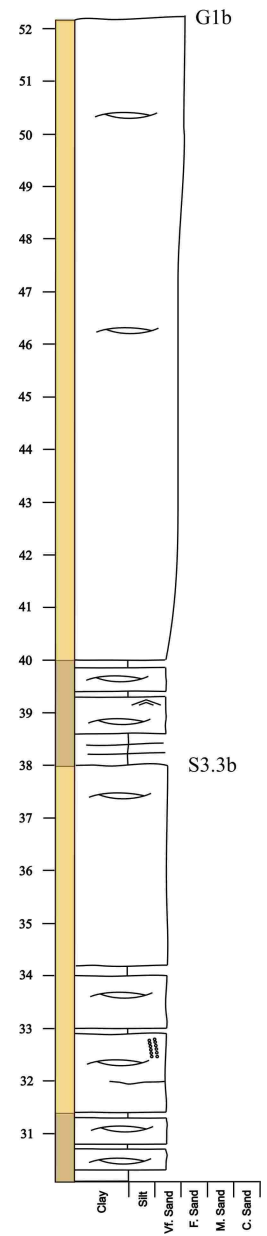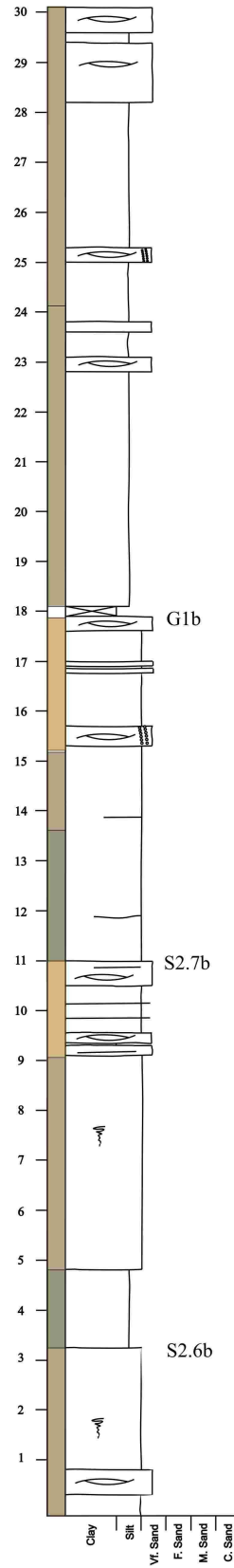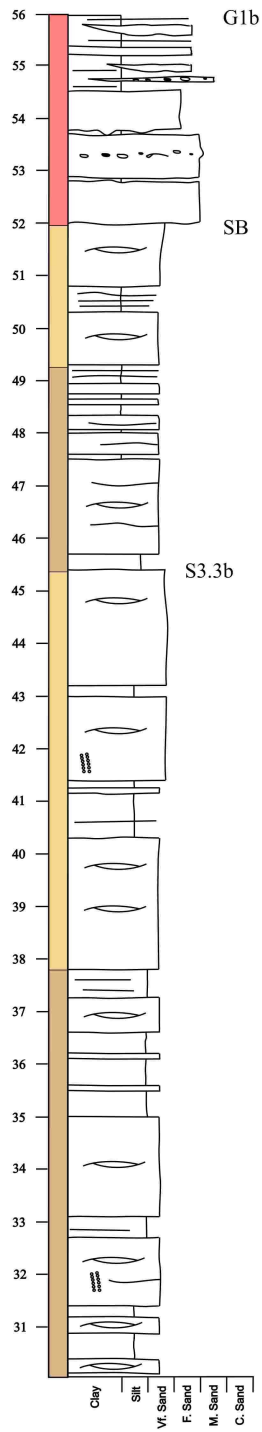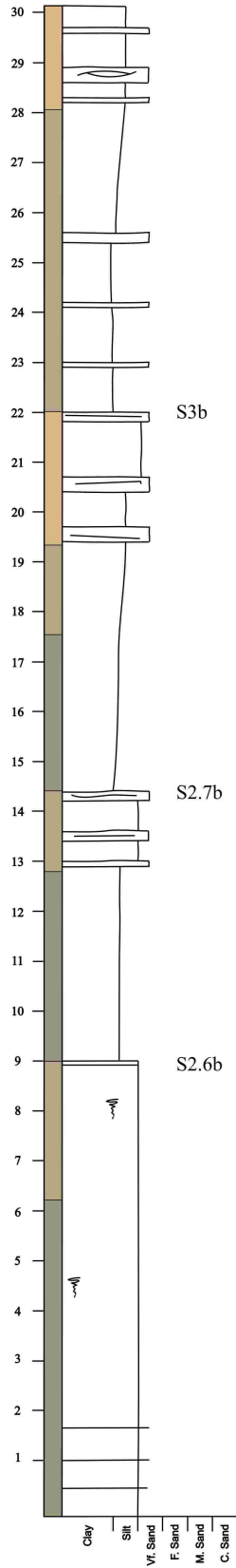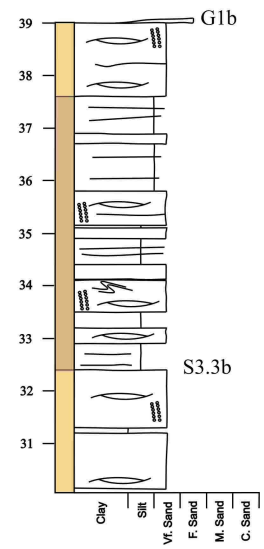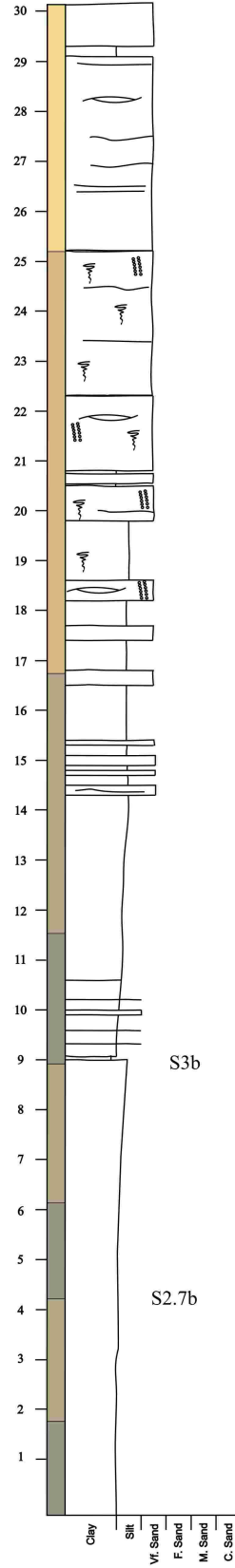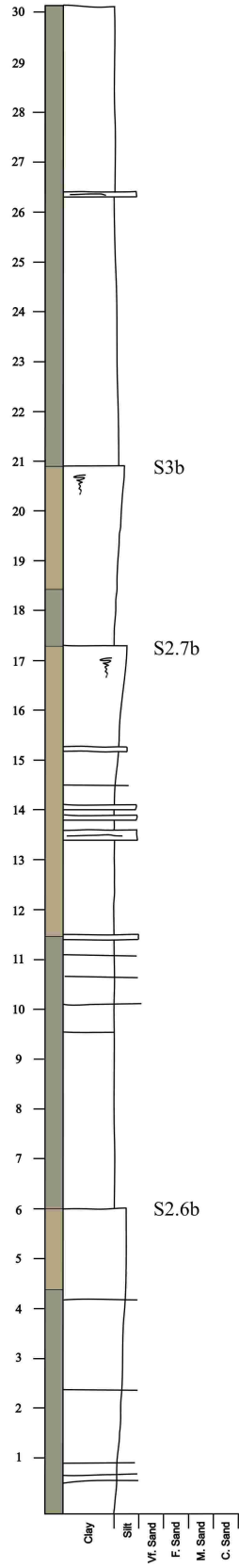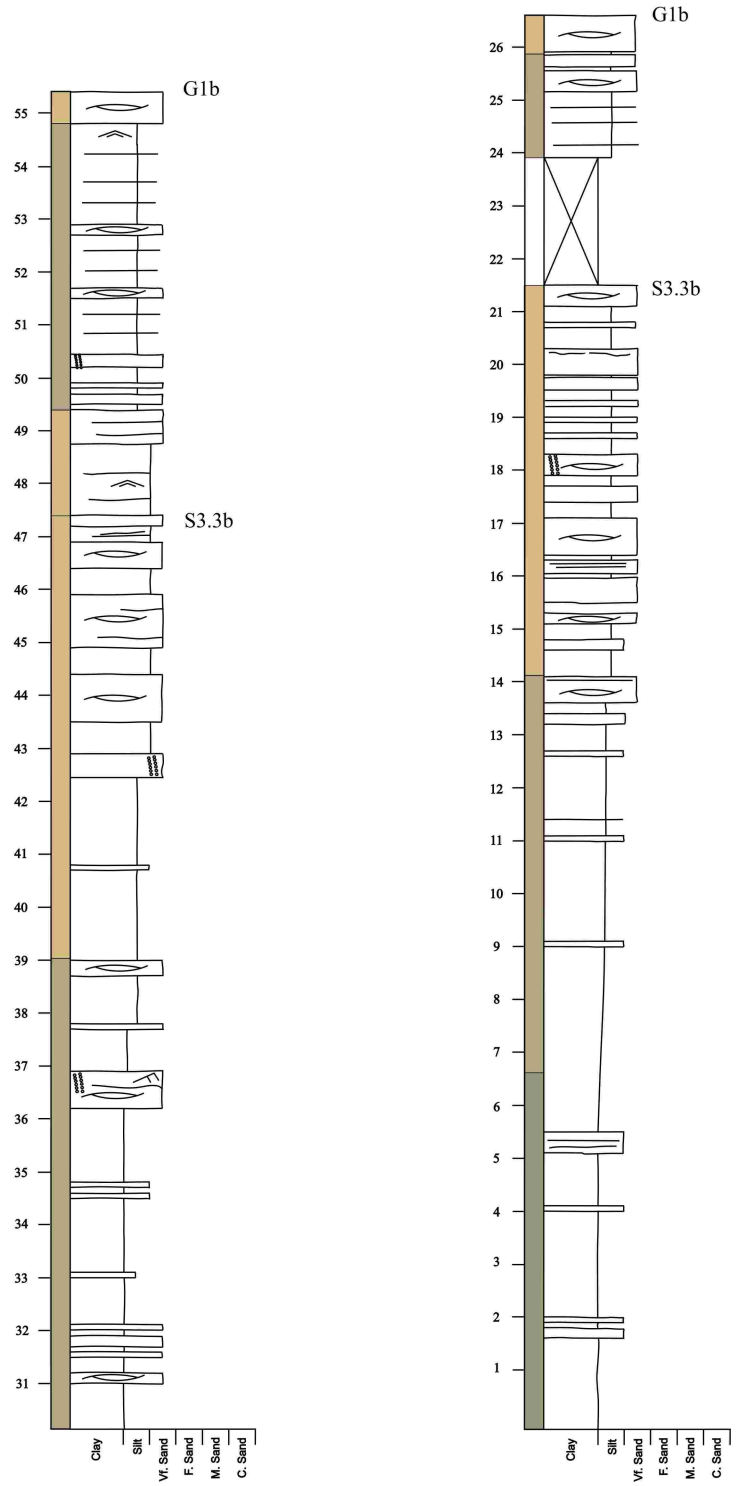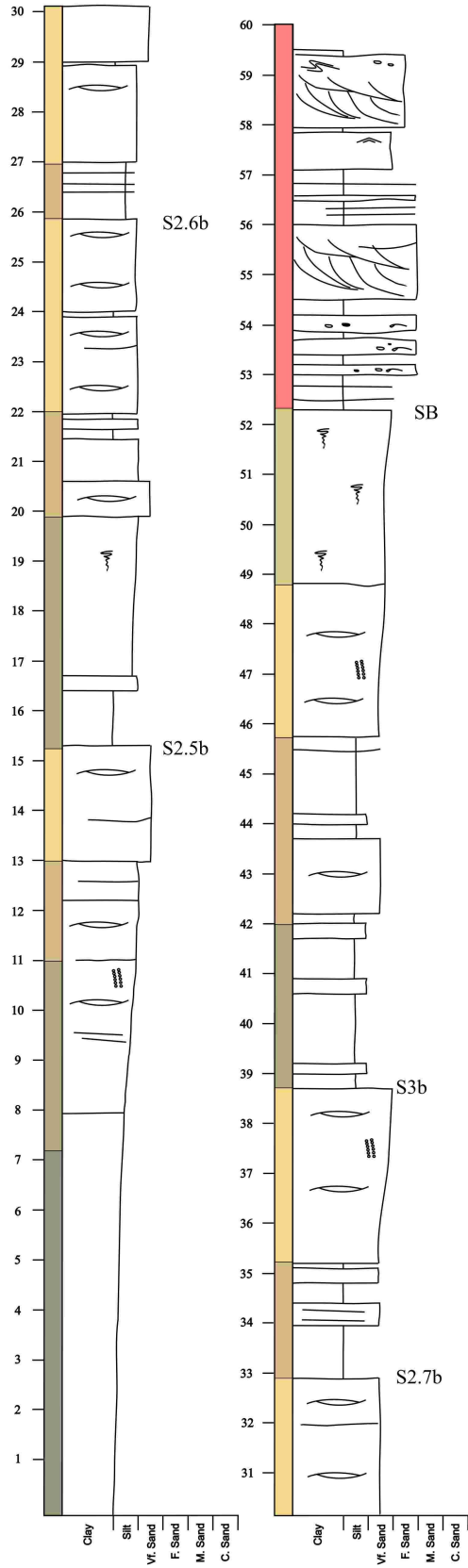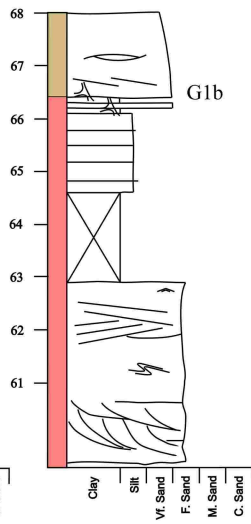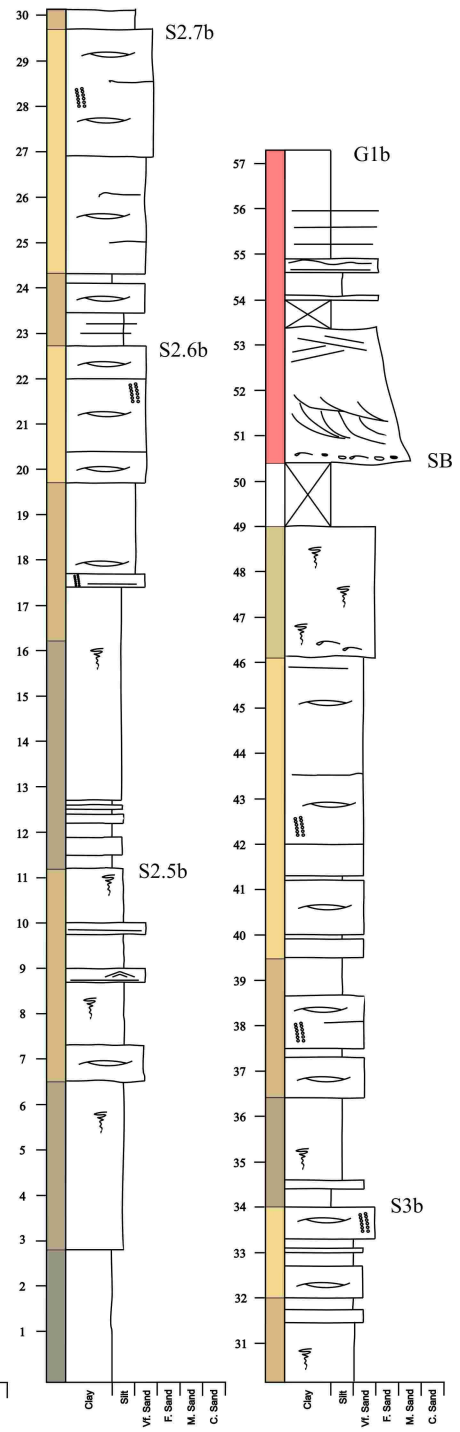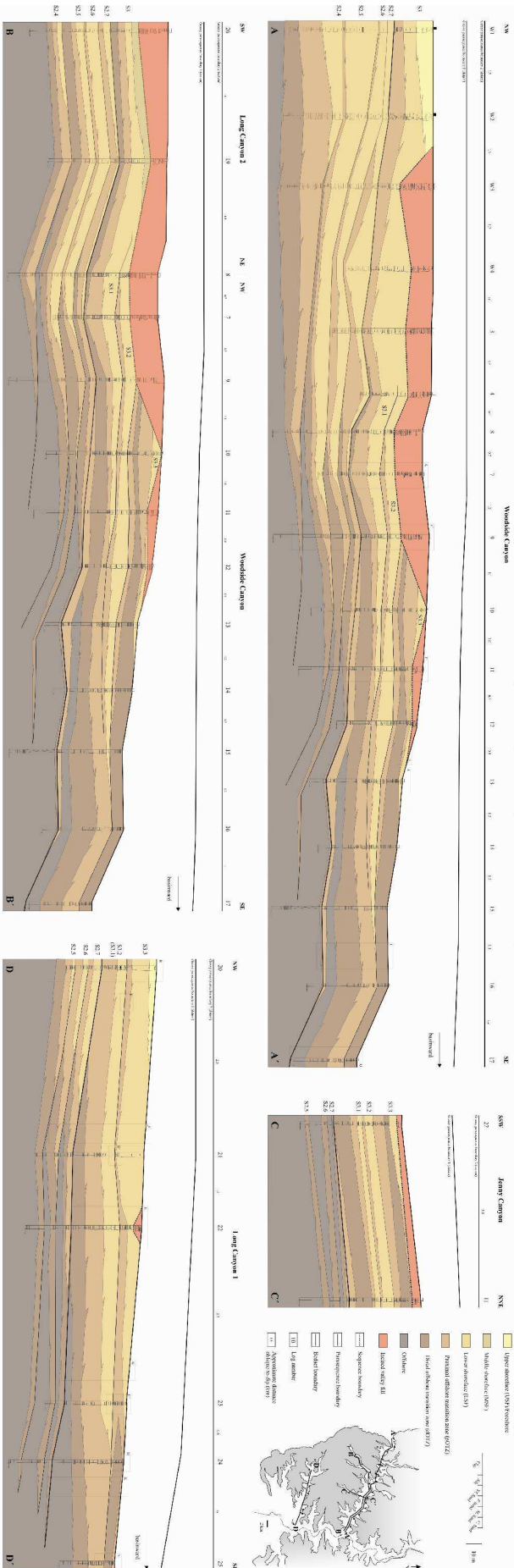
Log 26

Log 19

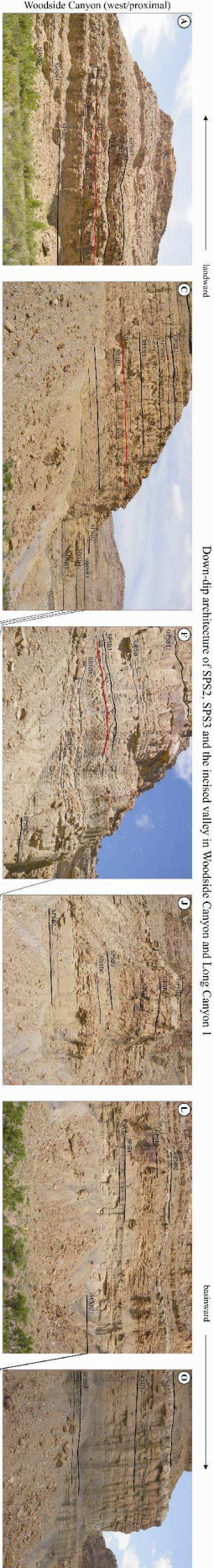Down-dip correlation panel of SPS2, SPS3 and the incised valley

Figure 3.4. Down-dip correlation panel documenting the sequence stratigraphic units and facies associations in the study area. Boxes (A-O) refer to the locations in Figure 3.5.
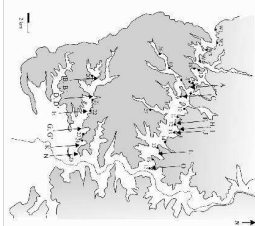
Woodside Canyon (west/proximal)

Long Canyon 1 (west/proximal)

landward

basinward

Down-dip architecture of SPS2, SPS3 and the incised valley in Woodside Canyon and Long Canyon 1

(A and C) SBSB5 pinches out into the LSF 2 km west of this location, and thickens towards the east. The incised valley fill is 10 m thick. BSB1-3 disappears into the subsurface. (B and B') SBSB6 is overlain by LSF deposits and water-lain by LSF subsurface, representing a landward shift of facies. SBS7 is composed of amalgamated HCS and is 15 m thick. SBSB6 disappears into the subsurface. (D and D') LSF HCS of BSB6 and 7 is repeated by 8.2 m.

(E) Evidence to incision in LC (e.g. 22), the unit is 4 m thick. (F) Thin (3 m) incised valley unit erodes underlying, fluvial-influenced OTZ deposits. SBSB5 pinches out. (G and G') SBS7 thin into several sandstone beds demonstrating mixed wave and fluvial influence. Thick bedrsock both the top and base of the unit which is 7 m thick. (H) The incised valley pinches out between Log12 and 13, and SBSB4 (I) is correlative SB. (I) SPS2 is composed of sandy OTZ deposits, and is overlain by a thin transgressive unit and SPS3. SBS7 (9 m) is becoming more lenticiline. (K, L and M) SBS7 is composed of thin sandstone beds indicating wave and current influence. The unit is approximately 5-7 m thick, thin heterolithic and is bounded by two distinct mudstone beds. SPS2 pinches out. (N and O) in the incised distal part, SBSB7 is approximately 5 m thick, and is composed of heterolithic, distal OTZ deposits.

SPSB2-3 = Sunnyside parasequence boundary 2-3

SPSB1-6 = Sunnyside parasequence boundary 1-6

GBSB = Grassy parasequence boundary 1-2

GBSB = Grassy bedset boundary

SB = Sequence boundary